Ecological observations of pelagic bacterial and archaeal communities in the Atlantic-Arctic boundary zone

Dissertation
zur Erlangung des Doktorgrades
der Naturwissenschaften
- Dr. rer. nat. -

dem Fachbereich Geowissenschaften
der Universität Bremen
vorgelegt von

Eduard Fadeev

Oktober 2018

Die vorliegende Doktorarbeit wurde im Rahmen des Programms International Max Planck Research School of Marine Microbiology (MarMic) in der Zeit von November 2015 bis Oktober 2018 in der HGF MPG Brückengruppe für Tiefsee-Ökologie und Technologie am Alfred-Wegener-Institut Helmholtz-Zentrum für Polar- und Meeresforschung und dem Max-Planck-Institut für Marine Mikrobiologie angefertigt.

Gutachter: Prof. Dr. Antje Boetius
Gutachter: Dr. Daniel Sher

Prüfer: PD Dr. Bernhard Fuchs
Prüfer: Prof. Dr. Kai-Uwe Hinrichs
Prüfer: Dr. Morten H Iversen

Tag des Promotionskolloquiums: 19 Dezember 2018

Summary

The global climate change has an unprecedented impact on the Arctic Ocean, resulting in warming of the Arctic surface air at much faster rates than the global average. The warming temperatures lead to constantly declining Arctic sea ice cover, which reached in September 2018 the sixth lowest summertime minimum extent in the satellite record (since the late 1970s). Shrinking sea ice has a strong impact on the entire Arctic marine ecosystem, through alterations of the primary production, grazers communities, and subsequently the biological carbon pump. Current predictions of entirely sea-ice free summers in the Arctic Ocean already in the second half of this century urges the need to understand the ongoing oceanographic and biological processes in order to predict how the Arctic ecosystem will respond to further environmental changes.

The differentiation between natural temporal ecosystem variability and anthropogenically-induced impact of the climate change requires long-term observations. The Ocean Observing System FRAM (FRontiers in Arctic marine Monitoring), which was established in 2014, is an Arctic long-term observatory for investigating the impact of changing ocean properties and sea ice conditions of the Arctic Ocean on its marine ecosystem. The starting point for the FRAM project was the already existing long-term observatory HAUSGARTEN, situated in the main gateway between the Arctic and the Atlantic Oceans - the Fram Strait. To date, despite their importance for the biogeochemical cycling, very little is known regarding the diversity and function of microbial communities in the Arctic Ocean in general, and specifically in the Fram Strait. In the framework of FRAM, a Molecular Observatory was established, for conducting standardized molecular-based high-resolution observations of the Arctic microbial communities.

This thesis was conducted as part of the FRAM Molecular Observatory, and as part of the establishment process of the observatory it contributes to the methodological and procedural standardization required for long-term microbial observations. This thesis provides a first comprehensive overview of currently existing long-term microbial observatories around the world, it provides guidelines for initial steps towards establishing a community network between them, and stresses the urgent need in community efforts towards methods standardization. Furthermore, as part of the methods standardization for long-term microbial observations, this thesis includes a performance comparison between two, broadly used in microbial oceanography, 16S rRNA gene primer sets.

The main focus of the thesis is on the ecology of pelagic bacterial and archaeal communities in the Fram Strait. Its overall objective was to investigate the distribution of these communities in the Fram Strait, and to identify environmental drivers of their diversity. The observations of this thesis reveal that sea ice has a strong impact on the development of the seasonal phytoplankton

bloom during the summer. As a result, sea ice conditions are affecting the bacterial diversity in surface water, and are leading to a distinct community in sea-ice free and sea-ice covered regions of the Fram Strait. However, the impact of the sea ice is not limited to the surface ocean, as it also heavily affects the vertical export of aggregated organic matter to the deep ocean. The results of this thesis also show that aggregates formed under the sea ice sink faster, and by that provide a stronger vector for transport of bacterial and archaeal taxa to the deep ocean, compared to ice-free waters.

Altogether, this thesis contributes to the baseline knowledge needed for further long-term observations of pelagic microbial communities in the Arctic marine ecosystem. Furthermore, it provides an important insight into the strong impact of the sea ice on bacterial and archaeal communities throughout the entire water column, underlining the potential impact of further environmental changes on the Arctic Ocean in the light of prevalent global warming and climate change.

Zusammenfassung

Der Einfluss des globalen Klimawandels ist an keinem Platz der Welt so deutlich sichtbar wie in dem Arktischen Ozean. Dies lässt sich besonders an der Erwärmung der Luft über der Arktis messen, die sich hier wesentlich schneller erwärmt als im globalen Durchschnitt. Diese warmen Temperaturen führten in den letzten Jahren zu einer konstant schmelzenden Eisdecke. Dieses Jahr im September wurde seit Anbeginn der Messungen (1970) die sechstniedrigste Eisstärke auf dem Arktischen Ozean gemessen.

Die Abschmelzung der Eisdecke auf dem Arktischen Ozean hat extreme Folgen für das gesamte marine Ökosystem, da es zu Veränderungen in der Primärproduktion und der Zooplanktonzusammensetzung kommt, was schlussendlich einen Effekt auf die biologische Kohlenstoffpumpe besitzt. Man geht momentan davon aus, dass bereits in der zweiten Hälfte dieses Jahrhunderts die Arktis im Sommer komplett eisfrei sein wird. Diese starken Veränderungen der Umwelt werden die ozeanografischen und biologischen Prozesse zwangsläufig beeinflussen. Daher ist es unabdingbar zu verstehen, wie sich die Klimaerwärmung bereits heute auf unsere Ökosysteme auswirkt, um zukünftige Veränderungen besser prognostizieren zu können.

Um den Einfluss des Klimawandels im Grundsatz zu verstehen und um unterscheiden zu können zwischen natürlicher, zeitlicher Variabilität des Ökosystems und anthropogenen Einflüssen, braucht es Langzeitstudien. Das Ozean-Beobachtungssystem FRAM (FRontiers in Arctic marine Monitoring) ermöglicht genau diese Langzeitbeobachtungen, welche sich auf den Einfluss der Veränderungen des Ozeans und der Eisverhältnisse auf das marine Ökosystem der Arktis konzentrieren. Den Grundstein für das FRAM Projekt legte das bereits seit langem bestehende Observatorium HAUSGARTEN, welches sich in dem Hauptzugang vom Arktischen zum Atlantischen Ozean befindet- der Framstraße.

Bis heute weiß man sehr wenig über die generelle Vielfalt und die Funktion mikrobiologischen Lebens in der Arktis, obwohl dies für das Verständnis des biogeochemikalischen Kreislaufs insbesondere in der Framstraße unbedingt notwendig ist. Im Rahmen des FRAM Projektes wurde daher ein Observatorium aufgebaut, welches es ermöglicht, genau diese Prozesse durch standardisierte molekulare Methoden hoch auflösend zu beobachten und besser zu verstehen wie die arktischen mikrobiologischen Gemeinschaften funktionieren.

Die Forschungsarbeit auf der diese Doktorarbeit basiert, wurde im Rahmen des mikrobiellen FRAM Observatoriums ermöglicht und trägt zu einer Methodenentwicklung und Prozessstandardisierung bei, die unbedingt für mikrobiologische Langzeitbeobachtungen dieser Region benötigt werden. Diese Arbeit gibt zudem den ersten allumfassenden Überblick aller derzeit existierenden mikrobiologischen Langzeitobservatorien, sowie Handlungsempfehlungen für erste

Schritte um ein Kommunikationsnetzwerk zwischen ihnen aufzubauen und betont die dringende Notwendigkeit Methoden zu standardisieren. Aus diesem Grunde werden in dieser Arbeit als erster Schritt Richtung Methodenentwicklung die zwei meist genutzten 16S rRNA Genprimersets miteinander verglichen.

Der Schwerpunkt dieser Doktorarbeit liegt auf der Ökologie der pelagischen bakteriellen und archaeellen Gemeinschaften in der Framstraße mit dem Ziel, die Verteilung dieser Gemeinschaften zu untersuchen und die Haupteinflüsse der Umwelt auf ihre Artenvielfalt zu identifizieren. Die Arbeit kommt zu zwei Hauptergebnissen: zum einen hat die Ausbreitung von Meereseis einen großen Einfluss auf die Entwicklung der saisonalen Planktonblüte im Sommer und die Vielfalt der Bakterien im Oberflächenwasser, was zu sich deutlich unterscheidenden Diversität der Gemeinschaften in vereisten und nicht vereisten Regionen auf allen Wasserebenen der Framstraße führt. Dies bedeutet, dass nicht nur das Oberflächenwasser von den Veränderungen beeinflusst ist, sondern genauso auch der vertikale Export aggregierter organischer Materie in die Tiefsee. Außerdem zeigt diese Arbeit, dass Aggregate, welche unter dem Meereis entstanden, schneller sinken und einen schnelleren Transportvektor bakterieller und archaeeller Taxa in die Tiefsee darstellen im Vergleich zu Aggregaten, die sich in eisfreien Gebieten bildeten.

Insgesamt liefert die Doktorarbeit einen entscheidenden Beitrag zum Aufbau des Basiswissens zur Langzeitbeobachtungen von pelagischen mikrobiellen Gemeinschaften des arktischen marinen Ökosystems, welches für zukünftige Forschung unabdingbar ist. Des Weiteren liefert sie wichtige Erkenntnisse über den Einfluss des Meereseis auf bakterielle und archaeelle Gemeinschaften innerhalb der gesamten Wassersäule, welches den potentiellen Einfluss von weiteren Veränderungen der Umwelt auf den Arktischen Ozean im Hinblick auf die globale Erwärmung und den Klimawandel weiter unterstreicht.

List of Figures

1.1 Bathymetry and hydrography of the Arctic Ocean . . . 3
1.2 Map of FRAM infrastructure in the Arctic Ocean and the Fram Strait . . . 15

2.1 Map of marine long term ecological time series sites with microbiome variables monitored . . . 34

3.1 Sampling coverage of bacterial communities used for primer sets comparison. . . 42
3.2 Mean sequence proportion of taxonomic classes in each habitat . . . 43
3.3 Differential abundance of bacterial families between the primer sets . . . 45
3.4 Relative abundance of bacterial taxa using 16S rRNA gene and CARD-FISH . . . 46
3.S1 Sequence retainment throughout the bioinformatic workflow . . . 50
3.S2 Linear correlation in sequence proportions between the primer sets . . . 51
3.S3 Correlation of 16S rRNA and CARD-FISH bacterial relative abundance . . . 52

4.1 Oceanographic overview of Fram Strait during June 2014 . . . 60
4.2 Modeled weekly surface chl a concentration in Fram Strait during June 2014 . . . 61
4.3 Comparison of bacterial community composition between the different regions and fractions . . . 62
4.4 Sequence proportion overview of overlapping bacterial OTUs . . . 63
4.5 Enriched bacterial families between the regions . . . 65
4.6 Sequence proportion overview of overlapping microbial eukaryote OTUs . . . 66
4.7 Bacterial community characteristics across the Fram Strait . . . 67
4.8 RDA ordination of bacterial community composition . . . 68
4.9 Overview of edge counts for selected taxonomic groups in each network . . . 69
4.10 Sub-networks of the FL and PA fractions in the chl. a max. . . . 70
4.S1 Regional separation of Fram Strait based on in situ biogeochemical parameters . . 80
4.S2 Rarefaction analysis of bacterial and eukaryotic communities . . . 81
4.S3 Differences in bacterial community composition between the regions . . . 82
4.S4 Venn diagram of shared OTU . . . 83
4.S5 Enriched microbial eukaryotic taxonomic groups between the regions . . . 84
4.S6 PCoA of microbial eukaryote community composition . . . 85
4.S7 Venn diagram of shared OTU . . . 85
4.S8 Monthly mean of surface chlorophyll a in FESOM-REcoM2 . . . 88
4.S9 Comparison of modeled and in situ measured parameters across the Fram Strait . 88

5.1 Oceanographic overview of Fram Strait during July 2016 . . . 98
5.3 Exemplary light microscopy images of marine aggregates in Fram Strait . . . 101
5.4 Sinking trajectories of particles . . . 102
5.5 Microbial community composition throughout the water column . . . 104
5.6 Free-living and particle-associated community dynamics throughout the water column of Fram Strait . . . 105
5.7 Differences in PA community composition between the the distinct water layers . 107
5.8 SourceTracker estimates of water mass contribution . . . 109
5.S1 Sample-size-based rarefaction curves of microbial communities . . . 116

5.S2 Chlorophyll a concentrations along Fram Strait during July 2016 116
5.S3 Vertical changes in communitiy richness and diversity 117
5.S4 Dissimilarities between microbial fractions throughout the water column. 117

6.1 Comparison of bacterial and archaeal communities between the central Arctic Ocean and the Fram Strait. 124
6.2 Schematic representation of Arctic Ocean water column. 132

List of Tables

2.1 Details of samples used in Polar Front study 22

3.S1 Details of samples used for primers comparison 53
3.S2 Details of CARD-FISH probes 55

4.1 Comparison of nutrient consumption, phytoplankton biomass and productivity . . 61
4.S1 Overview of sampled stations during RV Polarstern expedition PS85 89
4.S2 Bacterial cell abundance and activity 92
4.S3 Properties of the co-occurrence networks 93

5.1 Characteristics of particles in ice-free and ice-covered regions of Fram Strait. . . . 100
5.S1 Settings of particle tracking experiments 115
5.S2 Overview of sampled stations during RV Polarstern expedition PS99.2 118
5.S3 Microbial community alpha diversity estimations 120

List of acronyms

AW Atlantic Water

AtlantOS Atlantic Ocean Observing Systems

CARD-FISH CAtalyzed Reporter Deposition-Fluorescence In Situ Hybridization

CTD conductivity temperature depth

DOM dissolved organic matter

DNA deoxyribonucleic acid

daOTU differentially abundant operational taxonomic unit

EBDW Eurasian Basin Deep Water

EGC East Greenland Current

EMP Earth Microbiome Project

EOV Essential Ocean Variables

EPS extracellular polymeric substances

FL free-living

FISH Fluorescence In Situ Hybridization

FRAM FRontiers in Arctic marine Monitoring

HNA high nucleic acids

LNA low nucleic acids

LTER Long-term ecological research

MAW mixed Atlantic Water

MSC Marine Snow Catcher

MolObs Molecular Observatory

MI microbial indicator

OTU operational taxonomic unit

OM organic matter

PA particle-associated

PCR polymerase chain reaction

POM particulate organic matter

PPS PhytoPlankton Sampler

PW Polar water

RAS Remote Access water Sampler

RNA ribonucleic acid

rRNA ribosomal RNA

TEP transparent exopolymer particles

UVP Underwater Vision Profiler

WSC West Spitsbergen Current

Contents

Summary **iii**

Zusammenfassung **v**

List of Figures **viii**

List of Tables **ix**

List of Acronyms **x**

1 Introduction **1**
1.1 The Arctic Ocean . . . 1
1.2 Microbial ecology in the Arctic Ocean . . . 7
1.3 Observing changes in the Arctic Ocean . . . 10
1.4 Thesis objectives . . . 14
1.5 Publication outline . . . 16

2 Marine Microbes in 4D – Using time series observation to assess the dynamics of the ocean microbiome and its links to ocean health **19**
2.1 Abstract . . . 20
2.2 Highlights . . . 20
2.3 Introduction . . . 20
2.4 Monitoring the microbial role in ocean health . . . 31
2.5 Network for microbial observation . . . 33
2.6 Societal relevance of microbial observatories . . . 36

3 Primer selection for Arctic Ocean microbiome studies - a taxonomic resolution trade off **38**
3.1 Abstract . . . 39
3.2 Introduction . . . 39
3.3 Results and Discussion . . . 41
3.4 Concluding remarks . . . 47
3.5 Materials and methods . . . 47
3.6 Supplementary material . . . 50

4 Microbial communities in the East and West Fram Strait during sea-ice melting season **56**
4.1 Abstract . . . 57
4.2 Introduction . . . 57
4.3 Results . . . 59
4.4 Discussion . . . 70
4.5 Conclusions . . . 74
4.6 Materials and methods . . . 75
4.7 Supplementary material . . . 80

5 Arctic Ocean sea ice enhances vertical connectivity of microbial communities through sinking marine aggregates **94**
5.1 Abstract 95
5.2 Introduction 95
5.3 Results and Discussion 97
5.4 Conclusions 109
5.5 Materials and methods 110
5.6 Supplementary material 113

6 General discussion **123**
6.1 Towards integrated microbial observations of the Arctic Ocean 124
6.2 Observing seasonal dynamics in the Fram Strait using autonomous sampling . . . 125
6.3 Surface bacterial communities are driven by the seasonal phytoplankton bloom . 128
6.4 Sea ice promotes vertical connectivity of microbial communities 129
6.5 Future scenario for Arctic Ocean pelagic microbial communities 130

Perspectives **134**

References **135**

Acknowledgements **169**

Erklärung **170**

Chapter 1

Introduction

1.1 The Arctic Ocean

The Arctic Ocean is the smallest ocean on Earth, making up ~4% of the global ocean area and only ~1% of its volume (Jakobsson, 2002). The Arctic Ocean has a unique circumpolar oceanography, characterized by strong seasonal cycles in temperature, solar irradiation and seasonal formation of sea ice (Johannessen *et al.*, 1994). Unlike the Southern Ocean, the Arctic Ocean is almost completely enclosed by land and is classified as a mediterranean sea, comprising 35% of the world coastline (Tomczak and Godfrey, 2013). Furthermore, about 50% of the Arctic Ocean surface area is comprised of continental shelves, which are considered to be the most fertile regions of the Arctic Ocean (Carmack and Wassmann, 2006). Its central basin is separated by the subsurface Lomonosov Ridge into the Amerasian Basin, which connects to the North Pacific Ocean, and the Eurasian Basin, which connects the North Atlantic Ocean (Figure 1.1; Beszczynska-Möller *et al.*, 2011). Despite its small size, the Arctic Ocean has important functions in the global ocean circulation. It absorbs the heat from the north Atlantic thermohaline circulation, and produces the colder and denser waters that form the deep layers of the North Atlantic (Aagaard *et al.*, 1985). It also provides an oceanic connection between the North Atlantic and North Pacific Oceans that has an important role in the nutrient fluxes between these oceans (Torres-Valdés *et al.*, 2013).

1.1.1 Physical oceanography

The Arctic Ocean exchanges water with both the Pacific and the Atlantic Oceans through two main oceanic gateways, Bering Strait and Fram Strait (Beszczynska-Möller *et al.*, 2011). The low salinity Pacific waters are entering the Arctic Ocean through the shallow (50 m) Bering Strait. These waters are characterized by high silicate and phosphate concentrations, providing a large source of nutrients for the Arctic Ocean (Torres-Valdés *et al.*, 2013). However, they comprise only a small fraction of the total inflow to the Arctic Ocean. In contrast, Atlantic inflow through the Fram Strait is roughly 10 times larger than the Pacific inflow (Beszczynska-Möller *et al.*, 2011). The Atlantic waters (AW) are more saline and have higher nitrate to phosphate (N:P) ratio, compared to the Pacific waters. At depths of more than 1000 m, the Arctic Deep Water

layer begins (Smith Jr, 2013). This very dense homogeneous layer comprises the Arctic Ocean deep waters, and reaches the seafloor (Figure 1.1).

In general, the surface waters of the Arctic Ocean are stratified by salinity, with relatively weak vertical mixing (Carmack, 2007). In both basins, the water column is characterized by a low salinity polar mixed layer at the surface (10 m depth), separated by a cold halocline from the layers below (Rudels *et al.*, 1996). Being relatively fresher, the Pacific waters lie higher in the water column than Atlantic waters (AW), and provide part of the strong stratification of the Arctic water column. This strong water column stability isolates the surface waters from the heat of the Atlantic and the Pacific inflows, and allows formation of sea ice in winter (Rudels, 2012).

The most defining characteristic of the Arctic Ocean is the sea ice, that covers in winter the entire Arctic Ocean (Thomas, 2017). In the dark autumn and winter the temperature of surface waters drops below the freezing point. During that time the Arctic sea ice is formed, reaching its maximum seasonal coverage in March (Polyak *et al.*, 2010). The sea ice formation process results in brine rejection that increases the salinity of the underlying waters. Weakened stratification of the water column initiates deep vertical mixing, which forms the Arctic bottom water and "fills up" the nutrients budget in the surface (Korhonen *et al.*, 2013). In summer, as a result of solar radiation and warmer incoming waters, the sea ice melts, and reaches its seasonal minimum in September. The melting process releases freshwater and strengthens the stratification of the water column once again (Korhonen *et al.*, 2013).

The sea ice buffers interactions (e.g., heat exchange) between the atmosphere and the ocean, and governs light availability in the underlying water column (Perovich and Polashenski, 2012). Furthermore, it prevents surface and internal waves, and isolates the water surface from winds (Thomas and Dieckmann, 2003). As such, it is affected by both the winds above and the water currents below, and is carried with the transpolar drift towards the Fram Strait (Figure 1.2 Pfirman *et al.*, 1997).

The concentration and thickness of the sea ice are a result of thermodynamic processes and provide an important evidence for the global climate change (Gao *et al.*, 2015; Budikova, 2009). The shrinking sea ice extent results in surface warming twice as fast as the global average (Sun *et al.*, 2016; Dobricic *et al.*, 2016). Warmer surface waters are weakening the cold halocline layer, allowing stronger vertical mixing and upward AW heat flux, which further amplifies the sea-ice loss (Polyakov *et al.*, 2017). According to current model projections the Arctic Ocean may experience sea-ice free summers already by the second half of this century (Overland and Wang, 2013; Wang and Overland, 2015). Such fundamental change of the Arctic Ocean will lead to strong alterations of the marine ecosystem (Wassmann and Reigstad, 2011; Arrigo *et al.*, 2008).

1.1.2 Primary production

On a global scale, one of the key biological processes that occurs in the ocean is primary production by photosynthetic organisms (Falkowski *et al.*, 1998; Field, 1998). This process is fueled by solar radiation and provides the basis of the marine food web, as it converts inorganic carbon sources (such as carbon dioxide) into bioavailable organic carbon. Primary production by

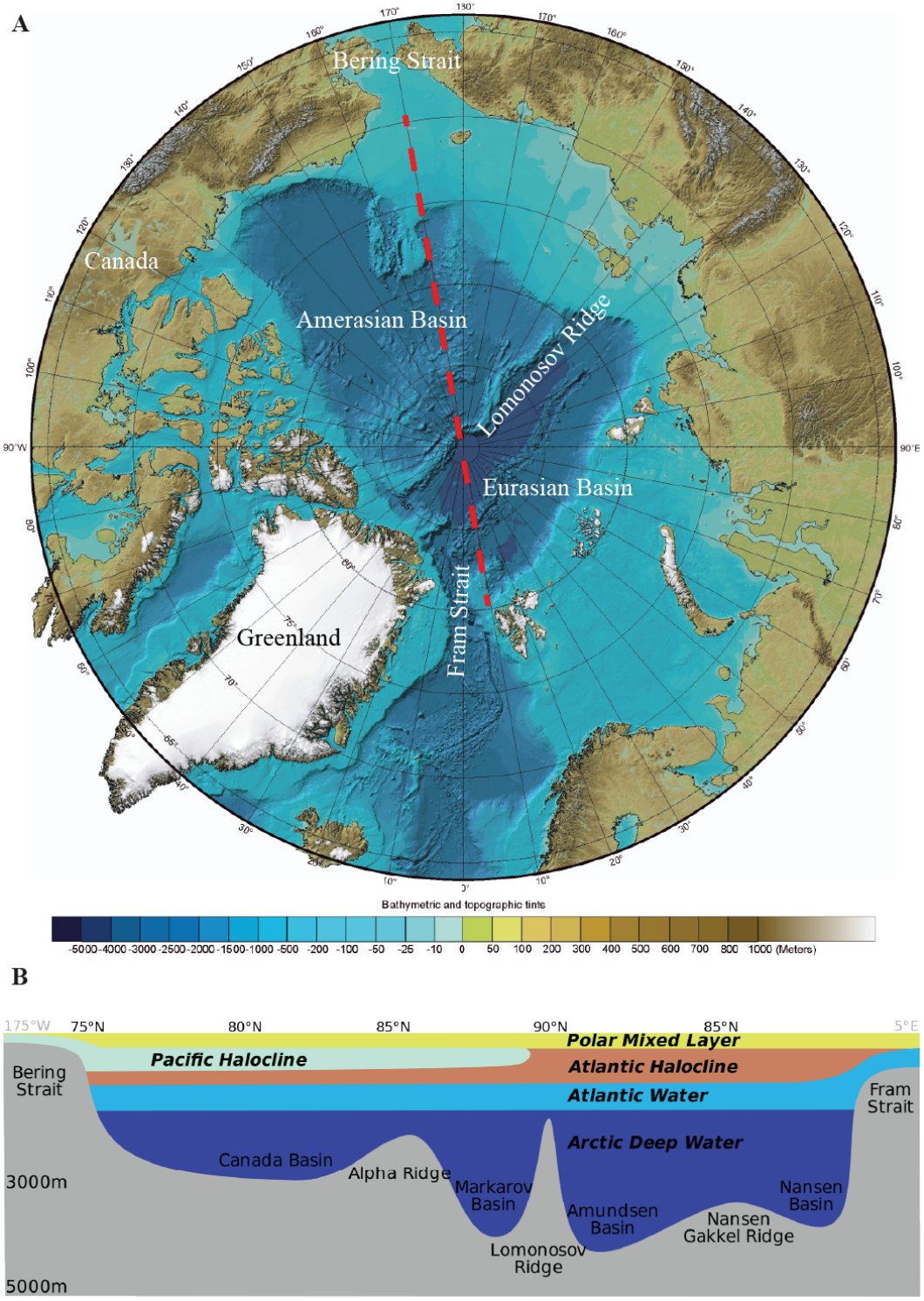

Figure 1.1: (**A**) Map of the Arctic Ocean seafloor features. Modified from: www.ngdc.noaa.gov/mgg/bathymetry/arctic/currentmap.html. The red line represent a hypothetical transect from Bering Strait to Fram Strait. (**B**) Schematic vertical distribution of the major water masses across the Arctic Ocean based on the hypothetical transect from Bering Strait to Fram Strait. Adapted from Gonçalves-Araujo (2016)

photosynthetic organisms is often limited by the availability of additional nutrients, such as nitrogen and phosphorous, which are required for the carbon fixation (Howarth, 1988). In the Arctic Ocean, primary production is also constrained by the availability of solar radiation, which is governed by the presence of sea ice (Popova *et al.*, 2012; Arrigo, 2014). Furthermore, due to the low angle of the sun, overall the Arctic Ocean receives less solar radiation and has a lower annual primary production compared with other oceanic regions (Lee *et al.*, 2015).

The primary production rates in the Arctic Ocean differ strongly between the deep central basin (i.e., central Arctic Ocean) and the continental shelves (Carmack and Wassmann, 2006). The broad shelf areas of the Arctic Ocean are seasonal sea-ice zones which receive 11% of the global river runoff and can sustain high primary productivity (Aagaard and Carmack, 1989; Tremblay and Gagnon, 2009; Carmack and Wassmann, 2006). The inflow shelves, through which nutrient rich sub-Arctic waters are entering the Arctic Ocean, are considered to be by far the most fertile regions in the Arctic Ocean (Wassmann, 2015). The central basin, on the other hand, due to high sea-ice coverage and low nutrient availability, is considered to be significantly less productive (Tremblay *et al.*, 2015; Sakshaug, 2004).

Unlike the sub-Arctic regions, the Arctic Ocean is shaped by extreme seasonality with three months a year of complete darkness (winter) and three months of permanent daylight (summer). During the dark winter time, as a result of vertical mixing and lack of active primary production, the nutrient level in the surface waters reaches its annual maximum (Codispoti *et al.*, 2013). In spring, with the increase in light availability the seasonal phytoplankton bloom begins (Leu *et al.*, 2011). There are two main sources for primary production in the Arctic Ocean, sea-ice algae and pelagic unicellular phytoplankton. Due to differences in light sensitivity, these two groups of primary producers differ in the timing of their bloom (Terrado *et al.*, 2013). The sea-ice algae are adapted to lower light conditions, and therefore able to start growing earlier in the spring (Hancke *et al.*, 2018; Arrigo, 2014). The total production of sea-ice algae is highly variable and depending on the sea-ice situation, however it is estimated between 5 and 10 g C m^{-2} yr^{-1} (Gosselin *et al.*, 1997; Leu *et al.*, 2011). The sea-ice algae contribute more than 50% of the primary production in the central Arctic Ocean, and only up to 25% of the primary production in the Arctic shelf regions (Gosselin *et al.*, 1997; Legendre *et al.*, 1992). With the increasing availability of solar radiation and due to retreating sea ice, the pelagic phytoplankton bloom usually occurs on the sea-ice edge in short massive bloom events (Arrigo *et al.*, 2012; Fernández-Méndez *et al.*, 2015), and is estimated to 12-50 g C m^{-2} yr^{-1} (Gosselin *et al.*, 1997; Leu *et al.*, 2011).

The primary production in the Arctic Ocean is carried out by unicellular eukaryotic algae, such as, diatoms, dinoflagellates and haptophytes (Poulin *et al.*, 2011; Terrado *et al.*, 2013). Overall, diatoms are considered to be the main contributors to primary production in the Arctic Ocean (Gosselin *et al.*, 1997). Diatoms are an extremely diverse taxonomic group with more than 10,000 species (Smetacek, 2000), characterized by a silicified cell wall which provides mechanical protection from grazers (Hamm *et al.*, 2003). They are unicellular organisms which may occur both as solitary cells and in colonies, ranging in size over several orders of magnitude (Smetacek, 2000). They are found in a wide range of freshwater and marine environments, and in the Arctic Ocean are present both in the water column and associated with sea ice (Arrigo, 2014). The most common pelagic diatom species in the Arctic Ocean belong to the lineages *Chaetoceros* and *Thalassiosira* (Lovejoy *et al.*, 2007a), and the most common diatoms found in

the sea ice are pennate diatoms, such as, *Nitzschia* and *Navicula* (Quillfeldt, 2005). In addition, the centric diatom *Melosira arctica* is known to form long filaments attached to the bottom of the sea ice (Boetius *et al.*, 2013).

1.1.3 Vertical export of organic matter

The oceans are the largest reservoir of carbon in the biosphere, on time scales of hundreds to thousands of years, and therefore they play a central role in the regulation of the increasing atmospheric CO_2 concentrations (Takahashi *et al.*, 2002). The Arctic Ocean is responsible for an uptake of 66-199 Tg C yr^{-1}, contributing up to 14% to the global uptake of CO_2 (Bates and Mathis, 2009). Part of the sequestered atmospheric CO_2 is due to production of organic carbon by the primary producers in the surface ocean. The vast majority of the produced organic carbon is respired, by heterotrophic organisms, back to carbon dioxide already in the surface ocean (Ducklow *et al.*, 2001). Nevertheless, up to 30% of it is exported to the deep ocean by sinking particles of organic matter (e.g., decaying phytoplankton and fecal pellets; Turner, 2002), a process also termed "the biological pump" (de La Rocha and Passow, 2003; De La Rocha and Passow, 2007). The sinking particles of organic matter (OM) which escape the photic layer of the ocean, provide the main source of food for the deep ocean biology (Ducklow *et al.*, 2001). Overall, less than 5% of the produced OM in the surface ocean are eventually reaching the seafloor (Jørgensen and Boetius, 2007).

The magnitude of the vertical export is greatly dependent on the presence of zooplankton, and microbial activity (i.e., the "microbial loop" - further discussed in section 1.2). In temperate and tropical latitudes the cycles of the phytoplankton bloom, and the zooplankton grazing, are varying within narrow limits. The relatively small community fluctuations allow strong retainment and large recycling of the produced OM in the upper part of the water column (Rivkin *et al.*, 1996; Calbert and Landry, Michael, 2004). In contrast, in the Arctic Ocean, the link between phytoplankton and grazers is less pronounced (Klein *et al.*, 2002). This results in an episodic vertical export of ungrazed OM in the beginning of the seasonal bloom (Wassmann *et al.*, 2004, 1996), especially on the Arctic Ocean shelves (Carmack and Wassmann, 2006). With increasing grazing activity throughout the season, the vertical export is declining and the ecosystem is shifting from an export food chain towards a retention food chain, at the end of the productive season (Wassmànn, 1997).

1.1.4 Climate change impacts

Global climate change is enhanced in high latitudes, resulting in a warming of the Arctic surface air at much faster rates than the global average (Dobricic *et al.*, 2016; Woodgate *et al.*, 2012). Combined with the increase of Atlantic heat flux into the Arctic Ocean (also termed "Atlantification"; Polyakov *et al.*, 2017), this causes strong reduction in sea-ice coverage and thickness (Peng and Meier, 2017; Kwok and Rothrock, 2009; Notz and Stroeve, 2016), at unprecedented rates over at least the last few thousand years (Polyak *et al.*, 2010; Kinnard *et al.*, 2011). With continuous anthropogenic release of CO_2, current projections suggest that the Arctic Ocean may experience sea-ice free summers already in the second half of this century (Overland and Wang, 2013). In addition to the significant sea-ice loss, Arctic surface waters are also getting warmer

(Steele and Dickinson, 2016) and fresher (Carmack *et al.*, 2016). All these phenomena are interconnected in a positive feedback process termed "Arctic amplification" (Serreze and Barry, 2011).

The decreasing coverage of sea ice, its thinning and early melting, results in higher light transmission into the water column (Arrigo *et al.*, 2008). Furthermore, increasing atmospheric CO_2 concentrations enhance the absorption of CO_2 in the seawater, causing a more pronounced acidification than in any other ocean (Steinacher *et al.*, 2009; Bates and Mathis, 2009; Popova *et al.*, 2014). These abiotic changes are clearly impacting the primary production under the sea ice and in the water column (Arrigo and van Dijken, 2015). Based on the predicted changes, there are environmental factors that may enhance the primary production, such as, higher light availability due to sea ice melt, and higher nutrient availability on the Arctic shelves, as a result of stronger discharge from rivers (Arrigo *et al.*, 2008). However, on the other hand, there are also environmental changes which may diminish the primary production, such as, stronger water column stratification as a result of sea ice melt, and lower light availability due to higher cloudiness (warmer temperatures will increase evaporation and cloud formation; Bélanger *et al.*, 2013). Thus, the direction, and the magnitude, of climate change impact on the total primary production in the Arctic Ocean is still heavily debated.

Not only a change in total primary production is expected. Numerous evidence for shifts in composition of the Arctic phytoplankton community towards very small (<2 μm diameter) phytoplankton groups, such as, *Prasinophytes* (Degerlund and Eilertsen, 2010; Metfies *et al.*, 2016; Li *et al.*, 2009). These small nanoflagellates are considered to be one of the main phytoplankton taxa impacting the biogeochemical cycles on a global scale (Schoemann *et al.*, 2005). Unlike diatoms which produce heavy silicate rich cells, the *Prasinophytes* form almost buoyant gelatinous colonies with very low sinking rates (Smetacek and Nicol, 2005; Wolf *et al.*, 2016). Longer retainment in the surface ocean allows higher recycling of the OM in the upper water column. Therefore, integrated estimates suggest that *Prasinophytes* contribute less than 5% to the vertical export in the Arctic Ocean (Reigstad and Wassmann, 2007). Thus, further shifts in the Arctic phytoplankton community from diatom- to flagellate- dominated communities will strongly impact the vertical export of OM to the deep ocean.

As primary production is the basis of the food web, its further alterations are most likely to cascade through the entire Arctic ecosystem (Leu *et al.*, 2011; Sakshaug, 2004). There are well documented ecological changes in larger organisms (Post *et al.*, 2009), such as, stronger mismatch between the phytoplankton bloom and the reproduction cycle of Arctic copepods (e.g., Leu *et al.*, 2011; Søreide *et al.*, 2010; Weydmann *et al.*, 2012), as well as, further migration northwards of the Atlantic cod (e.g., Drinkwater, 2005; McBride *et al.*, 2014; Hollowed *et al.*, 2013; Ingvaldsen *et al.*, 2017). On contrary, the ongoing changes in the microbial communities, and specifically the bacterial and archaeal communities, remain largely understudied. Nevertheless, the existing evidence suggests that these communities are also likely to be affected by the changing conditions (Piontek *et al.*, 2015; Brussaard *et al.*, 2013; Sala *et al.*, 2010; Kritzberg *et al.*, 2010).

1.2 Ecology of bacterial and archaeal communities in the Arctic Ocean

Microorganisms perform key functions in the oceanic biogeochemical cycles by mediating the fluxes of matter, and energy, through the ecosystem (Azam and Malfatti, 2007). A large fraction of the primary production in the ocean becomes dissolved in the water column (i.e., dissolved organic matter - DOM) and is almost exclusively accessible to heterotrophic bacteria and archaea (Thornton, 2014; Sarmento and Gasol, 2012). Heterotrophic microorganisms also utilize a significant fraction of the OM found in marine particles (i.e., particulate organic matter- POM) by enzymatic “digestion” (Biddanda and Benner, 1997; Arnosti *et al.*, 2011). As a result, a large fraction of the oceanic primary production is consumed by heterotrophic microorganisms, which has a strong impact on the global elemental cycle (Azam, 1998). The consumed OM is either directly respired to CO_2 or converted into biomass which is then channeled into the "microbial loop" (Azam *et al.*, 1983).

1.2.1 Microbial heterotrophic activity

The term "microbial loop" refers to a complex microbial food web of production and decomposition, based on the uptake and metabolism of DOM (Azam *et al.*, 1983). In the global ocean, heterotrophic bacteria are responsible for almost half of the community respiration, making them the main heterotrophic microoganisms involved in OM turnover (Robinson, 2008). Bacterial productivity is the key pathway which "fuels" the flux of OM through the loop, and therefore is an important proxy for microbial activity in the water column (Ducklow, 2002). The estimated bacterial productivity, in different seasons and regions of the Arctic Ocean, ranges over two orders of magnitude between 0.1 to 11 μg C l^{-1} day^{-1} (Kritzberg *et al.*, 2010; Sherr and Sherr, 2003; Sherr *et al.*, 2003; Malmstrom *et al.*, 2007; Nikrad *et al.*, 2012; Nguyen *et al.*, 2012; Kirchman *et al.*, 2009). These values are following the seasonal pattern of the primary production (Nikrad *et al.*, 2012; Nguyen *et al.*, 2012), and are in the same range with other oceanic regions (Rich *et al.*, 1997).

An additional way to observe microbial activity in the water column is through cell density dynamics (Ducklow, 2002). Similar to the bacterial productivity measurements, the cell densities in the Arctic Ocean show strong seasonal differences. Bacterial and archaeal cell densities in the surface waters of the Arctic Ocean are estimated in the range of 10^5 cells ml^{-1} in winter, and up to 10^8 cells ml^{-1} in summer (Sala *et al.*, 2010; Sherr *et al.*, 2003; Alonso-Sáez *et al.*, 2008; Kirchman *et al.*, 2007), which is similar to cell densities in other oceanic regions (Morris *et al.*, 2002; Sunagawa *et al.*, 2015). Interestingly, the proportion of *Archaea* in the community increases with depth (Kirchman *et al.*, 2007) and in winter (Alonso-Sáez *et al.*, 2008). Although very little is known regarding their role in the Arctic Ocean water column, these patterns suggest that *Archaea* may play an important role in the Arctic marine ecosystem.

1.2.2 Pelagic bacterial and archaeal diversity

In recent years, there were major efforts to survey the diversity of pelagic bacterial and archaeal communities in surface (e.g., TARA Oceans; Sunagawa *et al.*, 2015) and deep (e.g., Malaspina; Salazar *et al.*, 2016) waters of the global ocean, using molecular approaches. However, due to the harsh climatic conditions and the logistical challenge, no pan-Arctic surveys of pelagic *Bacteria* and *Archaea* have been done. A synthesis of the few existing regional diversity studies show that bacterial and archaeal communities are shaped by the hydrography of the Arctic Ocean, with distinct communities in surface and deep waters.

Surface waters communities exhibit a strong seasonality in their composition. During summer they are dominated by phytoplankton-bloom associated bacteria, such as, *Flavobacteria* and *Gammaproteobacteria*. In winter there is a strong increase in bacterial and archaeal diversity (Ladau *et al.*, 2013), and the community is dominated by oligotrophic taxonomic groups, such as, the SAR11 clade (*Alphaproteobacteria*; Wilson *et al.*, 2017). On contrary, deep waters communities show relatively small seasonal variation. These communities are dominated by poorly characterized taxonomic groups, such as, SAR202 clade and *Marinimicrobia* (Galand *et al.*, 2010; Ghiglione *et al.*, 2012), and to some extent resemble the surface winter communities (Wilson *et al.*, 2017). *Archaea* are present throughout the entire water column, especially the *Thaumarchaeota*, and comprise a significant fraction of the community in winter (Müller *et al.*, 2018). Below, is a brief review of the current state of knowledge on the diversity, biogeography, and potential functions of key taxonomic groups of Arctic pelagic microbial communities:

- **SAR11 clade** - of the *Alphaproteobacteria* is considered to be the most abundant bacterial lineage in the global ocean (Morris *et al.*, 2002). All members of the SAR11 clade are small, mostly free-living, aerobic chemoheterotrophs (Giovannoni, 2017). Their highly streamlined genomes minimize their nutrient requirement, which potentially explain their ecological success in the oligotrophic waters of the open ocean (Giovannoni *et al.*, 2014; Giovannoni, 2017). The diversity within the SAR11 clade often described by nine ecotypes, which were defined based on genomic phylogeny and spatiotemporal distribution (Vergin *et al.*, 2012; Brown *et al.*, 2012). Interestingly, the SAR11 surface-ocean 1a ecotype can be further divided into cold-water (1a.1) and warm-water (1a.3) subgroups, which have distinct latitudinal distribution (Brown *et al.*, 2012). In various molecular observations of the Arctic Ocean, the SAR11 clade comprised up to 30% of the sequences in the community and was present in the water column down to 1000 m (Alonso-Sáez *et al.*, 2008; Ghiglione *et al.*, 2012; Balmonte *et al.*, 2018; Wilson *et al.*, 2017).

- **Flavobacteria** - are one of the most abundant bacterial taxa in the surface waters of the Arctic Ocean (Wilson *et al.*, 2017; Ghiglione *et al.*, 2012; Balmonte *et al.*, 2018). Microscopic counts which targeted the broad flavobacterial genus *Polaribacter*, using fluorescent in-situ hybridization (FISH), revealed that this taxonomic group may reach up to 10% of summer bacterial communities in Arctic waters (Malmstrom *et al.*, 2007). Furthermore, *Flavobacteria* were identified to prevail in sea ice, where they comprise around 20% of the bacterial community (Rapp *et al.*, 2018; Boetius *et al.*, 2015; Bowman *et al.*, 2012; Brinkmeyer *et al.*, 2003). Interestingly, *Flavobacteria* have been identified to exhibit strong biogeographical partitioning both in the Southern Ocean and the North Atlantic Ocean. This has been suggested to be associated with niche separation between various clades

of this taxonomic group (Abell and Bowman, 2005; Gómez-Pereira *et al.*, 2010). The *Flavobacteria* can be found both free-living and associated with particles, and are one of the main groups responding to phytoplankton blooms in high-latitudes (Alderkamp *et al.*, 2006; Pinhassi and Hagström, 2000; Pinhassi *et al.*, 2004; Chafee *et al.*, 2018). They possess a large arsenal of hydrolytic enzymes which enable them to degrade and assimilate a wide variety of organic biopolymers (Williams *et al.*, 2013; Teeling *et al.*, 2012), making them important in remineralization of primary production products (Buchan *et al.*, 2014).

- **Gammaproteobacteria** - are one of the most abundant bacterial taxa throughout the entire water column of the Arctic Ocean, accounting for up to 30% of the bacterial community sequences (Kirchman *et al.*, 2010; Wilson *et al.*, 2017; Ghiglione *et al.*, 2012; Balmonte *et al.*, 2018). These organisms can be found both free-living and particle-associated, they possess a large enzymatic arsenal that allow them rapid adaption to a wide range of carbon sources (Buchan *et al.*, 2014). In polar regions, similar to *Flavobacteria*, the *Gammaproteobacteria* exhibit strong variability in cell densities and community composition, following the seasonal phytoplankton bloom (Wilson *et al.*, 2017; Williams *et al.*, 2012; Alonso-Sáez *et al.*, 2008). Seasonal metaproteomic analysis in Antarctic coastal waters revealed that diverse lineages of *Gammaproteobacteria* significantly increased their activity during summer in comparison to winter (e.g., *Alteromonadales* proportion increase from 1% in winter to 13% in summer; Williams *et al.*, 2012). Furthermore, *Gammaproteobacteria* are also one of the dominant taxonomic groups in sea ice (Rapp *et al.*, 2018; Bowman *et al.*, 2012; Boetius *et al.*, 2015). It has been suggested that the ecological success of *Flavobacteria* and *Gammaproteobacteria* in sea ice is related to their enzymatic potential to exploit the high concentrations of exopolymeric substances (EPS) and DOM that are produced by sea-ice algae (Grossmann and Dieckmann, 1994; Aslam *et al.*, 2012; Boetius *et al.*, 2015).

- **Verrucomicrobia** - are a widespread minority phylum found in various marine environments (Freitas *et al.*, 2012). Analyses of phenotypic, and genomic traits of a single *Verrucomicrobia* isolate strain revealed their specific adaptation to utilization of glycopolymers (Alonso-Sáez *et al.*, 2015; Spring *et al.*, 2016). Furthermore, this phylum has been identified as the most active polysaccharide degrading taxa in the waters of Smeerenburgfjord (Svalbard; Cardman *et al.*, 2014). In general, little is known regarding their ecological role, but there is increasing evidence for their potential importance in marine biogeochemical cycles.

- **Deltaproteobacteria** - have been identified as the second most abundant taxonomic group in deep waters of the Arctic Ocean (Galand *et al.*, 2010; Wilson *et al.*, 2017). They have been also found to comprise up to 10% of the sequences in surface communities during winter (Wilson *et al.*, 2017). Taxonomically, the majority of the *Deltaproteobacteria* sequences were associated with the SAR324 clade.Although, very little is known regarding this taxonomic clade, there are genomic evidences that link them to sulfur oxidation, as well as, oxidation of methylated compounds (Swan *et al.*, 2011). Thus, suggesting that they may play an important role in chemoautotrophic processed in the Arctic Ocean.

- **SAR202 clade** - of the class *Dehalococcoidia* is among the most dominant taxonomic groups in the meso- and bathy- pelagic waters of the global ocean (Salazar *et al.*, 2016), where they account for ∼10% of the cells in microbial communities (Morris *et al.*, 2004). In the

Arctic Ocean this group was one of the dominant members of deep water communities (Galand *et al.*, 2010; Bano and Hollibaugh, 2002). However, they also comprised a significant proportion of sequences in the upper part of the water column in winter (Wilson *et al.*, 2017). The ecological niche occupied by SAR202 clade is still not fully understood, but there is evidence for their potential role in the remineralization of recalcitrant OM in the deep ocean (Landry *et al.*, 2017; Colatriano *et al.*, 2018).

- **Marinimicrobia (SAR406 clade)** - were among the first bacterial groups detected in the deep ocean (Fuhrman *et al.*, 1993), and are found to be abundant in meso- and bathypelagic waters of the global ocean (Salazar *et al.*, 2016). They have higher abundance at low oxygen concentrations (Hawley *et al.*, 2017), and they were found to be especially abundant in oceanic oxygen minimum zones (Bertagnolli *et al.*, 2017). This taxonomic group comprised 9% of the 16S rRNA sequences in deep waters of the Arctic Ocean (Galand *et al.*, 2010), and also identified in surface waters during winter (Wilson *et al.*, 2017). Genomic observations of this taxonomic group linked it to sulfur cycling via a polysulfide reductase gene cluster (Wright *et al.*, 2014; Allers *et al.*, 2013), and to the nitrogen cycle via expression of a nitrous oxide reductase (Hawley *et al.*, 2017). Furthermore, it has been shown in a methanogenic bioreactor study that *Marinimicrobia* participate in a syntrophic interaction with metabolic partners to accomplish degradation of amino acids (Nobu *et al.*, 2015). Altogether, these traits suggest their potential importance in biogeochemical cycles of the deep ocean.
- **Thaumarchaeota** - often addressed as the ammonia-oxidizing archaea (AOA), are the most abundant pelagic archaeal group in both the surface and the deep ocean (Sunagawa *et al.*, 2015; Salazar *et al.*, 2016). They consist of several phylogenetic clades which are distributed through different water layers of the water column, with a general increase in abundance with depth. It has been shown that in mesopelagic waters (1000 m) of the Arctic Ocean, the *Thaumarchaeota* may comprise up to 25% of microbial community sequences (Wilson *et al.*, 2017; Müller *et al.*, 2018). In the surface waters of polar oceans they exhibit seasonal patterns with an increase in relative abundance during winter and a decline in summer (Alonso-Sáez *et al.*, 2008; Grzymski *et al.*, 2012). This seasonality was previously linked to the photoinhibition of ammonia oxidation (Merbt *et al.*, 2012), or potentially to a stronger competition for nutrients with phytoplankton during summer (Connelly *et al.*, 2014; Kirchman *et al.*, 2007).

1.3 Observing ecological changes in the Arctic Ocean

Since the beginning of the 20th century, oceanographers have recognized the need for extended sampling periods to monitor and understand processes that occur in the ocean ecosystem. The longest record of sustained oceanographic observations is obtained by the Continuous Plankton Recorder (CPR) which goes back to 1931 (Reid *et al.*, 2003). In 1988, as part of the Joint Global Ocean Flux Study (JGOFS), a new era of long-term observatories emerged, with the establishment of two major oceanographic time series programmes: the Hawaii Ocean Time-series in the Pacific Ocean (HOT; Karl and Church, 2014) and the Bermuda Atlantic Time-series Study in the Atlantic Ocean (BATS; Morris *et al.*, 2005). These Long-Term Ecological Research (LTER) obser-

vatories made a great contribution to our current understanding of the marine biogeochemistry, the biological pump (Karl *et al.*, 2001; Steinberg *et al.*, 2001), and the key role of microorganisms in them (Karl and Church, 2014). Furthermore, these long-term observatories provided a platform to observe impacts of climate change impact on the marine ecosystem (Ducklow *et al.*, 2009). As the value of such studies has become clear through the datasets produced at HOT and BATS, the number of oceanographic observatories has continued to grow. To date, there are more than 50 oceanographic observatories around the world. Among them the LTER observatory HAUSGARTEN in the Fram Strait, which is the only open ocean long-term observatory in the Arctic Ocean (Soltwedel *et al.*, 2005).

1.3.1 The Fram Strait and the LTER observatory HAUSGARTEN

The 450 km wide Fram Strait separates Northeast Greenland from the Svalbard Archipelago, and is the only deep gateway to the Arctic Ocean (sill depth of ~2600 m; Hop *et al.*, 2006). The exchange of water in the Fram Strait occurs in both directions, by two major opposing current systems, which generate distinct physical and chemical conditions between the eastern and western parts of the Strait (Figure 1.2).

The Atlantic inflow occurs through the West Spitsbergen Current (WSC) that flows above the eastern shelf slope of Fram Strait. It carries the relatively warm, and saline AW northward into the Central Arctic (Beszczynska-Moller *et al.*, 2012). Oceanographic time-series of the WSC reveals a positive linear trend of temperature, with an annual increase of 0.06°C in the upper 400 m of the water column, and an increase of 0.015°C at depth of 1000 m (Walczowski *et al.*, 2017). The Atlantic inflow through the Strait provides the largest input of heat into the Arctic Ocean, sufficient to melt its entire sea-ice cover (Østerhus *et al.*, 2005). Thus, the mass and the heat exchange through the Fram Strait have a strong impact on the entire Arctic region.

In the western Fram Strait, the East Greenland Current (EGC) carries cold polar water and sea ice into the North Atlantic (de Steur *et al.*, 2009). The exported freshwater and sea ice through EGC comprise roughly half of the total freshwater flux from the Arctic Ocean (Serreze *et al.*, 2006). While the freshwater outflow through Fram Strait may vary from year to year (due to an alternative exit through Bering Strait; Rabe *et al.*, 2009), almost the entire sea-ice flux from the Arctic Ocean is exported by EGC (Kwok, 2009). The area of the exported sea ice increases with a trend of 10% per decade since 1990 (Renner *et al.*, 2014). However, this positive trend is compensated by continuous thinning of the sea ice, and the total annually exported volume of sea ice does not show a significant increase (Zamani *et al.*, 2018). These observations suggest that the exported sea ice through the Fram Strait is changing, from a thicker old sea ice to thinner and younger sea ice.

The deep-sea LTER observatory HAUSGARTEN was established in 1999 by the Alfred Wegener Institute, Helmholtz-Center for Polar and Marine Research (AWI). It is located in a highly productive transitional area between sea-ice covered and sea-ice free regimes of the Fram Strait (i.e., marginal ice zone; Smith Jr *et al.*, 1987). The observatory consists of 21 permanent stations which are sampled repeatedly in annual summer expeditions since 1999, and includes monitoring the diversity of all faunal size classes, as well as, biogeochemical measurements (e.g., chlorophyll *a* and nutrient concentrations). The observations are complemented by continu-

ous year-round oceanographic measurements collected by autonomous instruments mounted on moorings (Soltwedel *et al.*, 2005). The observatory covers continental shelves with water depths of few hundred meters down to the deepest point of the Arctic Ocean - the Molloy Deep, at around 5600 m water depth. The stations array covers both the typically sea-ice covered area in the Arctic outflow (EGC), and the seasonally sea-ice covered area in the Atlantic inflow (WSC) (Soltwedel *et al.*, 2005). These distinct conditions between the current systems provide a valuable opportunity for studying ecological processes across strong gradients of temperature, and ice cover, in the deep water column and on the shallow continental shelves. Moreover, a comparison between the increasing Atlantic inflow in the east and the Arctic outflow in the west, allows the investigation of ongoing changes in the Arctic marine ecosystem. Throughout the years, the time-series at HAUSGARTEN observatory produced important insights into ecological processes, and temporal variability (Soltwedel *et al.*, 2016).

A comparison between the observations in the distinct pelagic regimes (EGC and WSC) revealed higher chlorophyll *a* concentration in the sea-ice free WSC (Nöthig *et al.*, 2015). There was no direct correlation identified between the chlorophyll *a* and the sea-ice concentration. However, as a result of sea-ice melt and solar radiation, the vertical stratification of the surface waters have shown to promote a higher phytoplankton growth (Cherkasheva *et al.*, 2014). There was also a clear difference in the phytoplankton community composition between the regimes, with a predominance of diatoms in the EGC and a mixed community of haptophytes, dinoflagellates and diatoms in the WSC (Nöthig *et al.*, 2015; Engel *et al.*, 2017). The heterotrophic bacterial communities also showed strong differences between the regimes, with cell densities in the range of 10^4-10^5 cells ml^{-1} in the EGC, and in the range of 10^6 cells ml^{-1} in the WSC. Bacterial productivity and cell-specific enzymatic activity showed strong differences between the regions as well, with higher values in the EGC, where the OM was enriched in combined carbohydrates (Piontek *et al.*, 2014). Showing that bacterial growth and degradation activity in WSC and EGC are regulated not only by the different physicochemical conditions, but also by the compositional differences in OM. To date, almost nothing was known about the bacterial diversity in the distinct pelagic regimes. The results of this thesis provide the first taxonomic comparison of these communities across the Fram Strait.

1.3.2 Ecological alterations in the Fram Strait as a result of a Warm-Water Anomaly

The oceanographic observations at the HAUSGARTEN observatory have captured an AW warm pulse between 2004 and 2007 (i.e., Warm-Water Anomaly), with temperature anomalies of up to 1°C along the AW inflow pathway (Beszczynska-Moller *et al.*, 2012). The ecological impact during the anomaly has been visible through the entire marine ecosystem of the Fram Strait. From a higher chlorophyll *a* concentrations in surface waters (Cherkasheva *et al.*, 2014), over a lower vertical export of POM (Lalande *et al.*, 2013), to a sharp change in the phytodetritus concentrations at the seafloor (Soltwedel *et al.*, 2016). While some of the monitored variables of the ecosystem returned to their previous state (e.g., benthic bacterial communities; Jacob, 2014), for others the original conditions have not been restored. One of the major changes in the pelagic ecosystem, which has remained after the end of the anomaly, is a shift from a diatom- to a flagellate- dominated phytoplankton community in the WSC (Metfies *et al.*, 2016;

Nöthig *et al.*, 2015; Lasternas and Agustí, 2010; Engel *et al.*, 2017). Aggregates formed by small flagellates, such as the haptophyte *Phaeocystis* spp., are more buoyant and sink slower in comparison to diatom aggregates. The longer retainment of the aggregates in the surface ocean allows stronger recycling in the upper water column (Lalande *et al.*, 2013).

Such a fundamental change in the nature of the OM and its vertical distribution, may have a strong impact on future carbon cycling processes, from the surface down to the seafloor (Vernet *et al.*, 2017). However, it is important to note that natural temporal variations of marine ecosystems may occur across a wide range of timescales from diurnal to decadal dynamics (e.g., Gilbert *et al.*, 2012; Fuhrman *et al.*, 2015). Moreover, they may be subject to even longer global cycles, such as the El Niño-Southern Oscillation or the North Atlantic Oscillation (Ikeda, 1990; Stenseth *et al.*, 2003). Thus, it cannot be concluded with absolute confidence that the observed alterations in the Fram Strait are a result of global climate change. However, they provide an important insight into the potential future of the Arctic marine ecosystem as a result of further warming of the Arctic Ocean.

1.3.3 Ocean Observing System FRAM

The extensive knowledge acquired from 15 years of observations in the Fram Strait, strengthened the urgent need for integrative, and interdisciplinary, observations not only in the Fram Strait but also in the central Arctic Ocean. In order to do so, in 2014, the AWI and partner institutes in Europe, established the long-term Arctic open-ocean infrastructure project FRAM (FRontiers in Arctic marine Monitoring Soltwedel *et al.*, 2013). The FRAM Ocean Observing System is designed according to the extensive knowledge baseline from the HAUSGARTEN observatory, which provides the starting point for the observing system infrastructure (Figure 1.2). The main novelty of the FRAM project is the integrated observation of physical (e.g., autonomous underwater vehicles; Wulff *et al.*, 2016), chemical (e.g., autonomous benthic crawlers; Wenzhoefer *et al.*, 2016) and biological (e.g., remotely operated vehicles; Katlein *et al.*, 2017) processes, in the water column and at the seafloor, using cutting edge technologies. In order to allow a comprehensive assessment of the ecosystem responses to global change processes in the Arctic Ocean in the next 25 years.

Due to their key role in biogeochemical processes, microorganisms are of central interest within FRAM. In the HAUSGARTEN observatory, the microbial research in the water column has been focused mainly on eukaryotic biota (Soltwedel *et al.*, 2016), with very little exploratory work on *Bacteria* and *Archaea*. However, in order to better understand natural dynamics of the marine ecosystem, and have the ability to detect consequences of the environmental changes, observations of all three domains of life are required (e.g., Steele *et al.*, 2011). In the framework of FRAM, all microbial observations are integrated into a Molecular Observatory (MolObs), which aims to conduct standardized molecular-based high-resolution observations of the Arctic Ocean microbiome. The molecular sampling is conducted synchronously with other observatories within FRAM (e.g., physical oceanography and biogeochemistry), which provides a unique opportunity for monitoring microbial communities in a comprehensive environmental context.

Unfortunately, extensive microbial long-term time-series studies in the framework of oceanographic observatories are rare. Unlike other research fields of oceanographic long-term obser-

vatories (e.g., physical oceanography), microbial oceanography lacks standardization in the application of high-throughput methodologies. Microbial observations are often dedicated to a specific research questions, and specific methodologies are applied. These discrepancies between studies challenge their comparability, and their incorporation into one large mechanistic system. Thus, one of the challenges currently faced in the FRAM MolObs is the development of a standardized, sustainable, methodological workflow for conducting long-term microbial observations, which is at the same time comparable to other molecular observatories.

1.4 Thesis objectives

The Arctic Ocean is rapidly changing towards a warmer conditions that are altering the entire ecosystem. Long-term time-series, such as the LTER HAUSGARTEN observatory in the Fram Strait, are essential for the detection and understanding of large-scale environmental changes. To date, the microbial research in the water column of the Fram Strait was mainly focused on phytoplankton communities. These primary producers play the key role in the oceanic uptake of CO_2 through the fixation of inorganic carbon, and are very important for estimating carbon fluxes between the atmosphere and the ocean. The heterotrophic bacterial and archaeal communities, on the other hand, respire a large fraction of the produced organic carbon back to CO_2. They are also involved in other nutrient cycles (e.g., nitrogen cycle) that can both enhance, and limit, the primary production by phytoplankton. Thus, marine microorganisms of all three domains of life are relevant for studying Arctic marine ecosystem and its biogeochemical cycles.

The aim of this thesis was to investigate the composition and diversity, of pelagic bacterial and archaeal communities in the Fram Strait. Addressing their distribution in space, both horizontally and vertically, in relation to environmental and biological parameters. In addition, this work contributed to the establishment of baseline knowledge for long-term microbial observations in the framework of the FRAM project. The ecological objectives of the thesis were: (i) to characterize the bacterial and archaeal communities associated with the different water masses of Fram Strait, and (ii) to identify environmental factors, which drive the diversity of these communities. Specifically the thesis addressed the following questions:

- **What are the requirements for long-term microbial observations in the Arctic Ocean?** - Time-series microbial observations are of a high relevance for the assessment of the ongoing changes, not only in the Arctic ecosystem, but in the entire global ocean. The observations should include various habitats (e.g., water column and seafloor), at various geographic locations, integrated into a holistic evaluation of the ecosystem state. Such a complex task requires an establishment of a network between various long-term microbial observatories, and methodological standardization for comparability of biological, and biogeochemical observations between them. In chapter 2 we reviewed existing microbial observatories, and suggest potential directions for the establishment of communication and data flows between them.
- **Which universal primer set for the 16S rRNA gene should be implemented in Arctic Ocean bacterial observations?** - The 16S rRNA gene-based studies of the marine sediment microbiome, often use the primer set 341F/785R that targets the V3-V4 hypervariable regions of the 16S rRNA gene. In contrast, the 16S rRNA gene based studies of the

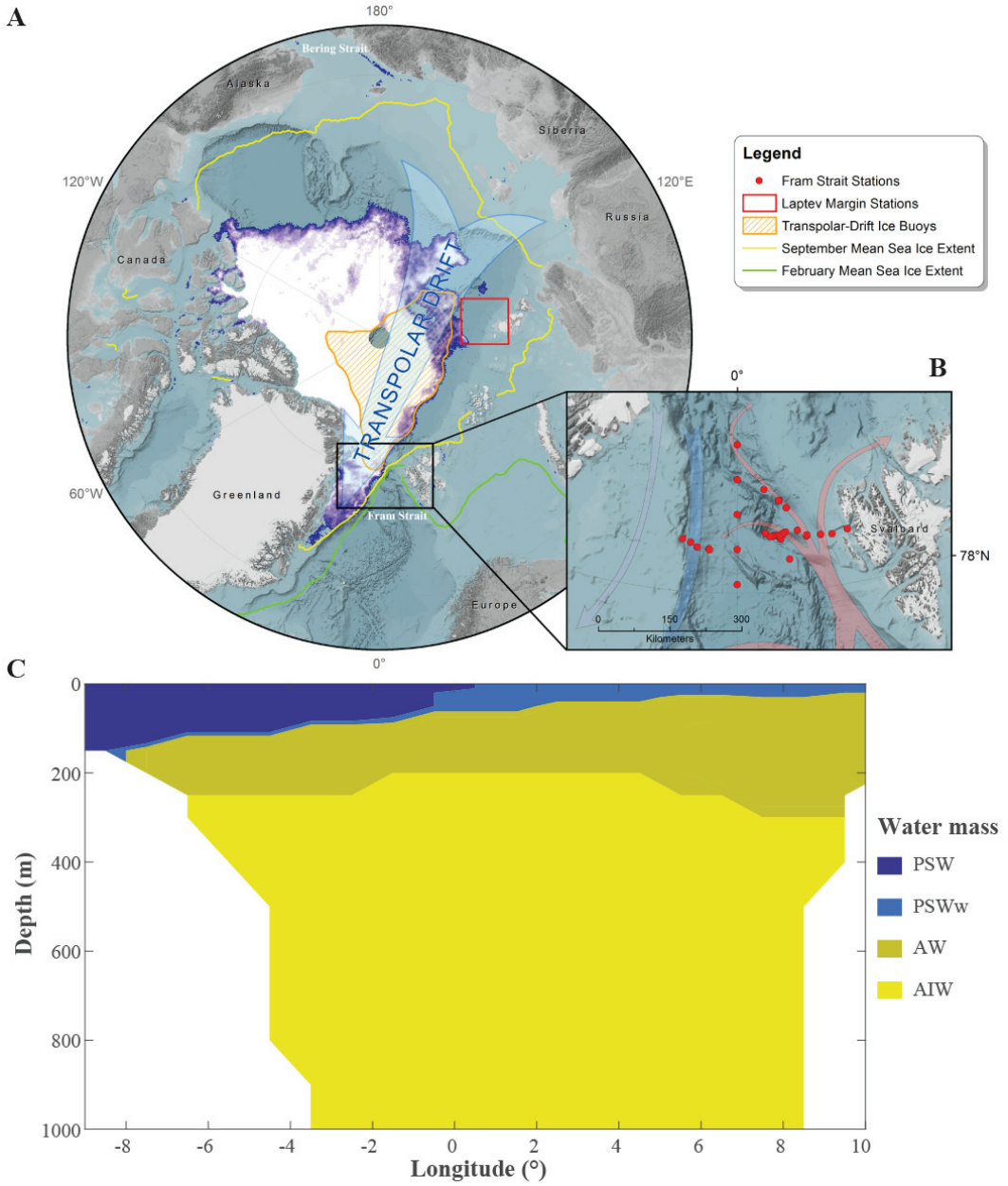

Figure 1.2: (**A**) Map of the FRAM infrastructure in the Arctic Ocean. The extremely low sea ice extent in September 2012 is shown as a white/blue area. (**B**) The section map represents the Fram Strait. The HAUSGARTEN observatory stations are shown by red dots, blue arrows indicate the EGC and the red arrows indicate the WSC. Map: AWI/ Laura Hehemann, Ingo Schewe. (**C**) A section across the Fram Strait at 79°N. The different colours represent the distinct water masses in the upper 1000 m of the water column. The Polar Surface Water (PSW), which are carried by the EGC, are originating in the Polar Mixed Layer and the Arctic halocline. The Atlantic Water (AW) are carried by the WSC. The Warm Surface Water (PSWw) are representing the sea-ice melting water, and the Arctic Intermediate Water (AIW) represent the mesopelagic water layer in the Arctic Ocean. The water masses were identified using PHC3.0 (updated from Steele *et al.*, 2001) annual temperature, salinity and density values, based on definitions in Rudels *et al.* (2005). Map: AWI/ Claudia Wekerle.

pelagic microbiome often implement the primer set 515F-Y/926R that targets the V4-V5 hypervariable regions of the 16S rRNA gene. In the framework of the FRAM MolObs, we aim to integrate microbial observations from the different habitats (water column and sediment) into one holistic ecosystem observation. Such integration requires methodological standardization between the sampling and analysis procedures of the different habitats. The methodological comparison of the different primer sets in chapter 3, will allow the selection of a single primer set for future standardized observations of bacterial communities in the Arctic marine ecosystem.

- **Which environmental parameters shape summer pelagic bacterial diversity in the photic layer of the Fram Strait?** - Temperature has been identified as the main driver of the microbial diversity in the surface waters of the global ocean. It has also been shown that light driven phytoplankton blooms have a strong impact on the associated bacterial diversity. In the Fram Strait, there is a strong temperature gradient across the EGC and WSC waters, ranging between -1°C and +8°C, respectively. Due to the distinct sea-ice conditions this temperature gradient is also coupled with strong differences in light penetration through the water column, which may have an impact on the phytoplankton bloom. This, suggests that bacterial diversity in the Fram Strait might be driven by both temperature and differences in sea ice cover. However, previous observations of bacterial activity in the Fram Strait revealed stronger correlation with phytoplankton bloom conditions, rather than physical characteristics of the water masses. Thus, the bacterial community is expected to exhibit stronger dissimilarity across the Fram Strait as a result of different sea-ice regimes, associated with different phytoplankton bloom conditions. Addressed in chapter 4.
- **How do sea-ice conditions affect the vertical connectivity between surface and deep ocean microbial communities?** - The OM produced by phytoplankton is exported to the deep ocean through sinking aggregates. It has been shown that these sinking aggregates may provide a connectivity vector between surface and deep ocean microbial communities. Sea ice plays a key role in regulating the primary production in the Arctic marine ecosystem. Furthermore, sea-ice covered and sea-ice free waters are characterized by different phytoplankton communities, which have different sinking velocities to the deep ocean. Thus, fast sinking diatom aggregates in sea-ice covered regions are expected to provide a stronger vertical connectivity between surface and deep ocean microbial communities. Addressed in chapter 5.

1.5 Publication outline

Chapter 2 - Marine Microbes in 4D – Using time series observation to assess the dynamics of the ocean microbiome and its links to ocean health

Pier Luigi Buttigieg, Eduard Fadeev, Christina Bienhold, Laura Hehemann, Pierre Offre and Antje Boetius

Current Opinion in Microbiology 43, 169–185. doi:10.1016/j.mib.2018.01.015

The review publication underlines the relevance of microbial observations in the marine environment for scientific and societal concerns, such as, ocean productivity, harmful algal blooms, and pathogen exposure. It provides a first comprehensive overview of the currently existing long-term microbial observatories around the world, and stresses the urgent need for the establishment of a network between them. Such a community network will provide an opportunity for data sharing and methodological standardization, and will allow to monitor shared environmental variables for an estimation of the global ocean state and health. Furthermore, the publication provides examples from existing community networks from other research fields, and makes suggestion for initial steps towards such a network through existing infrastructures.

Data synthesis and communication with coordinators of time-series projects was conducted by EF. The overview of the long-term observatories was conducted by EF and LH. The manuscript was written by PB and AB, with contribution from CB, PO, EF and LH.

Chapter 3 - Primer selection for Arctic Ocean microbiome studies - a taxonomic resolution trade off

Eduard Fadeev, Verena Carvalho, Massimiliano Molari, Magda Cardozo Mino, Josephine Z Rapp and Antje Boetius

This chapter is in preparation for a submission to F1000Research journal.

This study was conducted in the framework of FRAM MolObs development of ”best practices” for microbial monitoring in the Arctic Ocean. It also contributes to the methodology standardization of the Integrated Atlantic Ocean Observing Systems project (AtlantOS) . The study compared two 16S rRNA gene primer sets that are often applied in studies of marine bacterial communities. The performance of the primer sets was assessed on various marine samples (sea ice, surface and deep seawater, and seafloor sediment), from both the Fram Strait and central Arctic, in order to select the best suited primer set for long-term monitoring.

The study was designed and conducted by EF and AB. Samples included in the study were collected and processed by EF, MM and JR. M-CM and VC conducted the microscopy counting. EF conducted the data analysis and wrote the manuscript. All co-authors contributed to the manuscript preparation.

Chapter 4 - Microbial communities in the East and West Fram Strait during sea-ice melting season

Eduard Fadeev, Ian Salter, Vibe Schourup-Kristensen, Eva-Maria Nöthig, Katja Metfies, Anja Engel, Judith Piontek, Antje Boetius and Christina Bienhold

This chapter was accepted as an original research article to Front. Mar. Sci. - Marine Ecosystem Ecology.

This study focused on the spatial dynamics of the microbial communities in the photic layer of the Fram Strait, and their association with different ecosystem states in ice-free and

ice-covered regions. Using a combination of in-situ measured biogeochemical parameters and modeled data, we identified two ecological states in different parts of the Fram Strait: early bloom conditions in the ice-covered region, and late bloom conditions in the ice-free region. Using 16S rRNA gene and 18S rRNA gene sequencing we analyzed the composition and the diversity of microbial communities in each region, and statistically identified environmental factors which potentially affect these communities. We observed that bacterial diversity correlates with environmental factors that are associated with the distinct phytoplankton bloom conditions. Then, in order to identify potential associations between bacterial and phytoplankton microorganisms, we have conducted a co-occurrence network analysis between the bacterial and the microbial eukaryotes communities.

EF, CB, IS and AB designed and conducted the study. IS and KM collected the samples and provided the sequence data for the study. AE and JP provided the cell counts and bacterial productivity data. EN conducted the biogeochemical measurements. VK provided the modeled chl a estimates. EF conducted the data analysis and wrote the manuscript with guidance from CB, AB and IS.

Chapter 5 - Arctic Ocean sea ice enhances vertical connectivity of microbial communities through sinking marine aggregates

Eduard Fadeev, Morten H. Iversen, Claudia Wekerle, Andreas Rogge, Anya M. Waite, Christina Bienhold, Ian Salter, Laura Hehemann and Antje Boetius

This chapter is in preparation for a submission to the Proceedings of the National Academy of Science (PNAS) journal.

This study focuses on the vertical connectivity of bacterial and archaeal communities in the water column of the Fram Strait, and their association with different sea-ice regimes. We characterized on board the differences in size, composition and sinking velocities between aggregates in ice-covered and ice-free regions, supported by in-situ measured size distribution throughout the entire water column. We modeled the sinking trajectories of the aggregates in different regions of the Strait using the measured on board sinking velocities. Using 16S rRNA gene sequencing we analyzed the composition and the diversity of free-living and particle-associated bacterial and archaeal communities from surface to deep waters in both regions. Finally, using Bayesian modeling we estimated potential vertical connectivity of bacterial and archaeal communities throughout the water column. Revealing strong vertical connectivity between surface and deep ocean microbial communities in ice-covered waters.

EF, CB, IS and AB designed and conducted the study. MI conducted the sampling and on-board measurements of the marine aggregates. CW conducted the modeling of the sinking trajectories. AR and AW provided the in-situ particles size distribution. EF conducted data analysis and wrote the manuscript with guidance from MI, CB, AB and IS.

Chapter 2

Marine Microbes in 4D – Using time series observation to assess the dynamics of the ocean microbiome and its links to ocean health

Pier Luigi Buttigieg[1,2], Eduard Fadeev[1,2], Christina Bienhold[1,2], Laura Hehemann[1], Pierre Offre[3] and Antje Boetius[1,2,4]

[1] Alfred Wegener Institute for Polar and Marine Research, Bremerhaven, Germany

[2] Max Planck Institute for Marine Microbiology, Bremen, Germany

[3] NIOZ Royal Netherlands Institute for Sea Research, Department of Marine Microbiology and Biogeochemistry, and Utrecht University, Texel, The Netherlands

[4] MARUM - Center for Marine Environmental Sciences, University of Bremen, Bremen, Germany

This chapter was previously published in Buttigieg *et al.* (2018).

2.1 Abstract

Microbial observation is of high relevance in assessing marine phenomena of scientific and societal concern such as, ocean productivity, harmful algal blooms, and pathogen exposure. However, we have yet to realise its potential to coherently and comprehensively report on global ocean status. The ability of satellites to monitor the distribution of phytoplankton has transformed our appreciation of microbes as the foundation of key ecosystem services; however, more in-depth and localized understanding of microbial dynamics is needed to fully assess natural and anthropogenically induced variation in ocean ecosystems. While notable efforts exist, vast regions such as, the ocean depths, the open ocean, the polar oceans, and the coasts of the Indian Ocean, South Atlantic, and South West Pacific lack consistent observation. To secure a coordinated future for a global microbial observing system, existing long-term efforts must be better networked to generate shared bioindicators of the Global Oceans state and health.

2.2 Highlights

- Ocean ecosystem assessments require insight into the biosphere's microbial underpinnings
- Technologies are ripe to monitor marine microbes year-round with ocean physics and chemistry
- A global registry of marine microbial observatories with regular status updates and links to data portals is needed for higher impact
- Observatory output must be robust to rapidly developing practice and technology as well as societal challenges
- Microbial observatory data and results should be coherently linked to indicators of ocean health

2.3 Introduction

Despite decades of effort, the oceans remain strongly undersampled in space, hampering the estimation of global and regional element fluxes as well as assessments of the diversity and distribution of marine life. Well-structured and sustained temporal sampling is also limited, despite its central importance in detecting changes in ocean productivity, food webs, biodiversity, and habitat structure. Strategically distributed ocean time series are thus key to the assessment and quantification of ecosystem change, and doubly so in detecting anthropogenic impacts across decadal time scales. Unfortunately, these efforts are rare in the marine realm, follow no global strategy, and typically do not measure biological phenomena in the deep (see Table 2.1 and Smith Jr. *et al.*, 2015). The need to advance the status quo has never been more pressing: ocean ecosystems are facing rapidly warming and acidifying seas, compounded by the influence of pollutants, eutrophication, and the spread of hypoxia (Gruber, 2011). Additionally, industries such as, mineral, gas and oil extraction, tourism, international shipping, and large-scale fisheries are further impacting marine ecological assemblages and food webs at every scale (Halpern

et al., 2015; Seebens *et al.*, 2016). Microbial observation has a large role to play in monitoring the biogeochemical functioning and biotic structure of the ocean, but must transition into a spatiotemporally coherent and comprehensive activity to realise its full potential.

Taxonomically and functionally diverse assemblages of marine microbes from all three domains of life, along with their viruses, are the primary contributors to ocean productivity, biomass, and diversity. They are the core drivers of ocean biogeochemical cycles, control the emission of radiatively active gases, and constitute the foundations of many marine ecosystem services. Further, they are essential to the functioning of other trophic levels, providing animals with access to essential lipids and vitamins while supporting skin, tissue, and gut health (e.g. Bierlich *et al.*, 2017; Bik *et al.*, 2016; Apprill, 2017). These essential marine microbes - just as any other form of life - will respond to both natural and anthropogenic stressors; however, assessing how responses on the population and community level will contribute to ecosystem functions remains a challenging research target (Bourne *et al.*, 2016). Pioneering studies such as, the TARA Oceans expedition (Sunagawa *et al.*, 2015), and Ocean Sampling Day (OSD; Kopf *et al.*, 2015) have shown that the large-scale assessment of microbiome variations in space can be achieved, and their results have confirmed the need to extend observations through time. As autonomous technologies extend the spatiotemporal reach of marine sampling, archiving and measurement (Herfort *et al.*, 2016), we must establish a sustained and integrated system with which to provide novel microbiological insights into the changing state of the oceans.

In this contribution, we comment on the role of long-term microbial observatories in assessing ocean health: the degree to which the marine ecosystem provides its full range of ecosystem services in a temporally stable way when compared to past measurements or knowledge of its natural state (Halpern *et al.*, 2015). Anthropogenic activities altering the web of life in the sea can easily jeopardize the biodiversity which underpins many of these services, often indicated by a spectrum of ecological responses (see, e.g., Halpern *et al.*, 2012). We stress the value of microbial observatories as sites to develop trustworthy microbial indicators and ensure stable reporting in the face of changing technologies. Finally, we discuss the great need to rally microbial observatories towards a common goal: to provide science and society with coherent, global insight into the health and functioning of the microbially-driven ocean ecosystem.

Table 2.1: Overview of currently active long-term microbial observatories around the world. This overview table was generated based on search results in Google and Web of Science. Combinations of keywords for 'Microbial Observatory' OR 'Genomic Observatory' OR 'Long Term Ecological Research' OR 'Microbial LTER' OR 'Long Term Microbial Research' were used to initiate searches. In addition, we included (1) marine LTERs with microbial research programmes participating in LTER network initiatives (e.g. LTER and iLTER) and (2) phytoplankton monitoring observatories found using the NOAA Time Series Metabase. All information was manually collected from the website of each observatory or from direct contact with the corresponding researcher. These results are almost certainly incomplete, underscoring the need for the microbial observatory community to create a central registry to better align our collective efforts.

Labels	Observatory name	Region	Latitude (°N)	Longitude (°E)	Multiple sites?	Depths	Sampling frequency	Year of est.	Status
1	LTER HAUSGARTEN	Arctic Ocean (Fram Strait)	79	4	Yes	Epipelagic Zone (0-200m) and Benthos (sediment)	Annualy	1999	Active
2	Adventfjorden Time Series (IsA)	Arctic Ocean (West Spitsbergen)	78.26	15.53	Unknown	Unknown	Unknown	Unknown	Unknown
3	Icelandic monitoring programme	North Atlantic Ocean (Iceland)	63.33	-21.58	Yes	Unknown	Annually	1960	Active
4	Marine phytoplankton monitoring in Sweden (Svenskt HavsARKiv)	Baltic Sea	61	19	Yes	Epipelagic Zone (0-200m) and Mesopelagic Zone (200-1000m)	Monthly	1983	Active
5	Marine Scotland Science (MSS) CoastalEcosystem Monitoring Programme	Eastern North Atlantic Ocean	60.1	-1.4	Yes	Unknown	Unknown	2002	Active
6	Northern Gulf of Alaska (NGA) LTER	North Pacific Ocean	59.05	-148.7	Yes	Epipelagic Zone (0-200m)	Monthly	2017	Active
7	Linnaeus Microbial Observatory	Baltic Sea	56.91	17.05	Yes	Epipelagic Zone (0-200m)	Weekly	2011	Active

Labels	Observatory name	Region	Latitude (°N)	Longitude (°E)	Multiple sites?	Depths	Sampling frequency	Year of est.	Status
8	Cooperative Monitoring in the Baltic Marine Environment (COMBINE)	Baltic Sea	56.8	11.5	Yes	Unknown	Unknown	1992	Unknown
9	Atlantic Zone Off-Shelf Monitoring Program (AZOMP)	Western North Atlantic Ocean	55	-55	Yes (Transect)	Unknown	Annually	1998	Active
10	Helgoland Roads	North Sea (German Bight)	54.2	7.9	No	Epipelagic Zone (0-200m)	Daily	1962	Active
11	Phytoplankton Monitoring Programme of Marine Institute in Ireland	Eastern North Atlantic Ocean	52.79	-6.1	Unknown	Unknown	Unknown	1980	Active
12	UK Colne estuary microbial LTER	Eastern North Atlantic Ocean (English Channel)	51.78	0.98	Yes	Epipelagic Zone (0-200m)	Unknown	Unknown	Unknown
13	Western Channel Observatory	Eastern North Atlantic Ocean (English Channel)	50.25	-4.2	Yes	Unknown	Weekly	1988	Active
14	Line P Program	Eastern North Pacific Ocean	49	-135	Yes (Transect)	Unknown	3 cruises/yr	1950	Active
15	SOMLIT coastal network	Eastern North Atlantic Ocean (English Channel)	48.72	-3.98	Yes	Epipelagic Zone (0-200m)	Bi-weekly	1997	Active

Labels	Observatory name	Region	Latitude (°N)	Longitude (°E)	Multiple sites?	Depths	Sampling frequency	Year of est.	Status
16	VENUS Saanich Inlet cabled observatory	Eastern North Pacific Ocean (Strait of Georgia)	48.65	-123.48	Unknown	Unknown	Daily	2007	Active
17	Northwest Enhanced Moored Observatory (NEMO)	Eastern North Pacific Ocean (Strait of Juan de Fuca)	48.22	-123.41	Yes	Unknown	2 cruises/yr	2011	Active
18	JAMSTEC - K2 LTER	Western North Pacific Ocean	47	160	No	Unknown	Unknown	2010	Unknown
19	Bay of Fundy	Western North Atlantic Ocean	45.04	-66.84	Yes	Epipelagic Zone (0-200m)	Monthly	1988	Active
20	Bedford Basin Monitoring Program	Western North Atlantic Ocean	44.6	-63.6	Yes	Unknown	Weekly	1999	Active
21	Booth Bay	Western North Atlantic Ocean	43.84	-69.64	Yes	Epipelagic Zone (0-200m)	Weekly	2000	Active
22	REPHY	Western Mediterranean Sea (Ligurian Sea)	43.68	7.31	Yes (Transect)	Unknown	Monthly	1995	Active
23	AZTI Station D2	Eastern North Atlantic Ocean	43.45	-1.91	No	Epipelagic Zone (0-200m)	Monthly	1986	Unknown
24	DYFAMED Time Series	Western Mediterranean Sea (Ligurian Sea)	43.45	7.8	Yes	Unknown	Monthly	1991	Unknown
25	Thau Lagoon	Western Mediterranean Sea (Balearic Sea)	43.4	3.6	No	Unknown	Weekly	1971	Active

Labels	Observatory name	Region	Latitude (°N)	Longitude (°E)	Multiple sites?	Depths	Sampling frequency	Year of est.	Status
26	RADIALES Time Series	Eastern North Atlantic Ocean (Southern Bay of Biscay)	43.34	-3	Yes (Transect)	Unknown	Monthly	2007	Active
27	Atlantic Zone Monitoring Program (AZMP)	Western North Atlantic Ocean	43	-60	Yes	Unknown	Bi-weekly	1998	Active
28	Microbial Observatory of the Laboratoire Arago	Western Mediterranean Sea	42.5	3.12	Unknown	Unknown	Unknown	2001	Unknown
29	Les Medes Islands	Western Mediterranean Sea	42	3.23	Unknown	Unknown	Unknown	Unknown	Unknown
30	Blanes Bay Microbial Observatory (BBMO)	Western Mediterranean Sea (Blanes Bay)	41.66	2.9	Yes	Epipelagic Zone (0-200m)	Monthly	1992	Active
31	The Operational Observatory of the Catalan Sea (OOCS)	Western Mediterranean Sea (Blanes Canyon)	41.66	2.91	Yes	Epipelagic Zone (0-200m)	Weekly	2009	Active
32	Martha's vineyard observatory - MVCO	Western North Atlantic Ocean	41.33	-70.56	Yes	Epipelagic Zone (0-200m)	Daily	Unknown	Active
33	Gulf of Naples -LTER-MC	Eastern Mediterranean Sea (Gulf of Naples)	40.8	14.25	Yes	Unknown	Weekly	1984	Active
34	Northeastern U.S. Shelf (NES) LTER	Western North Atlantic Ocean	40.75	-70.65	Yes	Unknown	Unknown	2017	Active
35	Tohoku Ecosystem-Associated Marine Sciences - TEAMS - Otsuchi	Western North Pacific Ocean	39.31	142.09	Yes	Unknown	Unknown	2011	Active

Labels	Observatory name	Region	Latitude (°N)	Longitude (°E)	Multiple sites?	Depths	Sampling frequency	Year of est.	Status
36	Tohoku Ecosystem-Associated Marine Sciences - TEAMS - Onagawa	Western North Pacific Ocean	38.44	141.64	Yes	Unknown	Unknown	2011	Active
37	PROTEUS-LMER	Western North Atlantic Ocean (Chesapeake Bay)	37.52	-76.1	Unknown	Unknown	Unknown	1994	Not active
38	ECOMÁLAGA time-series	Western Mediterranean Sea (Alboran Sea)	36.8	-4.25	Yes	Epipelagic Zone (0-200m)	2 cruises/yr	2010	Active
39	Monterey Bay MBARI (Monterey Bay Microbial Observatory (MBMO))	Eastern Pacific Ocean (Monterey Bay)	36.6	-121.89	Unknown	Unknown	Unknown	Unknown	Active
40	IEO-RADMED monitoring program	Western Mediterranean Sea (Balearic Sea)	36.5	-3	Yes (Transect)	Epipelagic Zone (0-200m) and Mesopelagic Zone (200-1000m)		2007	Active
41	Tohoku Ecosystem-Associated Marine Sciences - TEAMS - Manazuru	Western North Pacific Ocean	35.12	139.22	Yes	Unknown	Unknown	2011	Active
42	Tohoku Ecosystem-Associated Marine Sciences - TEAMS - Sagami Bay	Western North Pacific Ocean	35	139.2	Yes	Unknown	Unknown	2011	Active

Labels	Observatory name	Region	Latitude (°N)	Longitude (°E)	Multiple sites?	Depths	Sampling frequency	Year of est.	Status
43	California Current Ecosystem (CCE-LTER)	Western North Pacific Ocean	33.9	-120.3	Yes	Unknown	Monthly	1996	Active
44	San Pedro Ocean Time series (SPOTS)	Eastern North Pacific Ocean (San Pedro Channel)	33.3	-118.3	Yes (Transect)	Epipelagic Zone (0-200m) and Mesopelagic Zone (200-1000m)	Monthly	1998	Active
45	Texas Aand M - University of Haifa Eastern Mediterranean Observatory - THEMO	Eastern Mediterranean Sea (Levant Basin)	33.15	34.85	No	Epipelagic Zone (0-200m) and Mesopelagic Zone (200-1000m)	Monthly	2017	Active
46	CENCOOS Scripps Pier	Western North Pacific Ocean	32.87	-117.25	No	Unknown	Unknown	Unknown	Active
47	Georgia Coastal Ecosystems LTER	Western Atlantic Ocean	31.5	-81.1	Yes	Unknown	Unknown	2000	Active
48	Oceanic Microbial Observatory- BIOSSCOPE	Western North Atlantic Ocean (Sargasso Sea)	31.4	-64.1	No	Epipelagic Zone (0-200m) and Mesopelagic Zone (200-1000m)	Monthly	1996	Active
49	JAMSTEC - S1 LTER	Western North Pacific Ocean	30	145	No	Unknown	Unknown	2010	Unknown
50	RAPROCAN Time Series	Eastern Atlantic Ocean (Canary Islands)	29.5	-25	Yes (Transect)	Epipelagic Zone (0-200m) and Mesopelagic Zone (200-1000m)	2 cruises/yr	2007	Active

Labels	Observatory name	Region	Latitude (°N)	Longitude (°E)	Multiple sites?	Depths	Sampling frequency	Year of est.	Status
51	ANTARES-Ubatuba	Western South Atlantic Ocean	23.75	-45	No	Epipelagic Zone (0-200m)	Monthly	2004	Active
52	Hawaii Ocean Time-series (HOT)	Western North Pacific Ocean (Hawaii)	22.75	-158	No	Epipelagic Zone (0-200m) and Mesopelagic Zone (200-1000m)	10 cruises/yr	1988	Active
53	Cape Verde Ocean Observatory	Eastern North Atlantic Ocean	17.6	-24.3	Yes	Epipelagic Zone (0-200m) and Mesopelagic Zone (200-1000m)	Monthly	2006	Active
54	Arabian Sea Time-Series (ASTS)	Indian Ocean (Arabian Sea)	17	68	Unknown	Unknown	6 cruises/year	2007	Active
55	Candolim Time-Series (CaTS)	Indian Ocean (Arabian Sea)	15.52	73.63	Unknown	Unknown	Monthly	1997	Active
56	CARIACO Ocean Time-Series Program	Western Atlantic Ocean	10.5	-64.67	Yes	Unknown	Monthly	1995	Active
57	IMARPE Time Series	Eastern South Pacific Ocean	-4.8	-82	Yes	Unknown	4cruises/yr	Unknown	Active
58	Darwin	Eastern Indian Ocean (Timor Sea)	-12.4	130.77	No	Epipelagic Zone (0-200m) and Mesopelagic Zone (200-1000m)		Unknown	Unknown
59	Moorea - MCR LTER	South Pacific Ocean (Moorea Island)	-17.5	-149.88	No	Epipelagic Zone (0-200m) and Benthos (sediment)	Monthly	2004	Active

Labels	Observatory name	Region	Latitude (°N)	Longitude (°E)	Multiple sites?	Depths	Sampling fre-quency	Year of est.	Status
60	Australian National Mooring Network - IMOS - Yongala	South Pacific Ocean (Coral Sea)	-19.31	147.62	No	Epipelagic Zone (0-200m) and Mesopelagic Zone (200-1000m)		2006	Active
61	Australian National Mooring Network - IMOS - North Strad-broke Island	South Pacific Ocean (Coral Sea)	-27.34	153.56	No	Epipelagic Zone (0-200m) and Mesopelagic Zone (200-1000m)		2006	Active
62	Australian National Mooring Network - IMOS - Rottness Island	Eastern Indian Ocean	-32	115.42	No	Epipelagic Zone (0-200m) and Mesopelagic Zone (200-1000m)		2006	Active
63	Australian National Mooring Network - IMOS - PS Hacking	Tasman Sea	-34.08	151.25	No	Epipelagic Zone (0-200m) and Mesopelagic Zone (200-1000m)		2006	Active
64	Australian National Mooring Network - IMOS - Kangaroo Island	Eastern Indian Ocean (Great Australian Bight)	-35.83	136.45	No	Epipelagic Zone (0-200m) and Mesopelagic Zone (200-1000m)		2006	Active
65	COPAS Time Series	Eastern South Pacific Ocean	-36.5	-73.13	Yes	Unknown	Monthly	2002	Active
66	Estacion Permanente de Estudios Ambien-tales (EPEA)	Western South Atlantic Ocean	-38.46	-57.68	No	Epipelagic Zone (0-200m)	Monthly	2000	Active

Labels	Observatory name	Region	Latitude (°N)	Longitude (°E)	Multiple sites?	Depths	Sampling frequency	Year of est.	Status
67	Australian National Mooring Network - IMOS - Maria Island	Tasman Sea	-42.6	148.23	No	Epipelagic Zone (0-200m) and Mesopelagic Zone (200-1000m)		2006	Active
68	Munida Time Series	South Pacific Ocean	-45.77	-170.72	Yes (Transect)	Epipelagic Zone (0-200m)	6 cruises/yr	Unknown	Unknown
69	Bay of Bengal Time-Series (BBTS)	Indian Ocean (Bay of Bengal)	-50.4	68.25	Unknown	Unknown	6 cruises/year	2010	Active
70	King Sejong Station (KOPRI)	Southern Ocean	-62.2	-58.8	Unknown	Unknown	2 cruises/yr	2012	Active
71	PALMER Antarctica	Southern Ocean	-64.77	-64.05	Yes	Unknown	Annually	1990	Active
72	RotheraOceanographic and Biological Time Series (RaTS)	Southern Ocean	-67.34	-68.13	Yes	Epipelagic Zone (0-200m) and Mesopelagic Zone (200-1000m)		1997	Active

2.4 Monitoring the microbial role in ocean health

Given their central place in the oceanic web of life, microbial assemblages are a prime indicator of ocean's state and health. Their metabolic and compositional responses to variations in light, temperature, oxygen, nutrients, and a vast host of metabolites make them excellent candidates for biosensing and bioindication of both short- and long-term dynamics. As a result, microbes have been used in the production of biosensors to detect, among other stimuli, the presence of organic substances, biofouling-linked compounds, toxins, and heavy metals. Further, microbial indicators (MIs) have been developed for hazard monitoring, primarily based on the detection of taxa such invasive or pathogenic species (e.g., Ramírez-Castillo *et al.*, 2015). For example, the close association of bacteria such as, *E. coli* with untreated sewage allows effective screening for faecal contamination in aquatic systems (Ramírez-Castillo *et al.*, 2015), while the temperature-dependent ranges and activity of pathogenic *Vibrio* strains can be predicted across global change scenarios (Baker-Austin and Oliver, 2017; Turner *et al.*, 2016). Eukaryotic MIs, which report on flagellates, ciliates, and diatoms (Pawlowski *et al.*, 2016), are also being developed to detect the occurrence of harmful algal blooms. The emergence of new microbial functions, such as, the metabolism of plastics (Yoshida *et al.*, 2016), promises to steadily increase this sensing repertoire, tracking the diversification of anthropogenic stressors. Undoubtedly useful, MIs of this kind have a narrow focus, centered on risks to human health and well-being. To report on ocean health, a suite of MIs, integrated into broader observational framework is urgently needed to fill pronounced gaps in marine assessment strategies (e.g., note the underrepresentation of microbial indicators in Piroddi *et al.*, 2015).

Holistic evaluations of ecosystem state require complex, community-level insight integrating both taxonomic and functional information over time (Fuhrman *et al.*, 2015; Chafee *et al.*, 2018). For example, studies on phytoplankton assemblages have detected compositional change tracking climate variation (Barton *et al.*, 2016; Nöthig *et al.*, 2015) and broader microbial community shifts have been detected in a rapidly warming Arctic Ocean (Soltwedel *et al.*, 2016; Boetius *et al.*, 2013). Unfortunately, heterogeneous and asynchronous reporting prevents these and other advancements, such as, the sensing of hydrocarbon pollution (Lozada *et al.*, 2014) and heavy-metal contamination (Moberly *et al.*, 2016), from contributing to more global assessments of ecosystem state. Credible baseline data and frameworks for integrated reporting (e.g., Racault *et al.*, 2014) are now needed to transition individual studies and time series into a globally coherent diagnosis of marine health. Indeed, this class of MIs can be fully utilized only if they allow the differentiation of baseline, natural variation (e.g., by seasonality, El Niño, or the North Atlantic Oscillation) from deviations explained by other factors, a challenge even for mature time series with strong microbial components (e.g., Soltwedel *et al.*, 2016).

The repertoire of technologies allowing the identification of community-level microbial bioindicators has been greatly augmented with multi-omic technologies and techniques to sense the metabolic capacities and behaviours of the uncultivable majority. Despite these technologies undergoing rapid transformations every 4-5 years in the past 20 years, a growing body of expertise in handling community metagenomes, metatranscriptomes, and environmental DNA (eDNA) is forming the basis of a new generation of MIs (Borja *et al.*, 2016; Thomsen and Willerslev, 2015; Goodwin *et al.*, 2017). Concurrently, omics approaches are increasing the efficiency and cost-effectiveness of MIs already in operation (e.g., Tan *et al.*, 2015). Importantly, these approaches

are allowing the use of functional genes as indicators (e.g., antibiotic resistance genes as indicators for aqua- and agricultural impacts Li *et al.*, 2015; Chen *et al.*, 2013; Raverty *et al.*, 2017), allowing more sensitive assessment of environmental change (Louca *et al.*, 2016) and have facilitated the application of well-established macroecological indicators such as, the AZTI (Centro Tecnológico Experto en Innovación Marina y Alimentaria) Marine Biotic Index (AMBI) to the microbial realm (microgAMBI, Aylagas *et al.*, 2017). It is clear that sequencing technologies will be a prime focus of future marine microbial observation and monitoring. Efforts here will be fuelled by progress in autonomous sampling and bioinformatics technologies (Ottesen, 2016), contextualisation by large-scale omics-focused sampling campaigns (e.g., Sunagawa *et al.*, 2015; Kopf *et al.*, 2015; Ottesen, 2016), and the applications of techniques such as, machine learning to omics data (e.g., Cordier *et al.*, 2017).

Regardless of what technologies can be applied to individual samples, the problem of meaningfully linking shifts in complex community composition and function to environmental change remains an issue of spatiotemporal coverage. In most regions, far too little is known and measured to reliably discriminate background microbial dynamics from all but a few, pronounced responses to climatic and anthropogenic factors. Consequently, we struggle to detect less obvious changes with profound consequences. For example, we lack MIs sensitive enough to detect the slight increases in the degradation rate of dissolved organic carbon expected to profoundly impact ocean's capacity to take up CO_2 (Kim *et al.*, 2015). Additionally, current MIs are not sophisticated enough to consistently report on functional changes caused by the synergistic action of multiple marine stressors (Hutchins and Fu, 2017). Long-term marine microbial observatories, with their sustained focus and highly developed understanding of their host ecosystem, represent our best chance to advance this front. These facilities can permit rigorous development and testing of MIs within multidisciplinary frameworks which which have established a background against which to compare new sources of variation. For example, the Hawaii Ocean Time-series (HOT; est. 1988) has sampled its ALOHA (A Long-term Oligotrophic Habitat Assessment) station monthly, providing deep insight into the North Pacific Subtropical Gyre (NPSG) for three decades (Bryant *et al.*, 2016). Here, recent analyses of data from dozens to hundreds of sampling events have thoroughly characterized the foundational relationship between sea surface irradiance, chlorophyll a concentration, and oxygen production (Letelier *et al.*, 2017; Laws *et al.*, 2016) and linked both local primary production and the large-scale climatic variation of the North Pacific Gyre Oscillation to monthly and annual mesozooplankton dynamics (Valencia *et al.*, 2016). Moreover, the cycling of methane and nitrous oxide, potent greenhouse gases, in the system's euphotic zone (5-175 m) was investigated over an eight year period, detecting regular oscillations in the former and a decline of methane concentrations linked to increased phosphate levels recorded in 2012-2013, furthering the understanding of microbial aerobic methane production in oligotrophic systems (Repeta *et al.*, 2016) while providing the raw knowledge to develop new MIs. Similarly, the only open ocean long-term ecological research station in the Arctic, HAUSGARTEN (est. 1999; now operated under the Frontiers in Arctic Marine Monitoring programme; (Soltwedel *et al.*, 2016)), has provided perspectives only possible with sustained observation while facilitating short-term process and methodological studies. In this remote site, work to improve the preservation of autonomously collected marine particles (e.g., Metfies *et al.*, 2017) is enhancing the temporal continuity of microbial data to match the output of the observatory's network of autonomous sensors, while yearly expeditions have generated more

multifaceted microbial data across its 5000 m depth gradient and 21 permanent sampling sites. Its 15 years of multidisciplinary observation have revealed fascinating properties of the rapidly changing Arctic, including: tight coupling of deep microbial communities to surface variability (Soltwedel *et al.*, 2016); interactive effects of temperature, acidification, and organic matter linked to increased bacterioplankton biomass production and extracellular enzyme activity (Piontek *et al.*, 2015); punctuated seasonal pico- and nanoplanktonic turnover during warm water anomalies as well as decadal increases in chlorophyll a concentration (Nöthig *et al.*, 2015); and the biological control of microbially derived transparent exopolymeric particles (TEP) concentrations involved in transporting carbon to deeper ecosystems and nucleating cloud and ice formation, thus increasingly influencing regional climatic conditions (Engel *et al.*, 2017).

From the above, it is clear that microbial observatories have created a refined, localized store of knowledge demonstrating that microbial dynamics are linked to multi-layered ecosystem states and events. Many more examples exist (e.g., increases in coccolithophore abundance in response to increased dissolved inorganic carbon at the Bermuda Atlantic Time-series Study Krumhardt *et al.*, 2016) and are readily apparent when exploring the resources listed in (Table 2.1). In the face of global challenges, the natural corollary for the next 5-10 years is two-part: 1) The microbial observatory community must align and create a coordinated and well-integrated global microbial observation system and 2) microbial phenomena which provide consistent information on issues of societal and scientific concern should be reported in a well-documented set of microbial indicators which can be consumed by the broader community. While both processes may occur in parallel, we believe the construction of a global marine microbial observatory network is of particular importance to catalyze a more globally integrated and sustained solution.

2.5 Building a network for marine microbial observation and monitoring

As illustrated above, long-term ocean observatories - as instituted and standardized acts of multidisciplinary observation - offer an ideal context to bring complex, prototypical MIs of ecosystem health to maturity. These facilities are necessarily concerned with ensuring the continuity and consistency of datasets spanning decades in order to detect change in ecosystem state. As such, observatories provide the baseline of data and knowledge needed to characterize an MI's behavior and relevance within a well-examined ecosystem. In the marine realm and spurred by initiatives such as, the Genomic Observatories Network (Davies *et al.*, 2014), a growing collection of observatories are now conducting regular microbial sampling. However, to be sustainable, extant efforts must seek to integrate with one another under a common, mutually reinforcing observatory framework (see (Scholes *et al.*, 2012) for an analogous case).

In (Table 2.1) and Figure 2.1, we have attempted to compile overview of existing oceanic microbial observatories to initialise a more formal community registry and encourage a more interconnected future. During our survey, we noted that most microbial observatories augment one of the three types of physicochemical ocean observatories, each with their strengths and weaknesses. Traditional observatories operated by ship-based transects (e.g., the Global Ocean Ship-based Hydrographic Investigations Program, GO SHIP) provide the best opportunities for biological

sampling due to the flexibility of ships as sampling platforms; however, they often lack temporal resolution due to uncertainties in securing ship time. Moorings and anchored buoys provide fixed platforms for autonomous observation through time, but lack sufficient energy stores to operate advanced in situ sensors and samplers. Lastly, tagged marine mammals and drifting Lagrangian observatories including Argo profiling floats, gliders, and buoys have considerable spatial reach and resolution, accessing depths of ca. 2000 m, but have limited capacities to carry equipment for handling microbial samples (Seegers *et al.*, 2015). All these options are challenged by high maintenance costs (Smith Jr. *et al.*, 2015), yet present our only options in detecting environmental trends and their links to microbial community structure and function. Encouragingly, many of these physicochemical frameworks have already established common practices and shared governance strategies, a feature that can be used to catalyze similar progress in the microbial observation domain.

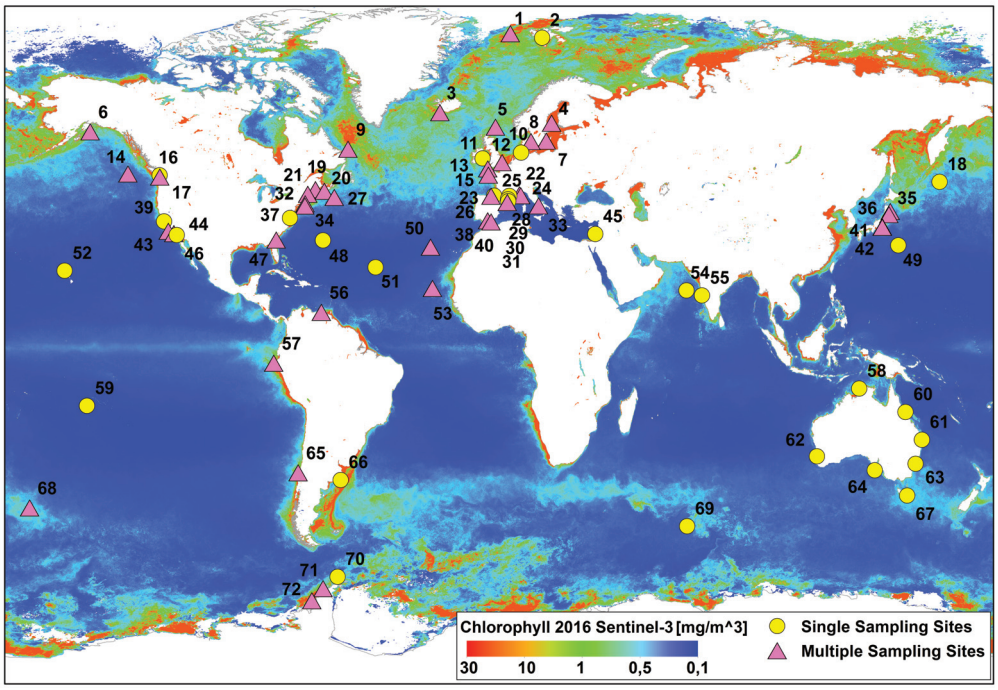

Figure 2.1: Map of marine long term ecological time series sites with microbiome variables monitored. Single sites are marked with yellow circles, regions where multiple sites are clustered are marked with pink triangles. Sites are identified by numbers, corresponding to rows in Table 1. Note that the map is likely incomplete, as it is the result of keyword searches of the scientific literature. It shows lack of observation in large ocean realms, especially areas of intensive fisheries in upwelling zones, in polar zones, in coastal regions of intense aquaculture, and in the Southern Ocean in general. The map features chlorophyll data from the GlobColour project, generating merged Level-3 ocean colour sensor products at a resolution of 4.6 km. The chlorophyll-a concentration (mg/m3), case 1 waters (CHL1) was derived from 2016 Sentinel-3 sensors: SeaWIFS, MERIS, MODIS AQUA, VIIRS and OLCI-A, using a weighted average and a GSM model method for the merging process. The data was further averaged over a 1-year period by AWI FRAM Remote-Sensing. Source of the continents data is ESRI.

The now global network of Continuous Plankton Recorder (CPR; http://www.globalcpr.org) sites presents an excellent example of interconnected and harmonized ecological and physicochem-

ical observation. The CPR network has used collecting instruments with conserved design and standardized processing protocols for many decades, which now acts as a platform upon which new sensors can be mounted. The integrity and coverage of this system has allowed the detection of numerous signals in the plankton, such as, population dynamics of invasive *Vibrio* species linked to warming waters (Vezzulli *et al.*, 2016), interannual variability in herring populations (Batten *et al.*, 2016), and planetary-scale regime shifts (Reid *et al.*, 2016). This knowledge has allowed the CPR community to identify essential, ecosystem-specific variables to improve global assessments (Constable *et al.*, 2016) and channel their collective outcomes into a wide array of policy development organizations. Of equal importance, the network is able to buffer loss of capacity by any of its members by, for example, maintaining sample records or stepping in when tows cannot be performed. At many levels, from governance to stakeholder engagement, the CPR network is a viable model upon which a global consortium of microbial observatories can be based; however, a graded approach to this goal is needed to progressively align initiatives in this complex and active domain.

As we noted above, the immense methodological variability and rapid development in microbial observation hinders the construction of a network unified by standardized methodology and technology. At the initial stages, it is more feasible that networking microbial observatories will be a question of aligning information flows via interoperable reporting standards along widely endorsed principles (notably, (Wilkinson *et al.*, 2016)). In this manner, frequent contact between existing and new initiatives will become more normalized, increasing the potential to perform meta-analyses and synthetic studies. This, in turn, is very likely to drive greater alignment at all levels to promote globally impactful studies. Some success is already visible through the grassroots development of standards for sequence-derived data (e.g., the BIOM format McDonald *et al.*, 2012) and its metadata (e.g., MIxS Yilmaz *et al.*, 2011), which are converging with more general biodiversity standards such as, Darwin Core (Wieczorek *et al.*, 2012) and Humboldt Core (Guralnick *et al.*, 2018) as well as resources in domains such as, Earth sensing through shared semantic technologies (e.g., Buttigieg *et al.*, 2016). The time is ripe for microbial observatories to interface through such standards, while collectively shaping them to be fit for purpose. Importantly, the use of these standards should be coupled to the stabilization of variable low-level information through some degree of information abstraction (see below). The community can then approach integrative reporting mechanisms aimed at a far broader base of stakeholders, including researchers from other domains, policy analysts, decision makers, educators and the general public.

Three emerging foci which could facilitate such integration present themselves: the Essential Ocean Variables (EOVs), the Essential Biodiversity Variables (EBVs Pereira *et al.*, 2013; Kissling *et al.*, 2018)) and the Ocean Health Index (OHI; Halpern *et al.*, 2015). The EOVs, championed by the Global Ocean Observing System (GOOS), are a developing mixture of low- and high-level variables deemed necessary to report on the state of the ocean. Microbiological variables, as most biological/ecological variables in this scheme, exist in a conceptual state with no established guidelines on measurement or assessment, in part due to the turnover of technologies, methodological variability, and the lack of low-price automated biosensors. The EBVs, promoted by the Group on Earth Observations Biodiversity Observation Network (GEO BON), play a somewhat different role: they aim to offer an intermediary layer of abstraction between raw biodiversity measurements, such as, genetic beta diversity, and high-level indicators (e.g., “connectivity /

fragmentation of ecosystems") used to monitor adherence to agreements such as, the Convention of Biological Diversity. With careful handling, this abstraction layer may allow harmonisation of biodiversity data generated using diverse, regionally-tuned methods across different observatories, preserving rationale-driven differentiation while promoting unified reporting. Researchers who operate and utilize microbial observatories are well-poised to report on some EBVs, such as ,"Taxonomic diversity" and "Physiological traits" through methods including marker gene analysis, labeled cell counts, enzymatic activity assays, and meta-omic approaches. However, there is a great need to build consensus on how data generated by local methodologies – many of which have been tuned to the ecosystems under scrutiny or are determined by local resource constraints – can be credibly merged across sites to provide global reporting. In our opinion, observatories should take stock of how their data streams can report on each essential variable, documenting caveats as appropriate and accounting for uncertainties. Subsequently, these strategies should be publically, allowing for peer review and comment prior to standardization by a task group of data analysts charged with formulating a robust set of aggregate indicators. Naturally, activities of this kind must be accompanied with diagnostic studies, continually testing whether integrative approaches centered on essential variables and indices adequately and accurately capture ecological signals. While this may sound daunting, similar activity reported almost a decade ago has provided the broader biodiversity community with a common basis to highlight increasingly urgent issues on a global scale and simultaneously conduct fascinating research (e.g., Butchart *et al.*, 2010). In this vein, the OHI (Halpern *et al.*, 2015) - now in its fifth year of operation – provides another framework which may benefit from harmonized microbial insight and novel MIs. The OHI integrates information about the ecological, social, and economic benefits that a healthy ocean provides to humans. Relatively low-level components of the OHI - including the counts of alien species and habitat destruction - are organized into the dimensions of status, resilience, pressures, and trend. Microbial components would have a natural home in the OHI's framework, but, as discussed above, need firmer scientific foundations and consensus within the observing community before they can be globally applied. For example, thresholds for declaring the detection of invasive species in molecular data are likely to vary across systems (due to varying degrees of natural turnover) and technologies (e.g., due to variation in error rates), thus well-documented and reproducible expert intervention is required prior to integration. Together, these reporting frameworks exemplify a challenging, but feasible, route towards global integration of marine microbial observation, especially when compared to the incredibly cumbersome and currently unsustainable option of attempting to standardize the use of samplers, filters, extraction technologies, primers and sequencing pipelines at a global scale. If taken up, we believe that this vital task of harmonized reporting will nucleate a tightly coordinated network of observatories, laying a solid foundation for further alignment.

2.6 Conclusion: Realizing the societal relevance of marine microbial observatories

Ocean biodiversity and its relationship to ecosystem health and human well-being has never been a more pressing target for research and monitoring (e.g., Egan and Gardiner, 2016; Lamb *et al.*, 2017; Russi *et al.*, 2016; Kite-Powell *et al.*, 2008). This urgency will only increase with

rapid growth of human settlements in coastal zones, increasing dependence on the ocean's resources and exposure to its biotic hazards. Indeed, UN Environment Chief, Erik Solheim, has recently called for the elevation of biodiversity monitoring to the same level as climate monitoring by 2020, and stressed the central importance of functioning ecosystems to societal well-being (COP12, Manila, 2017-10-25). Bolstering the capacity of long-term ocean observatory networks to coherently monitor microbes - the greatest store of biodiversity in the oceans - would do much to accomplish this target and enhance reporting on many components of the UN's Sustainable Development Goals (esp. SDGs 14:"Life Below Water" Malone *et al.*, 2014a,b). Indeed, much in the same way that the human microbiome is becoming increasingly relevant in monitoring human health, the ocean microbiome must be integrated into monitoring the health of our Blue Planet.

Microbial observing efforts at all scales can accelerate this mission if they are able to harmonise their outputs and function as a consolidated system capable of generating coherent, spatiotemporally comprehensive indicators and assessments tuned to societal priorities. Further, aligned observatories have the ability to cross-validate and test the validity and generalizability of existing and emerging methods and best practices, which are often developed in isolation. Observatories, projects, programs, and consortia such as, the Genomic Observatories Network (GON), DNAqua-Net (Leese *et al.*, 2016), the "Optimising and Enhancing the Integrated Atlantic Ocean Observing Systems" (AtlantOS) project, and the Association of European Marine Biological Laboratories Expanded (ASSEMBLE+) have an immense opportunity to align these efforts and collectively interface with broader coordination mechanisms offered by organisations such as, GOOS and the Marine Biological Observation Network (MBON). Such a convergence would greatly promote analyses and syntheses with greater coverage across time and space, which already draw from the findings of long-term observation efforts (e.g., Fuhrman *et al.*, 2015). Lastly, as societal needs associated with the marine ecosystems frequently cross the land-ocean interface, we must create operationalized links to observation infrastructures targeting more terrestrial systems (e.g., NEON Cesare, 2016). The scale of this challenge is immense, however, a concerted effort to establish stable microbial monitoring will vastly enhance our ability to understand, monitor, and protect the ocean's health. At an even larger scale, international microbiologists have already called for a unified microbiome initiative, with the overarching goal to take the next step from microbial monitoring to prediction of how Earth's microbiome will respond to the 21st century challenges (Blaser *et al.*, 2016). Marine microbiology must rally its capacities and prepare for the key role it will play in this process.

Chapter 3

Primer selection for Arctic Ocean microbiome studies - a taxonomic resolution trade off

Eduard Fadeev[1,2], Verena Salman-Carvalho[2], Massimiliano Molari[2], Magda Cardoz Mino[2], Josephine Z Rapp[1,2,3], Antje Boetius[1,2]

[1] Alfred Wegener Institute for Polar and Marine Research, Bremerhaven, Germany

[2] Max Planck Institute for Marine Microbiology, Bremen, Germany

[3] School of Oceanography, University of Washington, Seattle, Washington, USA

Keywords: bacterial communities, 16S rRNA gene, tag-sequencing, methods comparison, universal primers

This chapter is in preparation for submission to F1000Research journal.

3.1 Abstract

The microbiome of the Arctic Ocean is strongly understudied in comparison to other aquatic environments. However, the Arctic marine ecosystem harbors unique bacterial communities, which are strongly specialized to harsh environmental conditions (e.g., near-freezing temperatures), and extreme seasonality. The gene for the small ribosomal subunit (16S rRNA) is commonly used to study microbial communities in their natural environment. The primer sets for this marker gene were extensively tested using various environmental samples, but which typically originated from low-latitude locations. To-date, their performance in representing the bacterial communities of the Arctic Ocean was not yet evaluated. To select a suitable primer set for studying the bacterial communities in various habitats of the Arctic marine ecosystem (sea ice, surface and deep ocean, and deep-sea sediment), we have conducted a performance comparison between two commonly used primer sets, targeting different hypervariable regions of the 16S rRNA gene (V3-V4 and V4-V5). We observed differences between the primers and their representation of high-resolution taxonomic diversity (i.e., operational taxonomic units - OTUs), as well as differences in sequence proportions of taxonomically unresolved groups (e.g., *Marinimicrobia* and *Chloroflexi*). However, we also observed that throughout all tested habitats both primer sets were highly similar in representing the total bacterial community composition. Overall we do not endorse one primer set over the other but rather suggest that the decision should be made based on the presented strengths and weaknesses of each primer set.

3.2 Introduction

Methodologies of microbial research in general and environmental microbiology in particular went through significant changes in the last two decades with the improvements of molecular-based technologies and the establishment of the gene for the small ribosomal subunit (16S rRNA) as a molecular marker for microbial diversity (Pace *et al.*, 2012). The revolution of high-throughput sequencing technologies started a new era in microbiology, allowing large scale microbial biodiversity studies through massive parallel sequencing (Medini *et al.*, 2008; Reuter *et al.*, 2015; Morey *et al.*, 2013). The two most commonly used DNA-based approaches in environmental microbiology are: (1) polymerase chain reaction (PCR) based sequencing ("tag-sequencing"), which provides a taxonomic profile of the microbial community based on the phylogeny of the selected marker gene (e.g., 16S rRNA gene); and (2) shotgun sequencing of the total extracted DNA ("metagenomics") which provides, in addition to the taxonomic profile, a detailed functional information about the microorganisms within the community (Zinger *et al.*, 2012).

As each milliliter of seawater contains about one million microbial cells from different trophic groups (Glöckner *et al.*, 2012), these techniques allowed microbial oceanographers to investigate the massive diversity of the microbial assemblages, inferring their function in the biogeochemical cycles of the marine environment (Fuhrman and Steele, 2008; Rappé and Giovannoni, 2003; Karl, 2007; DeLong and Karl, 2005; Cullen *et al.*, 2007; Aristegui *et al.*, 2009). The increased awareness of global climate change and the deeper investigation of the global elemental cycles led to the understanding that microbial communities, as well as other relevant environmental

parameters should be monitored over time (Karl and Church, 2014). Time-series of microbial communities allow the detection of trends and irregularities in their dynamics, and may provide an insight into the main factors that control them (Fuhrman *et al.*, 2015).

Current time-series oceanographic research aims to understand large scale processes, and attempts to provide global estimates of the ongoing changes. For doing this, it is of uttermost importance to synchronize and standardize the data sampling between long-term time-series sites. The collection of samples in the open ocean is expensive and time consuming, which is mainly due to the remote locations of the sampling sites. Thus, unfortunately microbial long-term time-series studies in the framework of oceanographic observatories are rare, and are often conducted on a small geographic scale in a near-shore environment (further discussed in chapter 2). As a result, unlike other methodologies in long-term oceanographic observatories, the high-throughput technologies of microbial oceanography lack standardization and coordination. The studies are often dedicated to a specific research question, and apply a specific approach. Such discrepancies challenge the comparability and integration of these studies and their incorporation into one large mechanistic system, even within the same geographic region (e.g., Fuhrman *et al.*, 2015; Karl and Church, 2014; Giovannoni and Vergin, 2012).

Despite being the most rapidly changing marine environment on the planet (Vaughan *et al.*, 2013) the Arctic Ocean is undersampled (Wassmann *et al.*, 2011), and until recently consisted of only one long-term microbial time-series, of the HAUSGARTEN observatory in the Fram Strait (Soltwedel *et al.*, 2016, 2005). However, the recently established long-term Arctic open-ocean infrastructure project FRAM (FRontiers in Arctic marine Monitoring; Soltwedel *et al.*, 2013) set the goal to conduct year-round time-series observations of the Arctic marine environment over various sites in the Arctic Ocean. In the framework of the FRAM Molecular Observatory, we are aiming to develop a standardized methodology for conducting long-term microbial observations, across the diverse microbiomes of the Arctic Ocean (e.g., sea ice, seawater and seafloor; Boetius *et al.*, 2015), which will be comparable between them and other time-series sites (e.g., HOT and BATS). Unlike other time-series sites the harsh conditions in Arctic Ocean are limiting the accessibility of the sampling sites to the summer months. The sampling during the Arctic winter (which is generally low in microbial biomass; e.g., Alonso-Sáez *et al.*, 2008) is conducted using autonomous samplers with limited sampling capacities (Soltwedel *et al.*, 2013). These unique conditions constrain, with currently available technologies, the year-round time-series microbial observations to the PCR based approaches (i.e, "tag-sequencing"), which have lower DNA concentration thresholds (Hassan *et al.*, 2018; Thomas *et al.*, 2012). The 16S/18S rRNA gene sequencing taxonomic profiling is strongly supported by the existence of large curated taxonomic databases (e.g., SILVA Quast *et al.*, 2013), and it has been shown using a metagenomic approach that the functional capacity of a marine microbial community is strongly linked to its taxonomic composition (Galand *et al.*, 2018). Thus, despite the increasing use of metagenomics in microbial oceanography, tag-sequencing remains a valuable tool for addressing traditional community ecology questions.

One critical step step in 16S rRNA gene sequencing studies is the selection of PCR primers for the DNA amplification (Armougom, 2009). Throughout the years, many primer sets were designed for diversity studies of specific taxonomic groups, and in several attempts a universal 16S rRNA gene primer set was seeked, which could cover the entire diversity of the bacterial and archaeal communities (Wang and Qian, 2009). One of the most extensive primer evaluations

was conducted by Klindworth and colleagues, where they tested 512 primer sets in-silico, using the SILVA 16S rRNA gene non-redundant reference database (Klindworth *et al.*, 2013). Their evaluation resulted in the recommendation of using the 341F/785R (targeting the V3-V4 hypervariable regions of the 16S rRNA gene) as the 'best available' universal primer set for bacterial diversity studies, suitable for amplicon sequencing on Illumina platforms. At around the same time, the Earth Microbiome Project (EMP) was launched, aiming to catalog microbial diversity from different habitats across the world, and to create a microbial database that could facilitate global microbial community meta-analyses (Gilbert *et al.*, 2014, 2010). To ease comparability among the newly generated datasets, the EMP proposed standardized analysis protocols including the use of another primer set, 515F/806R, targeting the V4 hypervariable region of the 16S rRNA gene (Caporaso *et al.*, 2012, 2011). Unlike the V3-V4, the V4 primer set was able to capture not only bacterial but also archaeal diversity. However, later use of the primer set on marine microbiome samples revealed strong biases in the representation of dominant taxa in the water column (Apprill *et al.*, 2015; Parada *et al.*, 2016). Therefore, an alternative primer set, 515F-Y/926R (targeting the V4-V5 hypervariable regions) has been developed, and has since been proven to resolve the biases of the marine taxa representation known from the EMP primer set (Parada *et al.*, 2016). Since then, the V4-V5 primer set has been considered the 'best available' universal primer set for water column microbiome studies.

Both presented 16S rRNA gene primer sets, V3-V4 and V4-V5, are broadly used in current studies of marine pelagic microbial communities, and were extensively tested using mock and natural bacterial communities of temperate waters (e.g., Wear *et al.*, 2018). However, until today there were no systematic studies that tested the performance of these primer sets on the microbiome of the Arctic Ocean. In an attempt to select the most suitable primer set for future time-series microbial monitoring in the FRAM Molecular Observatory, we here present a performance comparison of the two 16S rRNA gene primer sets (V3-V4 and V4-V5) in representing the Arctic Ocean bacterial communities. Using 44 field samples collected from various habitats of the Arctic Ocean, we have conducted direct comparison of the taxonomic coverage and potential biases of the primers. Furthermore, based on extensive cell counting in two surface water samples, using CAtalyzed Reporter Deposition-Fluorescence In Situ Hybridization (CARD-FISH), we have estimated the primer-sets performance in representing the absolute abundance of key taxonomic groups in the Arctic microbiome.

3.3 Results and Discussion

3.3.1 The richness differs due to 16S rRNA gene sub-regions variability rates

Aliquotes of 44 DNA samples from the different habitats of the Arctic Ocean (i.e., sea ice, seawater, and seafloor) were sequenced on an Illumina MiSeq platform using both V3-V4 and V4-V5 primers (Table 3.S1). All samples were subject to the same 16S rRNA gene tag-sequencing analysis workflow, which consisted of quality control, operational taxonomic units (OTUs) clustering, and taxonomic assignment (Almeida *et al.*, 2018). Overall, both primers showed similar sequence reduction rates throughout the bioinformatic analysis, with slightly higher proportions

of retained sequences in the V4-V5 dataset. After quality filtering, removal of singletons and taxonomic assignment, both datasets accounted for slightly more than 50% of the initial sequences assigned to bacterial lineages. However, after the removal of sequences that were taxonomically assigned to chloroplast and mitochondria, only 35% of the initial sequences remained in the V4-V5 dataset, in comparison to 50% in the V3-V4 dataset (Fig. 3.S1). This suggests that the V4-V5 primer-set is less specific towards bacterial 16S rRNA gene sequences, and that large fractions of the sequences in each library (i.e., sampling effort) are a product of chloroplast and mitochondria rRNA amplification.

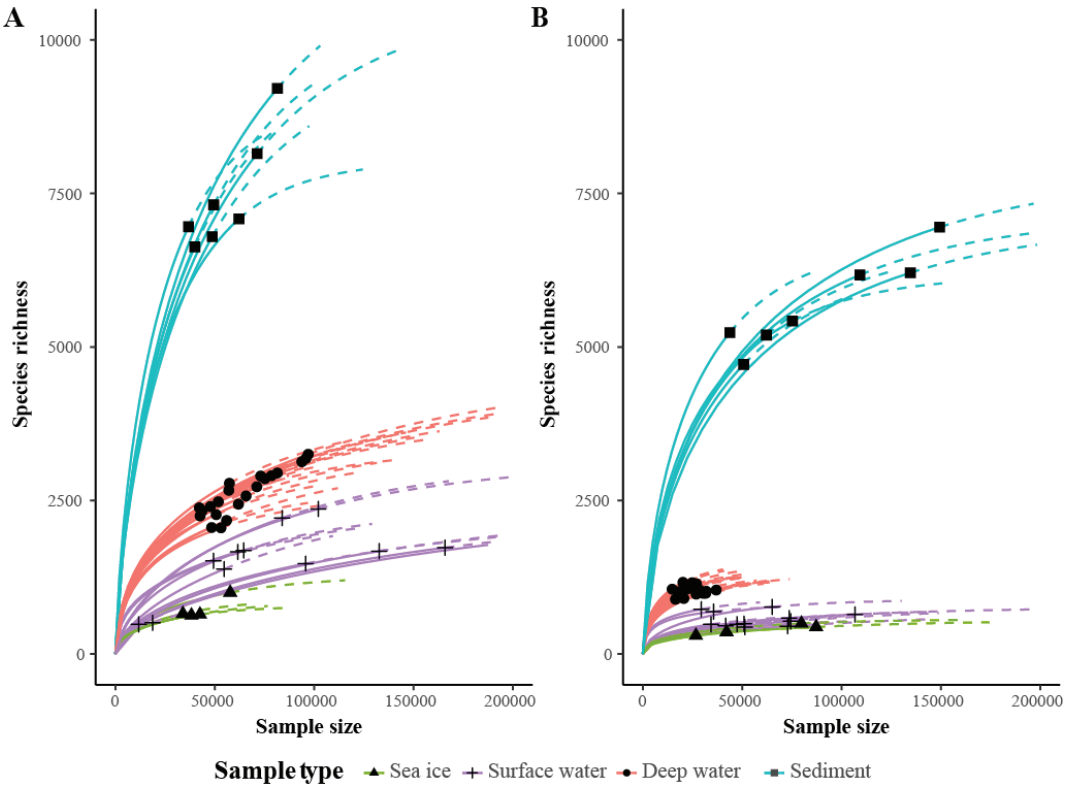

Figure 3.1: Rarefaction analysis of bacterial communities in each sample. (A,B) Sample-size-based rarefaction curves generated with iNEXT package, for V3-V4 (**A**) and V4-V5 (**B**) primer-sets. Based on the Hill numbers of order q = 0. The solid lines represent the observed accumulation with the number of sequences sampled, and the dashed lines represent the extrapolated accumulation up to double amount of sequences.

In all samples the rarefaction curves did not reach a plateau, and extrapolation with the double amount of sequences showed a further increase in richness ((Fig. 3.1) Chao and Jost, 2012; Chao *et al.*, 2014b), which suggests that additional OTUs are to be expected with larger sequencing effort. The observed richness (number of OTUs) in the V3-V4 dataset was significantly higher in comparison to the V4-V5 dataset (t-test, p value < 0.05; Table 3.S1). However, the Chao1 richness estimates, which take into account the sample size, revealed significantly higher community coverage in the V4-V5 dataset (mean coverage 71% and 78%, respectively; t-test, p value < 0.05). These observations suggest that the sensitivity of the V3-V4 primer set to bacterial diversity is higher in comparison to the V4-V5 primer set, potentially as a result of stronger hypervariability of the V3-V4 region of the 16S rRNA gene (Huse *et al.*, 2008; Yang *et al.*, 2016). Thus, in comparison to the V4-V5 primer set a smaller fraction of the bacterial diversity is covered

with the similar sampling depth (i.e., sampling effort). On the other hand, both Shannon and Simpson diversity indeces, which are less affected by rare OTUs (with low sequence abundance; Haegeman *et al.*, 2013), did not show statistically significant differences between the datasets. Altogether this suggests that the differences in richness are a result of a different representation of the rare biosphere, and the sequence abundant OTUs are represented in both datasets. Moreover, the coverage-based rarefaction estimations (i.e., Good's estimator) revealed that all samples had a completeness of more than 95%, independent of the primer set (Table 3.S1; Kang *et al.*, 2016).

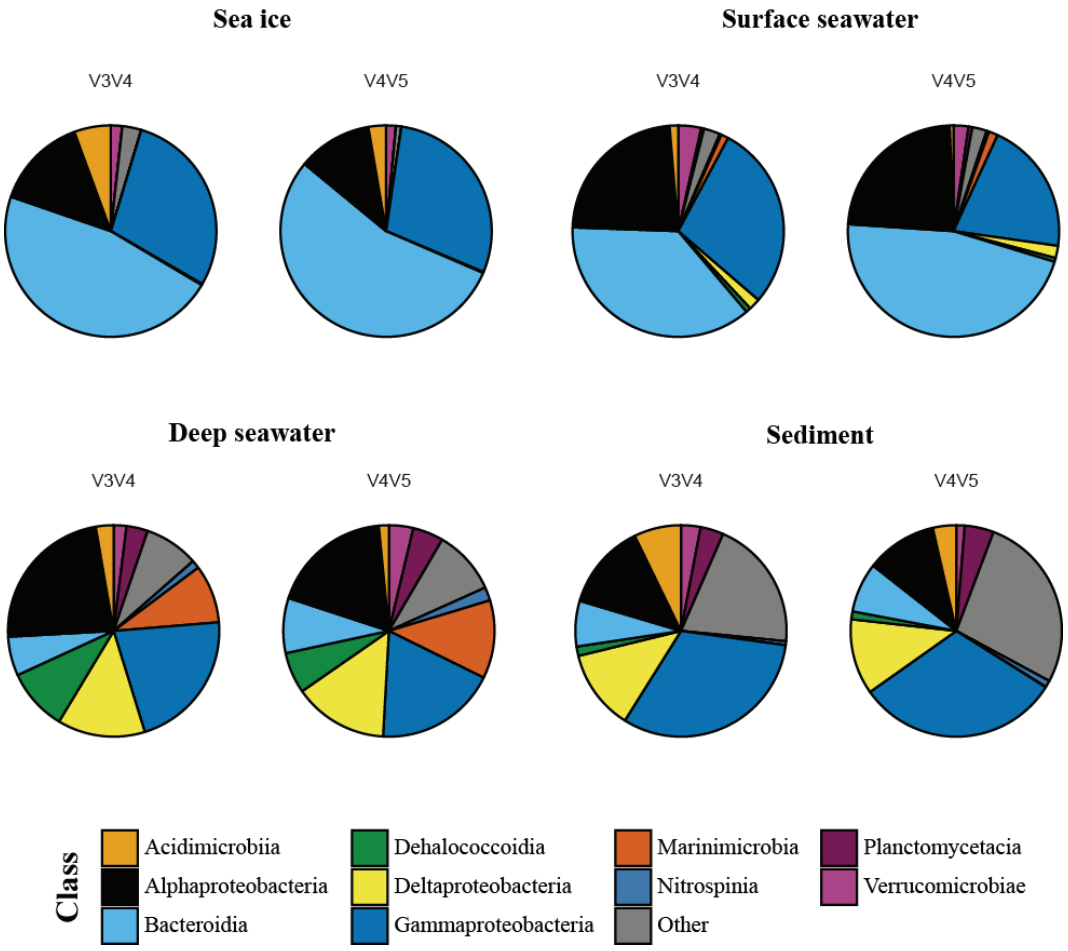

Figure 3.2: Mean sequence proportion of taxonomic classes in each habitat. The colours represent different dominant taxonomic classes, which were selected based on previous observations in the Arctic Ocean (Boetius *et al.*, 2015; Rapp *et al.*, 2018; Wilson *et al.*, 2017).

3.3.2 Similar representation of bacterial communities - different representation of populations with poor taxonomic classification

Both primer sets revealed bacterial community composition in line with previous reports for Arctic microbial diversity (Fig. 3.2). The sea ice and surface seawater communities were, in accordance with previously conducted studies, dominated by the classes *Alphaproteobacteria*, *Bacteroidia*, and *Gammaproteobacteria* (Boetius *et al.*, 2015; Rapp *et al.*, 2018; Wilson *et al.*, 2017). In the deep water column, a higher diversity was observed with increasing proportions of poorly

described taxonomic groups, such as, *Marinimicrobia* and *Dehalococcoidia* (Wilson *et al.*, 2017). The highest diversity was observed in the deep-sea sediment bacterial communities (Table 3.S1), with increasing number of low sequence abundance taxonomic classes, such as, *Acidobacteria* (Bienhold *et al.*, 2012; Rapp *et al.*, 2018). Overall, on a class level, both primer sets showed statistically significant (p value < 0.05) linear correlation in representation of the bacterial community composition (Fig. 3.S2), in consistency with previous observations (Wear *et al.*, 2018).

In order to investigate the differences between the primers on higher taxonomic resolution, we performed differential abundance tests for bacterial lineages at a family level, which were present in both datasets (V3-V4 and V4-V5). The families which had an average of at least 100 reads, a $\log_2$ change of absolute values higher than 1, and an adjusted p-value < 0.1 were defined as differentially abundant (Fig. 3.3). Out of 427 total bacterial lineages at family level only 58 showed differential abundance between the primer sets. Among them 54 lineages had higher representation in the V3-V4 dataset with absolute mean $\log_2$ fold change of 11.7, and only 4 lineages in the V4-V5 dataset with absolute mean $\log_2$ fold change of 8.2. The most abundant (in terms of number of sequences in each dataset) bacterial lineages, which showed differential abundance between the datasets, were members of taxonomic groups with poor classification, such as, *Deltaproteobacteria* (SAR324 clade and NB1-j), *Dehalococcoidia* (SAR202 clade) and *Marinimicrobia* (SAR406 clade). However, both primer sets were consistent in representing the sequence proportion of the bacterial families with high taxonomic resolution and most of the differentially abundant lineages were related to poorly classified taxonomic groups. The *Bacteroidia*, which are predominant members of the sea-ice community and sequence-abundant in the water column during the productive spring and summer months (Boetius *et al.*, 2015; Rapp *et al.*, 2018; Wilson *et al.*, 2017), did not show any differential abundance between the primer sets. The *Alphaproteobacteria* consisted of 5 distinct lineages with a higher sequence abundance in the V3-V4 dataset. Interestingly, despite the specific design of the V4-V5 primer set for representation of the SAR11 clade (Parada *et al.*, 2016), in our datatset there was one lineage of SAR11 clade in the deep seawater communities, which even had higher sequence abundance in the V3-V4 dataset.

3.3.3 High-throughput data provides semi-quantitative community composition

Due to the nature of PCR amplification, amplicon based sequencing may introduce biases into the dataset (Laursen *et al.*, 2017). Therefore, it is reasonable to assume that both primer sets have certain biases in representing specific taxa (e.g., Wear *et al.*, 2018), by either missing certain target groups or by misrepresenting their true abundance in the environment. In order to evaluate the two primer sets performance in representing the absolute abundances of bacterial taxa, we have conducted a comparison between the 16S rRNA gene community composition and microscopic cell counts using CARD-FISH (Fig. 3.4). The microscopy counts were conducted on two surface-water samples from the Fram Strait (Arctic Ocean). The taxonomic groups targeted by the CARD-FISH counting were selected based on their presence in the 16S rRNA gene dataset. The relative abundance of each targeted group was calculated based on total bacterial cell counts, acquired using the EUB338I-III CARD-FISH probe mix.

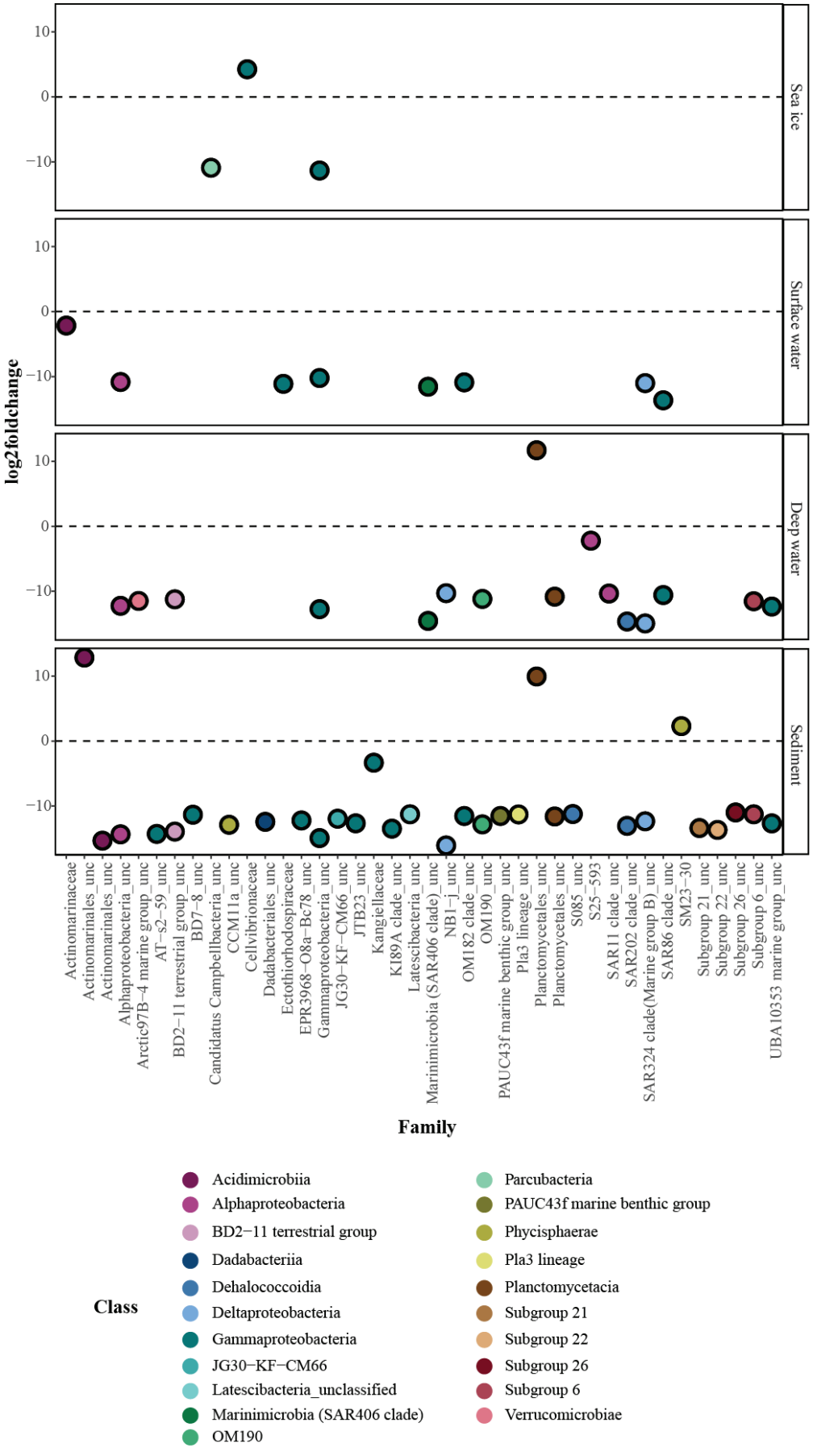

Figure 3.3: Differential abundance of bacterial lineages on a family level between the primer sets in each microbiome of the Arctic marine environment. Only lineages with absolute $\log_2$ fold change higher than 1 and statistically significance (adjusted p value < 0.1) were included in the data representation. The y axis represents values of $\log_2$ fold change. Positive values represent lineages which are enriched in the V4-V5 dataset and negative values represent lineages which are enriched in the V3-V4 dataset.

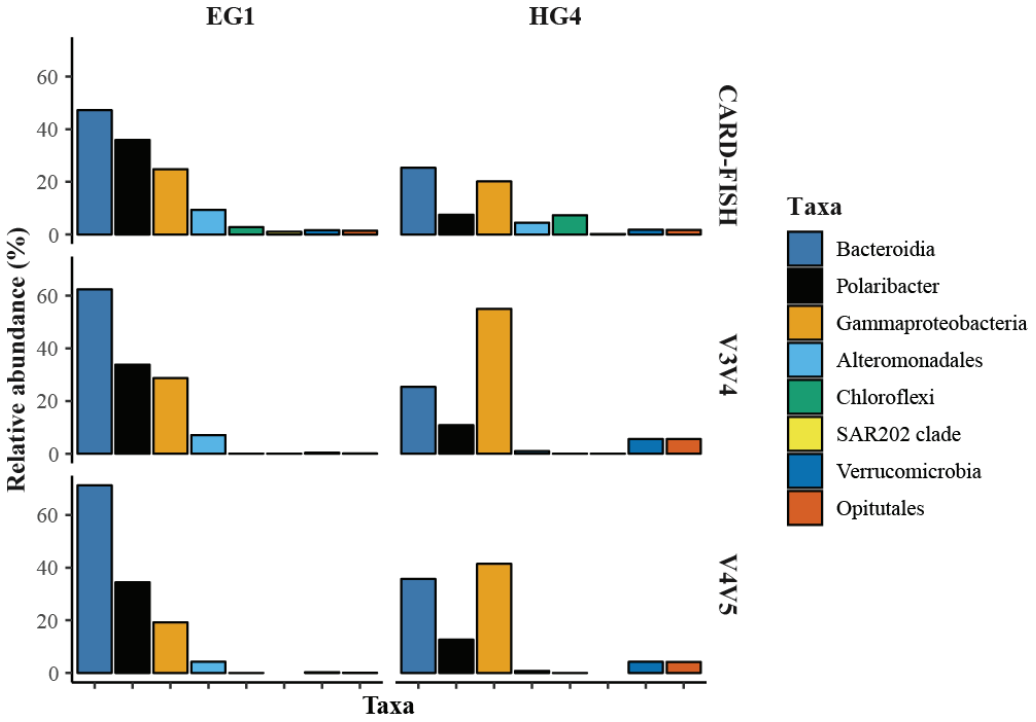

Figure 3.4: Relative abundance of selected bacterial taxa as inferred by CARD-FISH and sequence proportions in the 16S rRNA gene datasets, of various bacterial taxonomic groups. Both samples were collected in the HAUSGARTEN observatory, the EG1 station is located in the ice-covered part, and HG4 stations is located in the ice-free of part of the Fram Strait.

Overall the relative abundance in the CARD-FISH counts was lower than in the 16S rRNA gene datasets. Fluorescence in situ hybridization techniques have the clear advantage to provide absolute cell abundances that can be directly compared between samples, time-points, etc. However, the method itself surely also has internal technical hardships, which include the effectiveness to permeabilize the cell wall of the targeted organism, the high variability in the amount of intracellular ribosomes in environmentally interesting community members, and the steric differences for the accessibility of folded, double-stranded regions within the ribosome (Amann and Fuchs, 2008). The slightly lower representation of taxa in the cell counts could therefore be a consequence of these limitations, as well as the putative incomplete coverage of the target group by the probe(s) used. Nevertheless, in accordance with previous studies, both primer sets performed equally well in representing the patterns of absolute abundance in the selected taxonomic groups (e.g., Teeling *et al.*, 2016). Moreover, there was a statistically significant linear correlation between the sequence proportion in the 16S rRNA gene datasets and the relative abundance in microscopic cell counts (p value < 0.05; Figure 3.S3).

Although not addressed in the scope of this study, the high-throughput molecular techniques, such as 16S rRNA gene tag-sequencing, are limited in many other ways besides the primer biases, potentially in favor or against certain community members. Several other technical hardships, such as, different sampling procedures (Padilla *et al.*, 2015) or different DNA-extraction methodologies (Fouhy *et al.*, 2016; Starke *et al.*, 2014; Kennedy *et al.*, 2014) may impact the observations. Furthermore, various bioinformatic tools and approaches may have different sensitivities in sequence clustering into OTUs, which may also alter the observed patterns (Mahé

et al., 2015; Almeida *et al.*, 2018; Knight *et al.*, 2018). Thus, all these different parameters should be taken into account throughout the experimental design (Hugerth and Andersson, 2017), and standardized in case of continuous observation (i.e., time-series).

3.4 Concluding remarks

To understand the ongoing processes in the Arctic Ocean, and to estimate the future of this region, there is a need in holistic observations of the entire Arctic marine ecosystem. In order to conduct such observations, using a 16S rRNA gene tag-sequencing approach, a single primer set should be selected, which can be applied to all habitats of the Arctic Ocean (sea ice, water column, and deep-sea sediment). The most suitable primer set for 16S rRNA amplification and sequencing from environmental samples should produce high-quality 16S rRNA gene sequence amplicon libraries, and cover the desired organisms with minimum biases in relative abundance. We have found that both tested primer sets represent the major bacterial phyla at overall comparable levels, which correlates with their proportional representation via microscopic cell counting. Given the demonstrated similarity, we suggest that both primer sets are suitable for producing a high-quality overview of the bacterial communities in all tested habitats, and we cannot conclusively endorse one primer set over the other.

Despite the overall similar performance, our results have also shown that the V3-V4 primer set performs better in capturing the bacterial diversity on a higher taxonomic resolution. Such characteristic might be important in studies which are focusing on a specific bacterial taxonomic group and its diversity (e.g., oligotypes) or the rare biosphere. On the other hand, the V4-V5 primer has the clear advantage, which was not addressed in the scope of this study, of covering not only the bacterial domain but also the *Archaea*. It has already been demonstrated elsewhere that this domain may play an important ecological role in marine ecosystems, especially in the deep ocean water column, but they remain so far largely understudied. Thus, we suggest that the selection between these two primer sets should be done based on the aim of the study, and the research question.

3.5 Materials and methods

3.5.1 Sample collection

The samples were collected during the Polarstern cruise PS99.2 to the Long-term ecological research (LTER) site HAUSGARTEN in Fram Strait (June 24th – July 16th 2016), and Polarstern cruise PS101 to the central Arctic Ocean (September 9th – October 23rd 2016).

- The sea-ice cores were collected using an ice corer (9 cm diameter; Kovacs Enterprise, Roseburg, OR, United States), cut into two equal sections and melted in plastic containers (previously rinsed with ethanol and ultrapure water). The melting of the sea ice took around 24 hours and the samples were immediately filtered on 0.22 µm Sterivex© as soon as the last piece of sea ice melted.

- The water sampling was carried out using 12 L Niskin bottles mounted on a CTD rosette (Sea-Bird Electronics Inc. SBE 911 plus probe), and also filtered on 0.22 μm Sterivex© membranes.
- The deep-sea sediment cores were retrieved by a TV-guided multicorer and subsamples of the uppermost centimeter of the core was collected with syringes. All Sterivex© membranes and deep-sea samples were stored at −20° C until further processing.

3.5.2 DNA isolation and 16S amplicon sequencing

Genomic DNA was isolated in a combined chemical and mechanical procedure using the PowerWater DNA Isolation Kit for sea ice and water samples, and PowerSoil DNA Isolation Kit for sediment samples (MO BIO Laboratories, Inc., Carlsbad, CA, USA). Prior to DNA isolation, the 0.22 μm Sterivex© membrane cartridges of the seawater and sea ice samples were cracked open in order to place the filters into the kit-supplied bead beating tubes. The isolation was continued according to the manufacturer's instructions, and DNA was stored at −20° C. Library preparation was performed according to the standard instructions of the 16S Metagenomic Sequencing Library Preparation protocol (Illumina, Inc., San Diego, CA, USA). Two different hypervariable regions of the bacterial 16S rRNA gene were amplified using aliquots of the isolated DNA from each sample. The V3-V4 region was amplified using the S-D-Bact-0341-b-S-17 (5'-CCTACGGGNGGCWGCAG-3') and the S-D-Bact-0785-a-A-21 (5'-GACTACHVGGGTATCTAATCC-3') primer set (Klindworth *et al.*, 2013). And the V4-V5 regions was amplified using the 515F-Y (5'-GTGYCAGCMGCCGCGGTAA-3') and the 926R (5'-CCGYCAATTYMTTTRAGTTT-3') primer set (Parada *et al.*, 2016). Sequences were obtained on the Illumina MiSeq platform in a 2 × 300 bp paired-end run (CeBiTec Bielefeld, Germany), following the standard instructions of the 16S Metagenomic Sequencing Library Preparation protocol (Illumina, Inc., San Diego, CA, USA).

3.5.3 Bioinformatics and statistical analyses

The raw paired-end reads were primer-trimmed using cutadapt (Martin, 2011), quality trimmed using trimmomatic v0.32 with a sliding window of 4 bases and a minimum average quality of 15 (Bolger *et al.*, 2014), and merged using PEAR v0.9.5 (Bolger *et al.*, 2014). Clustering into OTUs was done with Swarm v.2.0 algorithm using default parameters (Mahé *et al.*, 2015). One representative sequence per OTU was taxonomically classified against Silva reference database (release 132; Quast *et al.*, 2013) using SINA v1.2.11 (SILVA Incremental Aligner), at a minimum alignment similarity of 0.9, and a last common ancestor consensus of 0.7 (Pruesse *et al.*, 2012). All OTUs that occurred with only a single sequence in the whole dataset (singleton), or were not taxonomically assigned to *Bacteria* were excluded from the analysis. Furthermore, the OTUs which were taxonomically assigned to mitochondria and chloroplast were removed from the datasets as well.

All the statistical analyses were conducted using R v3.4.1 (http://www.Rproject.org/) in RStudio v1.0.153 (RStudio Team, 2015). Sample data matrices were managed using the R package 'phyloseq' v1.20.0 (McMurdie and Holmes, 2013) and plots were generated using the R package 'ggplot2' v2.2.1 (Gómez-Rubio, 2017). All alpha diversity parameters and curves were obtained

using the R package 'iNEXT' v2.0.12 (Hsieh *et al.*, 2018). A prevalence threshold of 5% (2 samples) was applied to the OTU table prior to downstream analysis (i.e., in how many samples did a taxon appear at least once; Callahan *et al.*, 2016).

3.5.4 CAtalyzed reporter deposition Fluorescence In Situ Hybridization (CARD-FISH)

Water samples were filtered onto 0.2 μm polycarbonate Nucleopore Track-Etched filters (Whatman, Buckinghamshire, UK), and stored at -20°C. CARD-FISH was performed according to Pernthaler et al. (2002). Briefly, filters were embedded in 0.2% low-gelling-point agarose, treated with lysozyme (10 mg/mL in 0.05 M EDTA, pH 8.0, and 0.1 M Tris-HCl, pH 8.0; Sigma-Aldrich Chemie GmbH, Hamburg, Germany) for 1 hour at 37°C. After the inactivation of endogenous peroxidases with 0.15% H_2O_2 in methanol for 30 min filters were hybridized at 46°C with horseradish-peroxidase (HRP)-labelled oligonucleotide probes (biomers.net GmbH, Ulm, Germany), at 0.2 ng/ml final concentration of each probe, and the corresponding formamide concentration in the hybridization buffer (Table 3.S2). After washing at 48°C for 10 min the tyramide signal was amplified for 45 min at 46°C. Afterwards, the cells were counterstained with the nucleic acid dye 4,6-diamidino-2-phenylindole DAPI (Thermo Fisher Scientific GmbH, Bremen, Germany) at 1 μg/mL final concentration in water for 10 min at 46°C, followed by embedding the filter in 4:1 Citifluor (Citifluor Ltd, London, United Kingdom) and Vectashield (Vector Laboratories, Inc., Burlingame, United States), and freezing at -20°C.

3.5.5 Automated image acquisition and cell counting

CARD-FISH filters were evaluated microscopically using a Zeiss Axio Imager.Z2 stand (Carl Zeiss MicroImaging GmbH, Jena, Germany), which is equipped with a multipurpose fully automated microscope imaging system (MPISYS), a Colibri LED Light source illumination system (LED emitting 365 ± 4.5 nm for DAPI excitation, 470 ± 14 nm for Alexa Fluor 488 excitation, and 590 ± 17.5 nm for Alexa Fluor 594 excitation), and a multi-filter set 62HE (Carl Zeiss MicroImaging GmbH, Jena, Germany) to allow the passing of all desired wavelengths without physical rotation during recording. Pictures were taken via a cooled charged-coupled-device (CCD) camera (AxioCam MRm; Carl Zeiss AG, Oberkochen, Germany) coupled to the AxioVision Rel.4.8 software (Carl Zeiss AG, Oberkochen, Germany) After manual inspection of the filters, exposure times were adjusted in the AxioVision Rel.4.8 software to fit the DAPI and CARD-FISH signals. The filter pieces were located on the slides with the SamLoc 1.7 tool (Zeder et al. 2011), and 55 fields of view (FOV) with a minimum distance of 0.25 mm and in z-stack via autofocus were imaged per filter piece (Zeder and Pernthaler 2009) using a 63x oil objective with a numerical aperture of 1.4 (Carl Zeiss AG, Oberkochen, Germany), and a pixel size of 0.1016 μm/pixel.

Automated cell detection and counting was performed in the software Automated Cell Measuring and Enumeration Tool ACMEtool3 (2014; M. Zeder, Technobiology GmbH, Buchrain, Switzerland), where objects were counted in DAPI or FISH channels according to parameter thresholds set manually.

3.6 Supplementary material

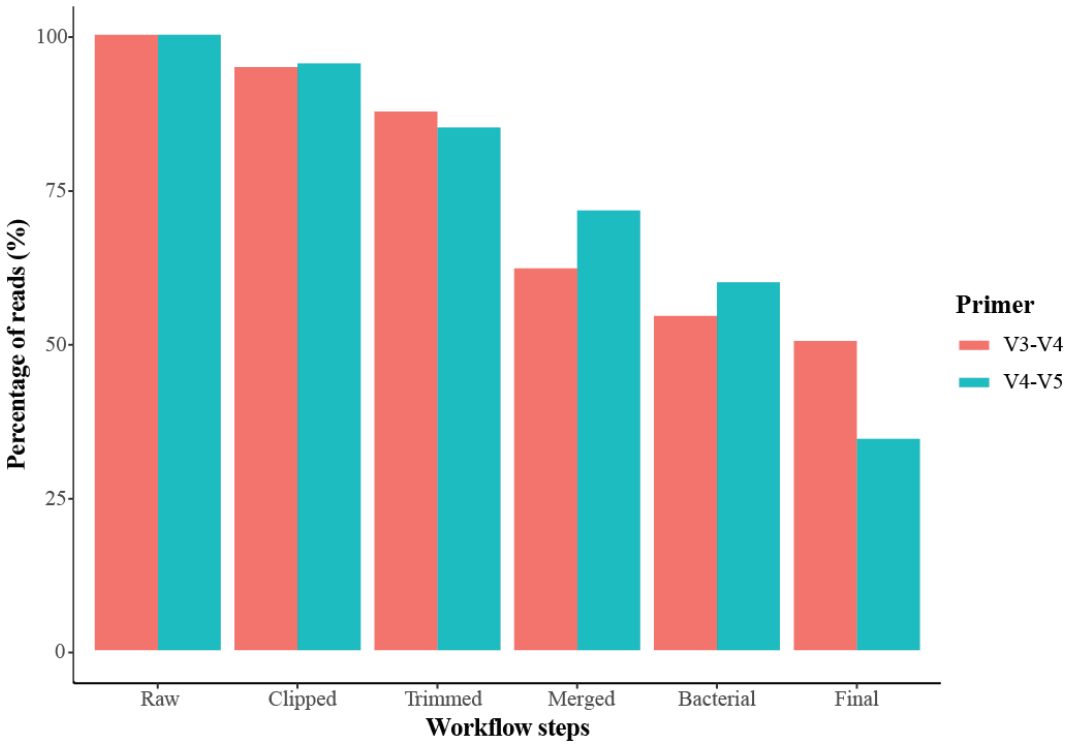

Figure 3.S1: Number of retained sequences after each step of the bioinformatic workflow. The 'Bacterial' value represents the number of sequences after quality control, singletons removal and taxonomic assignment to *Bacteria*. The 'Final' value represent the amount of sequences after exclusion of chloroplast and mitochondrial sequences.

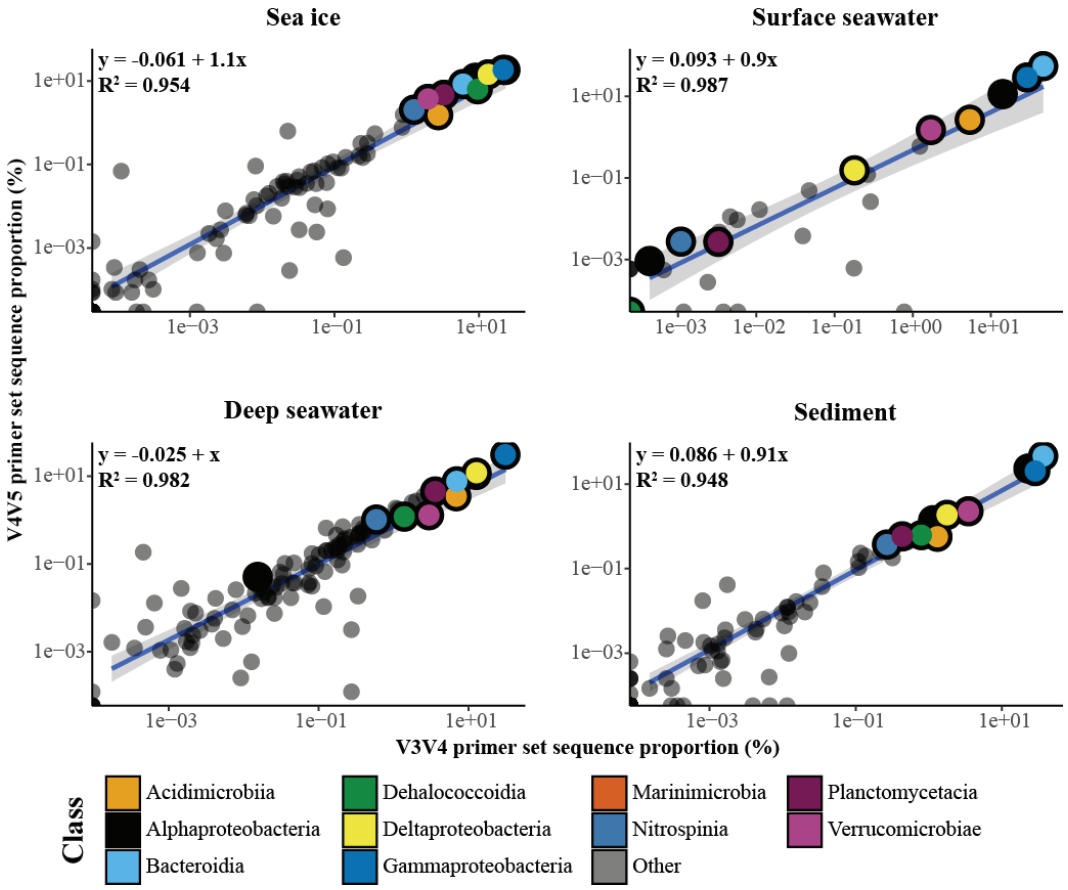

Figure 3.S2: Linear correlation in sequence proportions of different taxonomical classes between the V3-V4 and V4-V5 primer sets. The colored classes represent taxonomic lineages of interest in Arctic Ocean microbiome. The gray line represents 95% confidence interval.

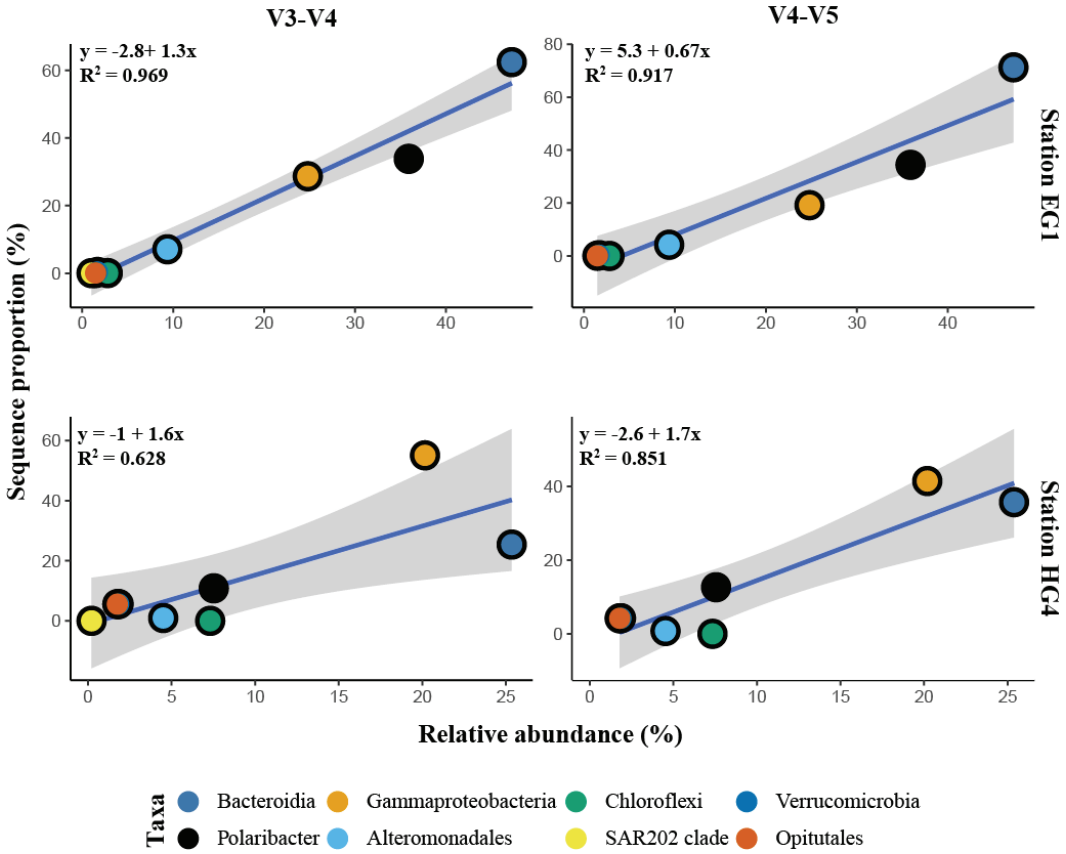

Figure 3.S3: Linear correlation of key taxonomic group representation, between 16S rRNA gene sequence proportion and relative abundance in cell counts using CARD-FISH. The colored classes represent taxonomic lineages of interest in Arctic Ocean microbiome. The gray line represents 95% confidence interval of the linear model.

Table 3.S1: Details of samples used for the primers comparison analysis. Number of sequences after QC represents the number of sequences after the bioinformatic workflow and removal of singletons. The number of bacterial sequences represents the final number of bacterial sequences, after removal of mitochondrial and chloroplast-associated sequences.

Expedition	StationID	PANGAEA stationID	Sample type	Sample depth (m)	No. of seq. after QC (V3-V4)	No. of bac. seq. (V3-V4)	Retained (%) (V3-V4)	No. of OTUs (V3-V4)	No. of seq. after QC (V4-V5)	No. of bac. seq. (V4-V5)	Retained (%) (V4-V5)	No. of OTUs (V4-V5)
PS99	48	PS99/48	Ice	0	217601	57841	26	1004	176743	95843	54	516
PS99	51	PS99/51	Ice	0	180343	38308	21	631	152382	54458	35	444
PS99	53	PS99/53	Ice	0	169777	42604	25	651	172048	86711	50	579
PS99	59	PS99/59	Ice	0	159668	34001	21	659	91326	30654	33	353
PS99	41	PS99/41	Sediment	2344	135067	81591	60	9219	288721	189113	65	12245
PS99	42	PS99/42	Sediment	2460	86775	49497	57	7320	382560	257806	67	13621
PS99	48	PS99/48	Sediment	2604	114178	62244	54	7089	204849	131711	64	10593
PS99	51	PS99/51	Sediment	1002	79007	48755	61	6797	351279	233191	66	12150
PS99	52	PS99/52	Sediment	2708	66784	40006	59	6635	157973	106588	67	10094
PS99	53	PS99/53	Sediment	2604	110525	71381	64	8155	144358	90425	62	9309
PS99	57	PS99/57	Sediment	1544	74420	36800	49	6964	118818	76349	64	9943
PS99	43	PS99/43	Water	10	216979	132797	61	1676	189207	75745	40	642
PS99	43	PS99/43	Water	28	190178	95773	50	1473	220098	49377	22	627
PS99	51	PS99/51	Water	5	52557	18730	35	509	135350	53229	39	615
PS99	51	PS99/51	Water	13	43250	11792	27	483	147127	37642	25	649
PS99	62	PS99/62	Water	10	263623	165960	62	1733	138043	54498	39	532
PS99	62	PS99/62	Water	20	332173	225131	67	1914	214565	114693	53	781
PS101	97	PS101/97	Water	50	96760	49359	51	1522	117601	57006	48	1060
PS101	97	PS101/97	Water	200	105109	47825	45	2403	123973	56420	45	1808
PS101	97	PS101/97	Water	400	119155	57107	47	2669	113597	53006	46	1996
PS101	97	PS101/97	Water	600	91680	43670	47	2334	123639	56663	45	2037
PS101	97	PS101/97	Water	853	91762	42285	46	2386	91129	40922	44	1958

Expedition	StationID	PANGAEA stationID	Sample type	Sample depth (m)	No. of seq. after QC (V3-V4)	No. of bac. seq. (V3-V4)	Retained (%) (V3-V4)	No. of OTUs (V3-V4)	No. of seq. after QC (V4-V5)	No. of bac. seq. (V4-V5)	Retained (%) (V4-V5)	No. of OTUs (V4-V5)
PS101	126	PS101/126	Water	10	167233	83909	50	2217	76331	43894	57	543
PS101	126	PS101/126	Water	200	93355	42658	45	2250	104382	48474	46	1739
PS101	126	PS101/126	Water	400	106434	51835	48	2482	88159	42764	48	1936
PS101	126	PS101/126	Water	600	131192	65779	50	2574	116848	61338	52	2067
PS101	126	PS101/126	Water	1000	111732	57405	51	2781	102131	46518	45	2110
PS101	149	PS101/149	Water	1.5	191021	102166	53	2365	119553	76303	63	693
PS101	149	PS101/149	Water	200	102198	55979	54	2175	74752	36213	48	1617
PS101	149	PS101/149	Water	400	135954	73133	53	2900	114809	55268	48	2077
PS101	149	PS101/149	Water	600	97822	50741	51	2271	119618	56250	47	2149
PS101	149	PS101/149	Water	750	145910	78558	53	2908	95485	43695	45	2077
PS101	172	PS101/172	Water	1	97457	54741	56	1383	118248	75436	63	543
PS101	172	PS101/172	Water	200	177595	93849	52	3132	104026	51371	49	1787
PS101	172	PS101/172	Water	400	140191	75218	53	2858	74619	36567	49	1838
PS101	172	PS101/172	Water	600	186160	95967	51	3187	108438	52965	48	2018
PS101	172	PS101/172	Water	620	183399	97112	52	3255	69513	35270	50	1829
PS101	175	PS101/175	Water	10	123796	64593	52	1688	104457	66680	63	879
PS101	175	PS101/175	Water	50	116327	61685	53	1667	88704	45777	51	1092
PS101	175	PS101/175	Water	200	163028	81546	50	2950	100926	55551	55	1743
PS101	175	PS101/175	Water	1000	118559	61952	52	2442	73229	38081	52	1645
PS101	175	PS101/175	Water	2000	137072	71178	51	2724	93667	50402	53	2063
PS101	175	PS101/175	Water	3000	98005	48460	49	2060	130479	70628	54	2096
PS101	175	PS101/175	Water	3230	101732	53165	52	2056	103380	55522	53	1916

Table 3.S2: Details of the selected CARD-FISH probes for microscopic cell counting. FA- formamide concentration in hybridization buffer.

Probe name	Target group	Sequence 5'-3'	FA (%)	Reference
EUB338-I	Bacteria	GCTGCCTCCCGTAGGAGT	35	Amann et al. (1990)
EUB338-II	Planctomycetales	GCAGCCACCCGTAGGTGT	35	Daims et al. (1999)
EUB338-III	Verrucomicrobia	GCTGCCACCCGTAGGTGT	35	Daims et al. (1999)
PSA184	Pseudoalteromonadaceae	CCCCTTTGGTCCGTAGAC	30	Eilers et al. (2000)
Gam42a	Gammaproteobacteria	GCCTTCCCACATCGTTT	35	Manz et al. (1992)
Bet42a	unlabeled competitor for Gam42a	GCCTTCCCACTTCGTTT	35	Manz et al. (1992)
POL740	Polaribacter	CCCTCAGCGTCAGTACATAGT	35	Malmstrom et al. (2007)
CF968	Bacteroidetes	GGTAAGGTTCCTCGCGTA	35	Acinas et al. (2014)
Opi346	Opitutae	TTCGAAACTGCTGCCACC	20	Reintjes et al. unpublished
Non338	Control	ACTCCTACGGGAGGCAGC	35	Wallner et al. (1993)

Chapter 4

Microbial communities in the East and West Fram Strait during sea-ice melting season

Eduard Fadeev[1,2], Ian Salter[1,3], Vibe Schourup-Kristensen[1], Eva-Maria Nöthig[1], Katja Metfies[1,4], Anja Engel[5], Judith Piontek[5], Antje Boetius[1,2] and Christina Bienhold[1,2]

[1] Alfred Wegener Institute for Polar and Marine Research, Bremerhaven, Germany

[2] Max Planck Institute for Marine Microbiology, Bremen, Germany

[3] Faroe Marine Research Institute, Torshavn, Faroe Islands

[4] Helmholtz Institute for Functional Marine Biodiversity, Oldenburg, Germany

[5] GEOMAR Helmholtz Centre for Ocean Research, Kiel, Germany

Keywords: Arctic Ocean, phytoplankton bloom, microbial interactions, bacterioplankton, network analysis

This chapter was previously published in Fadeev *et al.* (2018).

4.1 Abstract

Climate models project that the Arctic Ocean may experience ice-free summers already in the second half of this century. This may have severe repercussions on phytoplankton bloom dynamics and the associated cycling of carbon in surface waters. We currently lack baseline knowledge of the seasonal dynamics of Arctic microbial communities, which is needed in order to better estimate the effects of such changes on ecosystem functioning. Here we present a comparative study of polar summer microbial communities in the ice-free (eastern) and ice-covered (western) hydrographic regimes at the LTER HAUSGARTEN in Fram Strait, the main gateway between the Arctic and North Atlantic Oceans. Based on measured and modeled biogeochemical parameters, we tentatively identified two different ecosystem states (i.e., different phytoplankton bloom stages) in the distinct regions. Using Illumina tag-sequencing, we determined the community composition of both free-living and particle-associated bacteria as well as microbial eukaryotes in the photic layer. Despite substantial horizontal mixing by eddies in Fram Strait, pelagic microbial communities showed distinct differences between the two regimes, with a proposed early spring (pre-bloom) community in the ice-covered western regime (with higher representation of SAR11, SAR202, SAR406 and eukaryotic MALVs) and a community indicative of late summer conditions (post-bloom) in the ice-free eastern regime (with higher representation of *Flavobacteria*, *Gammaproteobacteria* and eukaryotic heterotrophs). Co-occurrence networks revealed specific taxon-taxon associations between bacterial and eukaryotic taxa in the two regions. Our results suggest that the predicted changes in sea-ice cover and phytoplankton bloom dynamics will have a strong impact on bacterial community dynamics and potentially on biogeochemical cycles in this region.

4.2 Introduction

In recent decades, Arctic warming has resulted in remarkable environmental changes in the Arctic Ocean, and the region is warming much faster than the global mean rate(Dobricic *et al.*, 2016; Sun *et al.*, 2016). Arctic sea-ice has been declining by approximately 50% since the late 1950s, and its extent is shrinking at approximately 10% per decade since the late 1990s (Kwok and Rothrock, 2009; Peng and Meier, 2017). Current predictions indicate that the Arctic Ocean may experience ice-free summers by the second half of this century (Polyakov *et al.*, 2017). In addition, recent observations suggest increasing temperatures of the Atlantic water inflow (Walczowski *et al.*, 2017). The combination of these environmental changes results in weakened stratification of the water column and increased vertical mixing of the deep Atlantic core water, a process also termed 'Atlantification' (Polyakov *et al.*, 2017). Based on these observations, the general agreement is that the Arctic Ocean is currently in a transitional phase towards warmer conditions (Dmitrenko *et al.*, 2008; Polyakov *et al.*, 2017, 2005).

The 450 km wide Fram Strait is the only deep gateway to the Arctic Ocean, and has two distinct hydrographic regimes. In the eastern part of Fram Strait, the northward flowing West Spitsbergen Current (WSC), transports relatively warm and saline Atlantic water into the Arctic Ocean (Beszczynska-Moller *et al.*, 2012; von Appen *et al.*, 2015). The East Greenland Current (EGC) flows southwards along the Greenland shelf, transporting cold polar water and exporting ap-

proximately 90% of the Arctic sea-ice to the North Atlantic (de Steur *et al.*, 2009). These distinct water masses are separated by the East Greenland Polar Front system (Paquette *et al.*, 1985). However, recent ocean simulation analyses show substantial horizontal mixing and exchange by eddies (Wekerle *et al.*, 2017a). Repeated summer sampling in the water column and at the seafloor of the Fram Strait, as part of the Long Term Ecological Research (LTER) site HAUSGARTEN, have revealed major ecological variations associated with anomalies of Atlantic Water inflow (Soltwedel *et al.*, 2016). Examples for such variations were a slow increase in phytoplankton biomass and shifts in microbial eukaryotic species composition which followed the Atlantic Water warming event in 2005-2007 (Nöthig *et al.*, 2015). This included a transition from diatom to flagellate (e.g., *Phaeocystis*) dominated communities during the summer months (Engel *et al.*, 2017; Nöthig *et al.*, 2015). Recent model predictions showed substantial differences in carbon export following diatom- or flagellate- dominated phytoplankton blooms (Vernet *et al.*, 2017; Wollenburg *et al.*, 2018). Depending on timing, flagellate dominated blooms may result in increasing abundance of microzooplankton (e.g., ciliates) and a more active microbial loop, or a more rapid export in connection with sea-ice formed mineral precipitation. Furthermore, a year round study of physical and biogeochemical hydrography in the WSC suggested that the ongoing 'Atlantification' in the region is leading to increased pelagic primary productivity (Randelhoff *et al.*, 2018). However, the harsh climatic conditions in the open Arctic Ocean during winter typically limit sampling opportunities to the Arctic summer season, so that seasonal dynamics within the pelagic ecosystem, especially in ice-covered parts of the Arctic, remain understudied (Nöthig *et al.*, 2015; Soltwedel *et al.*, 2016). Phytoplankton bloom dynamics may, to some extent, be monitored using remote sensing of chlorophyll a (chl a) by satellites in ice-free ocean areas, with substantial limits due to Arctic fog and the dark season (Perrette *et al.*, 2011). However, monitoring the dynamics of heterotrophic microorganisms requires physical sampling. Wilson and colleagues (2017) were the first to describe changes of bacterial community composition in the eastern Fram Strait throughout a polar year. In accordance with observations from other polar regions (Alonso-Sáez *et al.*, 2008; Ghiglione *et al.*, 2012; Iversen and Seuthe, 2011; Williams *et al.*, 2012), their results showed that the extreme seasonality of polar marine ecosystems, with ice-covered dark winter conditions and extended irradiance in summer, leads to pronounced seasonal differences in heterotrophic bacterial communities. Winter-time bacterial communities in the upper water column showed higher phylogenetic and functional diversity compared to the summertime, with increased importance of chemolithotrophic processes (e.g., Alonso-Sáez *et al.*, 2014; Müller *et al.*, 2018). During late spring, the increasing irradiance and decreasing sea-ice cover initiate large phytoplankton blooms, which can lead to major shifts in heterotrophic bacterial community composition.

Biological interactions among microbes are important drivers of the dynamics in pelagic microbial communities (Fuhrman *et al.*, 2015). Specific interactions between phytoplankton and heterotrophic bacteria have been documented, many of which are based on the exchange of energy sources, metabolites, including various forms of chemical signaling (Cole, 1982; Grossart *et al.*, 2006a; Grossart and Simon, 2007; Ramanan *et al.*, 2016). Analyses of bacterial communities co-occurring with diatoms, using advanced molecular approaches, revealed complex interspecies signaling (Amin *et al.*, 2012). While a full characterization of such interactions requires targeted experiments under laboratory conditions, currently available molecular methods in combination with network analyses allow us to identify potential interactions directly from

environmental samples (e.g., Chafee *et al.*, 2018; Gilbert *et al.*, 2012; Lima-Mendez *et al.*, 2015; Milici *et al.*, 2016; Peura *et al.*, 2015).

One such interaction with relevance to the proportion of pelagic recycling versus carbon export is the mechanical association of bacteria with plankton detritus. Pelagic bacteria have different strategies to tap into the detritus pool, free-living in the water column or associated with particulate matter (Stocker and Seymour, 2012). Previous studies of microbial associations revealed strong differences between potential associations of free-living (FL) and particle-associated (PA) bacteria with microbial eukaryotes (Lima-Mendez *et al.*, 2015; Milici *et al.*, 2016). While the FL fraction is often dominated by cosmopolitan oligotrophic bacteria that rely on the availability of organic matter in the dissolved fraction (Giovannoni *et al.*, 2014; Morris *et al.*, 2012), the PA fraction is usually represented by copiotrophic motile bacteria which colonize living or decaying microbial eukaryotes, fecal pellets, gel-like particles or other forms of particulate organic matter (Busch *et al.*, 2017; Herndl and Reinthaler, 2013; Simon *et al.*, 2002).

Microbiological studies of the photic layer of Fram Strait have so far focused on eukaryotic plankton (Kilias *et al.*, 2013; Metfies *et al.*, 2016; Nöthig *et al.*, 2015), and biogeochemical recycling of detritus by bacteria (Piontek *et al.*, 2014, 2015). Very little is known about the composition and dynamics of bacterial communities in this region. Bacteria are key players in the biogeochemical cycling of carbon and nutrients in the water column (Azam and Malfatti, 2007; Falkowski *et al.*, 2008), and baseline knowledge about these communities and their main drivers is needed, in order to project future changes in the pelagic ecosystem of Fram Strait, such as warming and acidification. Using a set of measured and modeled environmental parameters and sequence-based assessments of microbial community composition, the objectives of the study were: (1) to identify differences in bacterial community composition in the two hydrographic regimes of Fram Strait in relation to hydrographical and biogeochemical parameters; (2) to test whether these differences are related to specific productivity phases of the Arctic pelagic ecosystem; (3) to assess whether and to what extent these differences are reflected in specific taxon-taxon associations between bacterial and eukaryotic community members.

4.3 Results

4.3.1 Phytoplankton bloom dynamics across Fram Strait

Based on previously defined physical characteristics of the two main currents of Fram Strait (Rudels *et al.*, 2013), we identified two origins of our sample sets: (1) the eastern Fram Strait with warmer and more saline Atlantic Water of the WSC; (2) the western Fram Strait with colder and less saline Polar Water of the EGC (Figure 4.1). The two regions had distinct sea-ice conditions at the time of sampling, with an ice-covered regime in EGC and an ice-free regime in WSC (Figure 4.1). Furthermore, measured chl a concentrations showed higher concentrations in the WSC, and chl a was present down to water depths of more than 100 m in this region (Figure 4.1).

In WSC all measured inorganic nutrients (silicate - SiO3, nitrate - NO3 and phosphate - PO4) showed lower concentrations near the surface compared to deeper water layers below the pycnocline (roughly below 50 m). Contrary, in EGC there were only small differences in nutrient

concentrations throughout all measured depths. In addition, while measurements of SiO3 and PO4 concentrations in deeper water layers were similar between the regions, NO3 concentrations were lower in EGC (Figure 4.S1). The depth of the water column pycnocline represents the mixed layer depth during the last winter (Rudels *et al.*, 1996). Generally only the nutrients above the pycnocline within the photic zone (upper 50 m) are consumed by phytoplankton. Therefore, the calculated differences in nutrient concentrations (Δ) below and above the seasonal pycnocline provide a proxy estimation for phytoplankton productivity in the different regions, since the beginning of the seasonal bloom (Table 4.1). The estimated productivity (since the beginning of the seasonal bloom) based on the stoichiometry of consumed nutrients (see Material and Methods), as well as the integrated chl a and phytoplankton carbon biomass all showed higher values in WSC. Furthermore, based on a ratio 1:1 of NO3:SiO3 we estimated that the contribution of diatoms to the total productivity was roughly 30% in both regions. However, biomass estimates of diatoms showed a much larger fraction (50%) of the total phytoplankton biomass in EGC at the time of sampling.

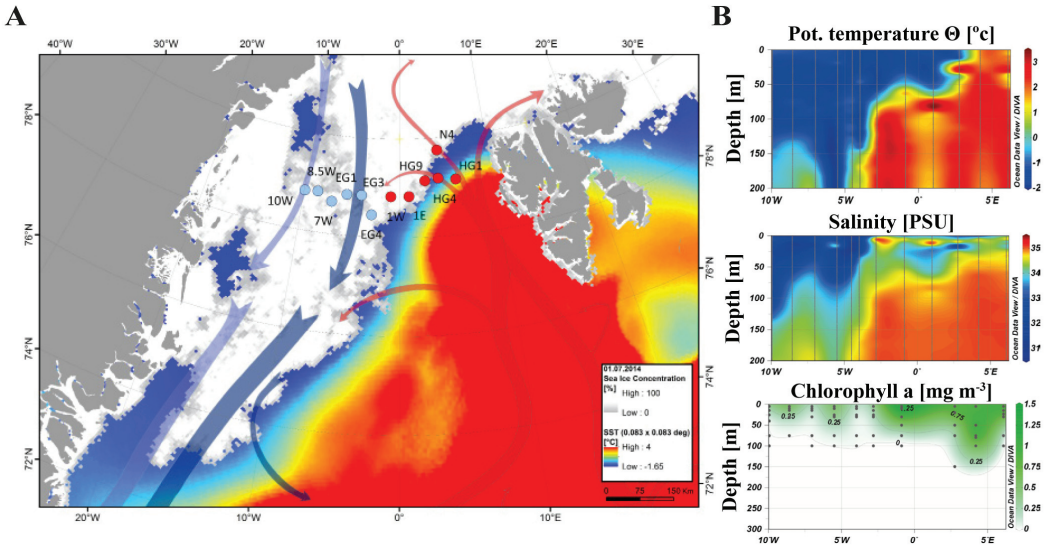

Figure 4.1: Regional separation of Fram Strait. The longitudinal coordinates of the EGC region are 10W-1W, and for the WSC region 1W-6E. (**A**) Monthly average of sea-ice coverage and sea surface temperature during June 2014. The satellite remote sensing sea-ice concentration data were obtained from http://www.meereisportal.de (Spreen et al., 2008). The ice concentration is represented by inverted grayscale (gray-low, white-high). Sea surface temperature was obtained from NOAA NCEP real-time analysis (http://polar.ncep.noaa.gov/sst/). The arrows represent general directions of the WSC (in red) and the EGC (in blue). Map: AWI/Laura Hehemann. The map was produced using ArcMap (ver.10.5) with Esri world countries dataset (www.esri.com) in a WGS 1984 Arctic Polar Stereographic map projection. (**B**) Physical characteristics of the water column from CTD (Conductivity-Temperature-Depth) sensors and chl a measured in situ. The plot was generated using Ocean Data View (v4.7.10; Schlitzer, 2015).

To verify that these differences in biogeochemical parameters represent different ecosystem states, we used surface chl a dynamics of the biogeochemical model FESOM-REcoM2 set to the studied dates, to estimate the phytoplankton bloom stages in the two regions. Because of the lack of remote sensing measurements of chl a for the ice-covered regions, we could only use the ice-free region for calibration (Figure 4.S9). In the model, a strong relationship between the

estimates of chl a and the shifting sea-ice edge was observed (Figure 4.2). In the beginning of June, surface chl a concentrations were elevated in the whole ice-free area of WSC, while they remained very low in the ice-covered EGC (Figure 4.2). In the second half of June 2014, with the ice thinning and the sea-ice edge shifting westwards, an increase in surface chl a concentrations was observed also in EGC (Figure 4.2).

Table 4.1: Comparison of nutrient consumption, phytoplankton biomass and productivity between the EGC and WSC regions. The values represent the mean and the standard deviation for each parameter and the number in parentheses represents the number of stations. Negative values in nutrient consumption were excluded from the mean calculation.

	EGC	WSC
Nutrient consumption (Δ)		
ΔNO3 (µmol Liter^{-1})	3.2 ± 1.2 (6)	6.4 ± 0.9 (5)
ΔSiO3 (µmol Liter^{-1})	1 ± 0.9 (5)	2.4 ± 0.9 (5)
ΔPO4 (µmol Liter^{-1})	0.07 ± 0.03 (4)	0.3 ± 0.2 (5)
Phytoplankton community		
Integrated chl. a conc. (mg m^{-3})	8.1 ± 4.8 (6)	43.3 ± 26.4 (5)
Estimated productivity since winter (g C m^{-2} yr^{-1})	250 ± 98 (6)	509 ± 73 (5)
Estimated diatom contribution to productivity (%)	32	37
Phytoplankton carbon estimate in chl a max. (mg m^{-3})	0.76 (4)	5.6 (3)
Diatom carbon estimate in chl a max. (mg m^{-3})	0.28 (4)	0.49 (3)
Estimated diatom contribution to phytoplankton biomass in chl a max. (%)	36	8

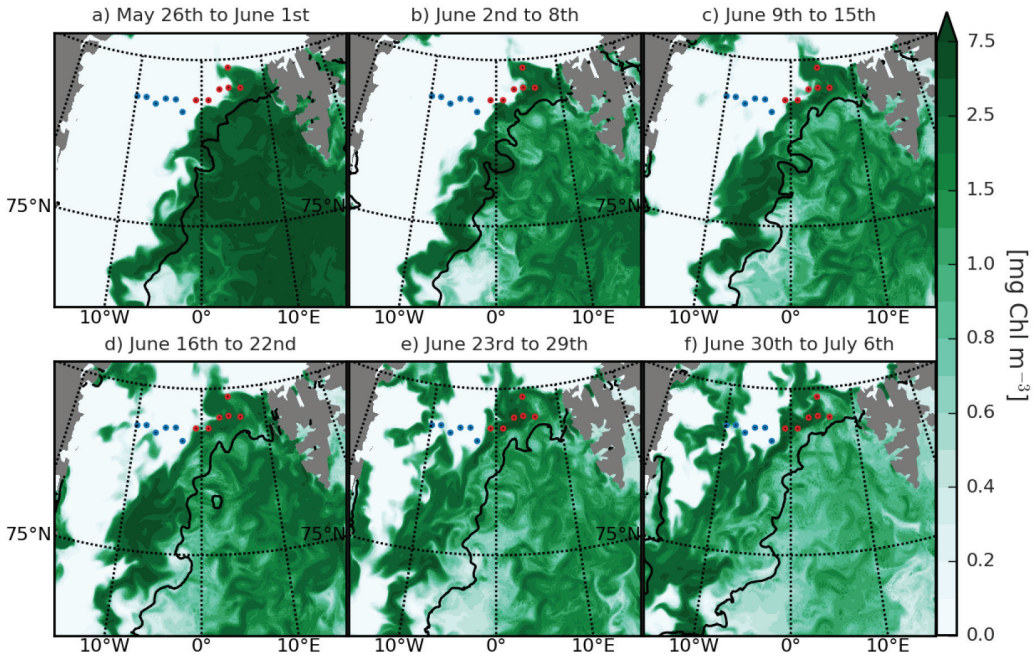

Figure 4.2: Modeled weekly surface chl a concentration in Fram Strait during June 2014. The black line marks the 10% ice concentration iso-line. Red and blue dots mark the location of sampling stations in the WSC and EGC regions, respectively, based on the observed characteristics in this study. For comparison between the modeled chl a with remote sensing and in-situ measurements, please refer to the supplementary material.

4.3.2 Differences in microbial community composition between the eastern and western regions of Fram Strait

Using Illumina 16S rRNA amplicon sequencing of the V3-V4 hypervariable region, we obtained a final dataset of 2,462,994 reads (amplicons) in 63 samples, which were assigned to 7,167 OTUs associated with 406 bacterial taxonomic lineages. The OTUs which were taxonomically assigned to chloroplasts or mitochondria were excluded from further analysis. The rarefaction curves did not reach a plateau in any of the samples, and on overage the samples covered 60% of the bacterial community richness (Figure 4.S2 and Table 4.S1). However, coverage-based rarefaction estimations (i.e., Good's estimator), revealed a sample completeness higher than 98% in all samples (autoreffig:ps85-supp-fig2; Chao and Jost, 2012; Chao *et al.*, 2014b). This suggests that although additional OTUs could be expected with additional sequencing, our sequencing depth was satisfactory to represent most of the diversity within the bacterial communities.

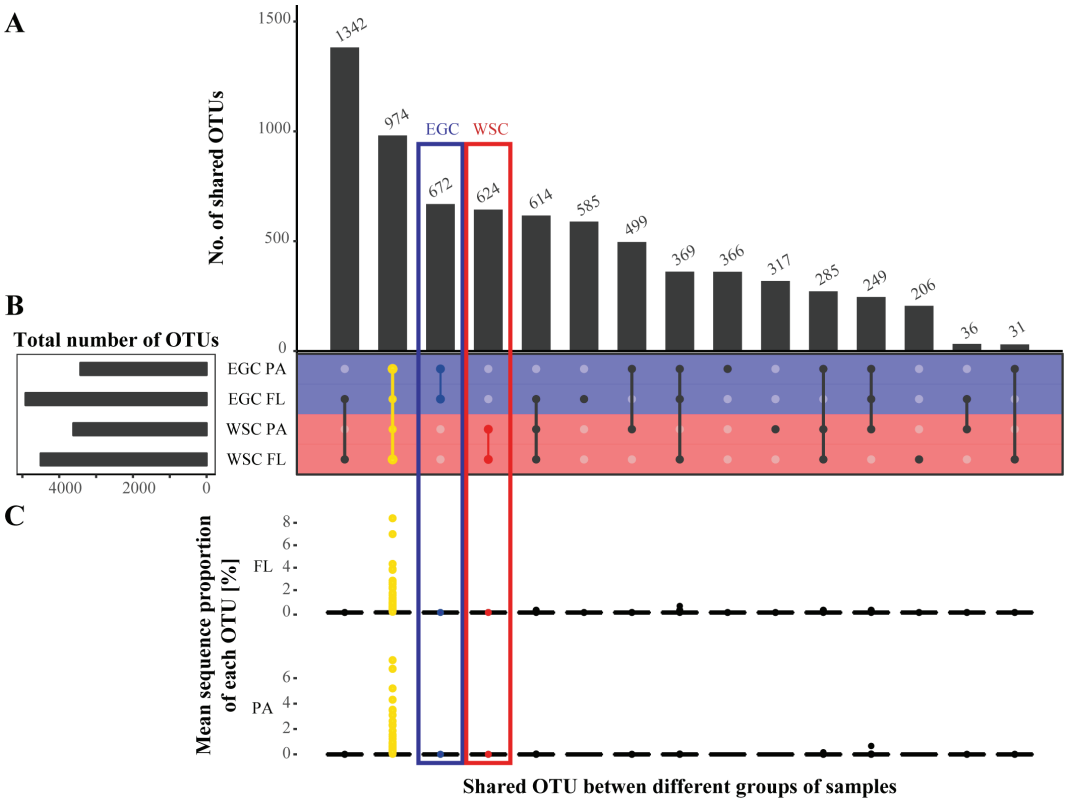

Figure 4.3: Comparison of bacterial community composition between the different regions and fractions. (**A**) Number of shared OTUs between the different regions and fractions. (**B**) Total number of OTUs in each category. (**C**) Mean sequence proportion of each OTU in each overlap group, separated by fractions. The yellow color marks the shared OTUs in the entire dataset, the red color the shared OTUs between fractions in WSC and the blue color the shared OTUs between fractions in EGC.

Comparison of bacterial community composition between the different regions and fractions was conducted based on the presence/absence of OTU (Figure 4.3). A total of 974 OTUs (13% of the total OTUs) were shared throughout the entire dataset, and represented more than 75% of all sequences. Especially the FL communities of both regions were similar. Hence, differences be-

tween the bacterial communities mainly resulted from variations in the proportional abundance of these taxa (Figure 4.4).

In order to further investigate the differences in community composition between the different regions, we performed differential abundance tests for all shared OTUs from both the FL and PA fractions using 'DESeq2'. The OTU which had a fold change of absolute values higher than 1 and an adjusted p-value <0.05 were defined as 'differentially abundant OTU' – daOTU. Furthermore, using 'GAGE' we tested for the enrichment of bacterial groups at a lower taxonomic resolution, i.e., that of bacterial families. Only bacterial families in which all OTUs were enriched in only one region and showed statistical significance (adjusted p value < 0.05), were considered to be enriched.

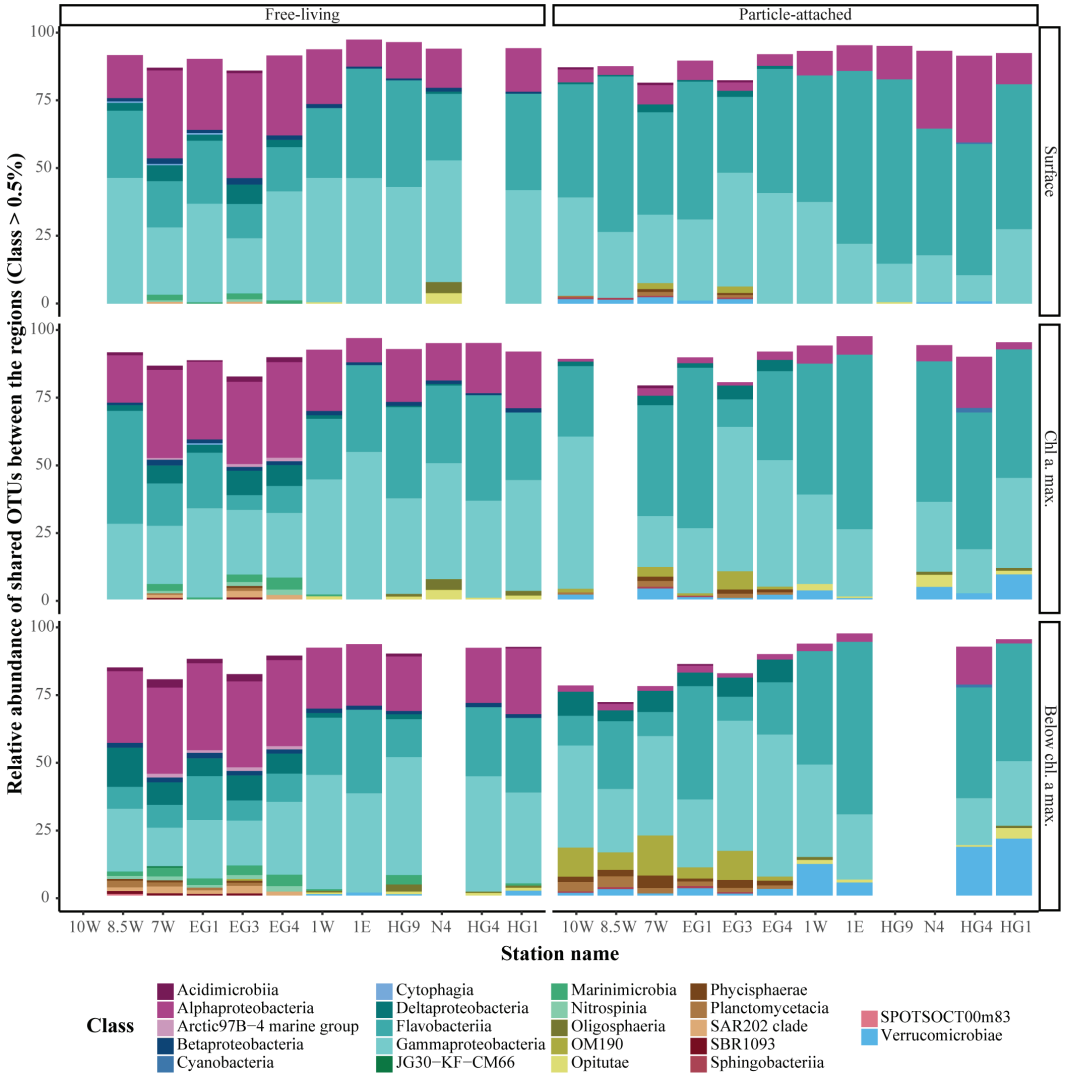

Figure 4.4: Sequence proportion overview of overlapping bacterial OTUs, between the regions in each fraction. The color code represents taxonomic classes. Only classes with sequence abundance higher than 0.5% were included in the figure.

A total of 757 (10% of all OTUs) and 869 (12% of all OTUs) daOTU were identified in the FL and PA fractions, respectively (Figure 4.S3). For both fractions, the EGC region was represented by a higher proportion of daOTU compared to the WSC (60% and 65% for FL and PA,

respectively), as well as by a higher number of sequence-enriched bacterial families (Figure 4.5). The WSC was characterized, in both fractions, by few significantly enriched families in various taxonomic groups, such as *Alphaproteobacteria* (*Rhodobacteraceae*), *Gammaproteobacteria* (*Piscirickettsiaceae*, *Porticoccaceae*). Furthermore, *Flavobacteria* (*Cryomorphaceae*) and *Gammaproteobacteria* (OM182 clade) were significantly enriched in the FL fraction of WSC. Enriched taxa in the EGC were distributed across a broader taxonomic range, with large differences also between the fractions. In the FL fraction the significantly enriched families were associated with the poorly classified *Chloroflexi* (SAR202), *Marinimicrobia* (SAR406) and *Deltaproteobacteria* (SAR324, *Bdellovibrionaceae*), as well as members of *Alphaproteobacteria* (SAR11, *Rhodospirillaceae*) and *Gammaproteobacteria* (*Colwelliaceae*, *Pseudoalteromonadaceae* and JTB255). In the PA fraction significantly enriched families were associated mainly with *Deltaproteobacteria* (*Bdellovibrionaceae*, *Bradymonadales*, *Oligoflexaceae*, NB1-j) and *Gammaproteobacteria* (*Pseudoalteromonadaceae*, *Shewanellaceae* and JTB255).

A similar workflow was applied to investigate microbial eukaryotic communities. Using Illumina 18S rRNA amplicon sequencing of the V4 hypervariable region, we obtained a final dataset of 2,396,433 reads (amplicons) in 33 samples, which were assigned to 4,419 OTUs associated with 173 eukaryotic taxonomic lineages. The eukaryotic OTUs which were taxonomically assigned to metazoa were excluded from further analysis. Rarefaction curves did not reach a plateau in any of the samples, and on overage the samples covered 75% of the eukaryotic community richness (Figure 4.S2 and Table 4.S1). Nevertheless, coverage-based rarefaction estimations (i.e., Good's estimator), revealed a sample completeness higher than 98% in all samples (autoreffig:ps85-supp-fig2; Chao and Jost, 2012; Chao *et al.*, 2014b). This suggests that although additional OTUs could be expected with additional sequencing, our sequencing depth was satisfactory to represent most of the diversity within the eukaryotic communities.

A corresponding OTU presence/absence analysis between eukaryotic communities in each region revealed that 2,502 OTUs (56% of the total OTUs) were shared between the regions (Figure 4.S4), comprising more than 80% of the sequences in all eukaryotic samples (Figure 4.6). Hence, the relatively high proportion of region-specific OTUs showed very low relative sequence abundances. Furthermore, the taxonomic groups *Syndiniales*, *Dinophyceae* (dinoflagellates) and *Diatomea* showed larger number of daOTU in EGC (Figure 4.S5). In the WSC on the other hand, the largest taxonomic group (in terms of number of daOTU) was the heterotrophic *Thecofilosea* (*Cercozoa*).

4.3.3 Environmental drivers of microbial communities in Fram Strait

Bacterial cell densities and production estimates based on leucine incorporation showed statistically significant differences between the two regions (t-test, $p < 0.001$; Figure 4.5 and Table 4.S2). The results show almost one order of magnitude higher bacterial cell densities in WSC compared to EGC, as well as higher ratios between high nucleic acid (HNA) and low nucleic acid (LNA) cells. Total bacterial productivity was higher in the WSC compared to the EGC region, while cell specific productivity (total productivity divided by cell concentration) did not show strong differences between the regions. Moreover, a principal coordinate analysis (PCoA) of bacterial community composition revealed significant differences between samples according to their geographic origin, in addition to clear differences in the community structure of FL

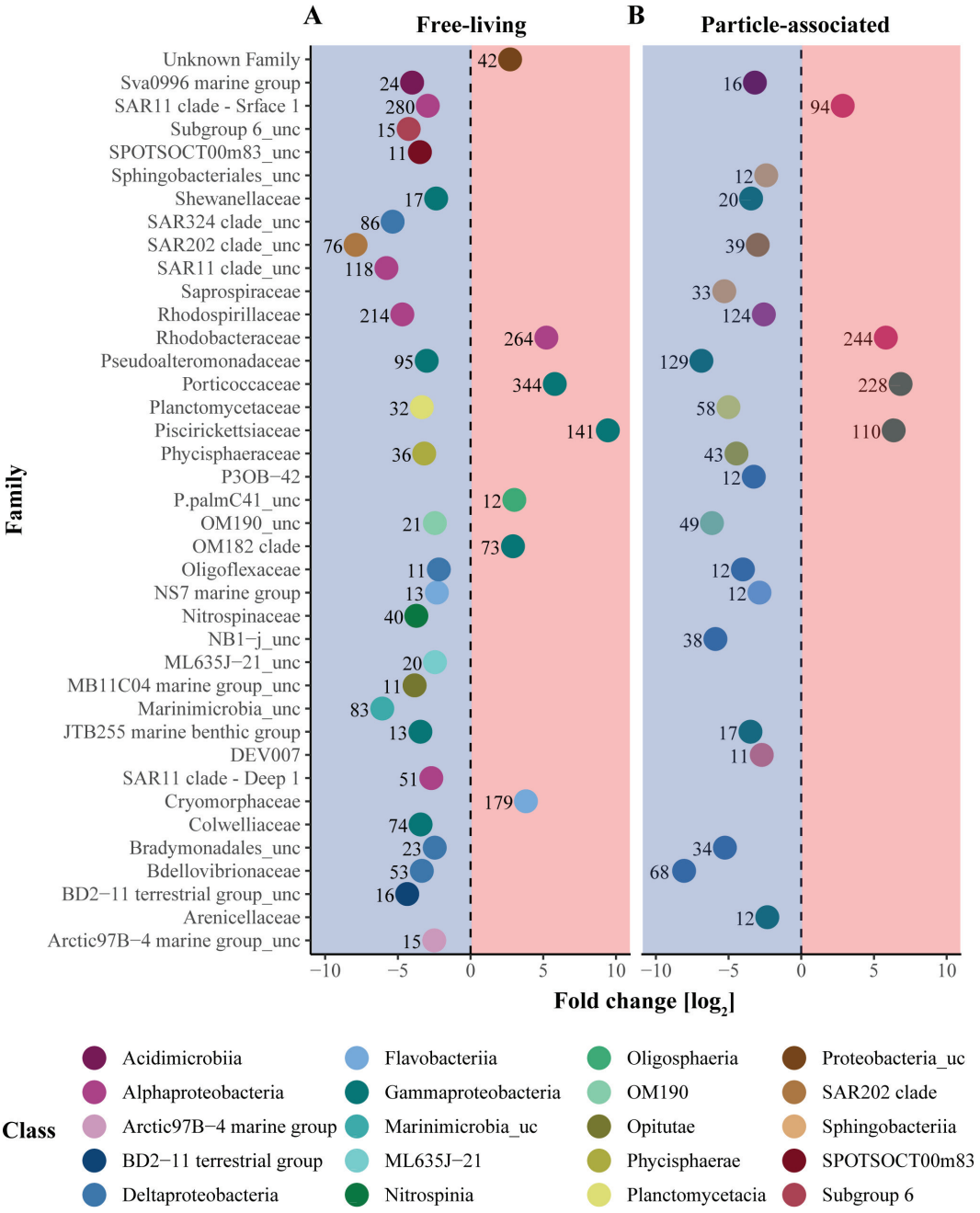

Figure 4.5: Enriched bacterial families between the regions. Taxonomic enrichment analysis was performed separately on the FL (**A**) and the PA (**B**) fractions, and only statistically significant taxa were included in data representation (adjusted p value < 0.05). The x-axis represents the $\log_2$ fold change in sequence abundance. Enrichment in the EGC region is represented in the blue area while enrichment in the WSC region is represented in the red area. The color code represents taxonomic classes and each point represents the $\log_2$ fold change of each taxonomic family. The number associated with each symbol represents the number of OTUs in the family.

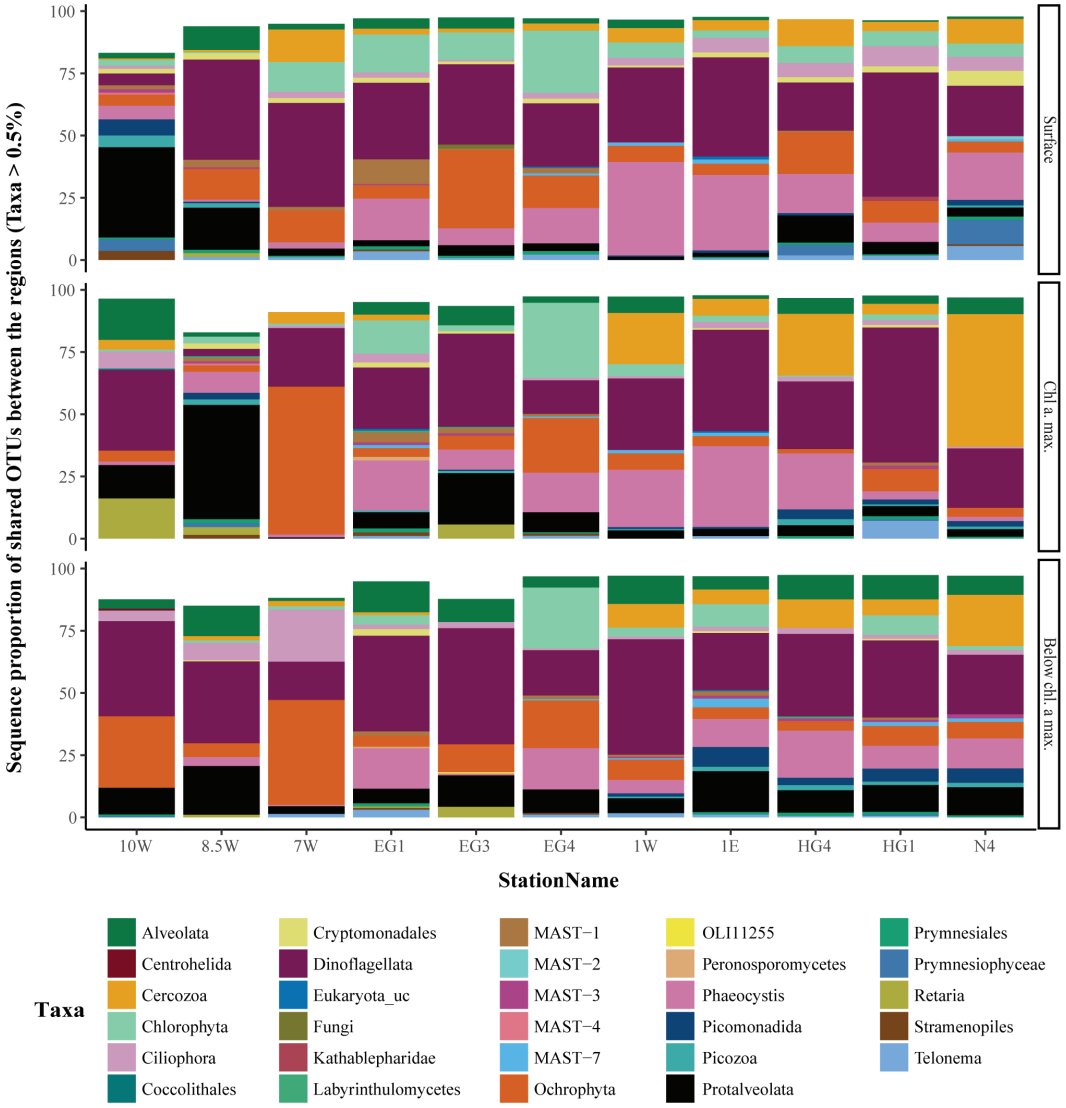

Figure 4.6: Sequence proportion overview of overlapping microbial eukaryote OTUs, between the regions. The color code represents taxonomic lineages. Only taxa with sequence abundance higher than 0.5% were included in the figure.

and PA fractions (Figure 4.7). Samples from different depths showed no clear clustering. The separation of samples according to their bacterial community structure was confirmed using a permutational multivariate analysis of variance. Similar differences between the regions were observed for the microbial eukaryotic community, with higher phytoplankton estimated biomass in the WSC (Table 4.1), and community composition clustering according to regions, although to a lesser extent than bacterial communities (Figure 4.S6).

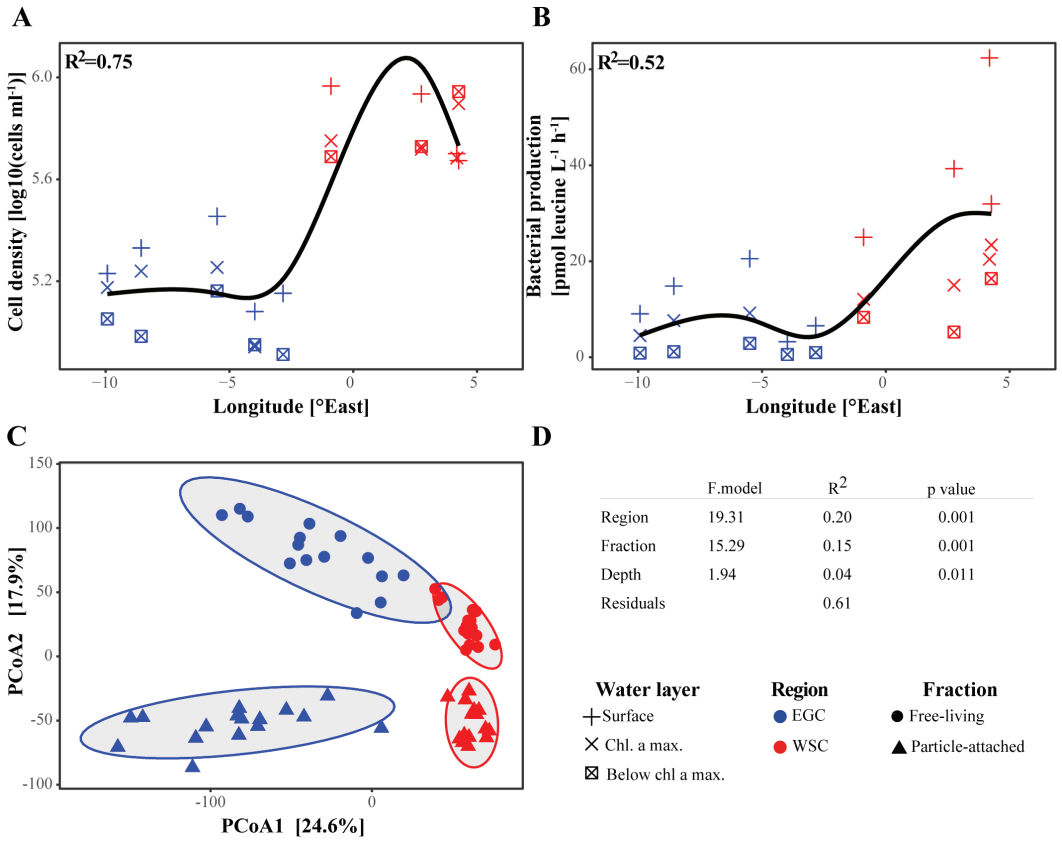

Figure 4.7: Bacterial community characteristics across the Fram Strait. (**A, B**) Bacterial cell density and production in three water layers: surface (5-10 m), chl a maximum (10-30 m) and below chl a maximum (30-60 m). By applying a generalized additive model with cubic spline we observed a longitudinal trend between the different regions (p value < 0.05, adjusted $r^2 > 0.75$). (**C**) PCoA of bacterial community composition in FL and PA fractions in all three water layers based on a Euclidean similarity matrix. The ellipses encompass each of the groups with normal confidence of 0.95. The percentages on both axes represent the explained variance of the axis. (**D**) Permutational multivariate analysis of variance between the groups of samples ('ADONIS' in R package 'vegan').

To compare the explanatory power of a range of environmental variables in structuring bacterial communities, we performed redundancy analysis (RDA) and constrained the ordination by the following environmental parameters: temperature, salinity, chl a, and consumed nutrients (ΔNO3, ΔSiO3 and ΔPO4). Due to the different environmental conditions in EGC and WSC regions, we selected these parameters to account for the combined effect of the different water masses (temperature and salinity) and different ecosystem states (chl a and nutrients). The analysis was performed separately for FL and PA bacterial communities, as the fractions may be influenced by different environmental factors (Figure 4.8). In accordance with the PCoA ordination (Figure 4.7), both FL and PA fractions exhibited a strong separation of bacterial com-

munities between EGC and WSC (mainly along RDA axis 1, which explained roughly 80% of the variance). Using a stepwise model selection test ('ordistep' algorithm in 'vegan' package), we identified that temperature, salinity and chl a were the strongest explanatory variables in the FL fraction, explaining 66% of the total variance. Community variation in the PA fraction was mainly explained by temperature, salinity, chl a and consumed nitrate (ΔNO3), which explained 63% of the total variance. A similar stepwise model selection test for the microbial eukaryotic community revealed that community variation was mainly explained by temperature, salinity, consumed silicate (ΔSiO3) and nitrate (ΔNO3), adding up to 38% of the total explained variance (Figure 4.S6).

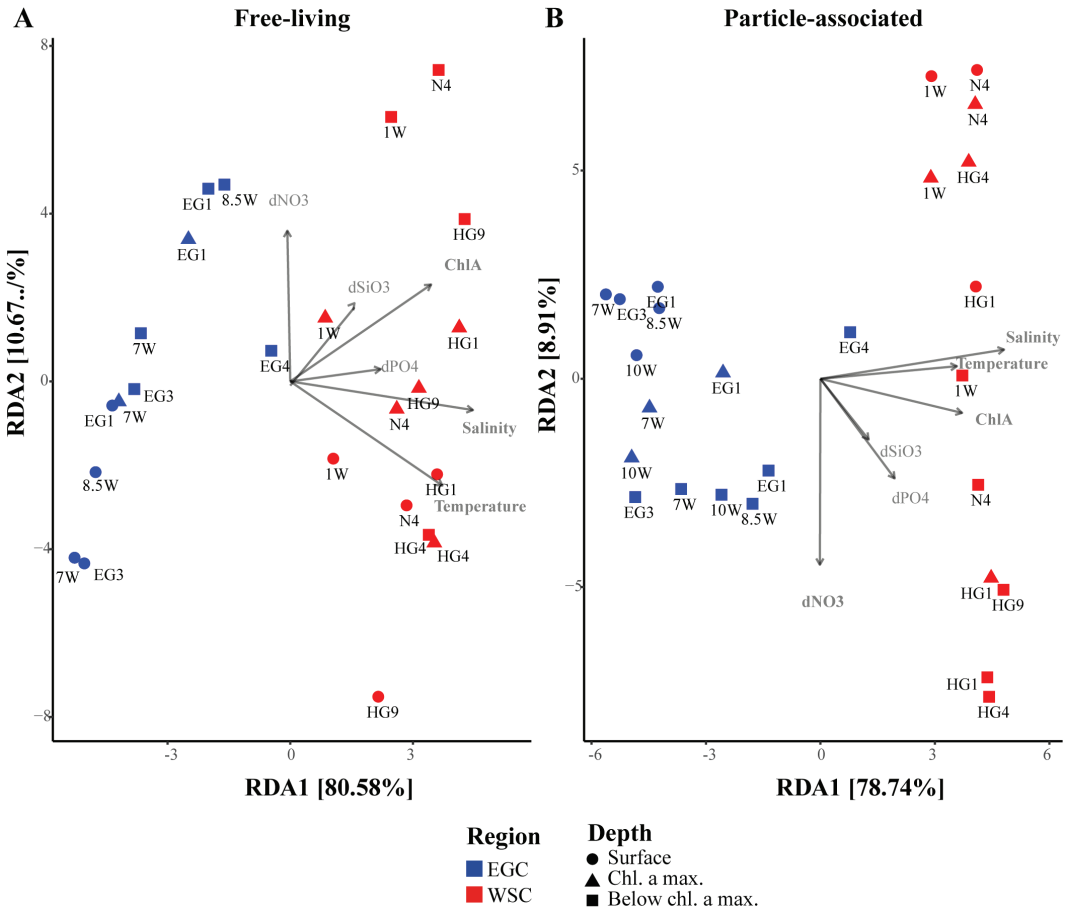

Figure 4.8: RDA ordination of bacterial community composition constrained by environmental variables. (**A**) Free-living bacteria, (**B**) particle-associated bacteria. The environmental variables are: Temperature, Salinity, ChlA - chlorophyll a, dSiO3 - ΔSiO3, dPO4 - ΔPO4 and dNO3 - ΔNO3.

4.3.4 Associations between bacteria and eukaryotic microbes - based on co-occurrence networks

Two separate networks were constructed to examine potential associations between free-living bacteria and microbial eukaryotes ('FL network') and between particle-associated bacteria and microbial eukaryotes ('PA network') at the chl a max. depth. In the FL network 85% of potential associations were positive, in the sense that sequence-richer taxa of bacteria were associated with

sequence-richer taxa of eukaryotes. The PA network consisted of a larger number of total potential associations, but only 71% of them were positive (Table 4.S3). An overview of both positive and negative associations (Figure 4.9) revealed two taxonomic groups that showed highest numbers of associations in both fractions together, the eukaryotic order *Syndiniales* (*Alveolata*) and the bacterial order *Flavobacteriales* (*Flavobacteriia*). In addition, high number of potential associations was associated with *Gammaproteobacteria*, such as *Alteromonadales*, and *Oceanospirillales* (Figure 4.9). Among the microbial eukaryotes, two groups showed relatively high numbers of associations: *Diatomea* and *Dinophyceae* (*Dinoflagellata*; Figure 4.9).

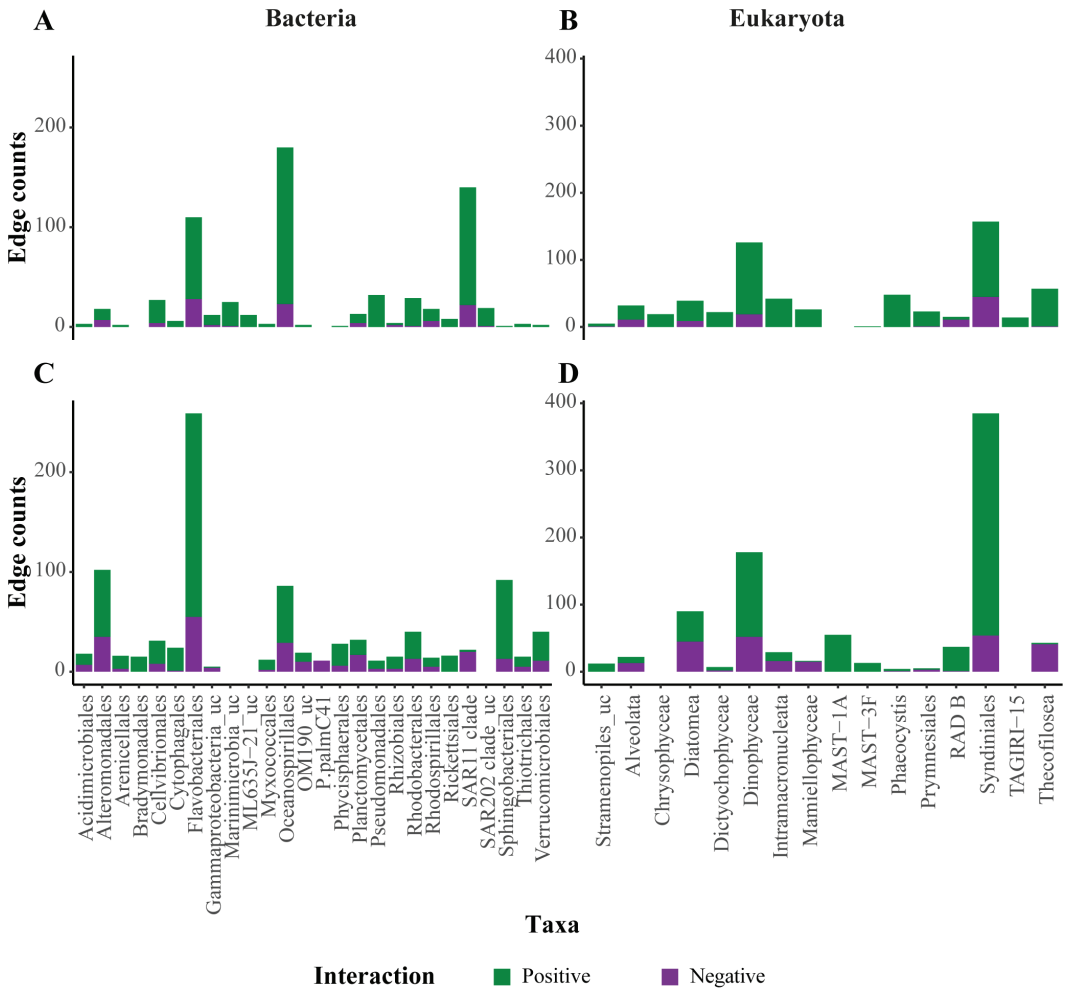

Figure 4.9: Overview of edge counts for selected taxonomic groups in each network. (**A**,**C**) Associations between bacteria and eukaryotes in the FL network. (**B**,**D**) Associations between bacteria and eukaryotes in the PA network. The y-axis represents the number of edges associated with the different taxa. Positive associations are represented in green, negative associations in purple. Only taxa with more than 3 edges were included in the figure.

In order to identify regionally specific associations of microbial eukaryotes with bacterial taxa, we generated for each fraction a sub-network of positive associations between eukaryotic OTUs and previously identified bacterial daOTU for the EGC and WSC, respectively (Table 4.S3). The sub-network topologies showed different patterns in the FL and the PA networks. Overall, the FL network consisted of 159 nodes of daOTU, out of a total 363 bacterial OTUs in the network (81 daOTU in EGC and 78 in WSC). In the PA network there were 226 nodes of daOTU, out

of a total 363 bacterial OTUs in the network (197 daOTU in EGC and 30 daOTU in WSC). Subsequently, the sub-networks were clustered into metanodes, each incorporating OTUs of a specific taxonomic group (Figure 4.10). The clustered sub-networks of both fractions revealed strong differences between the regions, with larger number of taxon-taxon associations in the EGC. The strongest associations, based on the number of connecting edges, in all sub-networks, were related to co-occurrences of *Syndiniales* (*Alveolata*) with various bacterial orders such as *Flavobacteriales* and *Oceanospirillales*.

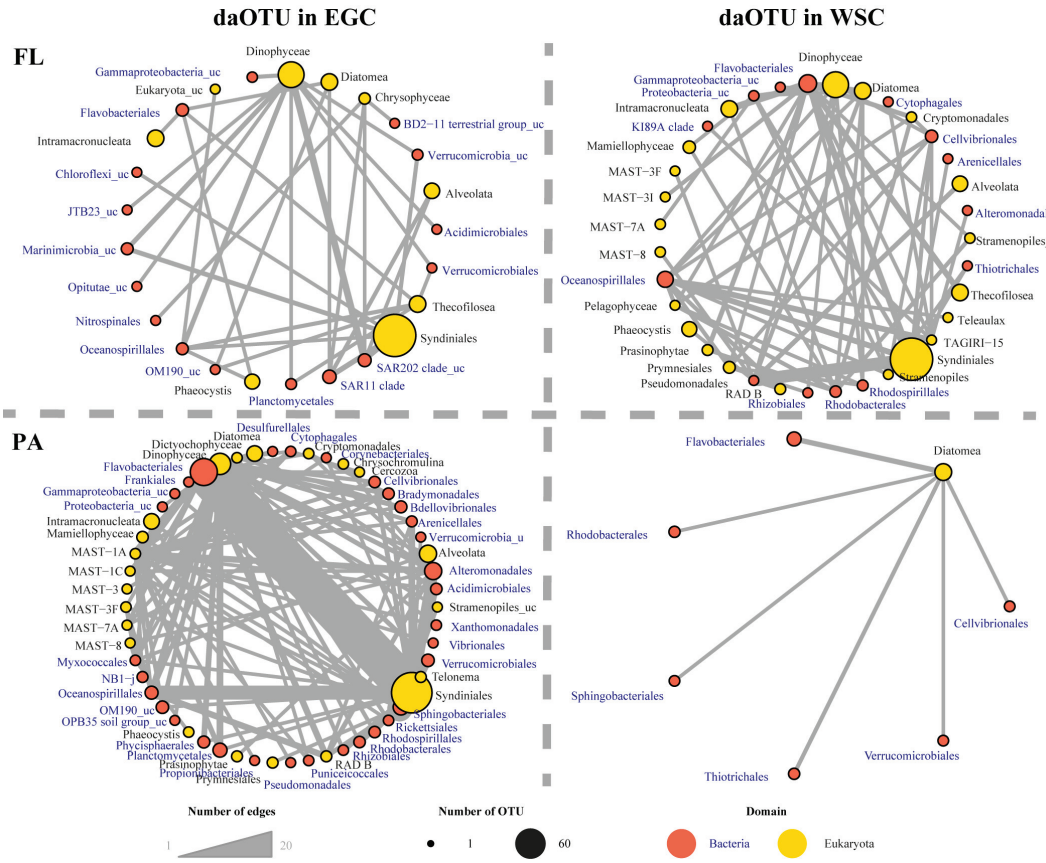

Figure 4.10: Sub-networks of the FL and PA fractions in the chl. a max. of EGC and WSC regions. Taxonomic groups were clustered into metanodes. Colors of the nodes represent the different taxonomic domains, while the size is proportional to the number of OTUs grouped together in the metanode. The edges represent taxon-taxon positive (co-occurrence) associations, and the width of the edges represents the number of associations between the metanodes.

4.4 Discussion

4.4.1 Pelagic ecosystem state - in situ and in silico observations

In our study we investigated the summer dynamics of pelagic bacterial communities from the photic zone of Fram Strait (top 60 m). Using measurements of physical and biogeochemical parameters, combined with sea-ice coverage, we separated the Strait into two main pelagic ecosystem regions (Figure 4.1). These different regions were directly related to the distinct

current systems in the Strait; one transporting Atlantic Water to the Arctic Ocean (WSC) and the other one exporting Polar Water and sea ice (EGC; Beszczynska-Möller *et al.*, 2011). These distinct current systems differed not only in physical characteristics of the water (temperature and salinity) but also in their nutrient concentrations (Table 4.1 and Figure 4.S1). The different geochemical and sea-ice conditions potentially affect biological processes in these distinct regions (e.g., nutrient and light limitation of the phytoplankton bloom). We thus used a combination of measured and modeled biogeochemical variables to further investigate the ecosystem states in the two regions.

The high phytoplankton biomass and production estimates (Table 4.1), as well as elevated bacterial cell densities in the WSC compared to the EGC (Figure 4.7), are likely related to the decaying phytoplankton bloom (Alonso-Sáez *et al.*, 2008; Buchan *et al.*, 2014; Pinhassi and Hagström, 2000; Riemann *et al.*, 2000). Further evidence for such a relationship has been detected by a previous study in Fram Strait, which showed correlations of bacterial activity with concentrations of amino acids and carbohydrates in the water (Piontek *et al.*, 2014). In the WSC region maximum integrated chl a values during seasonal blooms reach up to 100 mg/m3 (Nöthig *et al.*, 2015). Thus based on the chl a concentrations, fully depleted nutrients above the pycnocline and low pCO2 (Table 4.1 and Figure 4.S7), we conclude that we had sampled a post-phytoplankton bloom situation. In the EGC, the low nutrient depletion in surface waters, the low chl a concentration and the high pCO2 rather suggest a pre-phytoplankton bloom stage. Moreover, the stoichiometry-based estimate of new production in both regions was in a comparable range to previous estimates of Nöthig and colleagues in Fram Strait (Nöthig *et al.*, 2015), as well as to estimates in other regions of the Arctic Ocean (Arrigo *et al.*, 2008; Boetius *et al.*, 2013; Wassmann *et al.*, 2010). The generally high ratio between NO3 and PO4 concentrations in the EGC indicate a Pacific origin of the sampled Polar Water (Wilson and Wallace, 1990), and PO4 may be one of the limiting factors for the development of a phytoplankton bloom in this region (Taylor *et al.*, 1992).

In order to test whether the biogeochemical differences between the sampled regimes represent different ecosystem states, or simply represent hydrographical differences between Polar Water and Atlantic Water, we used surface chlorophyll a dynamics obtained from the coupled FESOM-REcoM2model (Figure 4.2 and Supplementary Material; Schourup-Kristensen *et al.*, 2014). In June 2014, when the sea-ice cover, hydrographical and nutrient conditions fit well with observations (Figure 4.S8 and Figure 4.S9), the annual dynamics produced by the model showed an increase in surface chl a concentration in EGC in the second half of June, associated with the seasonal thinning of the sea-ice in the region (Leu *et al.*, 2011; Nöthig *et al.*, 2015). Moreover, in the WSC the model showed a decline in surface chl a concentration throughout the month. In summary, our observations and the model results support the hypothesis that during the time of sampling early phytoplankton bloom conditions prevailed in the ice-covered EGC (first half of June), and that the phytoplankton bloom of the ice-free WSC was already in decline (second half of June).

4.4.2 Functional and regional differences in microbial communities across Fram Strait

Both WSC and EGC regions exhibited a large number of OTUs, which were unique to one of the regions (Figure 4.3). However, these OTUs represented only a small proportion of the total sequence abundance of the bacterial community, and consisted of taxa, which were previously identified as rare bacterial community members in the Arctic Ocean (Galand *et al.*, 2009a). The vast majority of the sequence proportion was related to OTUs which were shared between the regions and fractions (Figure 4.4). Moreover, bacterial community variations in the FL and PA fractions were explained by the same environmental parameters, suggesting that both fractions are subject to similar environmental drivers (Hanson *et al.*, 2012). Hence, we hypothesized that community variation was mostly driven by environmental factors such as bloom stage, selecting for different sequence proportions of shared OTUs. It is important to note that size-fractionated filtration may lead to different observations compared to bulk filtration (Padilla *et al.*, 2015). In this study we did not observe a clogging of filters, but cannot exclude effects on FL and PA fractions.

In order to investigate differences in the relative contributions of the shared OTUs to the communities in WSC and EGC, we identified differentially abundant OTUs (daOTU) in both the FL and PA fractions (Figure 4.S3). *Flavobacteria* and *Gammaproteobacteria* were the two main heterotrophic bacterial taxa which showed high numbers of daOTU and numerous enriched taxa in both fractions (Figure 4.5 and Figure 4.S3). For both fractions combined, the WSC consisted of almost twice the number of flavobacterial daOTU compared to EGC (176 and 107 daOTU, respectively), suggesting an enrichment of this taxonomic group by post-bloom conditions in this region. The *Flavobacteria* specialize on targeting complex organic biopolymers and were previously described to respond to phytoplankton blooms in high latitudes (Chafee *et al.*, 2018; Simon *et al.*, 1999; Williams, 2013; Teeling *et al.*, 2012). Moreover, *Cryomorphaceae*, a significantly enriched flavobacterial family in the FL fraction of WSC (Figure 4.5), was previously identified as one of the main taxa responding to a flagellate bloom in mesocosm experiments (Pinhassi *et al.*, 2004).

Additionally, in both fractions, there was a large number of daOTU and several significantly enriched families related to Gammaproteobacteria (Figure 4.5 and Figure 4.S3). These opportunistic copiotrophs, which have previously been described from both FL and PA fractions, are highly diverse and specialized in adapting to a wide range of carbon sources, also responding to different stages of phytoplankton blooms (Alonso-Sáez *et al.*, 2008; Nikrad *et al.*, 2014; Teeling *et al.*, 2012). Interestingly, the genus *Balneatrix* (*Oceanospirillales*) which was previously identified to strongly correlate with phytoplankton bloom presence in the North Sea (Wemheuer *et al.*, 2014), accounted for 30 daOTU in the WSC and only 5 daOTU in the EGC, which may be linked to the different phytoplankton bloom conditions in the region. Furthermore, the order *Pseudoalteromonadales* which consisted of several significantly enriched families in both fractions in EGC (Figure 4.5), contains several psychrophilic genera which were previously found in sea-ice (Bowman *et al.*, 1997; Brinkmeyer *et al.*, 2003; Brown, 2001; Collins *et al.*, 2010; Yu *et al.*, 2015), and their enrichment in the EGC may thus be partly a result of their release from sea-ice communities. An interesting observation was provided by two outlier samples. Although they originated from the WSC, the proximity of station 1W and HG9 to the sea-ice edge (Figure 4.1), potentially

resulted in bacterial communities more similar to stations from the EGC (Figure 4.7). This may indicate that the effect of the seasonal phytoplankton bloom extends into the zone where both water masses mix, e.g., by eddies (Wekerle *et al.*, 2017a).

Several cryptic taxonomic groups, such as *Chloroflexi* (SAR202), *Marinimicrobia* (SAR406) and various members of *Deltaproteobacteria*, were significantly enriched in EGC (Figure 4.5), and also consisted of a large number of unique OTUs in this region. These enriched taxonomic groups in the ice-covered EGC were previously reported from surface waters in the western Svalbard region (WSC) during the Arctic winter (Wilson *et al.*, 2017). Therefore, our results support and strengthen the hypothesis of Wilson and colleagues (2017) that bacterial community dynamics in Fram Strait are to a large extent affected by seasonal variability (e.g., availability of light under changing sea-ice conditions), rather than hydrographic differences between water masses.

Enriched eukaryotic taxa differed strongly between the EGC and WSC regions (Figure 4.S5), with the taxonomic groups being consistent with previously reported seasonal dynamics in the Arctic Ocean (Lovejoy, 2014). In the EGC region all enriched taxa were related to previously identified, dominant members of pelagic Arctic winter communities (e.g., *Syndiniales*; Guillou *et al.*, 2008; Jephcott *et al.*, 2016; Marquardt *et al.*, 2016). Two different taxonomic groups of phytoplankton were enriched in the WSC: the class of green algae *Prasinophytae* abundant photosynthetic organisms in late summer-autumn seasons in the Arctic (Joli *et al.*, 2017; Lovejoy *et al.*, 2007b; Marquardt *et al.*, 2016; Metfies *et al.*, 2016; Vader *et al.*, 2015). Furthermore, several heterotrophic eukaryotic taxa (e.g., *Thecofilosea*) were enriched in the WSC. These organisms are mainly grazers and depend on the presence of phytoplankton and bacteria (Monier *et al.*, 2014); their higher representation may thus be linked to the declining phytoplankton bloom in the WSC. Microbial eukaryotic community composition clearly differed between the two regions (Figure 4.S6). Interestingly, stations 10W and 8.5W showed some similarity to the WSC region, which may be related to a coastal phytoplankton bloom east of Greenland (Figure 4.S8). However, overall our observations of the microbial eukaryotic community further support our classification of early bloom conditions in the EGC and late bloom conditions in WSC.

4.4.3 Co-occurrence networks reveal potential candidates for cross-domain interactions

Numerous studies have described shifts in bacterial community composition during phytoplankton blooms (Chafee *et al.*, 2018; Teeling *et al.*, 2012; Wemheuer *et al.*, 2014), but very little is known about specific biotic interactions between bacteria and phytoplankton during blooms (Amin *et al.*, 2012; Hartmann *et al.*, 2013; Lima-Mendez *et al.*, 2015; Töpper *et al.*, 2010). Our results revealed an enrichment of specific bacterial taxa in the different regions, which we suggest to be related to the seasonal development of the phytoplankton bloom. Using network co-occurrence analyses (Faust and Raes, 2012), we therefore tested whether these enriched taxa exhibit potential associations with eukaryotic microbes in the chl a max. communities.

Both FL and PA networks consisted of a large number of edges (Figure 4.9 and Table 4.S3), which may indicate potential ecological interactions between taxa. Among the bacterial taxa in the FL network, a large number of associations was related to the typically free-living SAR11 clade (Giovannoni, 2017). In the PA network, on the other hand, large numbers of associa-

tions were related to typical particle-associated *Gammaproteobacteria*, such as *Alteromonadales* (Crespo *et al.*, 2013; Fontanez *et al.*, 2015). In both fractions, *Flavobacteria* and *Syndiniales* outnumbered all other taxonomic orders in terms of the number of associations. These observations are in line with a previous report from the global plankton interactome study conducted as part of the global Tara Oceans expedition (Lima-Mendez *et al.*, 2015), which did, however, not cover the Arctic Ocean.

Roughly 30% to 40% of bacterial nodes in the networks consisted of daOTU associated with one or more eukaryotic taxa. Interestingly, "regional" (WSC vs. EGC) sub-networks displayed strong differences between both regimes in the PA fraction, with a much higher number of associations in the EGC (Figure 4.10). Little is known about the lifestyle and physiology of many of the organisms identified in the networks, especially for the bacterial fraction, and the translation of observed associations into biological traits is thus extremely limited (Ramanan *et al.*, 2016). Furthermore, in many cases the association may represent a common response of taxonomic groups to environmental conditions, rather than direct interaction between them (Weiss *et al.*, 2016). Nevertheless, the observed cross-domain associations showed clear differences between the regions with different phytoplankton bloom conditions, resulting in the enrichment of specific bacterial taxa and the development of distinct ecological networks. It has been previously proposed that shifts in the timing and composition of phytoplankton blooms, as well as temporal mismatches with grazers resulting in an altered food web, are among the main impacts of climate change in the Arctic (Soltwedel *et al.*, 2016; Engel *et al.*, 2017). Our observations of specific associations between eukaryotes and bacteria in the plankton suggest that such ecological shifts may be accompanied by substantial changes in the microbial community structure.

4.5 Conclusions

Our study revealed strong differences in pelagic microbial community activity and structure in the photic layers of the ice-free eastern (WSC) and ice-covered western (EGC) Fram Strait during summer 2014. Measured and modeled biogeochemical parameters suggested distinct ecosystem states in the two regions, namely different stages of the summer phytoplankton bloom, as a result of differences in sea-ice cover and irradiance. Although it is challenging to conclusively decouple effects of water masses, seasonally driven biogeochemistry and biotic associations, our study shows that differences in bacterial communities between the regions could be explained by environmental parameters associated with phytoplankton bloom dynamics. This includes a strong increase in bacterial cell densities and activity in response to a declining phytoplankton bloom in the WSC, with an enrichment of phytoplankton bloom associated bacterial taxa commonly known to degrade phytoplankton products, such as Flavobacteria. In contrast, the EGC region showed high relative sequence proportions of bacterial taxa that have been associated with Arctic winter conditions (e.g., SAR202 clade, Marinimicrobia and Deltaproteobacteria). Moreover, co-occurrence networks provided evidence for a high variety of potential interactions between bacteria and microbial eukaryotes in the early bloom conditions, and their potential specialization with the advancement of the phytoplankton bloom. In times of a rapidly changing Arctic Ocean, our results highlight the potential impact of future ice-free summers on the structure and function of Arctic Ocean pelagic microbial communities. Additional sampling throughout

the year will help to better resolve seasonally driven microbial community dynamics and contrast them to long-term shifts.

4.6 Materials and methods

Field sampling

Samples were collected in Fram Strait during the Polarstern cruise PS85 (June 6th – July 3rd 2014) from the eastern Greenland shelf to the west coast of Spitsbergen (Figure 4.S2 and Table 4.S1). Sampling was carried out with 12 L Niskin bottles mounted on a CTD rosette (Sea-Bird Electronics Inc. SBE 911 plus probe) equipped with double temperature and conductivity sensors, a pressure sensor, altimeter, chlorophyll fluorometer, and transmissometer. The chlorophyll maximum depth (chl a max) was determined based on chl a fluorescence during the downcast, while the water samples were collected during the upcast. Along the transect samples were collected from surface water (5-10 m), the chl a max (10-30 m) and below the chl a max (30-60 m, Table 4.S1). Hydrographic data of the seawater including temperature and salinity were retrieved from the PANGAEA database (doi:10.1594/PANGAEA.837425). Water masses were identified based on their hydrographic characteristics, according to Rudels and colleagues (2013).

Sampling for bacterial communities

For assessing bacterial community composition, 2 L of water were filtered through successive membrane filters of 3 μm (Whatman Nucleopore, 47 mm polycarbonate), and 0.22 μm (Millipore Sterivex filters) using a peristaltic pump (Masterflex; Cole Parmer). All samples were stored at -20°C until DNA isolation.

Sampling for eukaryotic microbial communities

For assessing eukaryotic community composition, 2 L subsamples were taken in PVC bottles from the Niskin water samplers. Eukaryotic microbial cells were collected by sequential filtration using a Millipore Sterifil filtration system (Millipore, USA). Each water sample was filtered through three different mesh sizes (10, 3, and 0.4 μm) on 45 mm diameter Isopore Membrane Filters at 200 mbar. All samples were stored at -20°C until DNA isolation.

DNA isolation and amplicon sequencing

Bacteria

Genomic bacterial DNA was isolated from the 3 μm and the 0.22 μm filter membranes to analyze the particle-associated (PA) and the free-living (FL) community, respectively, in a combined chemical and mechanical procedure using the PowerWater DNA Isolation Kit (MO BIO Laboratories, Inc., Carlsbad, CA, USA). Prior to DNA isolation the sterivex cartridges of the 0.22

µm membranes were cracked open in order to place the filters in the kit-supplied bead beating tubes. The isolation was continued according to the manufacturer's instructions, and DNA was stored at -20°C. Library preparation was performed according to the standard instructions of the 16S Metagenomic Sequencing Library Preparation protocol (Illumina, Inc., San Diego, CA, USA). The hypervariable V3-V4 region of the bacterial 16S rRNA gene was amplified using bacterial primers S-D-Bact-0341-b-S-17 (5'-CCTACGGGNGGCWGCAG-3') and S-D-Bact-0785-a-A-21 (5'-GACTACHVGGGTATCTAATCC-3'; Klindworth *et al.*, 2013). Sequences were obtained on the Illumina MiSeq platform in a 2 × 300 bp paired-end run (CeBiTec Bielefeld, Germany), following the standard instructions of the 16S Metagenomic Sequencing Library Preparation protocol (Illumina, Inc., San Diego, CA, USA).

Eukaryotic microbes

Genomic eukaryotic DNA was isolated from the 10 µm, 3 µm, and 0.4 µm filter membranes using the NucleoSpin Plant Kit (Machery-Nagel, Germany), following the manufacturer protocol. The resulting DNA-extracts were stored at -20 °C. DNA concentrations were determined using the Quantus Fluorometer (Promega, USA) according to the manufacturer's protocol, and equal volumes of the isolated genomic DNA from the three different filter fractions were pulled together. Library preparation was performed according to the standard instructions of the 16S Metagenomic Sequencing Library Preparation protocol (Illumina, Inc., San Diego, CA, USA). The hypervariable V4 region of the eukaryotic 18S rRNA gene was amplified using 528iF (5'-GCGGTAATTCCAGCTCCAA-3') and 964iR (5'-ACTTTCGTTCTTGATYRR-3') primers. All PCRs had a final volume of 25 µL and contained 12.5 µl of KAPA HIFI Mix (Kapa Biosystems, Roche, Germany), 5 µl of each primer 1 µmol L^{-1} and 2.5 µl DNA-template 5 ng. The DNA-template was a mix of equal volumes of genomic DNA isolated from the three different filter fractions, i.e., 10 µm, 3 µm and 0.4 µm. PCR amplification was performed in a thermal cycler (Eppendorf, Germany) with an initial denaturation (95°C, 3 min) followed by 25 cycles of denaturation (95°C, 30 sec), annealing (55°C, 30 sec), and extension (72°C, 30 sec) with a single final extension (72°C, 5 min). The PCR products were purified from an agarose gel 1% w/v with the AMPure XP PCR purification kit (Beckman Coulter, Ing., USA) according to the manufacturer's protocol. Subsequent to purification DNA concentrations in the samples were determined using the Quantus Fluorometer (Promega, USA). Subsequently, indices and sequencing adapters of the Nextera XT Index Kit (Illumina, USA) were attached in the course of the Index PCR. All PCRs had a final volume of 50 µL and contained 25 µl of KAPA HIFI Mix (Kapa Biosystems, Roche, Germany), 5 µl of each Nextera XT Index Primer 1 µmol L-1, 5 µl DNA-template 5 ng and 10 µl PCR grade water. PCR amplification was performed in a thermal cycler (Eppendorf, Germany) with an initial denaturation (95°C, 3 min) followed by 8 cycles of denaturation (95°C, 30 sec), annealing (55°C, 30 sec), and extension (72°C, 30 sec) with a single final extension (72°C, 5 min). Prior to quantification of the amplification products with the Quantus Fluorometer (Promega, USA) for sequencing the final library was cleaned up using the AMPure XP PCR purification kit (Beckman Coulter, Ing., USA). Sequences were obtained on the Illumina MiSeq platform in a 2 × 300 bp paired-end run (AWI Bremerhaven, Germany), following the standard instructions of the 16S Metagenomic Sequencing Library Preparation protocol (Illumina, Inc., San Diego, CA, USA).

Bioinformatics and statistical analyses

Both bacterial and eukaryotic libraries were subject to similar bioinformatic pipelines. The raw paired-end reads were primer-trimmed using 'cutadapt' (Martin, 2011), quality trimmed using 'trimmomatic' with a sliding window of four bases and a minimum average quality of 15 (v0.32; Bolger *et al.*, 2014).The reads were merged using PEAR (v0.9.5; Zhang *et al.*, 2014), and all merged reads below 350 bp or above 450 bp were removed from the dataset. Clustering into OTUs was done with the 'swarm' algorithm using default parameters (v2.0; Mahé *et al.*, 2015). Chimeric sequences were identified and removed using 'uchime' function in VSEARCH (v1.9.7; Rognes *et al.*, 2016). One representative sequence per OTU was taxonomically classified using 'SINA' (SILVA Incremental Aligner; v1.2.11; Silva reference database release 128) at a minimum alignment similarity of 0.9, and a last common ancestor consensus of 0.7 (Pruesse *et al.*, 2012). The OTUs which were not taxonomically assigned to Bacteria/Eukarya or occurred with only a single sequence in the whole dataset ('singletons') were excluded from further analysis. Furthermore, OTUs in the bacterial dataset which were taxonomically assigned to chloroplast or mitochondria were excluded from further analysis, and OTUs in the eukaryotic dataset which were taxonomically assigned to metazoa were excluded as well.

All statistical analyses were conducted using R (v3.4.1; http://www.Rproject.org/) in RStudio (v1.0.153; RStudio Team, 2015). Sample data matrices were managed using the R package 'phyloseq' (v1.20.0; McMurdie and Holmes, 2013) and plots were generated using the R package 'ggplot2' (v2.2.1; Gómez-Rubio, 2017). A prevalence threshold (i.e., in how many samples did a taxon appear at least once) of 5% was applied to the OTU table prior to downstream analysis following (Callahan *et al.*, 2016). All alpha diversity parameters and curves were obtained using R package 'iNEXT' (v2.0.12; Hsieh *et al.*, 2018). The rarefaction curves for each sample were generated based on 40 equaly spaced rarefied sample sizes with 100 iterations.

Principal coordinate analysis (PCoA) was conducted on variance stabilized OTU abundance matrices (McMurdie and Holmes, 2014). The significance of the clustering was tested using the 'ADONIS' function in the R package 'vegan' (v2.4-5; Oksanen, 2016). To determine which environmental variables were significantly correlated with the community composition, a stepwise ordination significance test was performed using the 'ordistep' function in the R package 'vegan' (v2.4-5; Oksanen, 2016). The fold-change in abundance of each OTU between the regions was calculated using the R package 'DEseq2' (v1.16.1; Love *et al.*, 2014). The method applies a generalized exact binomial test on variance stabilized OTU abundance. The taxonomic enrichment test was performed using the generally applicable gene-set enrichment (GAGE) method in the R package 'GAGE' (v2.26.3; Luo *et al.*, 2009). The results were filtered by significance, after correction for multiple-testing according to Benjamini and Hochberg (1995) with an adjusted p-value <0.05. The shared OTUs calculations and visualization were conducted using R packages 'UpSetR' (v1.3.3; Conway *et al.*, 2017) and 'VennDiagram' (v1.6.18; Chen and Boutros, 2011).

Co-Occurrence Network Analysis

The network analysis was conducted separately using the chl a max. FL and PA bacterial communities. The cross-domain co-occurrence networks between bacteria and eukaryotes were constructed using CoNet (v1.1.1beta; Faust and Raes, 2016), as described in Lima-Mendez and col-

leagues (2015). The measure-specific p-values were merged using Brown's method (Brown, 1975) and correction for multiple-testing was performed according to Benjamini and Hochberg (1995). Edges with an adjusted p-value above 0.05 were discarded. The constructed networks were further analyzed and visualized using the R package 'igraph' (v1.1.2; Csardi and Nepusz, 2006).

Calculation of consumed inorganic nutrients

The raw nutrient concentration measurements were retrieved from PANGAEA (10.1594/PANGAEA.882217). The nutrient consumption (Δ) at each station was calculated by subtracting the mean value of all collected measurements above 50 m from the mean value of all collected measurements between 50 and 100 m (below the seasonal pycnocline). The integrated chlorophyll a and inorganic nutrient values were calculated according to (Boss and Behrenfeld, 2010). The productivity estimates were calculated using the Redfield ratio 106 C: 16 N : 1 P, and for diatom contribution the ratio of 1:1 N:Si was assumed.

Bacterial abundance and productivity

Bacterial abundance was determined by flow cytometry (FACSCalibur, Becton Dickinson). Samples were fixed with glutaraldehyde at 1% final concentration and stored at -20°C. Prior to analysis, samples were stained with the fluorescent dye SybrGreen I (Invitrogen) that binds to DNA. Bacterial cell numbers were estimated after visual inspection and manual gating of the bacterial population in the cytogram of side scatter vs. green fluorescence. Fluorescent latex beads (Polyscience, Becton Dickinson) were used to normalize the counted events to volume (Gasol *et al.*, 2000).

The incorporation of 3H-leucine (specific activity 100 Ci $mmol^{-1}$) was determined to estimate bacterial production (BP). The radiotracer was added at a saturating final concentration of 20 nmol L^{-1} before three replicate samples were incubated for 4-6 hours in the dark close to in situ temperature at 0-2°C. Incubations were stopped by the addition of trichloroacetic acid (TCA) at a final concentration of 5%. Samples were then processed by the centrifugation method according to Smith and Azam (1992). Briefly, samples were centrifuged at 14,000×g to obtain a cell pellet that was washed twice with 5% TCA. Incorporation into the TCA-insoluble fraction was measured by liquid scintillation counting after resuspension of the cell pellet in scintillation cocktail (Ultima Gold AB, Perkin Elmer).

Chlorophyll a measurements

The concentration of chlorophyll a (chl a) was determined from 0.5-2 L of seawater filtered onto glass fiber filters (Whatman GF/F) under low vacuum pressure (<200 mbar); the filters were stored at -20 °C before analysis. Pigments were extracted with 10 ml of 90% acetone. The filters were treated with an ultrasonic device in an ice bath for less than a minute, and then further extracted in the refrigerator for 2 h. Subsequently they were centrifuged for 10 minutes at 5000 rpm at 4°C prior to measurement. The concentration was determined fluorometrically (Turner

Designs), together with total phaeophytin concentration after acidification (HCl, 0.1 N) based on methods described in Edler, 1979 and Evans, 1980, respectively. The standard deviation of replicate test samples was < 10%.

The biogeochemical model FESOM-REcoM2

To estimate biological productivity in areas and time periods that were not covered by sampling, we used the biogeochemical model REcoM2 coupled to the Finite Element Sea-ice Ocean Model (FESOM; Schourup-Kristensen *et al.*, 2014). The model runs in a global setup and describes the ocean, sea-ice and marine biogeochemistry, thus making it possible for us to estimate the phytoplankton bloom development stage in both the western, ice-covered part of Fram Strait and the eastern ice-free part (see Supplementary Information).

Data Accession Numbers and Analyses Repository

Data are accessible via the Data Publisher for Earth & Environmental Science PANGAEA (www.pangaea.de): chlorophyll a measurements - 10.1594/PANGAEA.887840; bacterial counts and productivity - 10.1594/PANGAEA.887881. Raw paired-end sequence, primer-trimmed reads were deposited in the European Nucleotide Archive (ENA; Silvester *et al.*, 2018) under accession number PRJEB28027, or PRJEB26163 for Bacteria and PRJEB26288 for Microbial eukaryotes. The data were archived using the brokerage service of the German Federation for Biological Data (GFBio; Diepenbroek *et al.*, 2014). Scripts for processing data can be accessed at https://github.com/edfadeev/Bact-comm-PS85.

4.7 Supplementary material

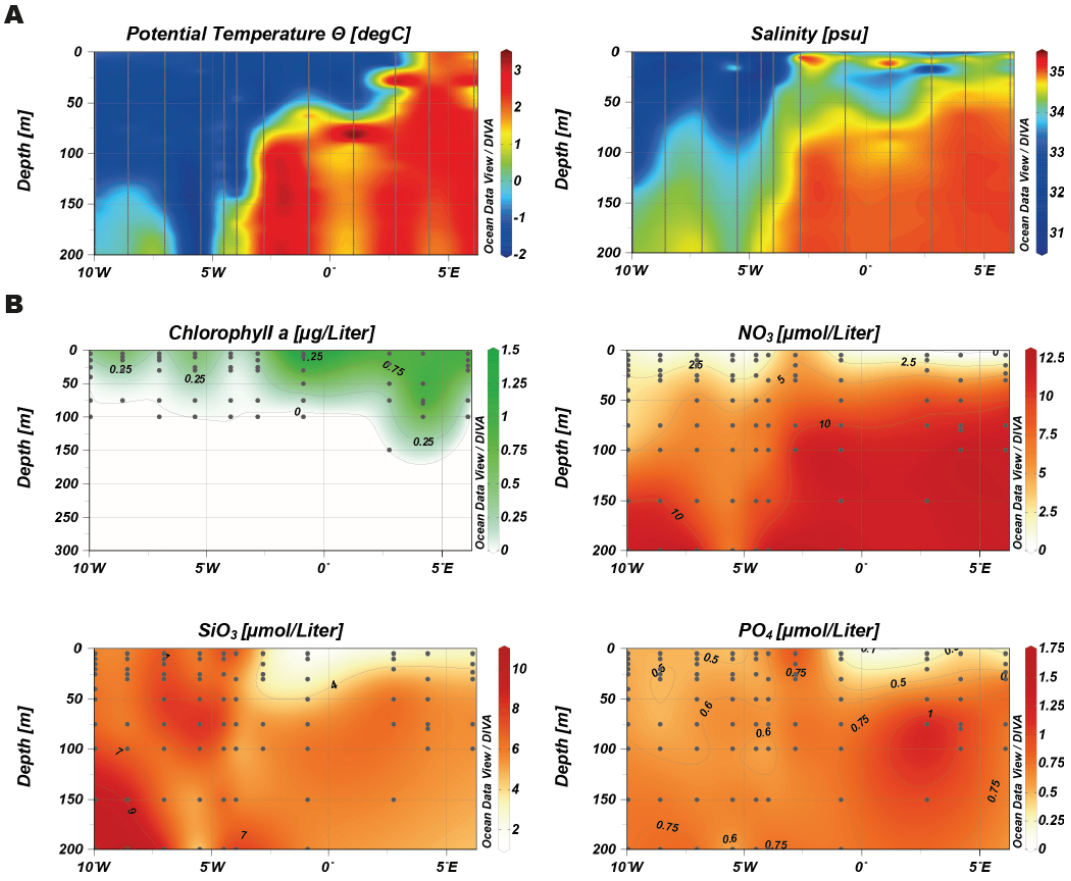

Figure 4.S1: Regional separation of Fram Strait based on in situ biogeochemical parameters. (**A**) Physical characteristics of the water column from CTD (Conductivity-Temperature-Depth) sensors. (**B**) Chl a and inorganic nutrients measured in situ. The longitudinal coordinates of EGC region are 10W-1W, and 1W-6E for the WSC region. The plot was generated using Ocean Data View (v4.7.10; Schlitzer, 2015).

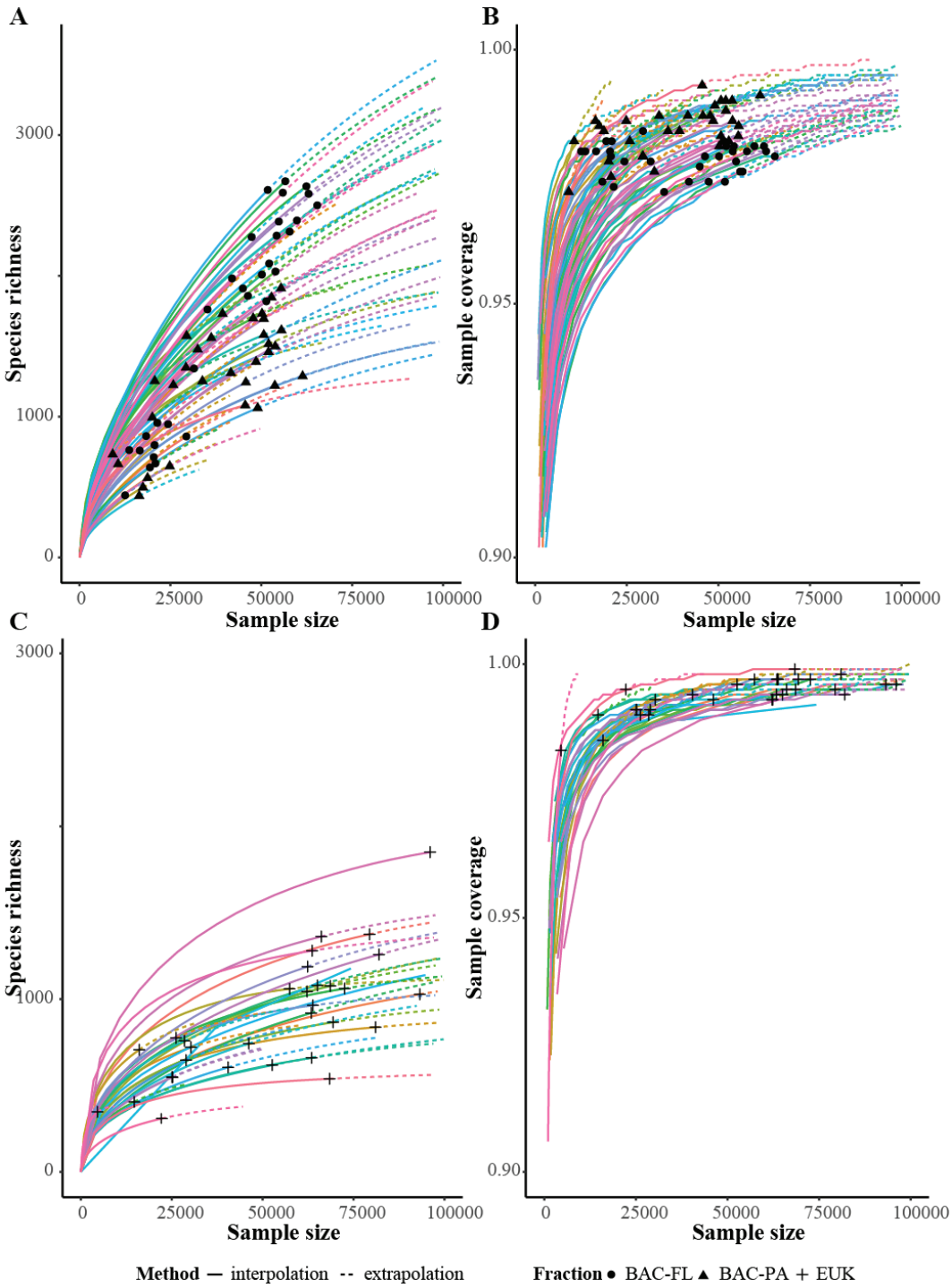

Figure 4.S2: Rarefaction analysis of bacterial and eukaryotic communities. (**A,C**) Sample-size-based rarefaction curves generated with the iNEXT package, for bacterial (A) and eukaryotic (C) communities. The solid lines represent the observed accumulation with the number of reads sampled, and the dashed lines represent the extrapolated accumulation up to the double amount of reads. Based on the Hill numbers of order q = 0. (**B,D**) Coverage-based sample completeness estimations for bacterial (B) and eukaryotic (D) communities. The observed values for each community are denoted by solid shapes.

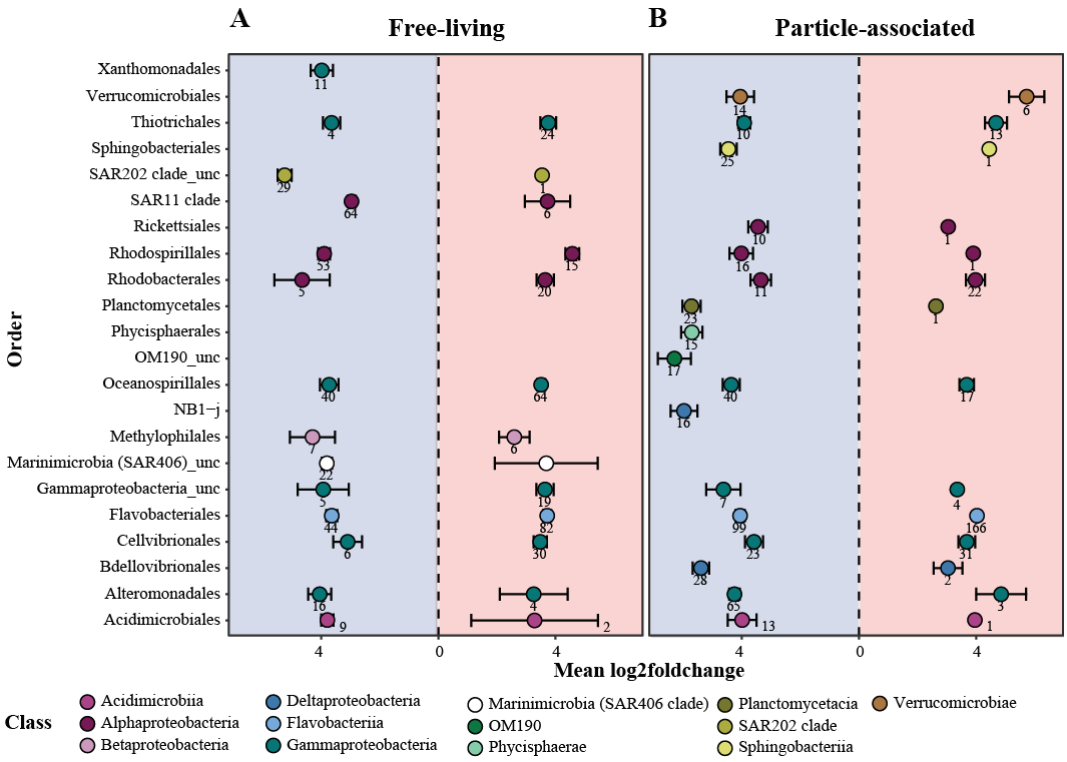

Figure 4.S3: Differences in bacterial community composition between the regions. OTU enrichment analysis was performed separately on the FL (**A**) and the PA (**B**) fractions, and only statistically significant daOTU were included in the data representation (adjusted p value < 0.01). The x axis represents absolute values of $\log_2$ fold change. Enrichment of daOTU in the EGC region is represented in the blue area, while enrichment in the WSC region is represented in the red area. The color code represents taxonomic classes and each point represents the average for orders with more than 10 daOTU (black bars indicate standard deviations). The numbers below the symbols represent the number of daOTU enriched in the region.

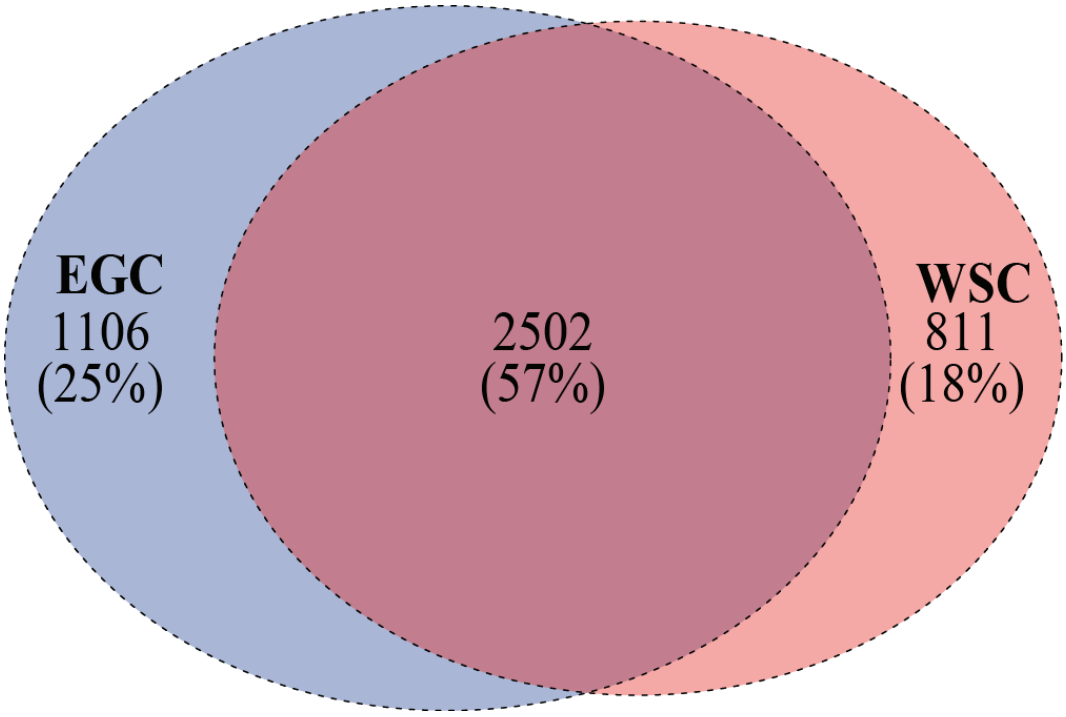

Figure 4.S4: Venn diagram of shared OTUs between microbial eukaryote communities in WSC and EGC.

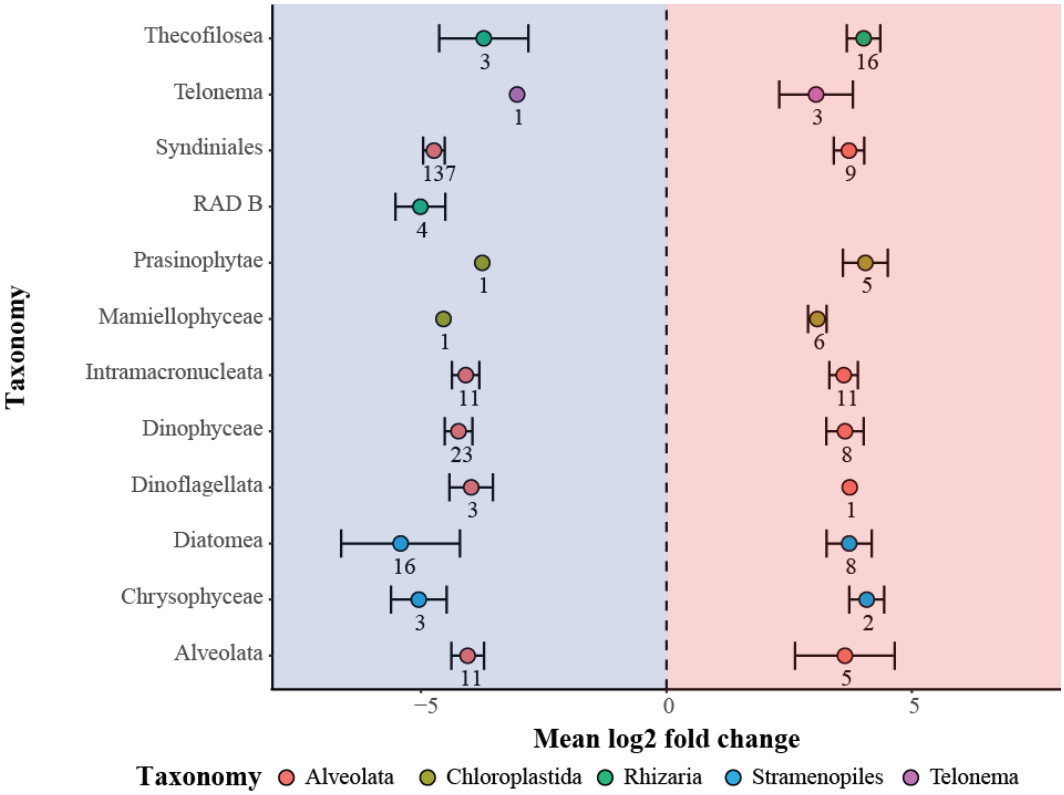

Figure 4.S5: Enriched microbial eukaryotic taxonomic groups between the regions. Only statistically significant taxa were included in data representation (p value < 0.01). The x axis represents the $\log_2$ fold change. Enrichment in EGC region is represented in the blue area while enrichment in the WSC region is represented in the red area. The color code represents higher taxonomic groups and each point represents the mean log2 fold change of all OTUs in the group (black bars indicate standard deviations).

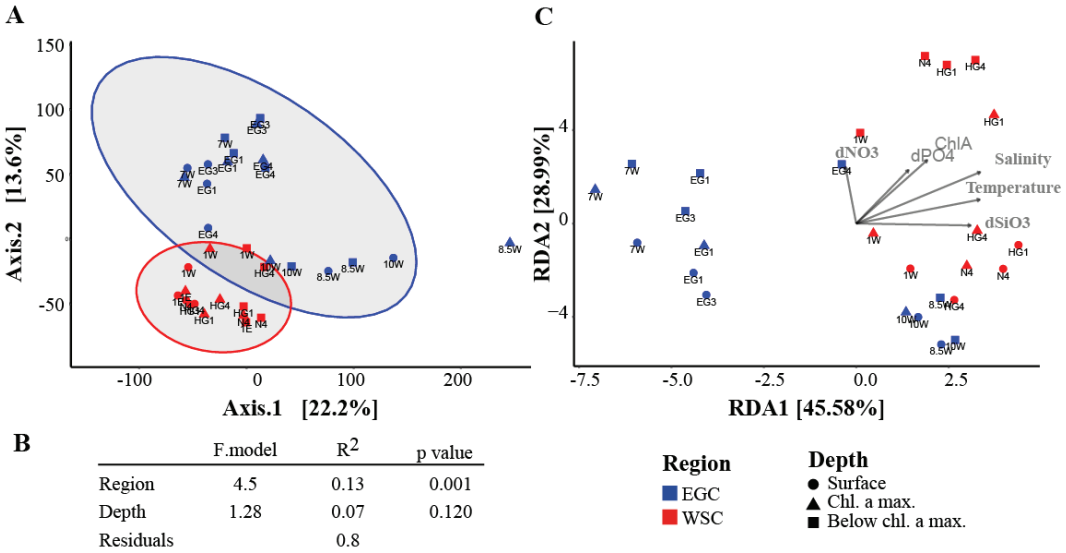

Figure 4.S6: (**A**) PCoA of microbial eukaryote community composition in all three water layers. The ellipses encompass each of the groups with normal confidence of 0.95. The percentages on both axes represent the explained variance of the axis. (**B**) Permutational multivariate analysis of variance between samples ('ADONIS' in R package 'vegan'). (**C**) RDA ordination of eukaryote community composition constrained by environmental variables. The environmental variables are: Temperature, Salinity, ChlA - chlorophyll a, dSiO3 - ΔSiO3, dPO4 - ΔPO4 and dNO3 - ΔNO3.

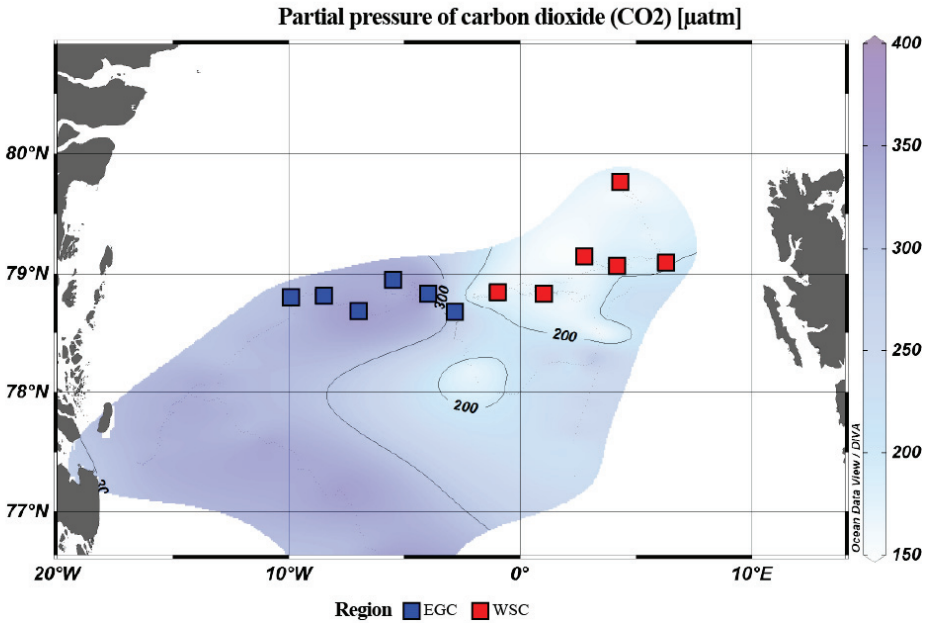

Figure 4.S7: Partial pressure of carbon dioxide (pCO_2) in surface waters across Fram Strait. The measurements were collected using an underway pCO_2 sensor mounted to the keel of the ship at 11 m depth (for further information: 10.1594/PANGAEA.865492).

Biogeochemical model FESOM-REcoM2

Description of the model

The biogeochemical model REcoM2 is a ratio model, in which stoichiometry is allowed to vary within set limits. The nutrients included in the model are nitrogen, silicon and iron, which describe the entire carbon cycle. The incoming photosynthetically available radiation (PAR) is prescribed by the JRA-55 reanalysis dataset (Kobayashi *et al.*, 2015), and thus varies in time and space. The amount of PAR reaching the ocean surface at a given time and location is scaled to the ice concentration in each point of the surface grid. PAR decreases exponentially with depth and is further reduced by the presence of chlorophyll in the water. The growth rate of the model's two phytoplankton classes, nano-phytoplankton (e.g., flagellates) and diatoms is affected by light and nutrient availability. Degradation occurs through zooplankton grazing and bacterial activity, the latter of which is parameterized.

The biogeochemical tracers of REcoM2 are transported by ocean currents and mixing, which are provided by the ocean general circulation model FESOM (Wang *et al.*, 2014a). FESOM is characterized by a triangulated surface grid, making it possible to have increased resolution in selected areas. The current run is carried out in a global setup with a resolution of 4.5km north of 60°N (Wekerle *et al.*, 2017b). After spin-up of the ocean model, the coupled model was started in 1980 and run until 2015. The modeled biogeochemistry of 2010 to 2015 has been comprehensively described and assessed against available data, showing that the model describes well the Arctic marine biogeochemistry (Schourup-Kristensen *et al.*, 2018). Moreover, in order to evaluate the modeled surface chlorophyll a trends, the modeled values in WSC (ice-free) were compared to remote sensing surface chlorophyll a measurements (Figure 4.S9). However, it is important to keep in mind that no model will perfectly catch the complexity of the biological systems; rather, the model results provide an insight into the biological processes and help us to look beyond the location and timing of in situ measurements.

Comparison of model output to satellite-based estimates of surface chlorophyll

To demonstrate the skill of the model we have plotted the monthly mean of surface chlorophyll a concentration from model output and from satellite-based estimates of chlorophyll (http://globcolor.com) for the year 2014 (Figure 4.S8). We compare to the satellite-based estimates as they provide a large-scale view of the development of the bloom in the area. Note that the satellite-based estimates use a specific algorithm for ocean color data (e.g., Maritorena *et al.*, 2010). The satellite-based estimates should thus be regarded as another type of model. Agreement in the spatial and temporal distribution between the output from FESOM-REcoM2 and the satellite-based estimates indicates that they provide realistic results. For discussions of satellite-based estimates of productivity in the Arctic region, see e.g., Lee *et al.* (2016).

In FESOM-REcoM2, the bloom starts in the warm and nutrient-rich water of the Norwegian Atlantic Current in April and in the coastal waters of Iceland (Figure 4.S8). This fits well with the satellite-based estimates. In May, the surface bloom covers the whole ice free area of the Nordic Seas in FESOM-REcoM2. This is also the case in the satellite-based estimates, but here the bloom is somewhat weaker compared to FESOM-REcoM2. The relatively strong bloom can

be attributed to a low concentration of grazers early in the growth season, allowing the modeled bloom to develop to higher chlorophyll concentrations than in the ocean. From June onwards, the modeled chlorophyll a in the ice-free part of the Nordic Seas has a very good fit with the satellite-based estimates. In the ice-covered region, the bloom begins as the ice concentration decreases in June, allowing PAR to reach the water column and initialize the bloom here. To summarize, the productivity is at a post-bloom stage in the ice-free part of the Fram Strait in June for both FESOM-REcoM2 and satellite-based estimates. In the ice-covered part, the bloom begins during the month of June in the model results.

Comparison between modeled and in situ measured parameters in a section across the Fram Strait

For the cruise transect across the Fram Strait from Greenland to Svalbard at 78textdegreeN, we have plotted the vertical section of the mean June model results for temperature, salinity, chlorophyll and dissolved inorganic nitrogen (DIN). The model sections have been overlaid with the in situ measurements from the cruise (Figure 4.S9). The division between warm and salty Atlantic Water (AW) in the eastern Fram Strait and cold and fresher Arctic water in the western Fram Strait is clear in both the modeled results and the in situ measurements. In FESOM-REcoM2, the AW brings DIN to the Fram Strait from the south. In the surface layer, where PAR allows for productivity to take place, the DIN has been drawn down below concentrations that allow for phytoplankton growth, and consequently, productivity takes place deeper in the water column at the depth of the nitracline in the modeled eastern Fram Strait. This feature is a so-called chlorophyll maximum (chl a max, Figure 4.S9). West of 5textdegreeE, where productivity starts later due to ice coverage, the nitracline is close enough to the surface that productivity can still take place in the uppermost part of the water column. In the in situ measurements, the nitracline is deeper in the eastern Fram Strait compared to FESOM-REcoM2, and the chl a max is thus also located deeper in the water column (Figure 4.S9). The process behind the chl a max, namely the downwards movement of the nutricline due to biological uptake, is, however, the same in the model results and the in situ measurements, and indicates a later stage of the bloom in the eastern Fram Strait as compared to the western.

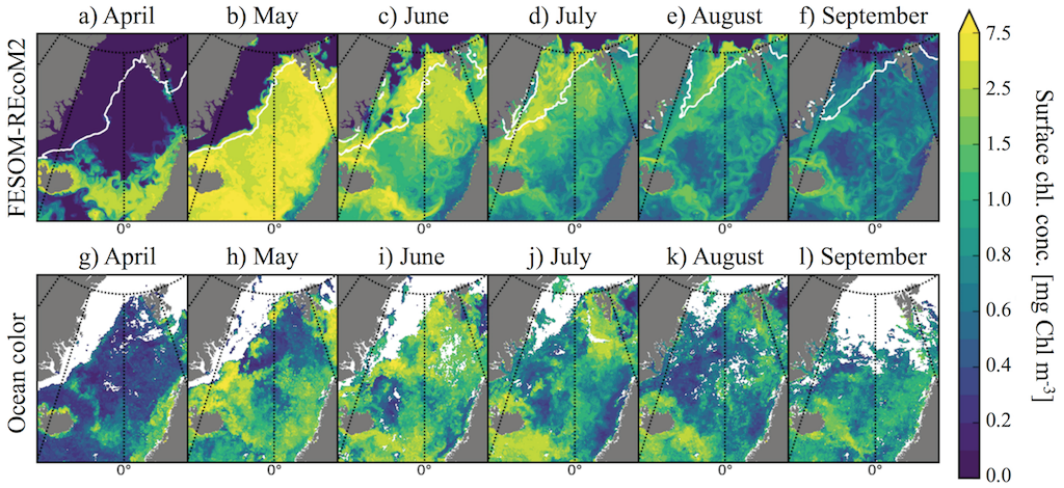

Figure 4.S8: Monthly mean of surface chlorophyll a in FESOM-REcoM2 (**a-f**) and in satellite-based estimates from Globcolor (**g-l**) downloaded from http://globcolor.com. Both model and satellite-based results are from 2014. The white line in subplot a-f marks the contour of the 10% ice concentration. White areas in subplots g-l are areas without data for the whole month, e.g., because of cloud cover or ice.

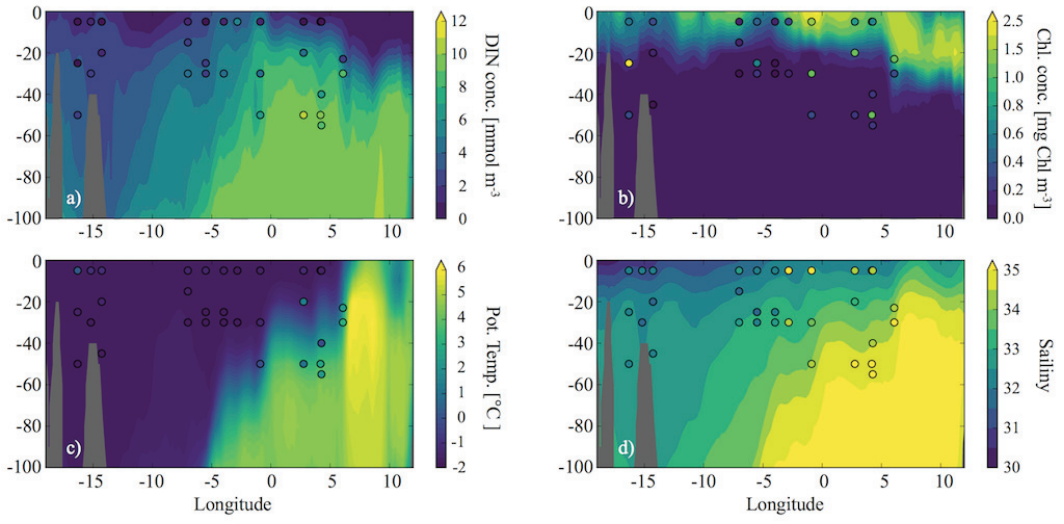

Figure 4.S9: Comparison of modeled and in situ measured parameters across the Fram Strait section at 78°N. The background represents the mean model results for June 2014, which have been overlaid with the in situ measurements from the PS85 expedition.

Table 4.S1: Overview of sampled stations during RV Polarstern expedition PS85. The table consists of sampling information for each station, number of sequences in each step of the bioinformatics workflow as well as alpha diversity estimations, conducted using the R package 'iNEXT'.

PANGAEA stationID	Station Name	Longitude (°E)	Latitude (°N)	Sampling Date (dd-mm-yyyy)	Sampled depths (m)	Community fraction	No. of raw amplicons	No. of amplicons after QC and merging	Final no. of amplicons after taxonomic assignment	Observed richness (no. of OTUs)	Chao1 richness estimator	Richness coverage (%)	Shanon diversity index	Sample completeness (%)
PS85/0426-1	10W	-9.93	78.81	16-06-2014	5	BAC-PA	80397	64742	33796	1253	1688	74%	96	98
						EUK	147259	96416	79400	1375	1626	85%	101	99
					25	BAC-PA	91123	72119	52012	1517	2195	69%	50	98
						EUK	150194	102204	72574	1061	1227	86%	59	99
					40	BAC-PA	32709	14861	10612	664	833	80%	109	98
						EUK	147314	100351	63842	964	1053	91%	83	99
PS85/0485-1	1E	1.01	78.84	28-06-2014	5	BAC-FL	36556	15425	12513	442	1048	42%	32	97
						BAC-PA	52802	26634	24811	649	1309	50%	30	98
						EUK	62815	42857	25060	549	894	61%	28	99
					15	BAC-FL	76337	36003	29384	860	1767	49%	38	98
						BAC-PA	41723	20613	17462	498	931	53%	30	98
						EUK	121572	78223	25238	548	866	63%	23	99
					60	BAC-FL	43652	20877	19360	640	1497	43%	77	98
						BAC-PA	35591	17538	16430	438	966	45%	26	98
						EUK	169597	109653	81993	1258	1766	71%	76	99
PS85/0482-1	1W	-0.9	78.83	28-06-2014	5	BAC-FL	77709	61309	46317	1858	3356	55%	61	97
						BAC-PA	90364	71325	52816	1847	3229	57%	61	98
						EUK	99943	62021	40492	605	925	65%	22	99
					30	BAC-FL	60089	48421	41956	1982	3679	54%	87	97
						BAC-PA	75761	61646	50193	1732	3330	52%	52	98
						EUK	116173	73992	28927	647	981	66%	25	99
					50	BAC-FL	76494	61438	55904	2591	4581	57%	103	97
						BAC-PA	84659	66948	55419	1912	3219	59%	48	98
						EUK	164612	108612	62359	1188	1662	71%	56	99
PS85/0432-1	7W	-7.01	78.66	17-06-2014	5	BAC-FL	70906	57234	44915	1911	3496	55%	122	97
						BAC-PA	78260	62880	29441	1574	2363	67%	155	97
						EUK	33567	7152	4598	348	381	91%	88	98
					15	BAC-FL	82651	65466	53898	2031	3823	53%	142	98
						BAC-PA	89928	70465	36222	1560	2122	74%	116	98
						EUK	104233	69591	22287	309	419	74%	17	99
					30	BAC-FL	89980	71294	62394	2636	4061	65%	202	98
						BAC-PA	91899	72800	47748	1699	2274	75%	80	98
						EUK	125204	80222	68398	539	587	92%	23	99
PS85/0429-1	8.5W	-8.56	78.83	16-06-2014	5	BAC-FL	41349	20557	18329	863	1958	44%	70	97
						BAC-PA	91168	79425	45569	1081	1365	79%	52	99
						EUK	122102	82354	66153	1362	1634	83%	110	99
					15	BAC-FL	41747	19198	16582	760	1316	58%	79	97
						EUK	181419	119906	96066	1850	1994	93%	185	99
					30	BAC-FL	32931	14862	13682	763	1139	67%	147	97
						BAC-PA	29010	13160	9141	733	984	74%	120	97
						EUK	129949	87319	63611	1280	1415	90%	186	99
PS85/0437-1	EG1	-5.5	78.83	17-06-2014	5	BAC-FL	85231	68633	57782	2314	3836	60%	85	98
						BAC-PA	78359	62571	29282	1349	2218	61%	79	97
						EUK	196875	131887	93201	1028	1308	79%	44	99

PANGAEA stationID	Station Name	Longitude (°E)	Latitude (°N)	Sampling Date (dd-mm-yyyy)	Sampled depths (m)	Community fraction	No. of raw amplicons	No. of amplicons after QC and merging	Final no. of amplicons after taxonomic assignment	Observed richness (no. of OTUs)	Chao1 richness estimator	Richness coverage (%)	Shanon diversity index	Sample completeness (%)
					25	BAC-FL	81707	66199	56587	2672	4327	62%	107	97
						BAC-PA	85414	70034	20038	995	1623	61%	55	97
						EUK	110323	72002	26192	775	1006	77%	56	99
					30	BAC-FL	95756	76869	65384	2501	4799	52%	145	97
						BAC-PA	81069	65846	25796	1225	1761	70%	107	98
						EUK	71733	49058	30306	721	911	79%	45	99
PS85/0444-1	EG3	-3.98	78.84	18-06-2014	5	BAC-FL	77088	61503	50149	2009	3734	54%	127	97
						BAC-PA	61815	49003	20694	1254	1973	64%	114	97
						EUK	140298	96787	81029	837	920	91%	31	99
					25	BAC-FL	78705	61132	54206	2286	3890	59%	173	98
						BAC-PA	72914	56244	39354	1731	2271	76%	82	98
						EUK	69062	25775	16066	707	974	73%	108	98
					30	BAC-FL	86092	68494	59783	2394	4015	60%	192	98
						BAC-PA	103314	79525	50683	1581	2034	78%	68	98
						EUK	111864	77280	57390	1059	1120	94%	106	99
PS85/0455-2	EG4	-2.83	78.45	21-06-2014	5	BAC-FL	76892	62268	47336	2276	4224	54%	92	97
						BAC-PA	75665	58788	32510	1478	2712	54%	58	97
						EUK	124988	82632	62200	1044	1571	66%	38	99
					20	BAC-FL	81102	64823	52158	2088	3396	61%	127	98
						BAC-PA	82155	66160	41640	1311	1849	71%	44	98
						EUK	138829	90341	69354	866	1029	84%	24	99
					30	BAC-FL	78368	61711	51762	2610	4652	56%	160	97
						BAC-PA	97030	74544	51986	1460	2038	72%	66	98
						EUK	124644	83373	68622	1076	1396	77%	31	99
PS85/0470-1	HG1	6.08	79.13	24-06-2014	5	BAC-PA	88309	69223	61358	1288	1858	69%	23	99
						EUK	118376	81039	63494	660	844	78%	34	99
					23	BAC-FL	44197	22004	20405	713	1586	45%	52	97
						BAC-PA	99612	76756	53722	1221	1806	68%	33	99
						EUK	114736	73485	52638	618	939	66%	45	99
					30	BAC-FL	47998	23509	21405	956	2383	40%	80	97
						BAC-PA	94944	74271	45745	1244	1997	62%	40	98
						EUK	106104	70476	28501	758	1097	69%	78	99
PS85/0460-1	HG4	4.19	79.19	22-06-2014	5	BAC-FL	58239	28496	24334	947	2171	44%	58	97
						BAC-PA	77468	62783	49002	1062	1824	58%	24	98
						EUK	24794	17367	14697	406	580	70%	49	98
					50	BAC-FL	51128	23529	20639	799	1725	46%	55	97
						BAC-PA	80709	64555	55532	1614	2817	57%	44	98
						EUK	122028	83737	63358	920	1477	62%	28	99
					60	EUK	127462	86970	65048	1079	1457	74%	39	99
PS85/0465-1	HG9	2.75	79.15	24-06-2014	5	BAC-FL	47806	23211	20885	669	1424	47%	40	98
						BAC-PA	40295	20267	18718	565	1206	47%	28	98
					20	BAC-FL	83762	40055	35179	1762	3372	52%	88	97
					50	BAC-FL	74227	35523	31476	1343	2580	52%	110	97
PS85/0473-1	N4	4.26	79.76	25-06-2014	5	BAC-FL	78003	61567	51392	1820	2985	61%	46	98
						BAC-PA	80864	64261	50661	1696	2866	59%	50	98
						EUK	104829	66993	46176	743	1159	64%	45	99
					40	BAC-FL	76360	59989	54801	2386	4029	59%	90	97
						BAC-PA	79049	62868	53831	1500	2607	58%	37	98

PANGAEA stationID	Station Name	Longitude (°E)	Latitude (°N)	Sampling Date (dd-mm-yyyy)	Sampled depths (m)	Community fraction	No. of raw amplicons	No. of amplicons after QC and merging	Final no. of amplicons after taxonomic assignment	Observed richness (no. of OTUs)	Chao1 richness estimator	Richness coverage (%)	Shanon diversity index	Sample completeness (%)
						EUK	1375615	932321	668065	2706	2969	91%	14	99
					55	BAC-FL	87573	69600	63000	2583	4378	59%	103	97
						BAC-PA	73018	57336	48538	1390	2243	62%	34	98
						EUK	184908	127835	100293	1163	1673	69%	39	99

Table 4.S2: Bacterial cell abundance and activity in East Greenland Current (EGC) and West Spitsbergen Current (WSC). The values represent the mean and the standard deviation for each parameter and the number in parentheses represents the number of samples. *HNA - high nucleic acids, LNA- low nucleic acids.

	EGC	**WSC**
Total bacterial cell conc. (cells ml^{-1})	5.1 ± 0.2 (11)	5.8 ± 0.1 (12)
HNA/LNA cells ratio*	1.8 ± 0.6 (11)	3.1 ± 1.2 (12)
Total bacterial productivity (pmol leucine $Lite^{-1}$ $hour^{-1}$)	6.3 (18)	25.4 (17)
Cell specific bac. prod. ($10e^{-8}$ pmol leucine $cell^{-1}$ $hour^{-1}$)	3.3 ± 2.4 (11)	3.7 ± 3.2 (12)

Table 4.S3: Properties of the co-occurrence networks in both Free-living (FL) and particle-attached (PA) size fractions.

	FL network	**PA network**
Nodes		
No. of nodes	555	514
Bacterial nodes (% of total)	55 (74%)	85 (64%)
Edges		
No. of edges	718	986
Pos. edges (% of total)	607 (85%)	702 (71%)
Topology		
No. clusters	49	52
Modularity	0.39	0.27
Diameter	23.09	15.68
Mean degree	2.58	3.83
Avg. path length	8.56	4.78
Betweenness	497.24	681.51

Chapter 5

Arctic Ocean sea ice enhances vertical connectivity of microbial communities through sinking marine aggregates

Eduard Fadeev[1,2], Morten H. Iversen[1,3], Claudia Wekerle[1], Andreas Rogge[1], Anya M. Waite[1,4], Christina Bienhold[1,2], Ian Salter[1,5], Laura Hehemann[1] and Antje Boetius[1,2,3]

[1] Alfred Wegener Institute for Polar and Marine Research, Bremerhaven, Germany

[2] Max Planck Institute for Marine Microbiology, Bremen, Germany

[3] Faculty of Geosciences and MARUM, University of Bremen, Bremen, Germany

[4] Ocean Frontier Institute, Dalhousie University, Halifax, Canada

[5] Faroe Marine Research Institute, Torshavn, Faroe Islands

Keywords: microbial source tracking, deep ocean, particles colonization, sinking trajectories, marine snow This chapter is in preparation for submission to the Proceedings of the National Academy of Science (PNAS) journal.

5.1 Abstract

The Arctic Ocean is characterized by a single seasonal phytoplankton bloom in late spring (May-June) to which the grazers are tuned. The bloom is terminated both by nutrient depletion, and by strong grazing pressure. A substantial export of matter follows, including decaying phytoplankton, fecal pellets and gels forming sinking aggregates. These aggregates are colonized at the surface by diverse particle-associating microbes, however little is known about their succession during the descent to deep waters. By combining in situ measurements with Lagrangian modeling we reconstructed sinking trajectories of marine aggregates in ice-free and ice-covered regions of the Fram Strait (0-2500 m water depth), and showed that ice-covered regions were characterized by larger (1-2 mm diameter) and faster-sinking (40-80 m/d) aggregates, composed mainly from diatoms. Using high-throughput sequencing of the 16S rRNA gene, we investigated the changes in particle-associated (>5 μm) and free-living (0.2-5 μm) microbial communities throughout the water column. We showed that aggregates were colonized mainly in the surface waters by heterotrophic bacteria (e.g., *Flavobacteria*), which were traceable using microbial source tracking in the deep ocean particle-associated communities (up to 4000 m depth). This vertical connectivity of microbial communities was especially strong in regions covered by sea ice, where almost half of the particle-associated communities at 1000 m depth were linked to surface-derived microbes. Our study reveals the magnitude at which surface-derived microbes may be transported to the deep ocean via large sinking aggregates. Highlighting that further sea-ice loss in the Arctic Ocean may impact this microbial connectivity, altering the current biogeochemical cycling in the Arctic.

5.2 Introduction

Global warming and climate change is currently affecting the Arctic Ocean at an unprecedented rate, causing warming at rates much faster than any other ocean (Dobricic *et al.*, 2016; Sun *et al.*, 2016). Arctic sea ice has declined by approximately 50% since the late 1950s (Kwok and Rothrock, 2009; Peng and Meier, 2017), and current projections suggest that the Arctic Ocean may experience sea-ice free summers by the second half of this century (Notz and Stroeve, 2016; Overland and Wang, 2013; Polyakov *et al.*, 2017). These remarkable environmental changes are likely to increase primary production in the water column (Arrigo and van Dijken, 2015; Randelhoff *et al.*, 2018; Tremblay *et al.*, 2015), and change the phytoplankton communities, grazers and the biological carbon pump (Boetius *et al.*, 2013; Li *et al.*, 2009). Shift from diatom to flagellate (e.g., *Phaeocystis* spp.) dominated phytoplankton communities has been already observed after the record Arctic sea-ice minimum of 2006 (Engel *et al.*, 2017; Nöthig *et al.*, 2015; Lasternas and Agustí, 2010).

The organic matter produced by phytoplankton in surface ocean is exported to the deep ocean through formation and gravitational settling of marine aggregates (Ducklow *et al.*, 2001). Aggregates formed by *Phaeocystis* spp. are more buoyant and sink slowly in comparison to diatom aggregates, remaining longer in the surface ocean, and allowing more recycling in the upper water column (Iversen and Ploug, 2010; Ploug *et al.*, 2008a,b). This is supported by recent model predictions that suggest that an ice-free Arctic Ocean will have a more active microbial loop in

surface waters and less carbon export to the deep ocean (Vernet *et al.*, 2017; Wollenburg *et al.*, 2018), where the availability of organic matter is usually extremely low (Aristegui *et al.*, 2009; Herndl and Reinthaler, 2013).

Marine aggregates are subject to colonization by microorganisms and are hotspots of microbial activity in the ocean (Azam and Long, 2001; Azam and Malfatti, 2007). The microbes play key roles in the recycling of particulate organic matter in the aggregates by hydrolytic enzymatic activity and the release of dissolved organic matter and nutrients into the water (Arnosti, 2011; Grossart *et al.*, 2007, 2006a; Karner and Herndl, 1992). There are strong experimental evidences showing that the PA communities are result of colonization by pioneers, followed by internal succession and continuous taxonomic exchange with the ambient FL microbial communities (Kiørboe *et al.*, 2003; Grossart *et al.*, 2003, 2006b; Datta *et al.*, 2016; Simon *et al.*, 2002; Kiørboe *et al.*, 2002; Stocker, 2012). From surface down to the bathypelagic waters (0-4000 m depth), particle-attached (PA) microbial communities have been shown to differ in composition from the surrounding free-living (FL) communities (Mestre *et al.*, 2017a; Salazar *et al.*, 2015). Furthermore, phylogenetic analyses showed that in the deep ocean the FL and PA communities are phylogenetically distant and cases of microbes being present in both fractions are rare (Salazar *et al.*, 2015). It has been also demonstrated, using a wide range of size-fractionated FL and PA communities, that sinking aggregates may act as vertical dispersal vectors between surface and deep ocean microbial communities, in tropical and subtropical waters (Mestre *et al.*, 2018).

Unlike in other open ocean environments, surface and deep waters of the Arctic Ocean both maintain similar near freezing point temperatures (Rudels *et al.*, 2013), which may allow surface waters particle-attached microbes to survive in the deep ocean despite the increasing hydrostatic pressure (Tamburini *et al.*, 2013). An evidence for potential connectivity of microbial communities from sea ice, water column and the seafloor in central Arctic was provided by identification of roughly 20% taxonomic overlap at the level of operational taxonomic units (OTUs) of total microbial communities between these environments (Rapp *et al.*, 2018). In contrast, in the Pacific Ocean only 12% of the OTUs were shared between the water column and the deep-sea sediment (Walsh *et al.*, 2016). However, in order to further understand the relevance of sinking particles to vertical connectivity of microbial communities in the Arctic Ocean, characterization of particle-associated microbes and identification of their sources is required.

Here, we characterized and compared sinking particles dynamics in sea-ice free and sea-ice influenced (partially or entirely covered by sea ice, further referred to as 'ice-covered') regions at the Long Term Ecological Research Observatory HAUSGARTEN in the Fram Strait (Soltwedel *et al.*, 2016), the only deep water gateway to the Arctic Ocean. Vertical profiles of particle abundance and size-distribution were obtained from the Underwater Vision Profiler (UVP; Picheral *et al.*, 2010). Aggregates were collected in situ with Marine Snow Catcher and measurements of their sizes and sinking velocities were made in a vertical flow chamber (Ploug *et al.*, 2010; Ploug and Jørgensen, 1999), and determined their composition microscopically. By combining the direct measurements of in situ particle distribution and size-specific sinking velocities, a Lagrangian modeling approach was developed to construct back-trajectories of the sinking aggregates from the deep ocean to their origin in the surface waters. We collected water samples from 4 distinct water layers down to 4500 m depth at 10 different sites within the LTER Observatory HAUSGARTEN. The water samples were divided into two size fractions: 0.2-5 μm (FL) and >5 μm

(PA) in order to distinguish between free-living and particle-associated communities. Based on high-throughput sequencing of the 16S rRNA gene, we targeted archaeal and bacterial communities (further referred to as 'microbes') within each size-fraction, and used a Bayesian microbial source tracking algorithm (SourceTracker; Knights *et al.*, 2011) to assess the potential connectivity between surface and deep Arctic Ocean microbial communities through association with particles.

5.3 Results and Discussion

5.3.1 The Fram Strait has two main distinct oceanographic regimes

Based on temperature and salinity characteristics, our sampling included four distinct water masses in the Fram Strait: the epipelagic - Polar water (PW) and Atlantic Water (AW), mesopelagic - mixed Atlantic Water (MAW) and bathypelagic - Eurasian Basin Deep Water (EBDW; Rudels *et al.*, 2005). In the epipelagic waters (0-200 m), two oceanographic regions across the Strait were also defined based on the physical characteristics, geographical location and sea-ice conditions (Figure 5.1): (i) the ice-covered region, which is mostly associated with the East Greenland Current (EGC) that flows southwards and transports PW as well as 90% of the Arctic sea ice (the 'EG' and 'N' stations; de Steur *et al.*, 2009); (ii) ice-free region, which includes the West Spitsbergen Current (WSC) which flows northward and transports AW into the Central Arctic basin (the 'HG' stations; Beszczynska-Moller *et al.*, 2012). These distinct sea ice and oceanography regimes have been previously shown to have different dynamics in the development of the seasonal phytoplankton bloom (chapter 4 and Nöthig *et al.*, 2015). However, at the time of the sampling during the PS99.2 expedition, the integrated chlorophyll a concentrations values suggest advanced phytoplankton bloom conditions in both regions, with highest values in the frontal boundary between the two sea-ice regimes (Figure 5.S2). The deeper layers of the Fram Strait are more homogeneous - the mesopelagic layer (200-1000 m) consists of mixed Atlantic Water (MAW), which transitions into Eurasian Basin Deep Water (EBDW) at bathypelagic depths (>1000 m; von Appen *et al.*, 2015).

5.3.2 Marine aggregates in different regions of the Fram Strait differ in their size distribution, velocities and sinking trajectories

In all stations of both ice-free and ice-covered regions, the particulate matter concentration profiles, acquired using the UVP, showed maxima at the upper 100 m of the water column (i.e., the photic layer; Figure 5.2). Both regions exhibited similar distribution of both small (64-512 μm) and large (0.512-10.3 mm) the particulate matter within the upper 100 m, with no statistically significant differences between the regions (Mann-Whitney-Wilcoxon Test, $p > 0.05$). However, deeper (100-1500 m), there was a significantly higher concentration of both small and large the particulate matter in the ice-free region (Mann-Whitney-Wilcoxon Test, $p < 0.01$). This potentially suggests that the particulate matter which was formed in the sea-ice covered waters was rapidly exported to the deep ocean.

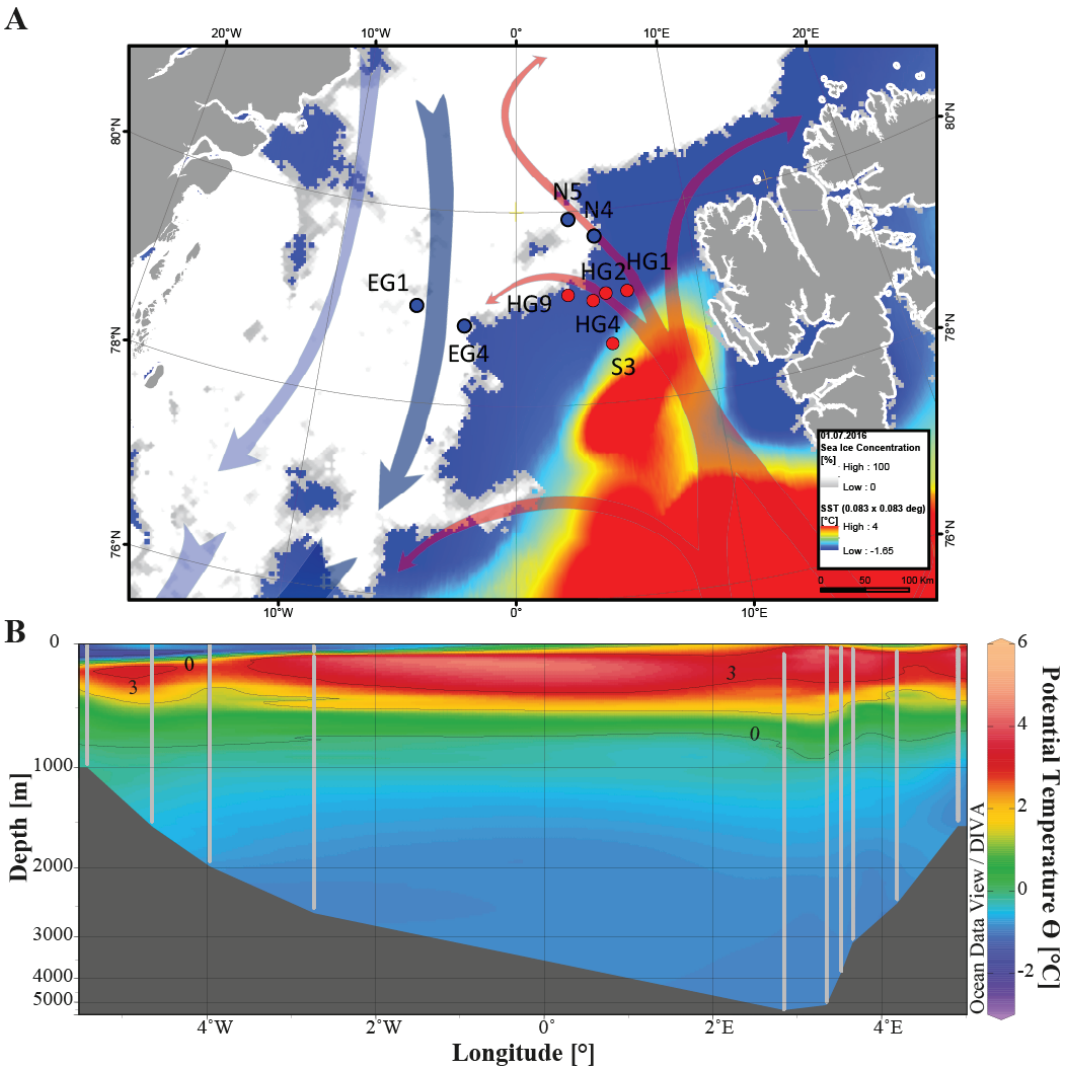

Figure 5.1: Oceanographic overview of Fram Strait during July 2016. (A) Monthly average of sea-ice coverage and sea surface temperature during July 2016. The sea ice concentration is represented by inverted grayscale (gray-low, white-high). The arrows represent general directions of the WSC (in red) and the EGC (in blue). Sampling stations are indicated and colored according to their sea-ice conditions: ice-covered EG stations (blue), ice-free HG stations (red), ice-influenced N stations (black). The map was generated using ArcMap (v.10.5) with Esri world countries dataset (www.esri.com) in a WGS 1984 Arctic Polar Stereographic map projection. (B) Potential temperature of the water, calculated based on physical characteristics measured by CTD (Conductivity-Temperature-Depth) sensors. Grey lines indicate the positions of the CTD profiles. The plot was generated using Ocean Data View (v4.7.10; Schlitzer, 2015).

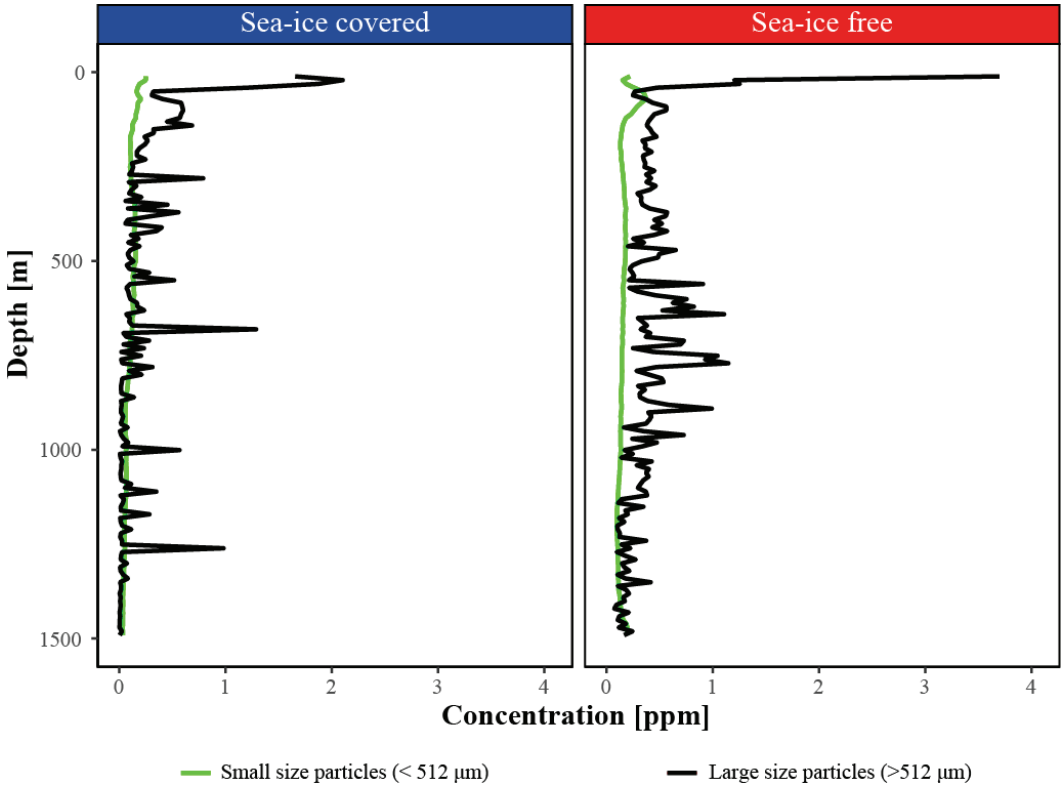

Figure 5.2: Mean vertical concentration profiles of small (64-512 µm; in green) and large (0.512-10.3 mm; in black) particles in sea-ice free (5 stations) and sea-ice covered (4 stations) regions of Fram Strait.

The combination of size, structure (e.g., porosity and density) and composition (e.g., diatoms with silica frustule as ballast mineral versus flagellate without any ballast minerals) of an aggregate determine its sinking velocity (Iversen and Ploug, 2010; Ploug *et al.*, 2008a). Intact marine aggregates were collected with a Marine Snow Catcher (MSC) below the sub-surface chl a maximum (60 m) in both ice-free (n = 23 aggregates) and ice-covered (n = 36 aggregates) regions of the Fram Strait. The size measurement of these aggregates revealed that on average in the ice-covered region aggregates were significantly larger (Mann-Whitney-Wilcoxon Test, $p < 0.001$; Table 5.1). According to microscopic analyses, more than half (12 out of 23) of the aggregates collected in ice-free region were smaller than 512 μm and composed primarily of flagellates, especially the Prymnesiophyte *Phaeocystis* spp. (Figure 5.3). On the other hand almost all (33 out of 36) collected aggregates in the ice-covered region were large aggregates (> 512 μm) and were dominated by diatoms (Figure 5.3), of both pelagic and sea ice origin (Arrigo, 2014; Boetius *et al.*, 2015). Due to the high abundance of silica-rich diatom frustules within aggregates at the ice-covered region; on average we observed significantly (Mann-Whitney-Wilcoxon Test, $p < 0.05$) higher sinking velocities for those aggregates (52.77±7.75 m/d) compared to the non-ballasted flagellate aggregates collected in the ice-free region (29.5±3.65 m/d; Table 2), which is in accordance with previous observations (Ploug *et al.*, 2008b; Iversen and Ploug, 2010; Reigstad and Wassmann, 2007; Wolf *et al.*, 2016).

Table 5.1: Characteristics of particles in ice-free and ice-covered regions of Fram Strait. The ± sign represents standard error.

	Sea-ice covered	Sea-ice free
Mean number of large particles in upper 100 m	19.3±3	18.2±4
Mean number of small particles in upper 100 m	3.9±1	5.5±1
Mean number of large particles 100-1500m	24.5±8	96.1±13***
Mean number of small particles 100-1500m	15.1±4	38±3**
Number of collected aggregates	36	24
Mean equivalent spherical diameter of aggregates (mm)	0.95±0.1***	0.58±0.1
Mean sinking velocity of aggregates (m/d)	52.8±8**	29.5±3

Interestingly, small aggregates (64-512 μm) of *Phaeocystis* spp. were also observed in the ice-covered region, where they exhibited significantly (Mann-Whitney-Wilcoxon Test, $p < 0.05$) higher sinking velocities (42.68±8.14 m/d) in comparison to the small aggregates in the ice-free region (23.37±3.98 m/d). Supporting recent observations which suggest that *Phaeocystis* spp. in ice-covered regions incorporates cryogenic gypsum resulting in its higher sinking velocities (Wollenburg *et al.*, 2018). Altogether our results support the recently observed dominance of flagellated phytoplankton over diatoms in the ice-free water column (Engel *et al.*, 2017), and suggest stronger retention rates of sinking aggregates throughout the water column in ice-free regions.

Using a Lagrangian particle tracking algorithm (SI Materials and Methods), we combined the measured on board sinking velocities of aggregates, with horizontal ocean velocities from an ocean-sea ice model FESOM, into statistical funnels which describe the sinking trajectories of aggregates from the surface ocean to the deep ocean (Wekerle *et al.*, 2015). The sinking trajectories were constructed based on the mean sinking velocities in each of the three sampled areas of the Fram Strait (Figure 5.1), the two ice-covered regions (EG and N), and the ice-free region (HG; Table 5.S1). The results revealed relatively similar catchment areas (i.e., area of potential

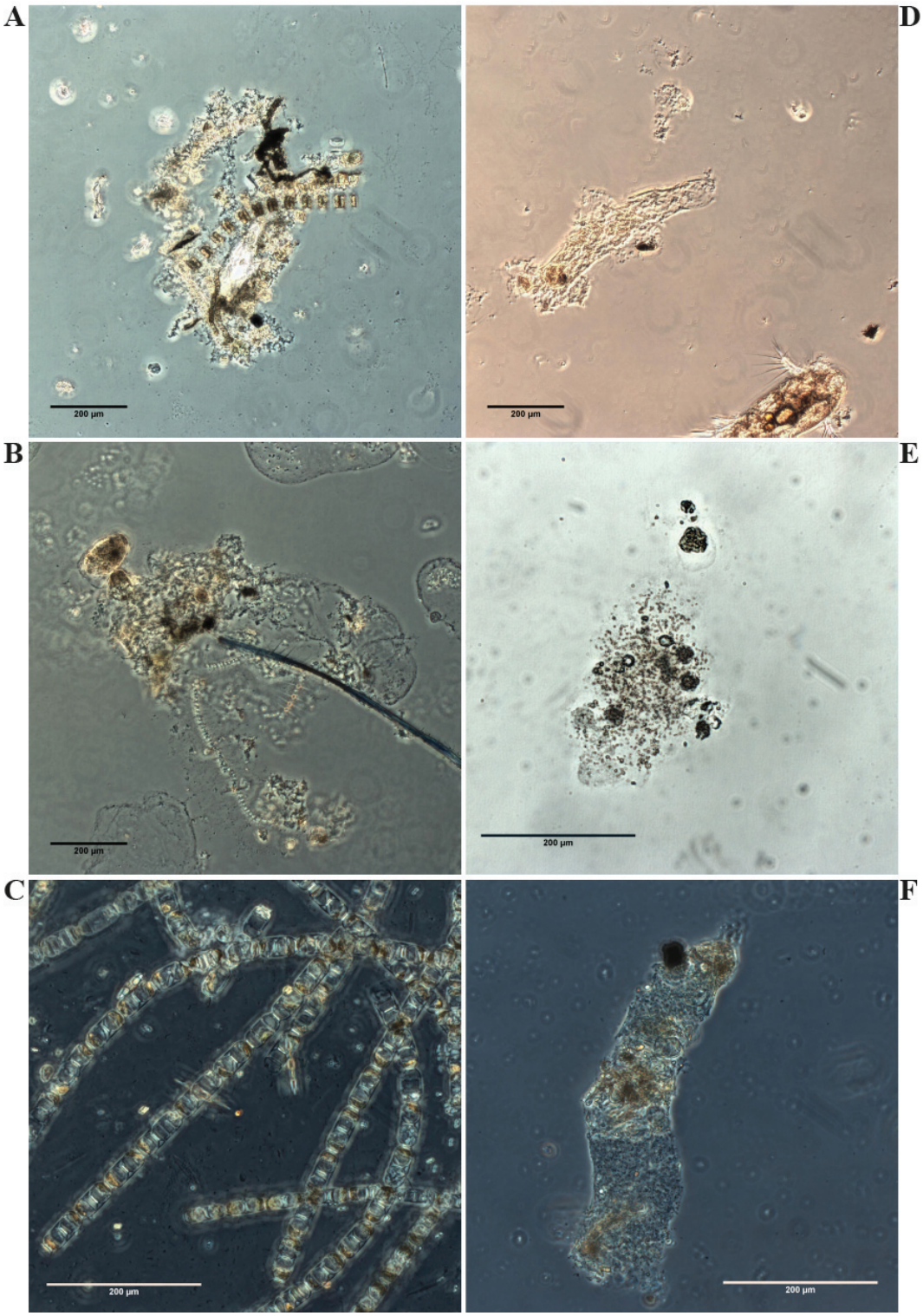

Figure 5.3: Exemplary light microscopy images of marine aggregates in Fram Strait. (**A,B**) Aggregates dominated by diatoms from ice-covered region -'EG', where A) is mainly diatoms and B) is diatoms together *Phaeocystis*. (C) Chains of *Melosira* spp., diatoms growing under the sea-ice. (**D,E**) Aggregates dominated by flagellates in ice-free region - 'HG', where E) is a copepod fecal pellet produced from *Phaeocystis* and E) is a marine snow aggregate formed from *Phaeocystis* colonies. (**F**) Calanus spp. (copepod) fecal pellets collected at the ice-covered region - 'N' and formed from mainly *Phaeocystis* colonies with a few diatoms. All scale bars are 200 µm long.

origin in surface waters) in the different regions (Figure 5.4), with lower values in comparison to previous simulations in other oceanic regions (Siegel *et al.*, 2008; Waniek *et al.*, 2000; Roullier *et al.*, 2014). Moreover, due to slower sinking velocities in the ice-free region, the dispersal of sinking trajectories was much higher in comparison to the ice-covered regions.

It is important to note that the reconstructed sinking trajectories rely on constant sinking velocity, and do not take into account the time of formation of the aggregate (De La Rocha and Passow, 2007), or changing characteristics of the aggregate as it descends through the water column (e.g., as a result of microbial degradation; McDonnell *et al.*, 2015). Slower sinking velocities may result in stronger horizontal displacement of the aggregate at depth. However, our measurements of sinking velocities were similar to those measured in situ at 1000 m from August 2016 to March 2017 using the Bio-Optical Platform (unpublished data). Combined with the well resolved meso-scale variability of the model (Wekerle *et al.*, 2017b,a), we therefore assume that there is little increase in horizontal displacement of the aggregates as they sink. Thus, our results suggest that aggregates formed in the surface water in ice-free regions are not laterally transported to the deep waters of ice-covered regions, and vice versa (Figure 5.4).

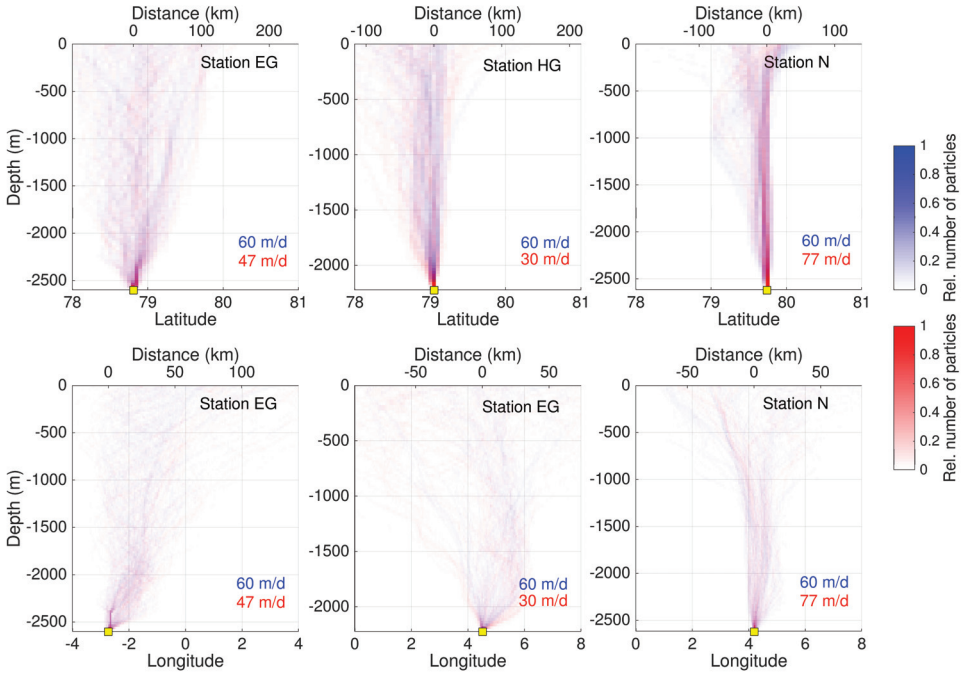

Figure 5.4: Vertical distribution of particles as a function of latitude (top) and longitude (bottom) for regions: ice-covered EG (left), ice-free HG (middle) and ice-covered N (right), released during the time period March-July 2016. Blue colours indicate trajectories computed with the measured on board mean sinking velocities (SI Appendix, Table S2). The yellow square indicates the starting point of the backward particle trajectory calculation. The dark gray bar on the top of the figures indicates the presence of sea ice in July 2016 (>15% concentration). The gray curves represent the seafloor bathymetry.

5.3.3 The pelagic microbial communities in Fram Strait show strong association with depth

The particle-associated (>5μm; PA) and the free-living (0.2-5μm; FL) microbial communities were sampled in the water column of the predefined regions across Fram Strait (Figure 5.1).Using Illumina 16S rRNA gene sequencing of the V4-V5 hypervariable region, we obtained a final dataset of 3,421,862 sequences (amplicons) in 66 samples (Table 5.S2), which were assigned to 17,868 operational taxonomic units (OTUs) associated with bacterial and archaeal lineages. All OTUs which were taxonomically assigned to chloroplasts or mitochondria were excluded from further analysis. In the FL fraction the sequences were affiliated to a total of 12,796 OTUs (12,293 bacterial and 503 archaeal OTUs), with a mean number of 1,901±108 OTUs per sample. In the PA fraction the sequences were affiliated to a total number of 10,604 OTUs (10,334 bacterial and 270 archaeal OTUs), with a mean number of 1,244±170 OTUs per sample. The rarefaction curves did not reach a plateau in any of the samples, suggesting that additional OTUs could be expected with additional sequencing (Figure 5.S1). Based on Chao1 richness estimator on overage the samples covered 71% of the bacterial and archaeal community (Table 5.S3; Chao *et al.*, 2014a; Hsieh *et al.*, 2016), with no statistically significant differences in coverage between the fractions.

The mean Chao1 richness estimator showed statistically significant differences with depth in both FL and PA fractions ('ANOVA', $F3,62 = 17.24$, $p < 0.001$; Figure 5.S3). Throughout the entire water column the PA communities exhibited a generally lower richness in comparison to the FL communities ('ANOVA', $F1,64 = 20.607$, $p < 0.001$), which is in concert with observations of other oceanic regions (Salazar *et al.*, 2015). The Pielou's evenness index (J') showed similar patterns to the richness estimates, with a statistically significant increase of evenness with depth in both fractions ('ANOVA', $F3,62 = 22.772$, $p < 0.001$; Figure 5.S3), indicating that OTUs were more evenly distributed in deep ocean communities. The deep waters of the Arctic Ocean are less affected by the frequent ecological perturbations typical for the surface waters (e.g., sea-ice dynamics and/or phytoplankton blooms; chapter 4), thus our results support previously suggested observations that high evenness is linked to functional stability in microbial ecosystems (Frank *et al.*, 2016; Wittebolle *et al.*, 2009).

The microbial communities in the surface (20 m depth) and the epipelagic (100 m depth) waters were dominated by sequences of typically phytoplankton bloom associated heterotrophic bacteria (Figure 5.5), such as *Gammaproteobacteria* and *Bacteroidia* (Bunse and Pinhassi, 2017; Buchan *et al.*, 2014). Previous study of the epipelagic microbial communities across the Fram Strait in 2014, showed that in summer the differences between the ice-covered and ice-free regions are closely related to the advancement of the seasonal phytoplankton bloom (chapter 4; Nöthig *et al.*, 2015). However, at the time of the sampling during the PS99.2 expedition, no statistically significant ('ADONIS', $p > 0.05$) differences in composition of the epipelagic microbial communities were observed, likely due to the late seasonal sampling in this study.

The microbial communities of meso- and the bathypelagic waters showed strong diversity increase, in comparison to the surface communities (Figure 5.5 and Table 5.S3). Large fraction of the sequences in these communities was related to globally present deep water bacterial taxa (Salazar *et al.*, 2016), such as *Deltaproteobacteria* (Swan *et al.*, 2011), *Dehalococcoidia* (Mehrshad *et al.*, 2018; Landry *et al.*, 2017), *Marinimicrobia* (Bertagnolli *et al.*, 2017; Hawley *et al.*,

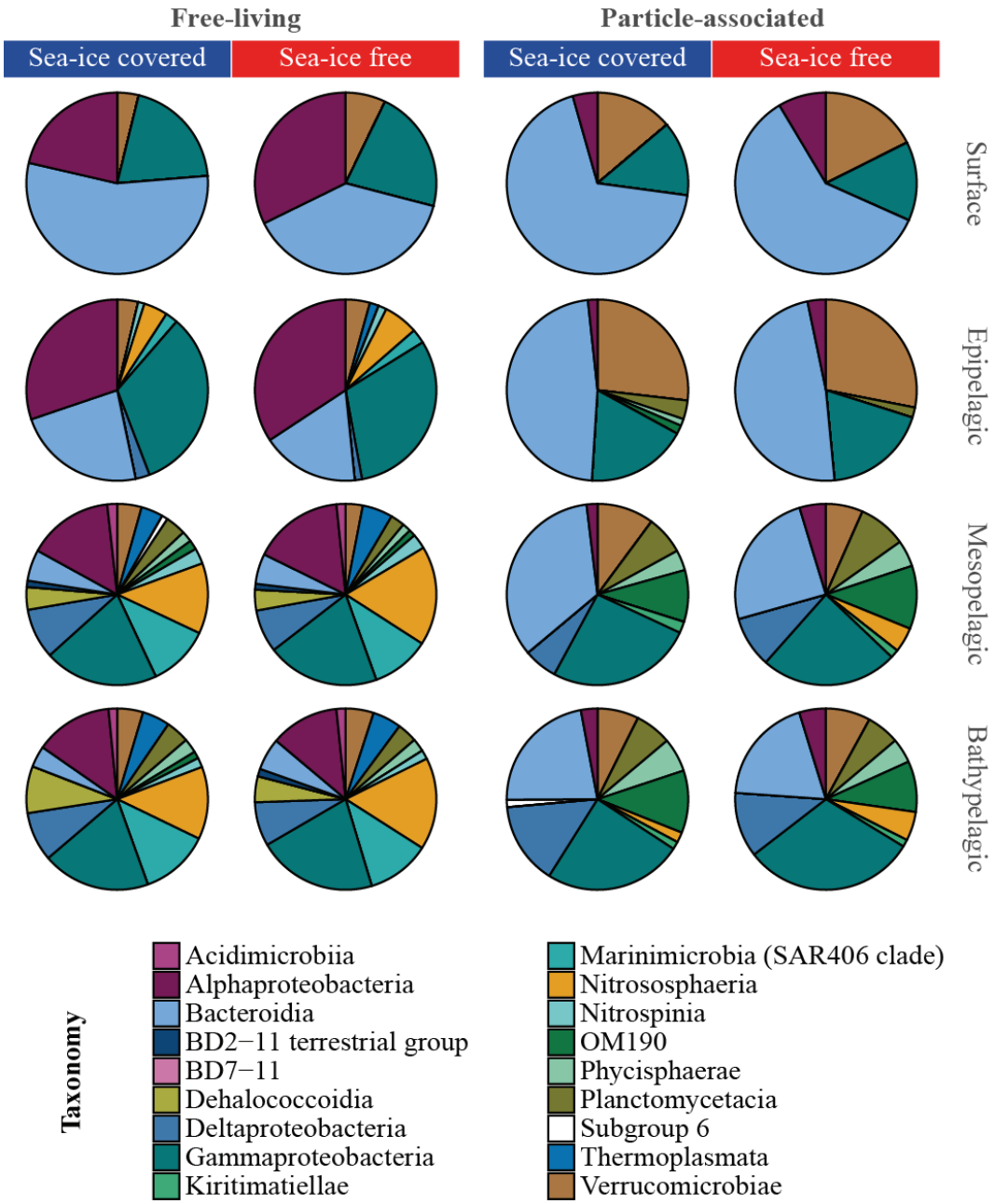

Figure 5.5: Mean sequence proportions of taxonomic classes in both FL and PA fractions throughout the water column, in each region. The colours represent different taxonomic classes according to the legend. Only classes which comprised more than 1% were included in the representation.

2017) and *Planctomycetes* (both *Phycisphaerae* and *Planctomycetacia* classes; Kuypers *et al.*, 2003; Strous *et al.*, 2006). Furthermore, the archaeal class *Nitrososphaeria* (i.e., *Thaumarchaeota*; Doxey *et al.*, 2015) consisted of up to 15% of the sequences in both mesopelagic and bathypelagic waters. Although the knowledge regarding these taxa is limited, the referenced genomic evidences suggest their potential importance in the deep ocean nutrient cycling.

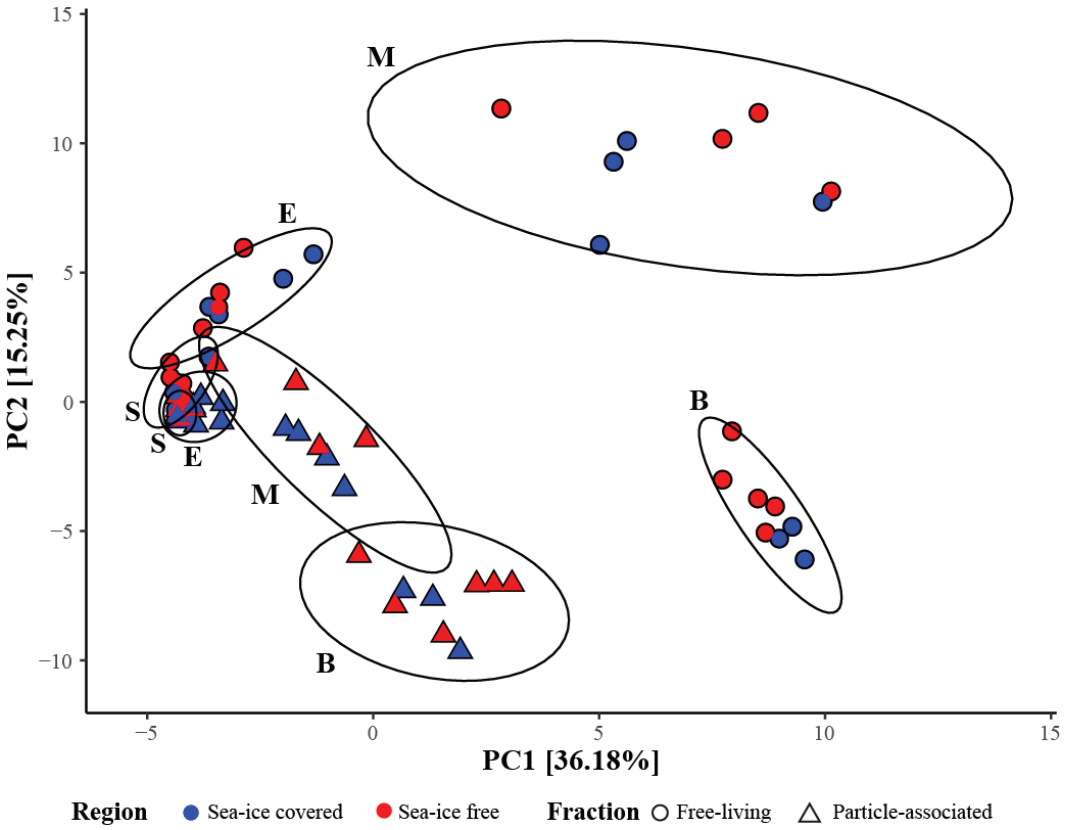

Figure 5.6: Free-living and particle-associated community dynamics throughout the water column of Fram Strait. (A) Principal component analysis (PCA) of microbial communities, based on Euclidean distances. Colours represent different geographic origins, and the shapes indicate free-living (FL) and particles-associated (PA) community fractions. Ellipses encompass each of the groups (by water layer and fraction) with normal confidence of 0.95, and the letters represent the water layer of the clustered samples (S- surface, E- epipelagic, M- mesopelagic, B- bathypelagic). The percentages on both axes represent the explained variance of the axis.

Overall, the communities of both FL and PA fractions showed statistically significant ('ADONIS', $F_{3,62} = 15.187$, $R^2 = 0.375$, $p < 0.001$; Figure 5.6) association with the distinct pelagic layers of the Fram Strait (surface 20 m, epipelagic - 100 m, mesopelagic - 1000 m and bathypelagic - >1000 m). However, the FL communities had significantly higher dissimilarity between the distinct pelagic layers in comparison to the PA communities (pairwise t-test, $p < 0.001$; Figure 5.S4). In all pelagic layers the FL and the PA fractions exhibited differences in the community composition with statistically significant increase in dissimilarity in depth (pairwise t-test, $p < 0.001$; Figure 5.S4). Taken together, these observations suggest that the high distinction of the suspended FL communities is a result of a well stratified water column (Marnela *et al.*, 2016), while the more similar PA communities are potential result of vertical transport of surface waters microbes on sinking aggregates, as was previously demonstrated by Mestre *et al.* (2018).

5.3.4 Particle associated communities go through internal succession throughout the water column

Sinking aggregates originate mostly, and are initially colonized, in the epipelagic waters (Mestre *et al.*, 2018; Thiele *et al.*, 2015). Thereafter, it is a matter of debate to what extent the attached bacteria undergo a succession during sinking, pick up more free-living microbes from surrounding water depths, and what factors influence this process (Datta *et al.*, 2016; Stocker, 2012; Yawata *et al.*, 2014). In order to test which taxonomic groups prevail on marine aggregates we have conducted enrichment tests of OTUs between the particle-associated communities between the different pelagic layers in consecutive order (i.e., surface-epipelagic, epipelagic-mesopelagic, mesopelagic-bathypelagic). The OTUs which had a fold-2 change (in their sequence abundance) of absolute value higher than 1 and an adjusted p-value < 0.1 were defined as enriched (Figure 5.7).

Our results revealed that altogether 749 OTUs showed significant enrichment with depth in the PA communities (176 OTUs between surface and epipelagic waters; 377 OTUs between epipelagic and mesopelagic waters; 196 OTUs between mesopelagic and bathypelagic waters). Throughout the entire water column the PA communities were enriched with OTUs of various 'master recycles' (Buchan *et al.*, 2014), members of the *Gammaproteobacteria* (93 OTUs) and *Bacteroidia* (84 OTUs; Figure 5.7). These taxonomic groups are known for possessing a wide range of carbohydrate-active enzymes to decompose algal-derived OM (Buchan *et al.*, 2014; Chow *et al.*, 2013; Teeling *et al.*, 2012, 2016), were previously described as associated with phytoplankton blooms, and identified as potential candidates for downward propagation of temporal changes to the deep ocean (Cram *et al.*, 2015b,a).

However, the largest number of enriched OTUs with depth was associated with various classes within the phylum *Planctomycetes* (233 OTUs) and the class *Deltaproteobacteria* (171 OTUs; Figure 5.7). It has been suggested that the high oxygen consumption by OM degrading bacteria (e.g., *Gammaproteobacteria* or *Bacteroidia*) creates anoxic and nutrient-enriched patches within the marine aggregates (Woebken *et al.*, 2007). These microniches then filled by organisms with anaerobic oxidation capabilities, such as anaerobic oxidation of ammonium by *Planctomycetes* (Kuypers *et al.*, 2003; Strous *et al.*, 2006) or sulfate-reduction by *Deltaproteobacteria* (Jones *et al.*, 2017; Muyzer and Stams, 2008). Thus, our results suggest that, despite the long sinking process to the deep ocean, the aggregates are still actively degraded by bacterial heterotrophs, which were potentially transported on the aggregates from the surface waters.

5.3.5 Sinking aggregates as potential vectors for the transport of surface-derived microbial taxa to the deep Arctic Ocean

In order to estimate whether the observed PA community dynamics are a result of internal succession within the sinking aggregates or a result of further colonization by surrounding microbes, we implemented a microbial source tracking (MST) Bayesian approach (SourceTracker; Knights *et al.*, 2011). This approach has been previously applied to identify contamination between microbial communities in coastal waters and lakes (e.g., Henry *et al.*, 2016; Neave *et al.*, 2014), and it is based on the assumption that the diversity in various 'source' communities (i.e., FL)

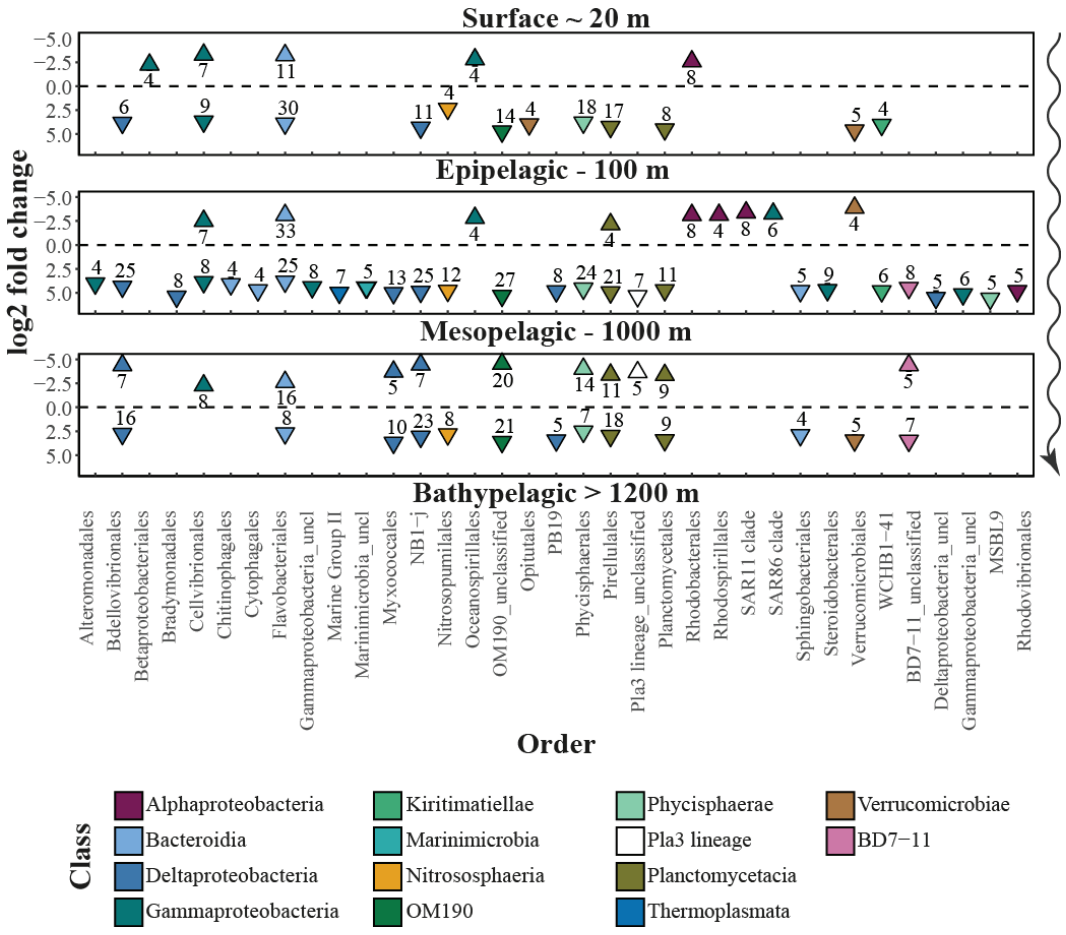

Figure 5.7: Differences in PA community composition between the the distinct water layers. The y axis represents log2 fold change. The color code represents taxonomic classes and each point represents the average for orders with more than 3 daOTU (black bars indicate standard deviations). The numbers below the symbols represent the number of daOTU enriched in the depth.

and corresponding 'sink' communities (i.e., PA) will allow the identification of statistically probable links between them. To our knowledge this approach has been so far applied only once in microbial oceanography to correlate microbial communities and water mass advections in the Southern Ocean (Wilkins *et al.*, 2013).

We used a model validation approach called 'leave-one-out' which tests the predictive accuracy across samples in the training dataset (i.e., the sources), that were each hidden, in turn, from the model when it was trained (Friedman *et al.*, 2001). The assessed performance of the model showed that the predicted water mass of each FL community matched its actual origin with a statistical significance ('ADONIS', $R^2 = 0.80$, $p < 0.001$; Figure 5.8). Indicating that the signal in this dataset is strong. The MST model identified that the FL microbial communities were closely associated with the distinct water masses of Fram Strait (Figure 5.1), with no evidences of vertical mixing between the FL communities. Furthermore, in the epipelagic boundary between the regions (stations HG4 and HG9) the model identified mixed communities of PW and AW water masses, supporting recent ocean simulations which showed horizontal mixing and water exchange by eddies in this boundary region (Wekerle *et al.*, 2017a).

The MST model showed that PA communities of the epipelagic waters were statistically associated with the FL communities (Figure 5.8). The contribution of different sources to deep ocean PA communities was less resolved, potentially due to the high diversity of the community, which consist of large number of rare OTUs (Figure 5.S3). Nevertheless the epipelagic FL communities contributed, as sources, up to <50% and <20% of the PA communities in meso- and bathypelagic waters, respectively. There was very little contribution of the deep ocean FL microbes to the PA communities, supporting previous observations of rare transitions between the lifestyles at depth (Thiele *et al.*, 2015; Salazar *et al.*, 2015).

It is important to note that the use of only two size fractions clusters all particles larger than 5 µm into one pool (Mestre *et al.*, 2017b,a). Consequently, our estimates represent an integration of large sinking aggregates as well as small buoyant particles. Such integration may influence our observations, especially in the deep ocean where large sinking aggregates are rare and small buoyant particles become more abundant (Baltar *et al.*, 2009; Herndl and Reinthaler, 2013). Thus, we suggest that considerable part of the estimated contribution of the bathypelagic FL communities to the PA fraction (i.e., colonization) represents small buoyant deep ocean particles, or alternatively resuspended particles of the nepheloid layer (Wells and Deming, 2003).

Deep-water PA communities of the sea-ice covered region contained more than twice as many surface-borne bacterial types compared to the ice-free region (Figure 5.8), suggesting that those communities retain an increased contribution of epipelagic community members. The presence of sea ice has already been considered a major factor influencing POC fluxes in the Arctic Ocean (Soltwedel *et al.*, 2016; Leu *et al.*, 2011), not only by controlling pelagic primary production in ice-melting regions, but also due to extensive primary production occurring underneath the sea ice, which produces rapidly sinking organic matter (Rapp *et al.*, 2018; Boetius *et al.*, 2013). In our study, we also observed significantly larger, faster-sinking particles in ice-covered regions formed by sea-ice diatoms, which evidently reach the seafloor rapidly. This was independently recorded by high-resolution seafloor imaging conducted during the same expedition, encountering large phytoplankton aggregates on the seafloor of the ice-covered region, but not of the ice-free region (Bergmann and Schewe, 2017). Taken together with our community turnover

projections, we conclude that sea ice promotes the formation of mainly diatom aggregates with a higher sinking velocity, leading to decreased retention times of the particles in the different water layers on their way down, ultimately shortening the time of re-colonization by the FL community. The attenuated turnover of communities, in turn, retains larger proportions of surface community members in these particles, and promotes a stronger connectivity between the surface and the deep ocean.

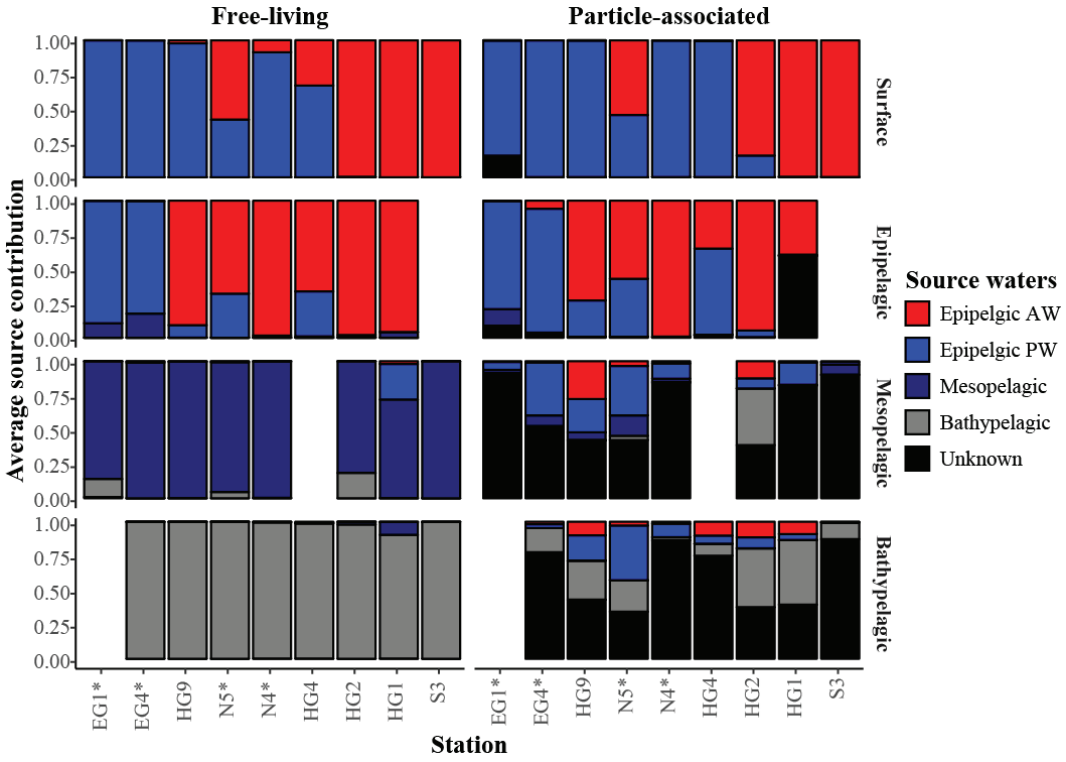

Figure 5.8: Water mass source contribution estimates for microbial communities along the water column, conducted using 'SourceTracker'. The source estimates for the FL communities were estimated using the leave-one-out approach, and the sources of the PA communities were estimated based on the FL communities. Asterisk represents stations associated with sea ice.

5.4 Conclusions

The impact of current decline of sea ice in the Arctic Ocean on the microbial communities in the water column remains largely unknown. Here we focused on the vertical connectivity between surface and deep oceans in ice-covered and ice-free regions. Our data suggests that the vertical flux of sinking particles during the Arctic summer is strongly associated with the sea-ice conditions, as the sea ice impacts the composition of the sinking aggregates (e.g., type of phytoplankton) as well as their sinking velocity and associated microbial community. The variation in size and composition influences sinking velocities between the regions of different sea-ice regimes, with larger and faster-sinking particles in ice-covered regions. The analysis of the microbial communities associated with the sinking particles showed increasing dissimilarity with depth between the particle-associated communities and the ambient free-living microbes. How-

ever, large number of taxa was shared between size-fractions at each depth, suggesting taxonomic exchange between them. Our approach of applying microbial source tracking to identify particle colonization and vertical connectivity patterns between surface and deep Arctic Ocean showed that surface water free-living microbes had a stronger contribution to the deep ocean particle-associated communities in ice-covered regions than in ice-free regions. Considering the similarities of conditions between the surface ice-covered waters and the deep ocean waters (e.g., temperature, oligotrophy), these surface-derived microbes may prevail and play an important role in the function of the deep waters communities. Ice-free regions produced smaller, more buoyant particles that exhibited a higher turnover of communities between the size-fractions. Due to lower sinking velocities, the particles in ice-free regions have longer time for community exchanges with ambient free-living microbes of the different water layers, allowing for more extensive re-colonization of the particles on their way down.

In conclusion, we suggest that vertical connectivity between the surface and deep waters microbial communities of the Arctic Ocean is effectively mediated by large, rapidly sinking marine particles, as found in sea-ice associated waters. In contrast, ice-free waters mediate a substantially weaker connectivity, lessening the influence of surface communities to carbon cycling in the deep waters of the Arctic Ocean. These scenarios can be directly projected to the future warmer ice-free summers in the Arctic Ocean, suggesting strong impact on the biogeochemical cycles in the water column and benthos of the Arctic Ocean basin.

5.5 Materials and methods

Sampling and metadata collection

Sampling was performed during the Polarstern cruise PS99.2 in HAUSGARTEN observatory in the Fram Strait (June 24th- July 16th 2016). Hydrographic data of the seawater including temperature and salinity were retrieved at PANGAEA (Tippenhauer *et al.*, 2017), as well as chlorophyll a concentrations in the water column (Nöthig *et al.*, 2018). The sea-ice concentration was retrieved from http://data.seaiceportal.de (Grosfeld *et al.*, 2016). Sea surface temperature was obtained from NOAA NCEP real-time analysis (http://polar.ncep.noaa.gov/sst/). To investigate the vertical structure and connectivity of free-living and particle-associated microbial communities, water samples (4-8 Liter) were collected from 4 distinct water layers throughout the entire water column (Table 5.S2).

In situ measured marine particle size distribution

The in situ profiling of marine particles was carried out using Underwater Vision Profiler 5hd (UVP; Hydroptic, France) mounted to the water sampler rosette (Picheral *et al.*, 2010). The UVP acquires images of particles within a measured volume of water, and the analyses of the images provide quantitative information on sizes of particles throughout the water column. For the purpose of this publication the particles were classified into two size classes, small particles with equivalent spherical diameter 60-512 μm, and large particles 0.512-10.3 mm. The particles

size is converted to biovolume assuming spherical structure. The concentrations are presented as biovolume / water volume (ppm). (further described in SI Materials and Methods).

On board characterization of marine aggregates and sinking velocity measurements

Using a marine snow catcher (MSC) we sampled intact aggregates, below the sub-surface chl a maxima (60 m depth). The aggregates were measured on board for their size, composition, and sinking velocities. Detailed information on the procedures can be found in SI Materials and Methods.

Modeled particles sinking trajectories

We use a Lagrangian particle tracking algorithm to track back sinking particles from the sampling depth to the surface. The backward particle computation is done by reversing the flow field, i.e., particles are treated as if they were rising from the sampling depth to the surface with a negative sinking speed, being horizontally displaced with the reversed horizontal velocity (further described in SI Materials and Methods and Wekerle *et al.*, 2015).

Microbial community analyses

Genomic bacterial and archaeal DNA was isolated in a combined chemical and mechanical procedure using the PowerWater DNA Isolation Kit (MO BIO Laboratories, Inc., Carlsbad, CA, USA). The hyper variable V4–V5 region of the 16S rRNA gene was amplified using 515F-Y and 926R primers (SI Materials and Methods; Parada *et al.*, 2016). The amplicons sequencing procedure on Illumina MiSeq platform was conducted following the standard instructions of the 16S Metagenomic Sequencing Library Preparation protocol (Illumina, Inc., San Diego, CA, USA). After quality control and merging the amplicons were clustered into OTU with Swarm (v2.0; Mahé *et al.*, 2015), and taxonomically classified using SINA v1.2.11 (SILVA Incremental Aligner; Silva reference database release 132). All the statistical analyses were conducted using R (v3.4.1; http://www.Rproject.org/) in RStudio (v1.0.153; RStudio Team, 2015). Detailed information on the bioinformatics procedures can be found in SI Materials and Methods.

Microbial source tracking

To determine potential colonization of marine particles by free-living microbes, and their export from surface water to the deep ocean, we used the R package 'SourceTracker' (v1.0; Knights *et al.*, 2011). Based on the assumption that the particles-associated microbial communities (i.e., 'sink' communities) are result of various events of colonization of particles by free-living microbes (i.e., 'source' communities), the 'SourceTracker' Bayesian model provided estimated proportions of each of the different 'source' communities within the 'sink' community. In case the 'sink' community contains mixture of taxa which do not match any of the 'source' communities, they are assigned to an 'unknown source' (further described in SI Materials and Methods).

Data availability

Data are accessible via the Data Publisher for Earth & Environmental Science PANGAEA (www.pangaea.de): Raw paired-end sequence, primer-trimmed reads were deposited in the European Nucleotide Archive (ENA; Silvester *et al.*, 2018) under accession number XXX. The data were archived using the brokerage service of the German Federation for Biological Data (GFBio; Diepenbroek *et al.*, 2014). Scripts for processing data can be accessed at https://github.com/edfadeev/XXX.

5.6 Supplementary material

In situ measured marine particle size distribution

The in situ profiling of marine particles was carried out using Underwater Vision Profiler 5hd (UVP; Hydroptic, France) mounted to the water sampler rosette (Picheral et al., 2010). The UVP5hd was operated in autonomous pressure mode (Picheral *et al.*, 2010), whereas acquisition was limited to the downcast. Maximum acquisition frequency was 20 Hz and the sampling volume was approximately 1L. The acquired images were analyzed using Zooprocess software (Picheral, 2008), and the particle size distribution was based on 26 size classes of equivalent spherical diameter sorted in a logarithmic scale from 64 μm to 26.79 mm. For the purpose of this publication the particles were classified into two size classes, small particles with equivalent spherical diameter 64-512 μm, and large particles 0.512-10.3 mm.

On board characterization of marine aggregates and sinking velocity measurements

Using a marine snow catcher (MSC) we sampled intact aggregates of both ice-free and ice-covered regions, and measured on board their size, composition, and sinking velocities. The aggregates were individually transferred to a vertical flow chamber (Ploug *et al.*, 2010; Ploug and Jørgensen, 1999) that was filled with GF/F filtered seawater collected from the same MSC and kept at in situ temperature. The x-,y-, and z-axis of each aggregate was measured in the vertical flow system using a horizontal dissection microscope and an ocular. The volume was thereafter calculated assuming an ellipsoid form, which was used to calculate the equivalent spherical diameter (ESD). The sinking velocity was measured by placing the aggregate in the middle of the flow chamber and increasing the upward flow until the aggregate was floating one diameter above the net. The sinking velocity was thereafter calculated by determining the flow speed three times, and dividing the average of these measurements by the area of the flow chamber. The composition of the aggregates was determined with an inverted light microscope using Utermöhl chambers.

Water sampling

Carried out with 12 L Niskin bottles mounted on a CTD rosette (Sea-Bird Electronics Inc. SBE 911 plus probe) equipped with double temperature and conductivity sensors, a pressure sensor, altimeter, chlorophyll fluorometer, and transmissometer. The chlorophyll maximum depth (chl a max) was determined based on chlorophyll a fluorescence during the downcast, while the water samples were collected during the upcast. At all stations, samples were collected from sub-surface chl a max (10 - 30 m), 100 m, 1000 m and 50 m above the seafloor. For assessing bacterial community composition 4L in epipelagic and 8-12L in meso- and bathypelagic waters were filtered with peristaltic pump (Masterflex; Cole Parmer) through successive membrane filters of 5 μm (Whatman Nucleopore, 47 mm polycarbonate), and 0.22 μm (Millipore Sterivex filters). All samples were collected in duplicates and stored at -20°C until DNA isolation.

DNA isolation and 16S amplicon sequencing. Genomic bacterial and archaeal DNA was isolated from the 5 μm- and the 0.22 μm- filter membranes to analyze the particle-associated (PA) and the free-living (FL) community, respectively, in a combined chemical and mechanical procedure using the PowerWater DNA Isolation Kit (MO BIO Laboratories, Inc., Carlsbad, CA, USA). Prior to DNA isolation the sterivex cartridges of the 0.22 μm Sterivex membranes were cracked open in order to place the filters in the kit-supplied bead beating tubes. The isolation was continued according to the manufacturer's instructions, and DNA was stored at - 20°C. Library preparation was performed according to the standard instructions of the 16S Metagenomic Sequencing Library Preparation protocol (Illumina, Inc., San Diego, CA, USA). The hyper variable V4–V5 region of the 16S rRNA gene was amplified using bacterial primers 515F-Y (5'-GTGYCAGCMGCCGCGGTAA-3') and 926R (5'-CCGYCAATTYMTTTRAGTTT-3" Parada *et al.*, 2016). Sequences were obtained on the Illumina MiSeq platform in a 2 × 300 bp paired-end run (CeBiTec Bielefeld, Germany), following the standard instructions of the 16S Metagenomic Sequencing Library Preparation protocol (Illumina, Inc., San Diego, CA, USA).

Bioinformatics and statistical analyses

The raw paired-end reads were primer-trimmed using cutadapt (Martin, 2011), quality trimmed using trimmomatic with sliding window of 4 bases and a minimum average quality of 15 (v0.32; Bolger *et al.*, 2014) and merged using PEAR (v0.9.5; Zhang *et al.*, 2014). Clustering into OTUs was done with Swarm algorithm using default parameters (v2.0; Mahé *et al.*, 2015). One representative sequence per OTU was taxonomically classified using SINA (SILVA Incremental Aligner; v1.2.11; Silva reference database release 132) at a minimum alignment similarity of 0.9, and a last common ancestor consensus of 0.7 (Pruesse *et al.*, 2012). The OTUs which were not taxonomically assigned to Bacteria/Archaea (based on the data set) or occurred with only a single sequence in the whole data set were excluded from further analysis. Furthermore, all OTU which were taxonomically assigned to mitochondria and chloroplast were removed from the dataset. All the statistical analyses were conducted using R (v3.4.1; http://www.Rproject.org/) in RStudio (v1.0.153; RStudio Team, 2015). Sample data matrices were managed using the R package 'phyloseq' (v1.20.0; McMurdie and Holmes, 2013) and plots were generated using R package 'ggplot2' (v2.2.1; Gómez-Rubio, 2017). The samples coverage and alpha diversity was estimated using R package 'iNEXT' (v2.0.12; Hsieh *et al.*, 2018). The rarefaction curves for each sample were generated based on 40 equally spaced rarefied sample sizes with 100 iterations. A prevalence threshold (i.e., in how many samples did a taxon appear at least once) of 5% was applied to the OTU table prior to downstream analysis following (Callahan *et al.*, 2016). Differences between FL and PA for richness and evenness were tested using t-test. Principal component analysis (PCA) was conducted on variance stabilized OTUs abundance matrix (McMurdie and Holmes, 2014). The significance of the clustering was tested using ADONIS function in R package 'vegan' (Permutational Multivariate Analysis of Variance Using Distance Matrices). The fold-change in abundance of each OTU between the regions was calculated using the R package 'DEseq2' (v1.16.1; Love *et al.*, 2014). The method applies a generalized exact binomial test on variance stabilized OTU abundance.

Modeled particles sinking trajectories

We use a Lagrangian particle tracking algorithm to track back particles from the sampling depth to the surface. The backward particle computation is done by reversing the flow field, i.e. particles are treated as if they were rising from the sampling depth to the surface with a negative sinking speed, being horizontally displaced with the reversed horizontal velocity. Particles were advected with daily averaged horizontal model velocities from the ocean general circulation model FESOM, whereas a constant sinking speed is used as vertical velocity. FESOM is an ocean-sea ice model based on unstructured meshes (Danilov *et al.*, 2015; Wang *et al.*, 2014b)). In this study, we use a FESOM configuration that was optimized for the Fram Strait, applying a mesh resolution of 1 km in this area (Wekerle *et al.*, 2017b). A more detailed description of the Lagrangian particle tracking approach, applied to study the catchment area of sediment traps deployed in the Fram Strait, is presented in the study by Wekerle *et al.* (2015).

The backward trajectory calculation was performed for all three sampled regions (ice free - HG , and ice covered – EG and N), using the measured on board sinking velocities. The duration of trajectories released at 2600 m depth (the seafloor) were thus 40 days. Trajectories were computed once per day during the time period March – July 2016. A time step of 1 hour was used for the trajectory calculation, and thus hourly positions and corresponding temperature and salinity values were stored. To quantify the vertical distribution of particles, particle positions are binned into a grid with bin size of 25 m depth x 0.05° Longitude/Latitude and then divided by the total number of particles to determine the fraction of particles originating from each grid box.

Table 5.S1: Settings of 3 particle tracking experiments performed in this study. For each experiment, backward particle trajectories were started once per day during the time period March-July 2016.

Settling location	Depth (m)	Sinking velocity (m/day)
EG (78.81°N / 2.729°W)	Seafloor (2600 m)	47
HG (79.06°N / 4.51°E)	Seafloor (2220 m)	30
N (79.74°N / 4.185°E)	Seafloor (2620 m)	77

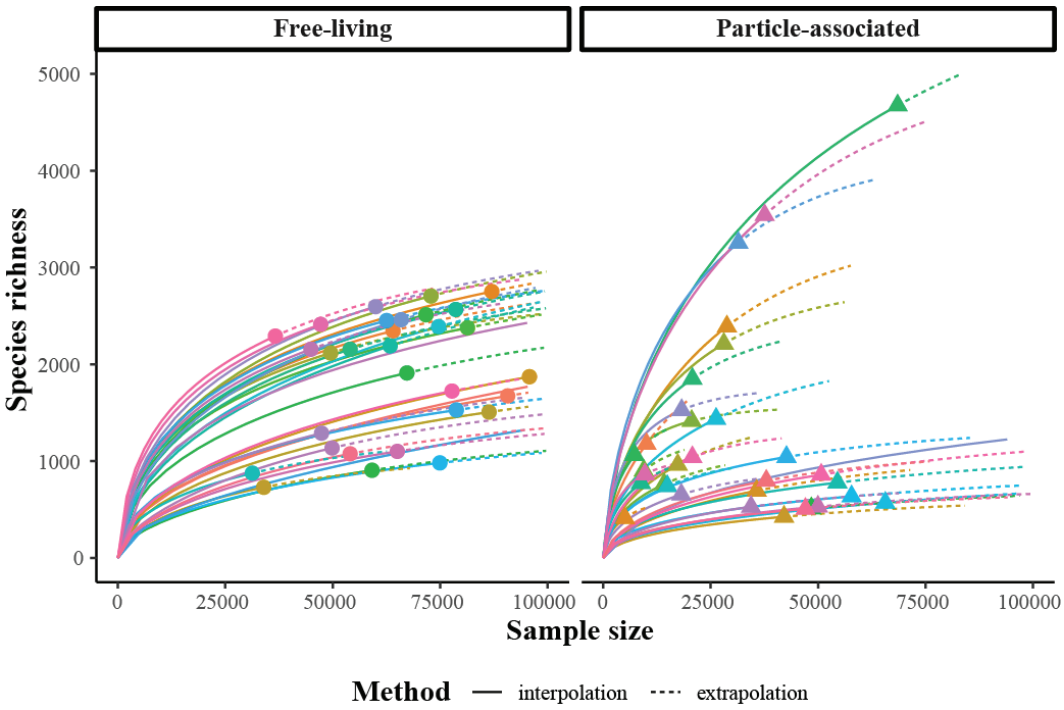

Figure 5.S1: Sample-size-based rarefaction curves for free-living and particle-associated samples.The solid lines represent the observed accumulation with the number of reads sampled, and the dashed lines represent the extrapolated accumulation up to the double amount of reads. Based on the Hill numbers of order q = 0, generated with the iNEXT package (Hsieh *et al.*, 2016).

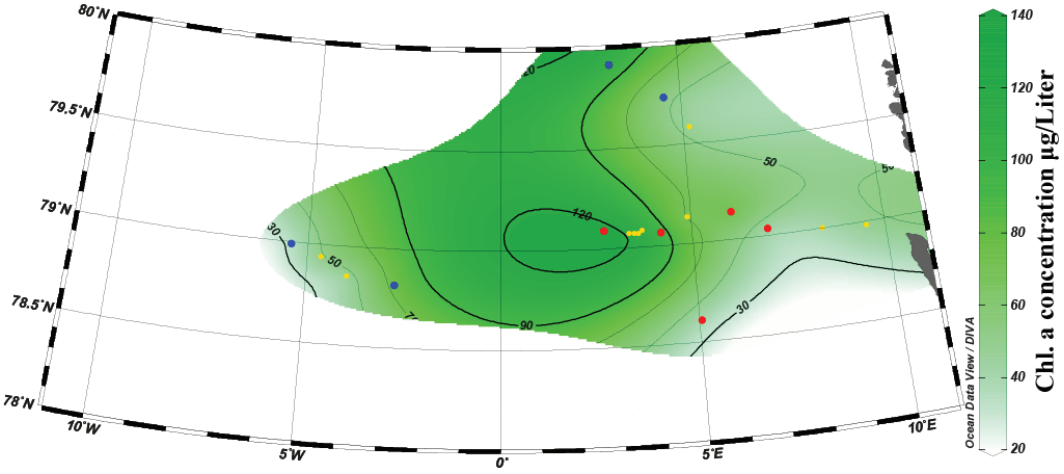

Figure 5.S2: Integrated chlorophyll a concentration (µm/Liter) quota, measured in situ during PS99.2 expedition. All dots represent locations of chlorophyll a sampling. The colored red and blue dots represent the stations where microbial samples were collected (ice-free and ice-covered regions, respectively). The integration of the water column quota was calculated according to (Boss and Behrenfeld, 2010).The plot was generated using Ocean Data View (v4.7.10; Schlitzer, 2015).

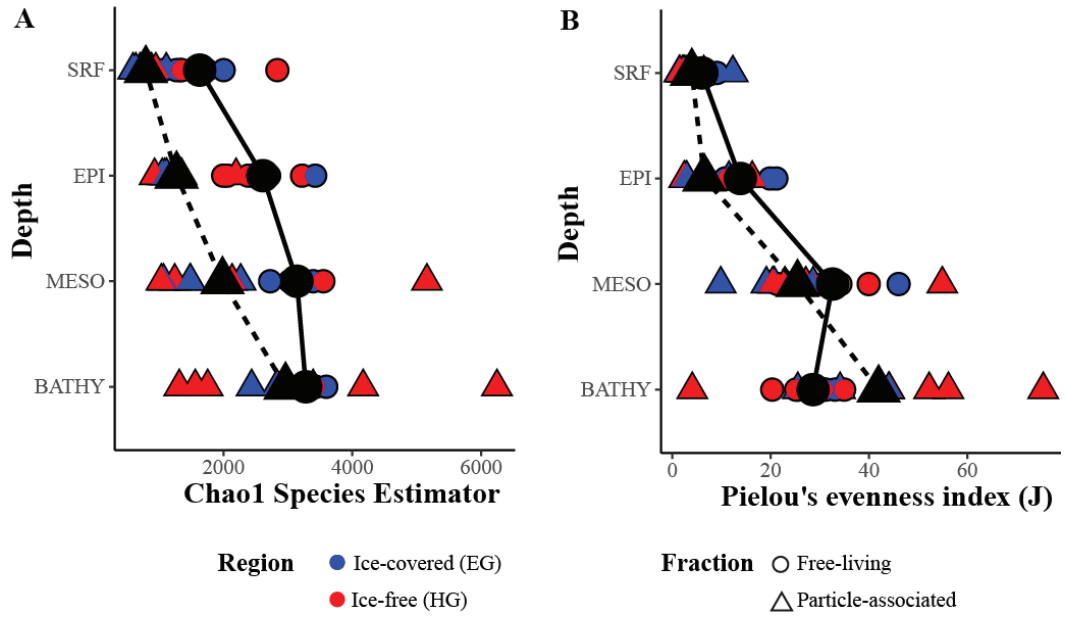

Figure 5.S3: Mean alpha-diversity of microbial communities by depth. (A) Chao1 species estimator. (B) Pielou's evenness index (J). Black points connected with a line represent the mean values for each fraction at each depth, and the coloured points represent individual samples and their geographic origin.

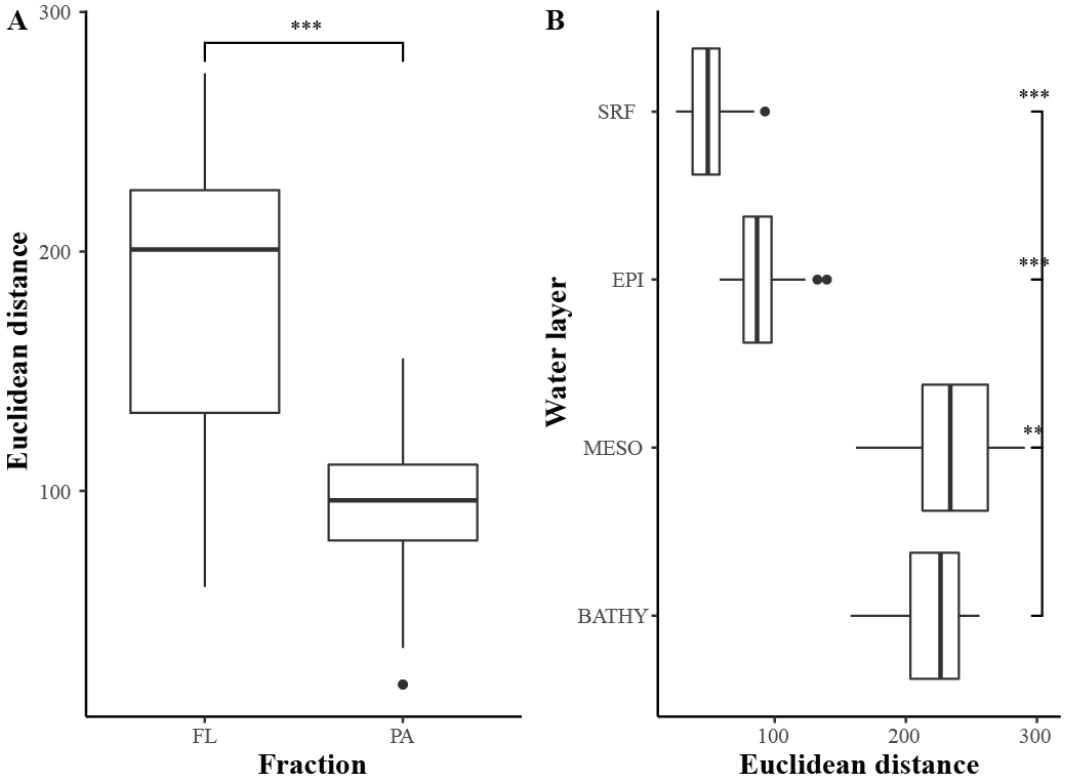

Figure 5.S4: Free-living and particle-associated community dynamics throughout the water column of Fram Strait. (**A**) Distribution of Euclidean distances between FL and PA communities in different depths. (**B**) Distribution of Euclidean distances between communities in each fraction throughout the water column. The asterisks represent levels of statistical significance: *- 0.05, **- 0.01, ***-0.001.

Table 5.S2: Overview of stations which were sampled for microbial community analysis, during RV Polarstern expedition PS99.2.

Station Name	Longitude (°E)	Latitude (°N)	PANGAEA stationID	Sampled depths (m)
EG1	005°24.56' W	78°59.45' N	PS99/0051-1	13 (Surface)
EG1	005°24.56' W	78°59.45' N	PS99/0051-1	100 (Epipelagic)
EG1	005°24.56' W	78°59.45' N	PS99/0051-1	971 (Mesopelagic)
EG4	002°43.73' W	78°48.96' N	PS99/0048-11	24 (Surface)
EG4	002°43.73' W	78°48.96' N	PS99/0048-11	100 (Epipelagic)
EG4	002°43.73' W	78°48.96' N	PS99/0048-1	1000 (Mesopelagic)
EG4	002°43.73' W	78°48.96' N	PS99/0048-1	2527 (Bathypelagic)
HG9	002°50.46' E	79°08.04' N	PS99/0059-2	24 (Surface)
HG9	002°50.46' E	79°08.04' N	PS99/0059-2	100 (Epipelagic)
HG9	002°50.46' E	79°08.04' N	PS99/0059-2	1000 (Mesopelagic)
HG9	002°50.46' E	79°08.04' N	PS99/0059-2	2500 (Bathypelagic)
HG4	004°10.55' E	79°03.93' N	PS99/0042-11	28 (Surface)
HG4	004°10.55' E	79°03.93' N	PS99/0042-11	100 (Epipelagic)
HG4	004°10.55' E	79°03.93' N	PS99/0042-1	1000 (Mesopelagic)
HG4	004°10.55' E	79°03.93' N	PS99/0042-1	2450 (Bathypelagic)
HG2	004°54.40' E	79°07.80' N	PS99/0057-1	22 (Surface)
HG2	004°54.40' E	79°07.80' N	PS99/0057-1	100 (Epipelagic)
HG2	004°54.40' E	79°07.80' N	PS99/0057-1	1000 (Mesopelagic)
HG2	004°54.40' E	79°07.80' N	PS99/0057-1	1492 (Bathypelagic)
HG1	006°04.92' E	79°08.34' N	PS99/0066-2	17 (Surface)
HG1	006°04.92' E	79°08.34' N	PS99/0066-5	100 (Epipelagic)
HG1	006°04.92' E	79°08.34' N	PS99/0066-5	500 (Mesopelagic)
HG1	006°04.92' E	79°08.34' N	PS99/0066-5	1253 (Bathypelagic)
N5	003°03.72' E	79°55.27' N	PS99/0053-2	19 (Surface)
N5	003°03.72' E	79°55.27' N	PS99/0053-2	100 (Epipelagic)
N5	003°03.72' E	79°55.27' N	PS99/0053-2	1000 (Mesopelagic)

Station Name	Longitude (°E)	Latitude (°N)	PANGAEA stationID	Sampled depths (m)
N5	003°03.72’ E	79°55.27’ N	PS99/0053-2	2427 (Bathypelagic)
N4	004°30.21’ E	79°44.49’ N	PS99/0055-1	22 (Surface)
N4	004°30.21’ E	79°44.49’ N	PS99/0055-1	100 (Epipelagic)
N4	004°30.21’ E	79°44.49’ N	PS99/0055-7	1000 (Mesopelagic)
N4	004°30.21’ E	79°44.49’ N	PS99/0055-7	2500 (Bathypelagic)
S3	005°02.84’ E	78°36.44’ N	PS99/0041-6	15 (Surface)
S3	005°02.84’ E	78°36.44’ N	PS99/0041-6	28 (Surface)
S3	005°02.84’ E	78°36.44’ N	PS99/0041-1	1000 (Mesopelagic)
S3	005°02.84’ E	78°36.44’ N	PS99/0041-1	2330 (Bathypelagic)

Table 5.S3: Overview of alpha diversity metrices for the 16S rRNA gene samples. The table consists of number of sequences after the bioinformatics workflow as well as alpha diversity estimations, conducted using the R package 'iNEXT'.

Station name	Water layer	Fraction	Number of sequences	Number of OTUs	Chao1 richness	Richness coverage %	Shannon index	Simpsons index	Evenness index	Completeness %
EG1	DCM	FL	86382	1507	2002.6	75.25	49.6	11.5	6.8	99.4
EG1	DCM	PA	5038	412	597.1	69.00	74	22	12.3	96.8
EG1	EPI	FL	67267	1911	2609.1	73.24	150	39.5	19.9	99
EG1	EPI	PA	14181	762	1113.4	68.44	76.4	23.9	11.5	98
EG1	MESO	FL	36646	2292	3117.9	73.51	356	65.7	46	98
EG1	MESO	PA	7301	1062	1484.4	71.54	133.2	11.6	19.1	94.4
EG4	DCM	FL	31292	876	1269.6	69.00	61.2	16.1	9	98.9
EG4	DCM	PA	54502	778	1113	69.90	15.9	4.6	2.4	99.5
EG4	EPI	FL	74645	2389	3423.2	69.79	164.5	44.5	21.1	98.8
EG4	EPI	PA	14909	742	1049.8	70.68	48.4	13.2	7.3	98.1
EG4	MESO	FL	78634	2567	3391.5	75.69	218.5	52.6	27.8	99
EG4	MESO	PA	8769	773	1069.1	72.30	137.8	40.9	20.7	96.7
EG4	BATHY	FL	54056	2155	2899	74.34	196.1	59.9	25.6	98.6
EG4	BATHY	PA	20737	1851	2436.9	75.96	331	81.7	44	96.9
HG1	DCM	FL	74929	982	1352.4	72.61	47.3	15	6.9	99.5
HG1	DCM	PA	57785	636	882.9	72.04	41.3	16.8	6.4	99.6
HG1	EPI	FL	78775	1528	2058.4	74.23	88.1	24.6	12	99.4
HG1	EPI	PA	42644	1043	1351.1	77.20	112.9	34.7	16.2	99.3
HG1	MESO	FL	62547	2452	3071.8	79.82	266.7	61.1	34.2	98.8
HG1	MESO	PA	26258	1437	2134.2	67.33	166.4	48	22.9	97.8
HG1	BATHY	FL	65940	2461	3323.1	74.06	196.3	55.9	25.1	98.7
HG1	BATHY	PA	31445	3255	4167.6	78.10	610.1	168	75.4	96.4
HG2	DCM	FL	106357	1406	2836.2	49.57	42.7	18	5.9	99.3

Station name	Water layer	Fraction	Number of sequences	Number of OTUs	Chao1 richness	Richness coverage %	Shannon index	Simpsons index	Evenness index	Completeness %
HG2	DCM	PA	65637	570	950.2	59.99	13.9	6.3	2.2	99.6
HG2	EPI	FL	114402	1922	3219.5	59.70	86	29.2	11.4	99.2
HG2	EPI	PA	169192	1530	2196	69.67	18.4	7.1	2.5	99.7
HG2	MESO	FL	122433	2630	3550	74.08	168.8	49.6	21.4	99.3
HG2	MESO	PA	37562	3541	5156.9	68.67	448.6	95.4	54.9	96.1
HG2	BATHY	FL	63364	2190	3416.7	64.10	156.2	51.9	20.3	98.6
HG2	BATHY	PA	68506	4674	6244.2	74.85	474.4	97.3	56.1	97.5
HG4	DCM	FL	49852	1136	1737.5	65.38	42.1	16.2	6	98.9
HG4	DCM	PA	34397	529	771.7	68.55	13.1	5.4	2.1	99.4
HG4	EPI	FL	47394	1289	1995.9	64.58	92.3	28.9	12.9	98.9
HG4	EPI	PA	18161	655	931.1	70.35	40.5	12.8	6.3	98.6
HG4	BATHY	FL	59986	2596	3346.5	77.57	274.6	75.2	34.9	98.7
HG4	BATHY	PA	18246	1528	1754.7	87.08	382.9	115.8	52.2	98.1
HG9	DCM	FL	65026	1101	1547.1	71.17	25.5	7	3.6	99.3
HG9	DCM	PA	49964	530	754.7	70.23	9.7	3.6	1.6	99.6
HG9	EPI	FL	77765	1724	2384.5	72.30	86.8	28.3	11.6	99.1
HG9	EPI	PA	50728	860	1328.6	64.73	16.2	5.9	2.4	99.3
HG9	MESO	FL	47208	2413	3147.1	76.67	311.1	70.7	39.9	98.4
HG9	MESO	PA	9670	863	1036.6	83.25	137.9	17.7	20.4	97.6
HG9	BATHY	FL	44936	2156	2934.8	73.46	234.8	68.4	30.6	98.4
HG9	BATHY	PA	20740	1041	1314.3	79.21	28.1	4.3	4	98.4
N4	DCM	FL	54053	1076	1548.3	69.50	42.5	16.6	6.1	99.2
N4	DCM	PA	47046	507	706.5	71.76	17.2	7	2.8	99.6
N4	EPI	FL	90722	1674	2489.1	67.25	79.7	26.3	10.7	99.3
N4	EPI	PA	37949	798	1118.3	71.36	19.6	7.4	2.9	99.2
N4	MESO	FL	64043	2346	3029.8	77.43	250.6	65.5	32.3	98.9

Station name	Water layer	Fraction	Number of sequences	Number of OTUs	Chao1 richness	Richness coverage %	Shannon index	Simpsons index	Evenness index	Completeness %
N4	MESO	PA	10060	1178	2267.3	51.96	202.5	56.5	28.6	94
N4	BATHY	FL	87025	2752	3595.1	76.55	261.8	84.7	33.1	99.1
N4	BATHY	PA	28778	2391	3391.1	70.51	198.4	40.7	25.5	96.6
N5	DCM	FL	33960	730	1060.7	68.82	22.9	7.5	3.5	99.1
N5	DCM	PA	42075	426	639.8	66.58	8.5	3.3	1.4	99.6
N5	EPI	FL	95782	1872	2708.4	69.12	82.4	25.6	10.9	99.2
N5	EPI	PA	35708	695	1087.7	63.90	18.7	7.2	2.9	99.1
N5	MESO	FL	49521	2117	2724.8	77.69	234.5	62.8	30.6	98.7
N5	MESO	PA	17343	962	1485.2	64.77	67.6	18.2	9.8	97.6
N5	BATHY	FL	72863	2706	3428	78.94	246.4	79.1	31.2	98.9
N5	BATHY	PA	28063	2212	2831.5	78.12	262.7	60.1	34.1	97.4
S3	DCM	FL	59153	906	1324.8	68.39	41.9	17.4	6.1	99.3
S3	DCM	PA	48430	513	740.1	69.31	28.1	13	4.5	99.6
S3	MESO	FL	81377	2377	3085.1	77.05	220.5	54.7	28.4	99.1
S3	MESO	PA	9428	902	1244.1	72.50	184.6	39.2	27.1	96.4
S3	BATHY	FL	71696	2512	3290.9	76.33	220.3	66.8	28.1	98.8
S3	BATHY	PA	20579	1415	1562.5	90.56	320.1	66.8	44.1	98.8

Chapter 6

General discussion

The Fram Strait is the Atlantic-Arctic boundary zone, and provides the main gateway for water exchange between the Arctic and the global oceans. The Fram Strait is the source of, by far, the largest inflow of water into the Arctic Ocean (Beszczynska-Möller *et al.*, 2011), which has already been shown to have a major impact on the entire Arctic Ocean (Polyakov *et al.*, 2017). Through the unique oceanography of the Strait, which includes both the Atlantic inflow and the Arctic outflow, associated with summer sea-ice free and sea-ice covered regimes (respectively), observations in this region provide an important insight into an Arctic marine ecosystem (Soltwedel *et al.*, 2005, 2013, 2016). In times of a rapidly changing Arctic marine ecosystem, as a result of sea-ice cover decline at unprecedented rates (Overland and Wang, 2013), and increasing impact of the Atlantic inflow (Polyakov *et al.*, 2017), an understanding of the main drivers of this ecosystem is urgently needed.

Despite being the sentinel region for the "Atlantification" processes of the Arctic Ocean, prior to this thesis, there were only two molecular studies of bacterial and archaeal communities in this region, Wilson *et al.* (2017), and Müller *et al.* (2018). Both these studies were limited to the first 1000 m of the sea-ice free eastern Fram Strait (the West Spitsbergen Current). Remaining unresolved the microbial communities of the sea-ice covered western Fram Strait (the East Greenland Current) and the deep ocean (> 1000 m). Furthermore, important ecological processes, such as, the impact of sea ice conditions on surface and deep waters microbial communities, remained unaddressed.

The results in this thesis provide the first comprehensive overview of pelagic bacterial and archaeal distribution in the Fram Strait. These communities revealed high taxonomic similarity between the Fram Strait and the central Arctic Ocean, both in the surface and in the deep ocean (Figure 6.1; Boetius *et al.*, 2015; Rapp *et al.*, 2018; Balmonte *et al.*, 2018). Thus, suggesting that the observed pelagic microbial dynamics in the Fram Strait can be, to some extent, extrapolated to the central Arctic Ocean. Moreover, it is reasonable to assume that the biogeochemical changes in the Fram Strait may foreshadow the future of the central Arctic Ocean.

In the following sections, I will discuss the importance of time-series microbial observations, propose a sampling strategy for observing seasonal dynamics in the Fram Strait, and underline the importance of a global integration of these observations. I will address the ecological research

questions of this thesis, and together with the results obtained here, will discuss the far-reaching contribution to our understanding of the bacterial and archaeal community dynamics in the Fram Strait. I will link them to the dynamics of sea ice and primary production in the region, and based on the acquired knowledge will propose a scenario for the future of Arctic Ocean microbial communities.

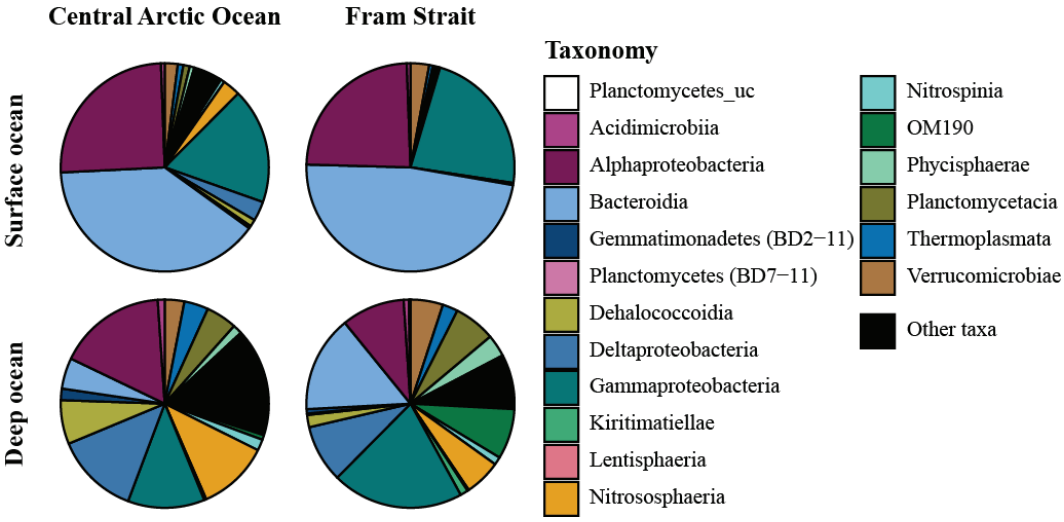

Figure 6.1: Relative sequence abundance comparison of taxonomic classes using the V4V5 region of the 16S rRNA gene, in surface (<50 m) and deep (500-1000 m) waters of central Arctic Ocean and the Fram Strait. The samples included in this comparison are further described in chapter 3.

6.1 Towards integrated microbial observations of the Arctic Ocean

The long-term goal of the Ocean Observing System FRAM is to improve our understanding of the impact changes in ocean circulation, water mass properties, and sea ice conditions, have on the Arctic marine ecosystem. The results in this thesis, as well as, other research projects within the FRAM Molecular Observatory (MolObs; e.g., Metfies *et al.*, 2017; Nöthig *et al.*, 2015; Wolf *et al.*, 2016; Hardge *et al.*, 2017; Engel *et al.*, 2017; Rapp *et al.*, 2018), are already expanding our knowledge of the Arctic marine ecosystem and its functioning. Most of currently existing knowledge regarding microbial communities in the Arctic Ocean in general, and the Fram Strait in particular, is derived from community composition analyses using 16S/18S rRNA gene sequencing. While this valuable knowledge provides an important baseline for answering the basic ecological question "who is out there?", often it is not sufficient for functional characterization of the community (i.e., "what are they doing?"). Therefore, an introduction of 'omics' methodologies (e.g., metagenomics, metatranscriptomics and metaproteomics) into studying the microbial communities will give the opportunity to look into their functional capacity, and potentially link specific phyla to a specific ecological function (e.g., Colatriano *et al.*, 2018).

Similar to other disciplines of oceanography, long-term microbial observations in the Arctic Ocean should be conducted based on well defined parameters, such as the Essential Ocean

Variables (EOVs; Constable *et al.*, 2016; Muller-Karger *et al.*, 2018). Through synthesis of the knowledge established in this thesis, and other studies within the FRAM MolObs (e.g., Metfies *et al.*, 2017; Nöthig *et al.*, 2015; Wolf *et al.*, 2016; Hardge *et al.*, 2017; Engel *et al.*, 2017), a set of microbial indicators (MIs; chapter 2) for environmental changes in the Arctic marine ecosystem should be established (e.g., *Flavobacteria* as an indicator for the seasonal phytoplankton bloom state). These MIs should be well defined, and have a standardized monitoring methodology (e.g., 16S rRNA gene primer set; chapter 3). Then, through a coordination and data integration among research institutions that are conducting molecular studies in the Arctic Ocean, integrated pan-Arctic microbial observations could be achieved.

Due to its structure, and its oceanography, the Arctic Ocean is strongly influenced by water input from the North Atlantic Ocean. This exchange is relevant for physical (Polyakov *et al.*, 2017) and chemical (Torres-Valdés *et al.*, 2013) dynamics between the oceans. However, it is also possible that this water exchange has a direct impact on the microbial communities, as microorganisms may be associated with specific water masses (e.g., Wilkins *et al.*, 2013; Galand *et al.*, 2010; Agogué *et al.*, 2011). In order to identify such transport of microorganisms and to understand its impact, the FRAM MolObs needs also to interact and exchange data with MolObs of the North Atlantic Ocean. One possible platform for such interaction is provided by the Integrated Atlantic Ocean Observing Systems (AtlantOS) project that aims to establish a coordinated network of oceanographic observatories, and associated ocean information systems around the Atlantic Ocean.

6.2 Observing seasonal dynamics in the Fram Strait using autonomous sampling

Surveying the microbial communities with high-throughput methodologies in annual summer expeditions provides an important insight into the spatial dynamics of the microbial communities in the Fram Strait. However, such sampling effort has a limited contribution to our understanding of the natural microbial community variability, and potential identification of the global climate change effects on them (Karl and Church, 2014). Highly resolved temporal dynamics of microbial communities in other oceanographic time-series (e.g., Teeling *et al.*, 2016; Karl and Church, 2014; Cram *et al.*, 2015a) revealed that natural temporal variability of microbial communities in the ocean may occur on a wide range of timescales: from hours - when observing a response to a phytoplankton bloom, up to years - when observing the impact of global oscillations (Ducklow *et al.*, 2009; Fuhrman *et al.*, 2015).

Several existing comparisons of winter-to-summer bacterial and archaeal communities in the Arctic Ocean suggest a strong seasonal variation (Iversen and Seuthe, 2011; Alonso-Sáez *et al.*, 2008; Wilson *et al.*, 2017). That corresponds to the extremely different environmental conditions between the seasons. In the summer, surface water microbial communities are strongly shaped by the availability of organic matter (OM), and are dominated by phytoplankton bloom associated taxonomic groups, such as, *Flavobacteria*, and *Gammaproteobacteria* (Alonso-Sáez *et al.*, 2008; Wilson *et al.*, 2017). In the dark winter, the communities are characterized by a higher diversity, and a higher presence of chemolithotrophes (Ladau *et al.*, 2013; Nikrad *et al.*,

2012; Connelly *et al.*, 2014; Alonso-Sáez *et al.*, 2014; Wilson *et al.*, 2017). These bulk observations provide an important insight into the seasonal differences, however, they do not fully reveal the impact of the strong temporal gradients in environmental conditions on the microbial communities. Thus, microbial seasonal dynamics in the Arctic Ocean remain largely unknown.

One of the main reasons for such scarce availability of winter microbial observations in the Arctic Ocean is the harsh climatic conditions, which limit the accessibility of the sampling sites. In order to overcome this limitation, the innovative McLane Research Laboratories® Remote Access water Sampler (RAS), and the Phytoplankton Sampler (PPS), were introduced to the fixed oceanographic and biogeochemichal mooring system in the HAUSGARTEN observatory, in the framework of the FRAM infrastructure project. These devices allow targeted autonomous water sampling throughout the entire polar year. Due to the limited number of such devices, and the expensive maintenance, their deployment should be carried out according to a well developed sampling strategy which consists of both spatial and temporal aspects:

- **Where to deploy the samplers?** There are clear differences in the development of a seasonal phytoplankton bloom between the West Spitsbergen Current (WSC; ice-free in summer), and the East Greenland Current (EGC; ice-covered in summer), regions of Fram Strait (chapter 4). Simultaneous sampling of both regions may provide an important insight into the seasonal drivers of the microbial communities, through a direct comparison between the regions.

- **At which depth to collect the samples?** Based on the results presented in this thesis, and previous observations from the eastern Fram Strait (Wilson *et al.*, 2017; Metfies *et al.*, 2016), the seasonality is pronounced mainly in the surface waters. However, deployment too close to the surface may put the sampler at risk of collision with sea-ice floats, which may reach a thickness of ~5 m (Bourke and Garrett, 1987). Taking into account that there are no strong differences between summer microbial communities of the surface waters (5-10 m) and the chlorophyll *a* maximum layer (~20 m; chapter 4), the recommended sampling depth would be between 10-20 m.

- **When to collect the samples?** One of the limiting factors in autonomous sampling is the amount of samples that can be collected between a deployment and a recovery. Based on the rapid development of phytoplankton blooms in the Arctic Ocean, and previous observations of changes in bacterial activity throughout a season (Alonso-Sáez *et al.*, 2008), it is reasonable to believe that in summertime the processes within the microbial communities occur much faster. Furthermore, the bacterial and the archaeal cell densities (i.e., biomass) in winter are one order of magnitude lower in comparison to the summer (10^5 and 10^6 cells ml^{-1}, respectively). Thus, a winter sampling may require a larger seawater volume, and a less frequent sampling event, than a summer. Based on these observations, and considering the capacity of 48 water samples by the RAS sampler, the recommended sampling frequency would be one sample per week in a summertime (April - September), and one sample every two weeks during a winter (October - March). The PPS, which consists of 24 samples, may be applied with half of the sampling frequency in comparison to the RAS.

- **For how long may the samples remain under water?** Collected samples are due to stay under the water for at least one year, and in some cases even longer, depending on a ship

time availability. Such long storage requires an efficient fixation, and preservation of the sample. This technical topic is not addressed in the scope of this discussion, however, is crucial of such seasonal observations.

The analysis of an autonomously collected sample is challenging. Throughout a year the microbial biomass in the surface waters is strongly fluctuating (Alonso-Sáez *et al.*, 2008), which might make it impossible to extract sufficient amount of DNA for a metagenomic analysis. Therefore, phylogenetic profiling using 16S rRNA gene is a more suitable approach, due to its lower DNA concentration thresholds (Hassan *et al.*, 2018; Thomas *et al.*, 2012). Heterotrophic bacterial communities clearly dominate Arctic surface waters during spring and summer (chapter 5 and Wilson *et al.*, 2017), associated with the ongoing seasonal phytoplankton bloom (chapter 5). It has been previously shown that the succession of a bacterial community during a bloom is tightly coupled to the phytoplankton bloom dynamics (Teeling *et al.*, 2012). Thus, the abundance, and diversity, of specific bacterial taxonomic groups may serve as a microbial indicator (MI) for different stages of the phytoplankton bloom. The results in this thesis suggest that taxonomic groups, such as the SAR324 clade (*Deltaproteobacteria*) or the SAR202 clade (*Dehalococcoidia*), are MIs for winter and a pre-bloom conditions in the water column (chapter 4). In contrast, taxonomic groups such as the *Rhodobacterales* (*Alphaproteobacteria*) or the *Flavobacteriia* (*Bacteroidetes*), are MIs for a well developed phytoplankton bloom (chapter 4). However, in some cases the succession may occur on a much higher taxonomic resolution (e.g., different strains of the same bacterial genus; Teeling *et al.*, 2016; Chafee *et al.*, 2018), which may have a strong impact on the functional capacity of the observed taxon (Xing *et al.*, 2015). Based on the conducted performance comparison (chapter 3), the higher phylogenetic sensitivity of the V3-V4 primer set, makes it a more suitable choice for 16S rRNA gene monitoring of specific MIs.

The results of this thesis (chapter 5), and previous observations, also suggest that not only *Bacteria* but also *Archaea* may play an important ecological role in the Arctic water column (Galand *et al.*, 2009b; Bano *et al.*, 2004; Alonso-Saez *et al.*, 2012). Furthermore, in previous observations in the Fram Strait during the Arctic winter, the *Archaea*, and especially the *Thaumarchaeota*, comprised a considerable fraction of sequences in surface waters communities (Wilson *et al.*, 2017; Müller *et al.*, 2018). Thus, suggesting that *Archaea* should be included in the long-term time-series monitoring of the FRAM MolObs. Altogether, based on the conducted performance comparison between the 16S rRNA gene primer sets (chapter 3), and the defined requirements of the monitoring scheme, I suggest that the V4-V5 primer set (Parada *et al.*, 2016) will be more suitable for observing the bulk annual dynamics within the surface water bacterial and archaeal communities.

It is also possible that in some cases the collected biomass will not be sufficient even for such sensitive molecular methods as 16S rRNA gene tag-sequencing. In such a case, alternative methodologies may be applied for gathering important insights into the microbial seasonal dynamics. For example, the samples from the PPS, which are collected directly on filter membranes, can be used for targeted Fluorescence In Situ Hybridization (FISH) monitoring of MIs. Furthermore, the RAS samples consist of fixed 500 ml of seawater. These water samples may also be used for FISH, however they can be also analyzed using flow-cytometry (e.g., high:low nucleic acid cell ratio as a biomarker for a phytoplankton bloom; Zubkov and Tarran, 2008; Piontek *et al.*, 2014). Single-cell techniques such as FISH, FISH-flow cytometry (Sekar *et al.*, 2004), and a direct-geneFISH (Barrero-Canosa *et al.*, 2017) have the clear power to greatly expanding the

information acquired via bulk community sequencing efforts. Using these methods it is possible to visualize and enumerate specific sub-groups in a microbial community, demonstrate their activity instead of their mere presence, and to preserve further information about life stages and possible interactions of the investigated microbial community members in their natural habitats (Amann and Fuchs, 2008). Such techniques are very tedious and are very time consuming, therefore, they should be applied on a small subset of key taxonomic groups (i.e., MIs) in the seasonal dynamics of the Arctic marine ecosystem.

6.3 Surface bacterial communities are driven by the seasonal phytoplankton bloom

The seasonal shift from a winter to a summer bacterial and archaeal community in the surface ocean follows a development of a seasonal phytoplankton bloom (Bunse and Pinhassi, 2017). Although very little is known regarding the relationship between phytoplankton and the associated microbial communities, the phytoplankton blooms are usually coupled with an increase in the rate of a bacterial growth and production (Tada *et al.*, 2011; Riemann *et al.*, 2000). The main taxonomic groups which are responding to the bloom are members of the classes *Bacteroidetes* and *Gammaproteobacteria*, and the *Roseobacter* clade within the class *Alphaproteobacteria* (Buchan *et al.*, 2014). A time-series study of the spring phytoplankton blooms in the German Bight (North Sea) has shown that various members of these taxonomic groups are blooming consecutively (Teeling *et al.*, 2016; Chafee *et al.*, 2018). These reoccurring succession patterns of bacterial taxa suggest that changes, over the course of the seasonal bloom, in the availability and composition of OM, are among the main forces that shape the bacterial community (Teeling *et al.*, 2012; Sperling *et al.*, 2017).

Recent observations by Wilson *et al.* (2017) in the surrounding waters of Svalbard (WSC) suggested that the bacterial communities are associated with the seasonal presence of sea ice, and chlorophyll *a* concentrations. During a summer, the surface communities are dominated by phytoplankton-bloom associated copiotrophs, such as *Gammaproteobacteria* and *Flavobacteriia* (Wilson *et al.*, 2017). These highly active heterotrophs may play a key role in the seasonal phytoplankton bloom, as they rapidly turn over the nutrients and make them once again available for further primary production (Azam and Malfatti, 2007). The results presented in this thesis further support these observations, and expand them through a comparison between the pelagic ecosystem of the Atlantic Water (AW) of the WSC, and the Polar Surface Water (PSW) of the EGC. We were able to show, that the diversity of the surface bacterial communities is driven by the succession of the seasonal phytoplankton bloom, which is controlled by a coupled impact of distinct water masses and distinct sea ice conditions (chapter 4).

The distinct water masses in the Fram Strait differ not only in their physical characteristics (Rudels *et al.*, 2005), but also in their nutrient budgets (Falck *et al.*, 2005), both of which may have an impact on the phytoplankton bloom (e.g., Tamminen and Andersen, 2007). Based on the nutrient consumption estimates in the water column, we were able to show that phytoplankton biomass in the sea-ice covered EGC consisted of a much larger fraction of diatoms compared to the sea-ice free waters of the WSC (chapter 4). The Arctic Ocean is a net exporter of silicate

that is exported by the EGC through the Fram Strait in to the North Atlantic (Torres-Valdés *et al.*, 2013). These general differences in silicate budgets between the water masses may potentially favor the conditions for siliceous diatoms in the EGC waters (Nöthig *et al.*, 2015; Krause *et al.*, 2018). However, during the short time period of a seasonal phytoplankton bloom, these differences may be further altered through the horizontal mixing, and a water exchange by meso-scale eddies (Wekerle *et al.*, 2017a,b).

The sea ice may affect the primary production by the phytoplankton through various processes. The seasonal sea-ice retreat increases the solar radiation that penetrates into the water column that results in a stronger phytoplankton bloom in the ice-free water column (Cherkasheva *et al.*, 2014; Rysgaard *et al.*, 1999). In addition, sea ice itself provides a habitat for the sea-ice algae that may be trapped within or hanging below the sea ice (Arrigo, 2014; Boetius *et al.*, 2015). These sea-ice associated algae may contribute a major fraction of the seasonal primary production, and as they detach from the sea ice or when the sea ice melts, may have a strong impact on the availability of OM in the water column. This tight relationship between the primary production and the sea ice is of a special importance for comparisons between the pelagic ecosystems of the EGC and WSC.

Overall, our observations suggest that a combination of the distinct physicochemical conditions, and the distinct sea-ice regimes in each region, drives the composition of surface waters bacterial communities, mainly through control of the seasonal phytoplankton bloom (Figure 6.2A). All these drivers are closely related, and estimating the individual contribution of each one of them is challenging. However, it is reasonable to assume that in addition to the impact of the phytoplankton bloom, each water mass (e.g., AW or PSW) encompasses endemic taxonomic groups (e.g., Agogué *et al.*, 2011), however, in our dataset we were not able to conclusively identify such taxa.

6.4 Sea ice promotes vertical connectivity of microbial communities

The deep ocean is the largest habitat in the biosphere that hosts the largest microbial diversity among the aquatic systems (Whitman *et al.*, 1998). This realm is strongly differs from the surface ocean (< 200 m) by its high pressure, high inorganic nutrient concentrations, and absence of solar radiation. Due to lack of primary production (as a result of insufficient light availability) the deep ocean microbial communities are strongly dependent on the exported organic carbon from the surface (Aristegui *et al.*, 2009). Nevertheless, the deep ocean is considered to be the largest reservoir of organic carbon in the biosphere, and plays an important role in the global biogeochemical cycles (Aristegui *et al.*, 2009; Herndl and Reinthaler, 2013).

The vertical export of OM (i.e., organic carbon) from surface to the deep ocean, by sinking aggregates, is considered to be the major input of OM to the deep ocean (Ducklow *et al.*, 2001; Herndl and Reinthaler, 2013). These sinking aggregates of phytoplankton cells and fecal pellets are subject to colonization by microorganisms, and are hotspots of microbial activity (Azam and Malfatti, 2007; Azam and Long, 2001). The colonized aggregates act not only as vectors for OM transport, but also as vertical dispersal vectors between surface and deep ocean microbial com-

munities (Mestre *et al.*, 2018). Furthermore, it has been shown that in the deep ocean bacterial association with aggregates is a phylogenetically conserved trait, and a transition between free-living and particle-associated lifestyles is rare (Salazar *et al.*, 2015). These observations suggests that most of the aggregate colonization occurs in the surface ocean.

This thesis provides the first observations from deep waters (>1000 m) of the Fram Strait, and includes one of the few studies characterizing deep ocean communities in the Arctic Ocean. The results presented here (chapter 5) revealed that the deep ocean communities are composed of several cosmopolitan taxonomic groups, such as, *Gammaproteobacteria* and *Thaumarchaeota*, and an increasing abundance of poorly characterized taxonomic groups, often addressed as the 'microbial dark matter' (e.g., SAR202 clade, *Marinimicrobia* (SAR406) and SAR324; Rinke *et al.*, 2013). This matches observations of a recent molecular survey of bacterial and archaeal communities in the deep waters of sub-tropical and temperate oceans (Salazar *et al.*, 2016), suggesting that despite physicochemical and biogeographical differences, there may be similar drivers of bacterial and archaeal diversity in deep waters of the global ocean.

The results of this thesis also further expand recent observations from the central Arctic Ocean, where excessive primary production by sea-ice associated algae was shown to provide a strong connectivity vector between sea ice and seafloor microbial communities (Rapp *et al.*, 2018). Through a comparison of marine aggregate characteristics, and microbial communities in sea-ice free and sea-ice covered waters of the Fram Strait, we showed that the vertical connectivity between bacterial and archaeal communities in the sea-ice covered water column is stronger. Sea ice promotes large, fast-sinking aggregates enriched with diatom cells that provide an export vector to the deep ocean for the "master recyclers", such as, *Flavobacteriales* and *Rhodobacterales* (Buchan *et al.*, 2014), where based on bacterial activity measurements in the central Arctic Ocean, they may play an active role in the degradation of OM (Tamelander, 2013; Balmonte *et al.*, 2018). This important observation suggests that despite the strong stratification of the Arctic Ocean water column, seasonal dynamics of microbial communities in surface waters (which are strongly driven by sea ice conditions), may propagate downwards to the deep ocean in a short period of time (Figure 6.2B).

6.5 Future scenario for Arctic Ocean pelagic microbial communities

The shift towards warmer conditions in the Arctic Ocean may have a strong impact on the Arctic marine ecosystem, and its functioning (Wassmann, 2015; Hollowed *et al.*, 2018; Wassmann and Reigstad, 2011). One of the main expected changes is in the magnitude of the seasonal primary production (i.e., amount of fixed carbon) that will have a cascading impact on the entire marine ecosystem. The continued thinning of the Arctic sea ice will increase the light transmission, resulting in earlier growth of the sea-ice associated algae (which have a large contribution to the primary production in the Arctic Ocean, e.g., Fernández-Méndez *et al.*, 2015). However, a stronger light transmission, and warmer waters, will also lead to an earlier breakout of the sea ice, and a stronger pelagic primary production by phytoplankton. Thus, due to the strong interdependencies between various environmental factors, which drive the sea-ice algae and the

phytoplankton blooms, the direction of the change in the primary production is not clear (Arrigo *et al.*, 2012; Arrigo and van Dijken, 2015; Leu *et al.*, 2011). The changing conditions may have an impact not only on the magnitude of the primary production but also on the community composition of the phytoplankton (Mock *et al.*, 2016). Such changes are already reported from the Arctic Ocean with shifting communities from diatom- to flagellate- dominant phytoplankton bloom communities (e.g., Degerlund and Eilertsen, 2010; Metfies *et al.*, 2016; Li *et al.*, 2009; Nöthig *et al.*, 2015). These changes in phytoplankton community composition may potentially shape the co-occurring heterotrophic bacterial communities through the interactions between them, many of which are based on exchange of metabolites and energy sources (Teeling *et al.*, 2012; Bertrand *et al.*, 2015; Grossart and Simon, 2007; Ramanan *et al.*, 2016; Amin *et al.*, 2012; Grossart, 1999; Lima-Mendez *et al.*, 2015; Aharonovich and Sher, 2016). Although understanding these interactions is of a high importance for deciphering energy fluxes and biogeochemical cycles in the ocean, the underlying mechanisms are largely unknown. However, a comparison of bacterial communities associated with blooming diatoms and flagellates revealed that the different blooming phytoplankton is associated with different bacterial communities (Pinhassi *et al.*, 2004).

Overall, it has been shown that bacterial communities correlate strongly with the abundance and the diversity of diatoms rather than other groups of phytoplankton (Rooney-Varga *et al.*, 2005). An extensive research of interaction mechanisms between diatoms and heterotrophic bacteria revealed that they tend to co-occur with specific bacterial groups, such as, *Marinobacter*, *Roseobacter* and *Sulfitobacter* (Grossart *et al.*, 2005; Sapp *et al.*, 2007b,a; Schafer *et al.*, 2002). It has also been suggested that co-occurring *Sulfitobacter*, *Colwellia* and *Pibocella*, protect the diatoms from oxidative stress, by catalyzing hydrogen peroxide that is produced by the phytoplankton (Hünken *et al.*, 2008). Furthermore, it has been shown that diatom-associated *Sulfitobacter* cells promote their cell-devision through secretion of the hormone indole-3-acetic acid (Amin *et al.*, 2015). However, not all interactions may be beneficial for the diatoms, and it has also been shown that transparent exopolymer particles (TEP), which are produced by heterotrophic bacteria, increase the aggregation of diatoms and enhance their sinking to the deep ocean (Gärdes *et al.*, 2011).

On the other hand, less is known regarding associations between bacteria and flagellated phytoplankton. There is evidence for a key function of bacteria in blooms of the coccolithophorid algae *Emiliania huxleyi*, which can be both enhanced (Segev *et al.*, 2016), and inhibited (Harvey *et al.*, 2016; Barak-Gavish *et al.*, 2018) by the co-occurring bacteria. Co-occurrence has also been observed between the Prymnesiophyte *Phaeocystis* spp. and bacterial lineages, such as, *Polaribacter* (*Flavobacteriia*) and *Oceanospirillum* (*Gammaproteobacteria*; e.g., Williams *et al.*, 2016; Ducklow *et al.*, 1999; Becquevort *et al.*, 1998; Delmont *et al.*, 2014). Furthermore, it has been shown that the associated *Bacteria* may inhibit the growth of *Phaeocystis* spp. colonies through solubilization of the algal mucus (i.e., the TEP; Davidson and Marchant, 1987). In recent years the Fram Strait phytoplankton blooms are dominated by colony forming *Phaeocystis* spp. that are strongly associated with a high abundance of TEP (Engel *et al.*, 2017). These polysaccharides have been shown to be an important factor in determining bacterial diversity during a phytoplankton bloom, and are selecting towards TEP utilizing taxa, such as, *Flavobacteriales* and *Rhodobacterales* (Taylor *et al.*, 2014). Thus, a combination of these observations with the results of this thesis (chapter 4) suggest that potential dominance of flagellated phytoplank-

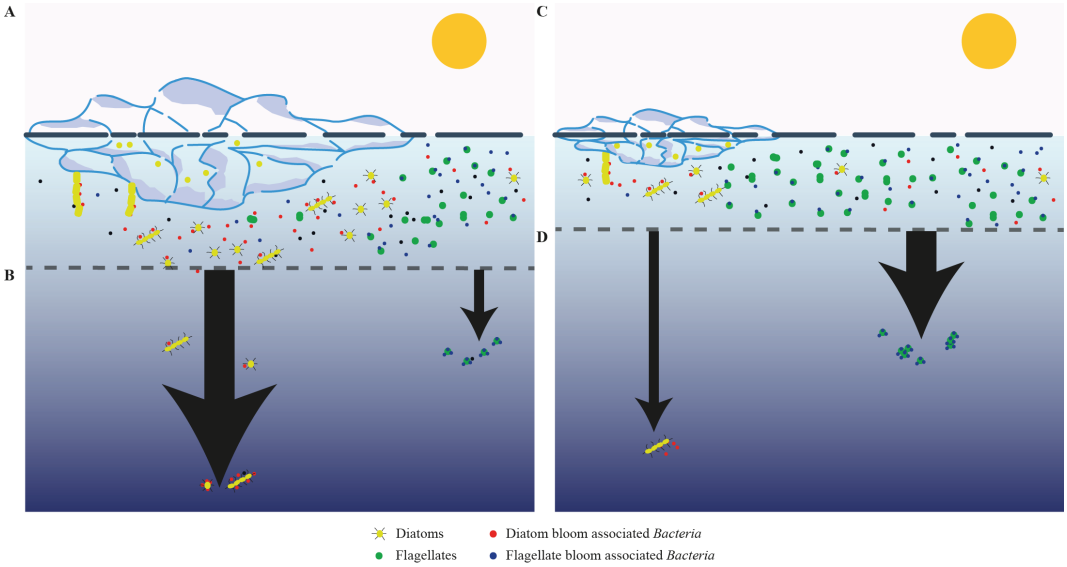

Figure 6.2: Schematic representation of an Arctic Ocean water column microbial community. (**A**) A hypothetical photic layer in current Arctic marine ecosystem, the phytoplankton communities and the associated heterotrophic communities. (**B**) Represents the hypothetical vertical export to the deep ocean in the distinct regions. The width of the arrows represent a hypothetical magnitude of the export. The dashed line represents the seasonal picnocline. (**C**,**D**) A hypothetical water column in a future Arctic Ocean, with decreased sea ice extent, shift in dominant phytoplankton and shift in vertical export.

ton over diatoms in the future ice-free summers in the Arctic marine ecosystem, will most likely have an impact on the phytoplankton-bloom associated bacterial communities (Figure 6.2C).

It is important to note that the suggested changes in the phytoplankton-bloom associated communities may not be apparent through a taxonomic profiling using 16S rRNA gene sequencing. It is possible that the different composition of the phytoplankton community will result in the shift of distinct gene function repertoires within the heterotrophic community, as a result of specialization. A potential functional group of genes in which such changes may occur is the carbohydrate-active enzymes (CAZymes; Cantarel *et al.*, 2009) that are responsible for the degradation of OM during a bloom. It has been shown that while there are differences of substrate preferences between broad taxonomic groups (Teeling *et al.*, 2012), in some cases specialization for distinct polysaccharides may occur within the same taxon (e.g., *Polaribacter*; Xing *et al.*, 2015). Thus, in parallel to further monitoring of the microbial communities 16S rRNA gene tag sequencing, it is vital to conduct further investigations using metagenomics in order to establish a deeper understanding of the functional capacities, and identify functional changes withing these communities (Galand *et al.*, 2018).

The shift in the phytoplankton communities may not be confined to the surface waters, and may propagate to the deep ocean microbial communities. Current model predictions suggest that in the future the Arctic Ocean will have a more active microbial loop in the surface waters, and less OM will be exported to the deep ocean (Vernet *et al.*, 2017). However, reduced availability of OM will not be the only impact on the deep water communities. There is increasing evidence for the importance of vertical connectivity between microbial communities through sinking particles (Frank *et al.*, 2016; Mestre *et al.*, 2018; Duret *et al.*, 2018). The results of this thesis further

extend these observations to the Arctic Ocean, and show for the first time, that sea ice enhances vertical taxonomic connectivity between the surface and the deep oceans (chapter 5). Altogether, this suggests that in future ice-free summers in the Arctic Ocean there may be a weakened genetic and taxonomic flow from the surface to the deep ocean communities (Figure 6.2D).

Perspectives

This thesis significantly contributes to our understanding of the microbial community dynamics in an Arctic marine ecosystem. It gives an extensive overview of the distinct pelagic bacterial and archaeal communities which dominate the surface waters, and their close association with the phytoplankton community. It further describes the key role of sea ice in driving the microbial diversity and in propagating dynamics of surface microbes into the deep waters of the Arctic Ocean. However, these observations, that were made based on taxonomic composition of the microbial communities, only provide a limited information regarding their functional capacity and activity. Building on the results of this thesis, an implementation of 'omics', such as, metagenomics and metaproteomics, is required to extend our understanding of the microbial dynamics in the Arctic marine ecosystem. These methodologies will allow to characterize the functional capabilities of the microbial communities as a whole, as well as link specific functions to specific taxonomic groups. Consequently, this will allow us to link the microbial communities to the biogeochemichal cycles, and to infer metabolic processes present in the Arctic marine ecosystem.

Episodic summer snapshot observations, such as the ones conducted in this thesis, are insufficient to fully understand the microbial dynamics in the Arctic Ocean. The Arctic marine ecosystem is characterized by an extreme seasonal variability, with an entirely phototrophically driven food web during the summer, and a heterotrophic, potentially also chemoautotrophic, food web during the winter. Revealing the succession dynamics of the microbial communities between these two fundamentally different ecosystem states will provide an important insight into the functional capacities of various microbial taxa and their role in the Arctic biogeochemichal cycles. However, due to the extreme conditions during the Arctic winter, this season is heavily undersampled compared to the summer, and almost nothing is known regarding the winter microbial communities in the Arctic marine ecosystem. For a two years now, we were able to overcome the sampling limitations during the harsh winter conditions through the deployment of advanced autonomous sampling platforms. Soon, the analysis of these and other samples will provide a unique opportunity to observe, for the first time in high temporal resolution, the seasonality of the Arctic microbial communities.

The bigger challenge, however, is to monitor processes associated with the changing climate of the Arctic Ocean. Only long-term observations that are well-designed with a standardized sampling scheme and with reasonable sampling reiterations, e.g., a varying sampling frequency according to seasonal variations throughout a year, will allow to effectively monitor ecological patterns. Over time, this might potentially allow to differentiate between the natural seasonal ecosystem variations, and the emerging impacts of climate change. Such observations should not be confined to a single location (e.g., the Fram Strait) and require a world-wide scientific

effort. It is of high importance that the methods development and standardization proceedings, that are developed in the framework of the FRAM Molecular Observatory, will be communicated across the entire Arctic research community in the near future, in order to achieve a standardized pan-Arctic monitoring of the microbial communities.

References

Aagaard K. and Carmack E. C. (1989). The role of sea ice and other fresh water in the Arctic circulation. *Journal of Geophysical Research*, 94(C10):14485.

Aagaard K., Swift J. H., and Carmack E. C. (1985). Thermohaline circulation in the Arctic Mediterranean Seas. *Journal of Geophysical Research*, 90(C3):4833.

Abell G. C. J. and Bowman J. P. (2005). Ecological and biogeographic relationships of class Flavobacteria in the Southern Ocean. *FEMS Microbiology Ecology*, 51(2):265–277.

Agogué H., Lamy D., Neal P. R., Sogin M. L., and Herndl G. J. (2011). Water mass-specificity of bacterial communities in the North Atlantic revealed by massively parallel sequencing. *Molecular Ecology*, 20(2):258–274.

Aharonovich D. and Sher D. (2016). Transcriptional response of Prochlorococcus to co-culture with a marine Alteromonas: differences between strains and the involvement of putative infochemicals. *The ISME Journal*, 10(12):2892–2906.

Alderkamp A. C., Sintes E., and Herndl G. J. (2006). Abundance and activity of major groups of prokaryotic plankton in the coastal North Sea during spring and summer. *Aquatic Microbial Ecology*, 45(3):237–246.

Allers E., Wright J. J., Konwar K. M., Howes C. G., Beneze E., Hallam S. J., and Sullivan M. B. (2013). Diversity and population structure of Marine Group A bacteria in the Northeast subarctic Pacific Ocean. *The ISME Journal*, 7(2):256–268.

Almeida A., Mitchell A. L., Tarkowska A., and Finn R. D. (2018). Benchmarking taxonomic assignments based on 16S rRNA gene profiling of the microbiota from commonly sampled environments. *GigaScience*, 7(5):1–10.

Alonso-Saez L., Waller A. S., Mende D. R., Bakker K., Farnelid H., Yager P. L., Lovejoy C., Tremblay J.-E., Potvin M., Heinrich F., Estrada M., Riemann L., Bork P., Pedros-Alio C., and Bertilsson S. (2012). Role for urea in nitrification by polar marine Archaea. *Proceedings of the National Academy of Sciences*, 109(44):17989–17994.

Alonso-Sáez L., Sánchez O., Gasol J. M., Balagué V., and Pedrós-Alio C. (2008). Winter-to-summer changes in the composition and single-cell activity of near-surface Arctic prokaryotes. *Environmental Microbiology*, 10(9):2444–2454.

Alonso-Sáez L., Zeder M., Harding T., Pernthaler J., Lovejoy C., Bertilsson S., and Pedrós-Alió C. (2014). Winter bloom of a rare betaproteobacterium in the Arctic Ocean. *Frontiers in Microbiology*, 5(AUG):1–9.

Alonso-Sáez L., Díaz-Pérez L., and Morán X. A. G. (2015). The hidden seasonality of the rare biosphere in coastal marine bacterioplankton. *Environmental microbiology*, 17(10):3766–3780.

Amann R. and Fuchs B. M. (2008). Single-cell identification in microbial communities by improved fluorescence in situ hybridization techniques. *Nature Reviews Microbiology*, 6(5):339–348.

Amin S. A., Hmelo L. R., van Tol H. M., Durham B. P., Carlson L. T., Heal K. R., Morales R. L., Berthiaume C. T., Parker M. S., Djunaedi B., Ingalls A. E., Parsek M. R., Moran M. A., and

Armbrust E. V. (2015). Interaction and signalling between a cosmopolitan phytoplankton and associated bacteria. *Nature*, 522(7554):98–101.

Amin S. A., Parker M. S., and Armbrust E. V. (2012). Interactions between Diatoms and Bacteria. *Microbiology and Molecular Biology Reviews*, 76(3):667–684.

Apprill A. (2017). Marine Animal Microbiomes: Toward Understanding Host–Microbiome Interactions in a Changing Ocean. *Frontiers in Marine Science*, 4.

Apprill A., McNally S., Parsons R., and Weber L. (2015). Minor revision to V4 region SSU rRNA 806R gene primer greatly increases detection of SAR11 bacterioplankton. *Aquatic Microbial Ecology*, 75(2):129–137.

Aristegui J., Gasol J. M., Duarte C. M., and Herndl G. J. (2009). Microbial oceanography of the dark ocean's pelagic realm. *Limnology and Oceanography*, 54(5):1501–1529.

Armougom F. (2009). Exploring Microbial Diversity Using 16S rRNA High-Throughput Methods. *Journal of Computer Science & Systems Biology*, 02(01):74–92.

Arnosti C. (2011). Microbial Extracellular Enzymes and the Marine Carbon Cycle. *Annual Review of Marine Science*, 3(1):401–425.

Arnosti C., Steen A. D., Ziervogel K., Ghobrial S., and Jeffrey W. H. (2011). Latitudinal gradients in degradation of marine dissolved organic carbon. *PLoS ONE*, 6(12):8–13.

Arrigo K. R., Perovich D. K., Pickart R. S., Brown Z. W., van Dijken G. L., Lowry K. E., Mills M. M., Palmer M. A., Balch W. M., Bahr F., Bates N. R., Benitez-Nelson C., Bowler B., Brownlee E., Ehn J. K., Frey K. E., Garley R., Laney S. R., Lubelczyk L., Mathis J., Matsuoka A., Mitchell B. G., Moore G. W. K., Ortega-Retuerta E., Pal S., Polashenski C. M., Reynolds R. A., Schieber B., Sosik H. M., Stephens M., and Swift J. H. (2012). Massive Phytoplankton Blooms Under Arctic Sea Ice. *Science*, 336(6087):1408–1408.

Arrigo K. R. (2014). Sea Ice Ecosystems. *Annual Review of Marine Science*, 6(1):439–467.

Arrigo K. R. and van Dijken G. L. (2015). Continued increases in Arctic Ocean primary production. *Progress in Oceanography*, 136:60–70.

Arrigo K. R., van Dijken G., and Pabi S. (2008). Impact of a shrinking Arctic ice cover on marine primary production. *Geophysical Research Letters*, 35(19):1–6.

Aslam S. N., Cresswell-Maynard T., Thomas D. N., and Underwood G. J. (2012). Production and Characterization of the Intra- and Extracellular Carbohydrates and Polymeric Substances (Eps) of Three Sea-Ice Diatom Species, and Evidence for a Cryoprotective Role for Eps. *Journal of Phycology*, 48(6):1494–1509.

Aylagas E., Borja Á., Tangherlini M., Dell'Anno A., Corinaldesi C., Michell C. T., Irigoien X., Danovaro R., and Rodríguez-Ezpeleta N. (2017). A bacterial community-based index to assess the ecological status of estuarine and coastal environments. *Marine Pollution Bulletin*, 114(2): 679–688.

Azam F., Fenchel T., Field J. G., Gray J. C., Meyer-Reil L. A., Thingstad F., and Graf J. S. (1983). The ecological role of water-column microbes in the sea. *Marine Ecology Progress Series*, 10 (3):257–263.

Azam F. (1998). Microbial Control of Oceanic Carbon Flux: The Plot Thickens. *Science*, 280 (5364):694–696.

Azam F. and Long R. A. (2001). Sea snow microcosms. *Nature*, 414(6863):495–498.

Azam F. and Malfatti F. (2007). Microbial structuring of marine ecosystems. *Nature Reviews Microbiology*, 5(10):782–791.

Baker-Austin C. and Oliver J. D. (2017). Vibrio vulnificus - new insights into a deadly opportunistic pathogen. *Environmental Microbiology*.

Balmonte J. P., Teske A., and Arnosti C. (2018). Structure and function of high Arctic pelagic, particle-associated, and benthic bacterial communities. *Environmental Microbiology*, (919).

Baltar F., Aristegui J., Gasol J. M., Sintes E., and Herndl G. J. (2009). Evidence of prokaryotic metabolism on suspended particulate organic matter in the dark waters of the subtropical North Atlantic. *Limnology and Oceanography*, 54(1):182–193.

Bano N. and Hollibaugh J. T. (2002). Phylogenetic composition of bacterioplankton assemblages from the Arctic Ocean. *Applied and Environmental Microbiology*, 68(2):505–518.

Bano N., Ruffin S., Ransom B., and Hollibaugh J. T. (2004). Phylogenetic Composition of Arctic Ocean Archaeal Assemblages and Comparison with Antarctic Assemblages. *Applied and Environmental Microbiology*, 70(2):781–789.

Barak-Gavish N., Frada M. J., Lee P. A., DiTullio G. R., Ku C., Malitsky S., Aharoni A., Green S. J., Rotkopf R., Kartvelishvily E., Sheyn U., Schatz D., and Vardi A. (2018). Bacterial virulence against an oceanic bloom-forming phytoplankter is mediated by algal DMSP. *bioRxiv*, pages 1–38.

Barrero-Canosa J., Moraru C., Zeugner L., Fuchs B. M., and Amann R. (2017). Direct-geneFISH: a simplified protocol for the simultaneous detection and quantification of genes and rRNA in microorganisms. *Environmental Microbiology*, 19(1):70–82.

Barton A. D., Irwin A. J., Finkel Z. V., and Stock C. A. (2016). Anthropogenic climate change drives shift and shuffle in North Atlantic phytoplankton communities. *Proceedings of the National Academy of Sciences*, 113(11):2964–2969.

Bates N. R. and Mathis J. T. (2009). The Arctic Ocean marine carbon cycle: Evaluation of air-sea CO2exchanges, ocean acidification impacts and potential feedbacks. *Biogeosciences*, 6(11): 2433–2459.

Batten S. D., Moffitt S., Pegau W. S., and Campbell R. (2016). Plankton indices explain interannual variability in Prince William Sound herring first year growth. *Fisheries Oceanography*, 25 (4):420–432.

Becquevort S., Rousseau V., and Lancelot C. (1998). Major and comparable roles for free-living and attached bacteria in the degradation of Phaeocystis-derived organic matter in Belgian coastal waters of the North Sea. *Aquatic Microbial Ecology*, 14(1):39–48.

Bélanger S., Babin M., and Tremblay J.-É. (2013). Increasing cloudiness in Arctic damps the increase in phytoplankton primary production due to sea ice receding. *Biogeosciences*, 10(6): 4087.

Bergmann M. and Schewe I. High resolution movies along OFOS profile PS99/048-14, 2017. URL `https://doi.org/10.1594/PANGAEA.873926`.

Bertagnolli A. D., Padilla C. C., Glass J. B., Thamdrup B., and Stewart F. J. (2017). Metabolic potential and in situ activity of marine Marinimicrobia bacteria in an anoxic water column. *Environmental Microbiology*, 19(11):4392–4416.

Bertrand E. M., McCrow J. P., Moustafa A., Zheng H., McQuaid J. B., Delmont T. O., Post A. F., Sipler R. E., Spackeen J. L., Xu K., Bronk D. A., Hutchins D. A., and Allen A. E. (2015). Phytoplankton–bacterial interactions mediate micronutrient colimitation at the coastal Antarctic sea ice edge. *Proceedings of the National Academy of Sciences*, 112(32):9938–9943.

Beszczynska-Moller A., Fahrbach E., Schauer U., and Hansen E. (2012). Variability in Atlantic water temperature and transport at the entrance to the Arctic Ocean, 1997-2010. *ICES Journal of Marine Science*, 69(5):852–863.

Beszczynska-Möller A., Woodgate R., Lee C., Melling H., and Karcher M. (2011). A Synthesis of Exchanges Through the Main Oceanic Gateways to the Arctic Ocean. *Oceanography*, 24(3): 82–99.

Biddanda B. and Benner R. (1997). Carbon, nitrogen, and carbohydrate fluxes during the production of particulate and dissolved organic matter by marine phytoplankton. *Limnology and Oceanography*, 42(3):506–518.

Bienhold C., Boetius A., and Ramette A. (2012). The energy-diversity relationship of complex bacterial communities in Arctic deep-sea sediments. *ISME Journal*, 6(4):724–732.

Bierlich K. C., Miller C., DeForce E., Friedlaender A. S., Johnston D. W., and Apprill A. (2017). Temporal and Regional Variability in the Skin Microbiome of Humpback Whales along the Western Antarctic Peninsula. *Applied and Environmental Microbiology*, 84(5).

Bik E. M., Costello E. K., Switzer A. D., Callahan B. J., Holmes S. P., Wells R. S., Carlin K. P., Jensen E. D., Venn-Watson S., and Relman D. A. (2016). Marine mammals harbor unique microbiotas shaped by and yet distinct from the sea. *Nature Communications*, 7:10516.

Blaser M. J., Cardon Z. G., Cho M. K., Dangl J. L., Donohue T. J., Green J. L., Knight R., Maxon M. E., Northen T. R., Pollard K. S., and Brodie E. L. (2016). Toward a Predictive Understanding of Earth's Microbiomes to Address 21st Century Challenges. *mBio*, 7(3).

Boetius A., Albrecht S., Bakker K., Bienhold C., Felden J., Fernandez-Mendez M., Hendricks S., Katlein C., Lalande C., Krumpen T., Nicolaus M., Peeken I., Rabe B., Rogacheva A., Rybakova E., Somavilla R., and Wenzhofer F. (2013). Export of Algal Biomass from the Melting Arctic Sea Ice. *Science*, 339(6126):1430–1432.

Boetius A., Anesio A. M., Deming J. W., Mikucki J. A., and Rapp J. Z. (2015). Microbial ecology of the cryosphere: Sea ice and glacial habitats. *Nature Reviews Microbiology*, 13(11):677–690.

Bolger A. M., Lohse M., and Usadel B. (2014). Trimmomatic: a flexible trimmer for Illumina sequence data. *Bioinformatics*, 30(15):2114–2120.

Borja A., Elliott M., Andersen J. H., Berg T., Carstensen J., Halpern B. S., Heiskanen A.-S., Korpinen S., Lowndes J. S. S., Martin G., and Rodriguez-Ezpeleta N. (2016). Overview of Integrative Assessment of Marine Systems: The Ecosystem Approach in Practice. *Frontiers in Marine Science*, 3.

Boss E. and Behrenfeld M. (2010). In situ evaluation of the initiation of the North Atlantic phytoplankton bloom. *Geophysical Research Letters*, 37(18):1–5.

Bourke R. H. and Garrett R. P. (1987). Sea ice thickness distribution in the Arctic Ocean. *Cold Reg. Sci. Technol*, 13:259–280.

Bourne D. G., Morrow K. M., and Webster N. S. (2016). Insights into the Coral Microbiome: Underpinning the Health and Resilience of Reef Ecosystems. *Annual Review of Microbiology*, 70(1):317–340.

Bowman J. P., McCammon S. a., Brown M. V., Nichols D. S., and McMeekin T. a. (1997). Diversity and association of psychrophilic bacteria in Antarctic sea ice. *Applied and Environmental Microbiology*, 63(8):3068–3078.

Bowman J. S., Rasmussen S., Blom N., Deming J. W., Rysgaard S., and Sicheritz-Ponten T. (2012). Microbial community structure of Arctic multiyear sea ice and surface seawater by 454 sequencing of the 16S RNA gene. *ISME Journal*, 6(1):11–20.

Brinkmeyer R., Knittel K., Jürgens J., Weyland H., Amann R., Helmke E., Jurgens J., Weyland H., Amann R., and Helmke E. (2003). Diversity and Structure of Bacterial Communities in Arctic versus Antarctic Pack Ice. *Applied and Environmental Microbiology*, 69(11):6610–6619.

Brown M. (2001). A molecular phylogenetic survey of sea-ice microbial communities (SIMCO). *FEMS Microbiology Ecology*, 35(3):267–275.

Brown M. V., Lauro F. M., Demaere M. Z., Muir L., Wilkins D., Thomas T., Riddle M. J., Fuhrman J. A., Andrews-Pfannkoch C., Hoffman J. M., McQuaid J. B., Allen A., Rintoul S. R., and Cavicchioli R. (2012). Global biogeography of SAR11 marine bacteria. *Molecular Systems Biology*, 8(595):1–13.

Brown M. B. (1975). 400: A Method for Combining Non-Independent, One-Sided Tests of Significance. *Biometrics*, 31(4):987.

Brussaard C. P. D., Noordeloos A. A. M., Witte H., Collenteur M. C. J., Schulz K., Ludwig A., and Riebesell U. (2013). Arctic microbial community dynamics influenced by elevated CO2 levels. *Biogeosciences*, 10(2):719–731.

Bryant J. A., Aylward F. O., Eppley J. M., Karl D. M., Church M. J., and DeLong E. F. (2016). Wind and sunlight shape microbial diversity in surface waters of the North Pacific Subtropical Gyre. *The ISME Journal*, 10(6):1308–1322.

Buchan A., LeCleir G. R., Gulvik C. A., Gonzalez J. M., González J. M., and Gonzalez J. M. (2014). Master recyclers: features and functions of bacteria associated with phytoplankton blooms. *Nature Reviews Microbiology*, 12(10):686–698.

Budikova D. (2009). Role of Arctic sea ice in global atmospheric circulation: A review. *Global and Planetary Change*, 68(3):149–163.

Bunse C. and Pinhassi J. (2017). Marine Bacterioplankton Seasonal Succession Dynamics. *Trends in Microbiology*, 25(6):494–505.

Busch K., Endres S., Iversen M. H., Michels J., Nöthig E.-M., and Engel A. (2017). Bacterial Colonization and Vertical Distribution of Marine Gel Particles (TEP and CSP) in the Arctic Fram Strait. *Frontiers in Marine Science*, 4.

Butchart S. H. M., Walpole M., Collen B., van Strien A., Scharlemann J. P. W., Almond R. E. A., Baillie J. E. M., Bomhard B., Brown C., Bruno J., Carpenter K. E., Carr G. M., Chanson J., Chenery A. M., Csirke J., Davidson N. C., Dentener F., Foster M., Galli A., Galloway J. N., Genovesi P., Gregory R. D., Hockings M., Kapos V., Lamarque J.-F., Leverington F., Loh J., McGeoch M. A., McRae L., Minasyan A., Morcillo M. H., Oldfield T. E. E., Pauly D., Quader S., Revenga C., Sauer J. R., Skolnik B., Spear D., Stanwell-Smith D., Stuart S. N., Symes A., Tierney M., Tyrrell T. D., Vie J.-C., and Watson R. (2010). Global Biodiversity: Indicators of Recent Declines. *Science*, 328(5982):1164–1168.

Buttigieg P. L., Pafilis E., Lewis S. E., Schildhauer M. P., Walls R. L., and Mungall C. J. (2016). The environment ontology in 2016: bridging domains with increased scope, semantic density, and interoperation. *Journal of Biomedical Semantics*, 7(1):57.

Buttigieg P. L., Fadeev E., Bienhold C., Hehemann L., Offre P., and Boetius A. (2018). Marine microbes in 4D — using time series observation to assess the dynamics of the ocean microbiome and its links to ocean health. *Current Opinion in Microbiology*, 43:169–185.

Calbert A. and Landry, Michael R. (2004). Phytoplankton growth, microzooplankton grazing, and carbon cycling in marine systems. *Limnology and Oceanography*, 49(1):51–57.

Callahan B. J., Sankaran K., Fukuyama J. A., McMurdie P. J., and Holmes S. P. (2016). Bioconductor Workflow for Microbiome Data Analysis: from raw reads to community analyses. *F1000Research*, 5(3):1492.

Cantarel B. L., Coutinho P. M., Rancurel C., Bernard T., Lombard V., and Henrissat B. (2009). The Carbohydrate-Active EnZymes database (CAZy): an expert resource for Glycogenomics. *Nucleic Acids Research*, 37(Database):D233–D238.

Caporaso J. G., Lauber C. L., Walters W. A., Berg-Lyons D., Lozupone C. A., Turnbaugh P. J., Fierer N., and Knight R. (2011). Global patterns of 16S rRNA diversity at a depth of millions of sequences per sample. *Proceedings of the National Academy of Sciences*, 108(Supplement_1): 4516–4522.

Caporaso J. G., Lauber C. L., Walters W. A., Berg-Lyons D., Huntley J., Fierer N., Owens S. M., Betley J., Fraser L., Bauer M., Gormley N., Gilbert J. A., Smith G., and Knight R. (2012). Ultra-high-throughput microbial community analysis on the Illumina HiSeq and MiSeq platforms. *ISME Journal*, 6(8):1621–1624.

Cardman Z., Arnosti C., Durbin A., Ziervogel K., Cox C., Steen A. D., and Teske A. (2014). Verrucomicrobia Are Candidates for Polysaccharide-Degrading Bacterioplankton in an Arctic Fjord of Svalbard. *Applied and Environmental Microbiology*, 80(12):3749–3756.

Carmack E. C., Yamamoto-Kawai M., Haine T. W., Bacon S., Bluhm B. A., Lique C., Melling H., Polyakov I. V., Straneo F., Timmermans M. L., and Williams W. J. (2016). Freshwater and its role in the Arctic Marine System: Sources, disposition, storage, export, and physical and biogeochemical consequences in the Arctic and global oceans. *Journal of Geophysical Research G: Biogeosciences*, 121(3):675–717.

Carmack E. and Wassmann P. (2006). Food webs and physical-biological coupling on pan-Arctic shelves: Unifying concepts and comprehensive perspectives. *Progress in Oceanography*, 71 (2-4):446–477.

Carmack E. C. (2007). The alpha/beta ocean distinction: A perspective on freshwater fluxes, convection, nutrients and productivity in high-latitude seas. *Deep-Sea Research Part II: Topical Studies in Oceanography*, 54(23-26):2578–2598.

Cesare C. (2016). Ecology's $434,000,000 test. *Nature*, 529(7586):274–276.

Chafee M., Fernàndez-Guerra A., Buttigieg P. L., Gerdts G., Eren A. M., Teeling H., and Amann R. I. (2018). Recurrent patterns of microdiversity in a temperate coastal marine environment. *The ISME Journal*, 12(1):237–252.

Chao A., Gotelli N., Hsieh T., Sander E., Ma K., RK C., and Ellison A. (2014). Rarefactionand extrapolation with Hill numbers: a framework for sampling and estimation in species diversity studies. *Ecological Monographs*, 84(1):45–67.

Chao A. and Jost L. (2012). Coverage-based rarefaction and extrapolation: Standardizing samples by completeness rather than size. *Ecology*, 93(12):2533–2547.

Chao A., Gotelli N. J., Hsieh T. C., Sande E. L., Ma K. H., Colwell R. K., and Ellison A. M. (2014). Rarefaction and extrapolation with Hill numbers: a framework for sampling and estimation in species diversity studies. *Ecological Monographs*, 84:45–67.

Chen B., Yang Y., Liang X., Yu K., Zhang T., and Li X. (2013). Metagenomic Profiles of Antibiotic Resistance Genes (ARGs) between Human Impacted Estuary and Deep Ocean Sediments. *Environmental Science & Technology*, 47(22):12753–12760.

Chen H. and Boutros P. C. (2011). VennDiagram: a package for the generation of highly-customizable Venn and Euler diagrams in R. *BMC Bioinformatics*, 12(1):35.

Cherkasheva A., Bracher A., Melsheimer C., Köberle C., Gerdes R., Nöthig E. M., Bauerfeind E., and Boetius A. (2014). Influence of the physical environment on polar phytoplankton blooms: A case study in the Fram Strait. *Journal of Marine Systems*, 132:196–207.

Chow C.-E. T., Sachdeva R., Cram J. A., Steele J. A., Needham D. M., Patel A., Parada A. E., and Fuhrman J. A. (2013). Temporal variability and coherence of euphotic zone bacterial communities over a decade in the Southern California Bight. *The ISME Journal*, 7(12):2259–2273.

Codispoti L. A., Kelly V., Thessen A., Matrai P., Suttles S., Hill V., Steele M., and Light B. (2013). Synthesis of primary production in the Arctic Ocean: III. Nitrate and phosphate based estimates of net community production. *Progress in Oceanography*, 110(December 2012):126–150.

Colatriano D., Tran P. Q., Guéguen C., Williams W. J., Lovejoy C., and Walsh D. A. (2018). Genomic evidence for the degradation of terrestrial organic matter by pelagic Arctic Ocean Chloroflexi bacteria. *Communications Biology*, 1(1):90.

Cole J. J. (1982). Interactions Between Bacteria and Algae in Aquatic Ecosystems. *Annual Review of Ecology and Systematics*, 13(1):291–314.

Collins R. E., Rocap G., and Deming J. W. (2010). Persistence of bacterial and archaeal communities in sea ice through an Arctic winter. *Environmental Microbiology*, 12(7):1828–1841.

Connelly T. L., Baer S. E., Cooper J. T., and Bronk D. A. (2014). Urea uptake and carbon fixation by marine pelagic bacteria and archaea during the Arctic summer and winter seasons. *Applied and Environmental Microbiology*, 80(19):6013–6022.

Constable A. J., Costa D. P., Schofield O., Newman L., Urban E. R., Fulton E. A., Melbourne-Thomas J., Ballerini T., Boyd P. W., Brandt A., de la Mare W. K., Edwards M., Eléaume M., Emmerson L., Fennel K., Fielding S., Griffiths H., Gutt J., Hindell M. A., Hofmann E. E., Jennings S., La H. S., McCurdy A., Mitchell B. G., Moltmann T., Muelbert M., Murphy E., Press A. J., Raymond B., Reid K., Reiss C., Rice J., Salter I., Smith D. C., Song S., Southwell C., Swadling K. M., Van de Putte A., and Willis Z. (2016). Developing priority variables ("ecosystem Essential Ocean Variables" — eEOVs) for observing dynamics and change in Southern Ocean ecosystems. *Journal of Marine Systems*, 161:26–41.

Conway J. R., Lex A., and Gehlenborg N. (2017). UpSetR: an R package for the visualization of intersecting sets and their properties. *Bioinformatics*, 33(18):2938–2940.

Cordier T., Esling P., Lejzerowicz F., Visco J., Ouadahi A., Martins C., Cedhagen T., and Pawlowski J. (2017). Predicting the Ecological Quality Status of Marine Environments from eDNA Metabarcoding Data Using Supervised Machine Learning. *Environmental Science & Technology*, 51(16):9118–9126.

Cram J. A., Chow C.-E. T., Sachdeva R., Needham D. M., Parada A. E., Steele J. A., and Fuhrman J. A. (2015). Seasonal and interannual variability of the marine bacterioplankton community throughout the water column over ten years. *The ISME Journal*, 9(3):563–580.

Cram J. A., Xia L. C., Needham D. M., Sachdeva R., Sun F., and Fuhrman J. A. (2015). Cross-depth analysis of marine bacterial networks suggests downward propagation of temporal changes. *ISME Journal*, 9(12):2573–2586.

Crespo B. G., Pommier T., Fernández-Gómez B., and Pedrós-Alió C. (2013). Taxonomic composition of the particle-attached and free-living bacterial assemblages in the Northwest Mediterranean Sea analyzed by pyrosequencing of the 16S rRNA. *MicrobiologyOpen*, 2(4):541–552.

Csardi G. and Nepusz T. (2006). The igraph software package for complex network research. *InterJournal*, Complex Sy:1695.

Cullen J., Doolittle W. F., Levin S., and Li W. (2007). Patterns and Prediction in Microbial Oceanography. *Oceanography*, 20(2):34–46.

Danilov S., Wang Q., Timmermann R., Iakovlev N., Sidorenko D., Kimmritz M., Jung T., and Schröter J. (2015). Finite-Element Sea Ice Model (FESIM), version 2. *Geoscientific Model Development*, 8(6):1747–1761.

Datta M. S., Sliwerska E., Gore J., Polz M. F., and Cordero O. X. (2016). Microbial interactions lead to rapid micro-scale successions on model marine particles. *Nature Communications*, 7 (May):11965.

Davidson A. T. and Marchant H. J. (1987). Binding of manganese by Antarctic Phaeocystis pouchetii and the role of bacteria in its release. *Marine Biology*, 95(3):481–487.

Davies N., Field D., Amaral-Zettler L., Clark M. S., Deck J., Drummond A., Faith D. P., Geller J., Gilbert J., Glöckner F. O., Hirsch P. R., Leong J.-A., Meyer C., Obst M., Planes S., Scholin C., Vogler A. P., Gates R. D., Toonen R., Berteaux-Lecellier V., Barbier M., Barker K., Bertilsson S., Bicak M., Bietz M. J., Bobe J., Bodrossy L., Borja A., Coddington J., Fuhrman J., Gerdts G., Gillespie R., Goodwin K., Hanson P. C., Hero J.-M., Hoekman D., Jansson J., Jeanthon C., Kao R., Klindworth A., Knight R., Kottmann R., Koo M. S., Kotoulas G., Lowe A. J., Marteinsson V. T., Meyer F., Morrison N., Myrold D. D., Pafilis E., Parker S., Parnell J. J., Polymenakou P. N., Ratnasingham S., Roderick G. K., Rodriguez-Ezpeleta N., Schonrogge K., Simon N., Valette-Silver N. J., Springer Y. P., Stone G. N., Stones-Havas S., Sansone S.-A., Thibault K. M., Wecker

P., Wichels A., Wooley J. C., Yahara T., and Zingone A. (2014). The founding charter of the Genomic Observatories Network. *GigaScience*, 3(1):2.

de La Rocha C. L. and Passow U. (2003). The biological pump. *Treatise on Geochemistry*, 6: 83–111.

De La Rocha C. L. and Passow U. (2007). Factors influencing the sinking of POC and the efficiency of the biological carbon pump. *Deep-Sea Research Part II: Topical Studies in Oceanography*, 54 (5-7):639–658.

de Steur L., Hansen E., Gerdes R., Karcher M., Fahrbach E., and Holfort J. (2009). Freshwater fluxes in the East Greenland Current: A decade of observations. *Geophysical Research Letters*, 36(23):L23611.

Degerlund M. and Eilertsen H. C. (2010). Main Species Characteristics of Phytoplankton Spring Blooms in NE Atlantic and Arctic Waters (68-80° N). *Estuaries and Coasts*, 33(2):242–269.

Delmont T. O., Hammar K. M., Ducklow H. W., Yager P. L., and Post A. F. (2014). Phaeocystis antarctica blooms strongly influence bacterial community structures in the Amundsen Sea polynya. *Frontiers in Microbiology*, 5(DEC):1–13.

DeLong E. F. and Karl D. M. (2005). Genomic perspectives in microbial oceanography. *Nature*, 437(7057):336–42.

Diepenbroek M., Glöckner F. O., Grobe P., Güntsch A., Huber R., König-Ries B., Kostadinov I., Nieschulze J., Seeger B., Tolksdorf R., and Triebel D. Towards an integrated biodiversity and ecological research data management and archiving platform: the German federation for the curation of biological data (GFBio). In Plödereder E., Grunske L., Schneider E., and Ull D., editors, *Informatik 2014*, pages 1711–1721, Bonn, 2014. Gesellschaft für Informatik e.V.

Dmitrenko I. A., Polyakov I. V., Kirillov S. A., Timokhov L. A., Frolov I. E., Sokolov V. T., Simmons H. L., Ivanov V. V., and Walsh D. (2008). Toward a warmer Arctic Ocean: Spreading of the early 21st century Atlantic Water warm anomaly along the Eurasian Basin margins. *Journal of Geophysical Research*, 113(C5):C05023.

Dobricic S., Vignati E., and Russo S. (2016). Large-scale atmospheric warming in winter and the arctic sea ice retreat. *Journal of Climate*, 29(8):2869–2888.

Doxey A. C., Kurtz D. A., Lynch M. D., Sauder L. A., and Neufeld J. D. (2015). Aquatic metagenomes implicate Thaumarchaeota in global cobalamin production. *ISME Journal*, 9 (2):461–471.

Drinkwater K. F. (2005). The response of Atlantic cod (Gadus morhua) to future climate change. *ICES Journal of Marine Science*, 62(7):1327–1337.

Ducklow H. (2002). Bacterial Production and Biomass in the Oceans. *Microbial Ecology of the Ocean*, pages 1–47.

Ducklow H., Carlson C., and Smith W. (1999). Bacterial growth in experimental plankton assemblages and seawater cultures from the Phaeocystis antarctica bloom in the Ross Sea, Antarctica. *Aquatic Microbial Ecology*, 19(3):215–227.

Ducklow H., Steinberg D., and Buesseler K. (2001). Upper Ocean Carbon Export and the Biological Pump. *Oceanography*, 14(4):50–58.

Ducklow H. W., Doney S. C., and Steinberg D. K. (2009). Contributions of Long-Term Research and Time-Series Observations to Marine Ecology and Biogeochemistry. *Annual Review of Marine Science*, 1(1):279–302.

Duret M. T., Lampitt R. S., and Lam P. (2018). Prokaryotic Niche Partitioning Between Suspended and Sinking Marine Particles. *Environmental Microbiology Reports*.

Egan S. and Gardiner M. (2016). Microbial Dysbiosis: Rethinking Disease in Marine Ecosystems. *Frontiers in Microbiology*, 7.

Engel A., Piontek J., Metfies K., Endres S., Sprong P., Peeken I., Gäbler-Schwarz S., and Nöthig E.-M. (2017). Inter-annual variability of transparent exopolymer particles in the Arctic Ocean reveals high sensitivity to ecosystem changes. *Scientific Reports*, 7(1):4129.

Fadeev E., Salter I., Schourup-Kristensen V., Nöthig E.-M., Metfies K., Engel A., Piontek J., Boetius A., and Bienhold C. (2018). Microbial communities in the East and West Fram Strait during sea-ice melting season. *Frontiers in Marine Science*, 5:429.

Falck E., Kattner G., and Budéus G. (2005). Disappearance of Pacific Water in the northwestern Fram Strait. *Geophysical Research Letters*, 32(14):1–4.

Falkowski P. G., Fenchel T., and Delong E. F. (2008). The Microbial Engines That Drive Earth's Biogeochemical Cycles. *Science*, 320(5879):1034–1039.

Falkowski P. G., Barber R. T., and Smetacek V. (1998). Biogeochemical Controls and Feedbacks on Ocean Primary Biogeochemical Controls and Feedbacks on Ocean Primary Production. 200 (July):200–207.

Faust K. and Raes J. (2012). Microbial interactions: from networks to models. *Nature Reviews Microbiology*, 10(8):538–550.

Faust K. and Raes J. (2016). CoNet app: inference of biological association networks using Cytoscape. *F1000Research*, 5:1519.

Fernández-Méndez M., Katlein C., Rabe B., Nicolaus M., Peeken I., Bakker K., Flores H., and Boetius A. (2015). Photosynthetic production in the central Arctic Ocean during the record sea-ice minimum in 2012. *Biogeosciences*, 12(11):3525–3549.

Field C. B. (1998). Primary Production of the Biosphere: Integrating Terrestrial and Oceanic Components. *Science*, 281(5374):237–240.

Fontanez K. M., Eppley J. M., Samo T. J., Karl D. M., and DeLong E. F. (2015). Microbial community structure and function on sinking particles in the North Pacific Subtropical Gyre. *Frontiers in Microbiology*, 6(MAY):1–14.

Fouhy F., Clooney A. G., Stanton C., Claesson M. J., Cotter P. D., Shendure J., Ji H., Glenn T., Mardis E., Shokralla S., Spall J., Gibson J., Hajibabaei M., Weinstock G., Raoult D., Henrissat B., Walker A., Martin J., Scott P., Parkhill J., Flint H., Scott K., Yu Z., Morrison M., Nelson M., Morrison H., Benjamino J., Grim S., Graf J., McOrist A., Jackson M., Bird A., Claesson M., Cusack S., O'Sullivan O., Greene-Diniz R., Weerd H., Flannery E., Aronesty E., Edgar R., Haas B., Clemente J., Quince C., Knight R., Allard G., Ryan F., Jeffery I., and Claesson M. (2016). 16S rRNA gene sequencing of mock microbial populations- impact of DNA extraction method, primer choice and sequencing platform. *BMC Microbiology*, 16(1):123.

Frank A. H., Garcia J. A. L., Herndl G. J., and Reinthaler T. (2016). Connectivity between surface and deep waters determines prokaryotic diversity in the North Atlantic Deep Water. *Environmental Microbiology*, 18(6):2052–2063.

Freitas S., Hatosy S., Fuhrman J. A., Huse S. M., Mark Welch D. B., Sogin M. L., and Martiny A. C. (2012). Global distribution and diversity of marine Verrucomicrobia. *ISME Journal*, 6 (8):1499–1505.

Friedman J., Hastie T., and Tibshirani R. *The elements of statistical learning*, volume 1. Springer series in statistics New York, NY, USA:, 2001.

Fuhrman J. A. and Steele J. A. (2008). Community structure of marine bacterioplankton: Patterns, networks, and relationships to function. *Aquatic Microbial Ecology*, 53(1):69–81.

Fuhrman J. A., Mccallum K., and Davis A. A. (1993). Phylogenetic Diversity of Subsurface Marine Microbial Communities from the Atlantic and Pacific Oceans. *Applied and environmental microbiology*, 59(5):1294–1302.

Fuhrman J. A., Cram J. A., and Needham D. M. (2015). Marine microbial community dynamics and their ecological interpretation. *Nature Reviews Microbiology*, 13(3):133–146.

Galand P. E., Casamayor E. O., Kirchman D. L., and Lovejoy C. (2009). Ecology of the rare microbial biosphere of the Arctic Ocean. *Proceedings of the National Academy of Sciences*, 106 (52):22427–22432.

Galand P. E., Casamayor E. O., Kirchman D. L., Potvin M., and Lovejoy C. (2009). Unique archaeal assemblages in the Arctic Ocean unveiled by massively parallel tag sequencing. *The ISME journal*, 3(7):860–869.

Galand P. E., Potvin M., Casamayor E. O., and Lovejoy C. (2010). Hydrography shapes bacterial biogeography of the deep Arctic Ocean. *The ISME Journal*, 4(4):564–576.

Galand P. E., Pereira O., Hochart C., Auguet J. C., and Debroas D. (2018). A strong link between marine microbial community composition and function challenges the idea of functional redundancy. *ISME Journal*, pages 1–9.

Gao Y., Sun J., Li F., He S., Sandven S., Yan Q., Zhang Z., Lohmann K., Keenlyside N., Furevik T., and Suo L. (2015). Arctic sea ice and Eurasian climate: A review. *Advances in Atmospheric Sciences*, 32(1):92–114.

Gärdes A., Iversen M. H., Grossart H.-P., Passow U., and Ullrich M. S. (2011). Diatom-associated bacteria are required for aggregation of Thalassiosira weissflogii. *The ISME Journal*, 5(3): 436–445.

Gasol J. M., Del Giorgio P. A., Giorgio P. a. D. E. L., and Del Giorgio P. A. (2000). Using flow cytometry for counting natural planktonic bacteria and understanding the structure of planktonic bacterial communities. *Scientia Marina*, 64(2):197–224.

Ghiglione J.-F., Galand P. E., Pommier T., Pedros-Alio C., Maas E. W., Bakker K., Bertilson S., Kirchman D. L., Lovejoy C., Yager P. L., and Murray A. E. (2012). Pole-to-pole biogeography of surface and deep marine bacterial communities. *Proceedings of the National Academy of Sciences*, 109(43):17633–17638.

Gilbert J. A., Meyer F., Antonopoulos D., Balaji P., Brown C. T., Brown C. T., Desai N., Eisen J. A., Evers D., Field D., Feng W., Huson D., Jansson J., Knight R., Knight J., Kolker E., Konstantindis K., Kostka J., Kyrpides N., Mackelprang R., McHardy A., Quince C., Raes J., Sczyrba A., Shade A., and Stevens R. (2010). Meeting Report: The Terabase Metagenomics Workshop and the Vision of an Earth Microbiome Project. *Standards in Genomic Sciences*, 3(3):243–248.

Gilbert J. A., Steele J. A., Caporaso J. G., Steinbrück L., Reeder J., Temperton B., Huse S., McHardy A. C., Knight R., Joint I., Somerfield P., Fuhrman J. A., and Field D. (2012). Defining seasonal marine microbial community dynamics. *The ISME Journal*, 6(2):298–308.

Gilbert J. A., Jansson J. K., and Knight R. (2014). The Earth Microbiome project: successes and aspirations. *BMC Biology*, 12(1):69.

Giovannoni S. J. and Vergin K. L. (2012). Seasonality in Ocean Microbial Communities. *Science*, 335(6069):671–676.

Giovannoni S. J. (2017). SAR11 Bacteria: The Most Abundant Plankton in the Oceans. *Annual Review of Marine Science*, 9(1):231–255.

Giovannoni S. J., Cameron Thrash J., and Temperton B. (2014). Implications of streamlining theory for microbial ecology. *The ISME Journal*, 8(8):1553–1565.

Glöckner F., Gasol J., McDonough N., and Calewaert J. (2012). Marine Microbial Diversity and its role in Ecosystem Functioning and Environmental Change. *Marine Board-ESF Report*, (May):84.

Gómez-Pereira P. R., Fuchs B. M., Alonso C., Oliver M. J., van Beusekom J. E. E., and Amann R. (2010). Distinct flavobacterial communities in contrasting water masses of the North Atlantic Ocean. *The ISME Journal*, 4(4):472–487.

Gómez-Rubio V. (2017). ggplot2 - Elegant Graphics for Data Analysis (2nd Edition). *Journal of Statistical Software*, 77(Book Review 2).

Gonçalves-Araujo R. *Tracing environmental variability in the changing Arctic Ocean with optical measurements of dissolved organic matter*. PhD thesis, Universität Bremen, 2016.

Goodwin K. D., Thompson L. R., Duarte B., Kahlke T., Thompson A. R., Marques J. C., and Caçador I. (2017). DNA Sequencing as a Tool to Monitor Marine Ecological Status. *Frontiers in Marine Science*, 4.

Gosselin M., Levasseur M., Wheeler P. A., Horner R. A., and Booth B. C. (1997). New measurements of phytoplankton and ice algal production in the Arctic Ocean. *Deep-Sea Research Part II: Topical Studies in Oceanography*, 44(8):1623–1644.

Grosfeld K., Treffeisen R., Asseng J., Bartsch A., Bräuer B., Fritzsch B., Gerdes R., Hendricks S., Hiller W., Heygster G., Krumpen T., Lemke P., Melsheimer C., Nicolaus M., Ricker R., and Weigelt M. (2016). Online sea-ice knowledge and data platform. *Polarforschung*, 85(2):143–155.

Grossart H.-P., Kiørboe T., Tang K., and Ploug H. (2003). Bacterial Colonization of Marine Snow Particles: Growth and Inter-Specific Interactions. *Appl. Environ. Microbiol.*, 69(6):3500–3509.

Grossart H. P., Levold F., Allgaier M., Simon M., and Brinkhoff T. (2005). Marine diatom species harbour distinct bacterial communities. *Environmental Microbiology*, 7(6):860–873.

Grossart H.-P., Tang K. W., KiÃ¸rboe T., and Ploug H. (2007). Comparison of cell-specific activity between free-living and attached bacteria using isolates and natural assemblages. *FEMS Microbiology Letters*, 266(2):194–200.

Grossart H.-P. P., Czub G., and Simon M. (2006). Algae-bacteria interactions and their effects on aggregation and organic matter flux in the sea. *Environmental Microbiology*, 8(6):1074–1084.

Grossart H., Kiørboe T., Tang K., Allgaier M., Yam E., and Ploug H. (2006). Interactions between marine snow and heterotrophic bacteria: aggregate formation and microbial dynamics. *Aquatic Microbial Ecology*, 42(1):19–26.

Grossart H. H.-P. and Simon M. (2007). Interactions of planktonic algae and bacteria: effects on algal growth and organic matter dynamics. *Aquatic Microbial Ecology*, 47(3):163–176.

Grossart H. H. P. (1999). Interactions between marine bacteria and axenic diatoms (Cylindrotheca fusiformis, Nitzschia laevis, and Thalassiosira weissflogii) incubated under various conditions in the lab. *Aquatic Microbial Ecology*, 19(1):1–11.

Grossmann S. and Dieckmann G. S. (1994). Bacterial Standing Stock, Activity, And Carbon Production During Formation And Growth Of Sea-Ice In The Weddell Sea, Antarctica. *Applied And Environmental Microbiology*, 60(8):2746–2753.

Gruber N. (2011). Warming up, turning sour, losing breath: ocean biogeochemistry under global change. *Philosophical Transactions of the Royal Society A: Mathematical, Physical and Engineering Sciences*, 369(1943):1980–1996.

Grzymski J. J., Riesenfeld C. S., Williams T. J., Dussaq A. M., Ducklow H., Erickson M., Cavicchioli R., and Murray A. E. (2012). A metagenomic assessment of winter and summer bacterioplankton from Antarctica Peninsula coastal surface waters. *ISME Journal*, 6(10):1901–1915.

Guillou L., Viprey M., Chambouvet A., Welsh R. M., Kirkham A. R., Massana R., Scanlan D. J., and Worden A. Z. (2008). Widespread occurrence and genetic diversity of marine parasitoids belonging to Syndiniales (Alveolata). *Environmental Microbiology*, 10(12):3349–3365.

Guralnick R., Walls R., and Jetz W. (2018). Humboldt Core - toward a standardized capture of biological inventories for biodiversity monitoring, modeling and assessment. *Ecography*, 41 (5):713–725.

Haegeman B., Hamelin J., Moriarty J., Neal P., Dushoff J., and Weitz J. S. (2013). Robust estimation of microbial diversity in theory and in practice. *ISME Journal*, 7(6):1092–1101.

Halpern B. S., Longo C., Hardy D., McLeod K. L., Samhouri J. F., Katona S. K., Kleisner K., Lester S. E., O'Leary J., Ranelletti M., Rosenberg A. A., Scarborough C., Selig E. R., Best B. D., Brumbaugh D. R., Chapin F. S., Crowder L. B., Daly K. L., Doney S. C., Elfes C., Fogarty M. J., Gaines S. D., Jacobsen K. I., Karrer L. B., Leslie H. M., Neeley E., Pauly D., Polasky S., Ris B., St Martin K., Stone G. S., Sumaila U. R., and Zeller D. (2012). An index to assess the health and benefits of the global ocean. *Nature*, 488(7413):615–620.

Halpern B. S., Longo C., Stewart Lowndes J. S., Best B. D., Frazier M., Katona S. K., Kleisner K. M., Rosenberg A. A., Scarborough C., and Selig E. R. (2015). Patterns and emerging trends in global ocean health. *PLoS ONE*, 10(3):e0117863.

Hamm C. E., Merkel R., Springer O., Jurkojc P., Maier C., Prechtel K., and Smetacek V. (2003). Architecture and material properties of diatom shells provide effective mechanical protection. *Nature*, 421:841.

Hancke K., Lund-Hansen L. C., Lamare M. L., Højlund Pedersen S., King M. D., Andersen P., and Sorrell B. K. (2018). Extreme Low Light Requirement for Algae Growth Underneath Sea Ice: A Case Study From Station Nord, NE Greenland. *Journal of Geophysical Research: Oceans*, 123(2):985–1000.

Hanson C. A., Fuhrman J. A., Horner-Devine M. C., and Martiny J. B. H. (2012). Beyond biogeographic patterns: processes shaping the microbial landscape. *Nature Reviews Microbiology*, 10 (7):497–506.

Hardge K., Peeken I., Neuhaus S., Lange B. A., Stock A., Stoeck T., Weinisch L., Met K., and Metfies K. (2017). The importance of sea ice for exchange of habitat-specific protist communities in the Central Arctic Ocean. *Journal of Marine Systems*, 165:124–138.

Hartmann M., Zubkov M. V., Scanlan D. J., and Lepère C. (2013). In situ interactions between photosynthetic picoeukaryotes and bacterioplankton in the Atlantic Ocean: Evidence for mixotrophy. *Environmental Microbiology Reports*, 5(6):835–840.

Harvey E. L., Deering R. W., Rowley D. C., Gamal A. E., Schorn M., Moore B. S., Johnson M. D., Mincer T. J., and Whalen K. E. (2016). A bacterial quorum-sensing precursor induces mortality in the marine coccolithophore, Emiliania huxleyi. *Frontiers in Microbiology*, 7(FEB):1–12.

Hassan M., Essam T., and Megahed S. (2018). Illumina sequencing and assessment of new cost-efficient protocol for metagenomic-DNA extraction from environmental water samples. *Brazilian Journal of Microbiology*, pages 1–8.

Hawley A. K., Nobu M. K., Wright J. J., Durno W. E., Morgan-Lang C., Sage B., Schwientek P., Swan B. K., Rinke C., Torres-Beltrán M., Mewis K., Liu W.-T., Stepanauskas R., Woyke T., and Hallam S. J. (2017). Diverse Marinimicrobia bacteria may mediate coupled biogeochemical cycles along eco-thermodynamic gradients. *Nature Communications*, 8(1):1507.

Henry R., Schang C., Coutts S., Kolotelo P., Prosser T., Crosbie N., Grant T., Cottam D., O'Brien P., Deletic A., and McCarthy D. (2016). Into the deep: Evaluation of SourceTracker for assessment of faecal contamination of coastal waters. *Water Research*, 93:242–253.

Herfort L., Seaton C., Wilkin M., Roman B., Preston C. M., Marin R., Seitz K., Smith M. W., Haynes V., Scholin C. A., Baptista A. M., and Simon H. M. (2016). Use of continuous, real-time observations and model simulations to achieve autonomous, adaptive sampling of microbial processes with a robotic sampler. *Limnology and Oceanography: Methods*, 14(1):50–67.

Herndl G. J. and Reinthaler T. (2013). Microbial control of the dark end of the biological pump. *Nature Geoscience*, 6(9):718–724.

Hollowed A. B., Barange M., Beamish R. J., Brander K. M., Cochrane K., Drinkwater K. F., Foreman M. G. G., Hare J. A., Holt J., Ito S.-i., Kim S., King J. R., Loeng H., Mackenzie B. R., Mueter F. J., Okey T. A., Peck M. A., Radchenko V. I., Rice J. C., Schirripa M. J., Yatsu A., and Yamanaka Y. (2013). Projected impacts of climate change on marine fish and fisheries. *ICES Journal of Marine Science*, 70(5):1023–1037.

Hollowed A. B., Cheng W., Loeng H., Logerwell E., and Reist J. (2018). Regional Assessment of Climate Change Impacts on Arctic Marine Ecosystems. II.

Hop H., Falk-Petersen S., Svendsen H., Kwasniewski S., Pavlov V., Pavlova O., S??reide J. E., and Søreide J. E. (2006). Physical and biological characteristics of the pelagic system across Fram Strait to Kongsfjorden. *Progress in Oceanography*, 71(2-4):182–231.

Howarth R. W. (1988). Primary Production in Marine Ecosystems. pages 89–110.

Hsieh T. C., Ma K. H., and Chao A. (2016). iNEXT: an R package for rarefaction and extrapolation of species diversity (Hill numbers). *Methods in Ecology and Evolution*, 7(12):1451–1456.

Hsieh T. C., Ma K. H., and Chao A. *iNEXT: Interpolation and Extrapolation for Species Diversity*, 2018. URL `http://chao.stat.nthu.edu.tw/blog/software-download/`.

Hugerth L. W. and Andersson A. F. (2017). Analysing microbial community composition through amplicon sequencing: From sampling to hypothesis testing. *Frontiers in Microbiology*, 8(SEP): 1–22.

Hünken M., Harder J., and Kirst G. O. (2008). Epiphytic bacteria on the Antarctic ice diatom Amphiprora kufferathii Manguin cleave hydrogen peroxide produced during algal photosynthesis. *Plant Biology*, 10(4):519–526.

Huse S. M., Dethlefsen L., Huber J. A., Welch D. M., Relman D. A., and Sogin M. L. (2008). Exploring microbial diversity and taxonomy using SSU rRNA hypervariable tag sequencing. *PLoS Genetics*, 4(11).

Hutchins D. A. and Fu F. (2017). Microorganisms and ocean global change. *Nature Microbiology*, 2(6):17058.

Ikeda M. (1990). Decadal oscillations of the air-ice-ocean system in the northern hemisphere. *Atmosphere - Ocean*, 28(1):106–139.

Ingvaldsen R. B., Gjøsæter H., Ona E., and Michalsen K. (2017). Atlantic cod (Gadus morhua) feeding over deep water in the high Arctic. *Polar Biology*, 40(10):2105–2111.

Iversen K. R. and Seuthe L. (2011). Seasonal microbial processes in a high-latitude fjord (Kongsfjorden, Svalbard): I. Heterotrophic bacteria, picoplankton and nanoflagellates. *Polar Biology*, 34(5):731–749.

Iversen M. H. and Ploug H. (2010). Ballast minerals and the sinking carbon flux in the ocean: carbon-specific respiration rates and sinking velocity of marine snow aggregates. *Biogeosciences*, 7(9):2613–2624.

Jacob M. *Influence of Global Change on microbial communities in Arctic sediments*. PhD thesis, University of Bremen, 2014.

Jakobsson M. (2002). Hypsometry and volume of the Arctic Ocean and its constituent seas. *Geochemistry, Geophysics, Geosystems*, 3(5):1–18.

Jephcott T. G., Alves-de Souza C., Gleason F. H., van Ogtrop F. F., Sime-Ngando T., Karpov S. A., and Guillou L. (2016). Ecological impacts of parasitic chytrids, syndiniales and perkinsids on populations of marine photosynthetic dinoflagellates. *Fungal Ecology*, 19:47–58.

Johannessen O. M., Muench R. D., and Overland J. E., editors. *The Polar Oceans and Their Role in Shaping the Global Environment*. Geophysical Monograph Series. American Geophysical Union, Washington, D. C., 1994. ISBN 9781118663882. doi: 10.1029/GM085. URL `http://doi.wiley.com/10.1029/GM085`.

Joli N., Monier A., Logares R., and Lovejoy C. (2017). Seasonal patterns in Arctic prasinophytes and inferred ecology of Bathycoccus unveiled in an Arctic winter metagenome. *ISME Journal*, 11(6):1372–1385.

Jones Z. L., Jasper J. T., Sedlak D. L., and Sharp J. O. (2017). Sulfide-Induced Dissimilatory Nitrate Reduction to Ammonium Supports Anaerobic Ammonium Oxidation (Anammox) in an Open-Water Unit Process Wetland. *Applied and Environmental Microbiology*, 83(15):1–14.

Jørgensen B. B. and Boetius A. (2007). Feast and famine — microbial life in the deep-sea bed. *Nature Reviews Microbiology*, 5(10):770–781.

Kang S., Rodrigues J. L., Ng J. P., and Gentry T. J. (2016). Hill number as a bacterial diversity measure framework with high-throughput sequence data. *Scientific Reports*, 6(November): 1–4.

Karl D. M. (2007). Microbial oceanography: Paradigms, processes and promise. *Nature Reviews Microbiology*, 5(10):759–769.

Karl D. M., Dore J. E., Lukas R., Michaels A. F., Bates N. R., and Knap A. (2001). Building the long-term picture. *Oceanography*, 14(6).

Karl D. and Church M. (2014). Microbial oceanography and the Hawaii Ocean Time-series programme. *Nature reviews. Microbiology*, 12(10):699–713.

Karner M. and Herndl G. J. (1992). Extracellular enzymatic activity and secondary production in free-living and marine-snow-associated bacteria. *Marine Biology*, 113(2):341–347.

Katlein C., Schiller M., Belter H. J., Coppolaro V., Wenslandt D., and Nicolaus M. (2017). A New Remotely Operated Sensor Platform for Interdisciplinary Observations under Sea Ice. *Frontiers in Marine Science*, 4:281.

Kennedy N. A., Walker A. W., Berry S. H., Duncan S. H., Farquarson F. M., Louis P., Thomson J. M., Satsangi J., Flint H. J., Parkhill J., Lees C. W., and Hold G. L. (2014). The impact of different DNA extraction kits and laboratories upon the assessment of human gut microbiota composition by 16S rRNA gene sequencing. *PLoS ONE*, 9(2):1–9.

Kilias E., Wolf C., Nöthig E.-M., Peeken I., and Metfies K. (2013). Protist distribution in the Western Fram Strait in summer 2010 based on 454-pyrosequencing of 18S rDNA. *Journal of Phycology*, pages n/a–n/a.

Kim T.-H., Kim G., Lee S.-A., and Dittmar T. (2015). Extraordinary slow degradation of dissolved organic carbon (DOC) in a cold marginal sea. *Scientific Reports*, 5(1):13808.

Kinnard C., Zdanowicz C. M., Fisher D. A., Isaksson E., De Vernal A., and Thompson L. G. (2011). Reconstructed changes in Arctic sea ice over the past 1,450 years. *Nature*, 479(7374):509–512.

Kiørboe T., Grossart H.-P., Ploug H., and Tang K. (2002). Mechanisms and rates of colonisation of sinking aggregates. *Applied and Environmental Microbiology*, 68(8):3996–4006.

Kiørboe T., Tang K., Grossart H.-p., and Ploug H. (2003). Dynamics of Microbial Communities on Marine Snow Aggregates : Colonization , Growth , Detachment , and Grazing Mortality of Attached Bacteria. 69(6):3036–3047.

Kirchman D. L., Elifantz H., Dittel A. I., Malmstrom R. R., and Cottrell M. T. (2007). Standing stocks and activity of Archaea and Bacteria in the western Arctic Ocean. *Limnology and Oceanography*, 52(2):495–507.

Kirchman D. L., Morán X. A. G., and Ducklow H. (2009). Microbial growth in the polar oceans — role of temperature and potential impact of climate change. *Nature Reviews Microbiology*, 7(juNE):451–459.

Kirchman D. L., Cottrell M. T., and Lovejoy C. (2010). The structure of bacterial communities in the western Arctic Ocean as revealed by pyrosequencing of 16S rRNA genes. *Environmental Microbiology*, 12(5):1132–1143.

Kissling W. D., Ahumada J. A., Bowser A., Fernandez M., Fernández N., García E. A., Guralnick R. P., Isaac N. J. B., Kelling S., Los W., McRae L., Mihoub J.-B., Obst M., Santamaria M.,

Skidmore A. K., Williams K. J., Agosti D., Amariles D., Arvanitidis C., Bastin L., De Leo F., Egloff W., Elith J., Hobern D., Martin D., Pereira H. M., Pesole G., Peterseil J., Saarenmaa H., Schigel D., Schmeller D. S., Segata N., Turak E., Uhlir P. F., Wee B., and Hardisty A. R. (2018). Building essential biodiversity variables (EBVs) of species distribution and abundance at a global scale. *Biological Reviews*, 93(1):600–625.

Kite-Powell H. L., Fleming L. E., Backer L. C., Faustman E. M., Hoagland P., Tsuchiya A., Younglove L. R., Wilcox B. A., and Gast R. J. (2008). Linking the oceans to public health: current efforts and future directions. *Environmental Health*, 7(Suppl 2):S6.

Klein B., LeBlanc B., Mei Z. P., Beret R., Michaud J., Mundy C. J., Von Quillfeldt C. H., Garneau M. È., Roy S., Gratton Y., Cochran J. K., Bélanger S., Larouche P., Pakulski J. D., Rivkin R. B., and Legendre L. (2002). Phytoplankton biomass, production and potential export in the North Water. *Deep-Sea Research Part II: Topical Studies in Oceanography*, 49(22-23):4983–5002.

Klindworth A., Pruesse E., Schweer T., Quast C., Horn M., Glo F. O., Peplies J., Quast C., Horn M., and Glöckner F. O. (2013). Evaluation of general 16S ribosomal RNA gene PCR primers for classical and next-generation sequencing-based diversity studies. *Nucleic Acids Research*, 41(1):e1–e1.

Knight R., Vrbanac A., Taylor B. C., Aksenov A., Callewaert C., Debelius J., Gonzalez A., Kosciolek T., McCall L. I., McDonald D., Melnik A. V., Morton J. T., Navas J., Quinn R. A., Sanders J. G., Swafford A. D., Thompson L. R., Tripathi A., Xu Z. Z., Zaneveld J. R., Zhu Q., Caporaso J. G., and Dorrestein P. C. (2018). Best practices for analysing microbiomes. *Nature Reviews Microbiology*, 16(7):410–422.

Knights D., Kuczynski J., Charlson E. S., Zaneveld J., Mozer M. C., Collman R. G., Bushman F. D., Knight R., and Kelley S. T. (2011). Bayesian community-wide culture-independent microbial source tracking. *Nature Methods*, 8(9):761–763.

Kobayashi S., Ota Y., Harada Y., Ebita A., Moriya M., Onoda H., Onogi K., Kamahori H., Kabayashi C., Endo H., Miyaoka K., and Takahashi K. (2015). The JRA-55 Reanalysis: General Specifications and Basic Characteristics. *Journal of the Meteorological Society of Japan. Ser. II*, 93(1): 5–48.

Kopf A., Bicak M., Kottmann R., Schnetzer J., Kostadinov I., Lehmann K., Fernandez-Guerra A., Jeanthon C., Rahav E., Ullrich M., Wichels A., Gerdts G., Polymenakou P., Kotoulas G., Siam R., Abdallah R. Z., Sonnenschein E. C., Cariou T., O'Gara F., Jackson S., Orlic S., Steinke M., Busch J., Duarte B., Caçador I., Canning-Clode J., Bobrova O., Marteinsson V., Reynisson E., Loureiro C. M., Luna G. M., Quero G. M., Löscher C. R., Kremp A., DeLorenzo M. E., Øvreås L., Tolman J., LaRoche J., Penna A., Frischer M., Davis T., Katherine B., Meyer C. P., Ramos S., Magalhães C., Jude-Lemeilleur F., Aguirre-Macedo M. L., Wang S., Poulton N., Jones S., Collin R., Fuhrman J. A., Conan P., Alonso C., Stambler N., Goodwin K., Yakimov M. M., Baltar F., Bodrossy L., Van De Kamp J., Frampton D. M., Ostrowski M., Van Ruth P., Malthouse P., Claus S., Deneudt K., Mortelmans J., Pitois S., Wallom D., Salter I., Costa R., Schroeder D. C., Kandil M. M., Amaral V., Biancalana F., Santana R., Pedrotti M. L., Yoshida T., Ogata H., Ingleton T., Munnik K., Rodriguez-Ezpeleta N., Berteaux-Lecellier V., Wecker P., Cancio I., Vaulot D., Bienhold C., Ghazal H., Chaouni B., Essayeh S., Ettamimi S., Zaid E. H., Boukhatem N., Bouali A., Chahboune R., Barrijal S., Timinouni M., El Otmani F., Bennani M., Mea M., Todorova N., Karamfilov V., ten Hoopen P., Cochrane G., L'Haridon S., Bizsel K. C., Vezzi A., Lauro F. M., Martin P., Jensen R. M., Hinks J., Gebbels S., Rosselli R., De Pascale F., Schiavon R., dos Santos A., Villar E., Pesant S., Cataletto B., Malfatti F., Edirisinghe R., Silveira J. A. H., Barbier M., Turk V., Tinta T., Fuller W. J., Salihoglu I., Serakinci N., Ergoren M. C., Bresnan E., Iriberri J., Nyhus P. A. F., Bente E., Karlsen H. E., Golyshin P. N., Gasol J. M., Moncheva S., Dzhembekova N., Johnson Z., Sinigalliano C. D., Gidley M. L., Zingone A., Danovaro R., Tsiamis G., Clark M. S., Costa A. C., El Bour M., Martins A. M., Collins R. E., Ducluzeau A.-L., Martinez J., Costello M. J., Amaral-Zettler L. A., Gilbert J. A., Davies N., Field D., and Glöckner F. O. (2015). The ocean sampling day consortium. *GigaScience*, 4(1):27.

Korhonen M., Rudels B., Marnela M., Wisotzki A., and Zhao J. (2013). Time and space variability

of freshwater content, heat content and seasonal ice melt in the Arctic Ocean from 1991 to 2011. *Ocean Science*, 9(6):1015–1055.

Krause J. W., Duarte C. M., Marquez I. A., Assmy P., Fernández-Méndez M., Wiedmann I., Wassmann P., Kristiansen S., and Agustí S. (2018). Biogenic silica production and diatom dynamics in the Svalbard region during spring. *Biogeosciences Discussions*, 2(May):1–25.

Kritzberg E. S., Duarte C. M., and Wassmann P. (2010). Changes in Arctic marine bacterial carbon metabolism in response to increasing temperature. *Polar Biology*, 33(12):1673–1682.

Krumhardt K. M., Lovenduski N. S., Freeman N. M., and Bates N. R. (2016). Apparent increase in coccolithophore abundance in the subtropical North Atlantic from 1990 to 2014. *Biogeosciences*, 13(4):1163–1177.

Kuypers M. M. M., Sliekers A. O., Lavik G., Schmid M., Jorgensen B. B., Kuenen J. G., S. S. D. J., Strous M., and Jetten M. S. M. (2003). Anaerobic Ammonium Oxidation by Anammox Bacteria in the Black Sea. *Nature*, 422(6932):608–611.

Kwok R. (2009). Outflow of Arctic Ocean Sea Ice into the Greenland and Barents Seas: 1979–2007. *Journal of Climate*, 22(9):2438–2457.

Kwok R. and Rothrock D. A. (2009). Decline in Arctic sea ice thickness from submarine and ICESat records: 1958-2008. *Geophysical Research Letters*, 36(15):n/a–n/a.

Ladau J., Sharpton T. J., Finucane M. M., Jospin G., Kembel S. W., O'Dwyer J., Koeppel A. F., Green J. L., and Pollard K. S. (2013). Global marine bacterial diversity peaks at high latitudes in winter. *ISME Journal*, 7(9):1669–1677.

Lalande C., Bauerfeind E., Nöthig E. M., and Beszczynska-Möller A. (2013). Impact of a warm anomaly on export fluxes of biogenic matter in the eastern Fram Strait. *Progress in Oceanography*, 109:70–77.

Lamb J. B., van de Water J. A. J. M., Bourne D. G., Altier C., Hein M. Y., Fiorenza E. A., Abu N., Jompa J., and Harvell C. D. (2017). Seagrass ecosystems reduce exposure to bacterial pathogens of humans, fishes, and invertebrates. *Science*, 355(6326):731–733.

Landry Z., Swan B. K., Herndl G. J., Stepanauskas R., and Giovannoni S. J. (2017). SAR202 Genomes from the Dark Ocean Predict Pathways for the Oxidation of Recalcitrant Dissolved Organic Matter. *mBio*, 8(2):e00413–17.

Lasternas S. and Agustí S. (2010). Phytoplankton community structure during the record Arctic ice-melting of summer 2007. *Polar Biology*, 33(12):1709–1717.

Laursen M. F., Dalgaard M. D., and Bahl M. I. (2017). Genomic GC-content affects the accuracy of 16S rRNA gene sequencing bsed microbial profiling due to PCR bias. *Frontiers in Microbiology*, 8(OCT):1–8.

Laws E., Bidigare R., and Karl D. (2016). Enigmatic relationship between chlorophyll a concentrations and photosynthetic rates at Station ALOHA. *Heliyon*, 2(9):e00156.

Lee Y. J., Matrai P. A., Friedrichs M. A. M., Saba V. S., Ardyna M., Asanuma I., Babin M., and Bélanger S. (2015). An assessment of phytoplankton primary productivity in the Arctic Ocean from satellite ocean color / in situ chlorophyll- a based models. *Journal of Geophysical Research : Oceans*, (SEPTEMBER):1–34.

Lee Y. J., Matrai P. A., Friedrichs M. A. M., Saba V. S., Aumont O., Babin M., Buitenhuis E. T., Chevallier M., de Mora L., Dessert M., Dunne J. P., Ellingsen I. H., Feldman D., Frouin R., Gehlen M., Gorgues T., Ilyina T., Jin M., John J. G., Lawrence J., Manizza M., Menkes C. E., Perruche C., Le Fouest V., Popova E. E., Romanou A., Samuelsen A., Schwinger J., Séférian R., Stock C. A., Tjiputra J., Tremblay L. B., Ueyoshi K., Vichi M., Yool A., and Zhang J. (2016). Net primary productivity estimates and environmental variables in the Arctic Ocean: An assessment of coupled physical-biogeochemical models. *Journal of Geophysical Research: Oceans*, 121(12):8635–8669.

Leese F., Altermatt F., Bouchez A., Ekrem T., Hering D., Meissner K., Mergen P., Pawlowski J., Piggott J., Rimet F., Steinke D., Taberlet P., Weigand A., Abarenkov K., Beja P., Bervoets L., Björnsdóttir S., Boets P., Boggero A., Bones A., Borja Á., Bruce K., Bursić V., Carlsson J., Čiampor F., Čiamporová-Zatovičová Z., Coissac E., Costa F., Costache M., Creer S., Csabai Z., Deiner K., DelValls Á., Drakare S., Duarte S., Eleršek T., Fazi S., Fišer C., Flot J.-F., Fonseca V., Fontaneto D., Grabowski M., Graf W., Guðbrandsson J., Hellström M., Hershkovitz Y., Hollingsworth P., Japoshvili B., Jones J., Kahlert M., Kalamujic Stroil B., Kasapidis P., Kelly M., Kelly-Quinn M., Keskin E., Kõljalg U., Ljubešić Z., Maček I., Mächler E., Mahon A., Marečková M., Mejdandzic M., Mircheva G., Montagna M., Moritz C., Mulk V., Naumoski A., Navodaru I., Padisák J., Pálsson S., Panksep K., Penev L., Petrusek A., Pfannkuchen M., Primmer C., Rinkevich B., Rotter A., Schmidt-Kloiber A., Segurado P., Speksnijder A., Stoev P., Strand M., Šulčius S., Sundberg P., Traugott M., Tsigenopoulos C., Turon X., Valentini A., van der Hoorn B., Várbíró G., Vasquez Hadjilyra M., Viguri J., Vitonytė I., Vogler A., Vrålstad T., Wägele W., Wenne R., Winding A., Woodward G., Zegura B., and Zimmermann J. (2016). DNAqua-Net: Developing new genetic tools for bioassessment and monitoring of aquatic ecosystems in Europe. *Research Ideas and Outcomes*, 2:e11321.

Legendre L., Ackley S., Dieckmann G., Gulliksen B., Horner R., Hoshiai T., Melnikov I., Reeburgh W., Spindler M., and Sullivan C. (1992). Ecology of sea ice biota. *Polar Biology*, 12(3-4):429–444.

Letelier R. M., White A. E., Bidigare R. R., Barone B., Church M. J., and Karl D. M. (2017). Light absorption by phytoplankton in the North Pacific Subtropical Gyre. *Limnology and Oceanography*, 62(4):1526–1540.

Leu E., Søreide J. E., Hessen D. O., Falk-Petersen S., and Berge J. (2011). Consequences of changing sea-ice cover for primary and secondary producers in the European Arctic shelf seas: Timing, quantity, and quality. *Progress in Oceanography*, 90(1-4):18–32.

Li B., Yang Y., Ma L., Ju F., Guo F., Tiedje J. M., and Zhang T. (2015). Metagenomic and network analysis reveal wide distribution and co-occurrence of environmental antibiotic resistance genes. *The ISME Journal*, 9(11):2490–2502.

Li W. K. W., McLaughlin F. A., Lovejoy C., and Carmack E. C. (2009). Smallest Algae Thrive As the Arctic Ocean Freshens. *Science*, 326(5952):539–539.

Lima-Mendez G., Faust K., Henry N., Decelle J., Colin S., Carcillo F., Chaffron S., Ignacio-Espinosa J. C., Roux S., Vincent F., Bittner L., Darzi Y., Wang J., Audic S., Berline L., Bontempi G., Cabello A. M., Coppola L., Cornejo-Castillo F. M., D'Ovidio F., De Meester L., Ferrera I., Garet-Delmas M.-J., Guidi L., Lara E., Pesant S., Royo-Llonch M., Salazar G., Sanchez P., Sebastian M., Souffreau C., Dimier C., Picheral M., Searson S., Kandels-Lewis S., Gorsky G., Not F., Ogata H., Speich S., Stemmann L., Weissenbach J., Wincker P., Acinas S. G., Sunagawa S., Bork P., Sullivan M. B., Karsenti E., Bowler C., de Vargas C., and Raes J. (2015). Determinants of community structure in the global plankton interactome. *Science*, 348(6237):1262073–1262073.

Louca S., Parfrey L. W., and Doebeli M. (2016). Decoupling function and taxonomy in the global ocean microbiome. *Science*, 353(6305):1272–1277.

Love M. I., Huber W., and Anders S. (2014). Moderated estimation of fold change and dispersion for RNA-seq data with DESeq2. *Genome Biology*, 15(12):550.

Lovejoy C., Massana R., and Pedros-Alio C. (2007). Diversity and Distribution of Marine Microbial Eukaryotes in the Arctic Ocean and Adjacent Seas. *Applied and Environmental Microbiologyl*, 72(5):3085–3095.

Lovejoy C. Changing views of Arctic protists (marine microbial eukaryotes) in a changing Arctic, 2014.

Lovejoy C., Vincent W. F., Bonilla S., Roy S., Martineau M.-J. J., Terrado R., Potvin M., Mas-

sana R., and Pedrós-Alió C. (2007). Distributions, Phylogeny, and Growth of Cold-Adapted Picoprasinophytes in Arctic Seas. *Journal of Phycology*, 43(1):78–89.

Lozada M., Marcos M. S., Commendatore M. G., Gil M. N., and Dionisi H. M. (2014). The Bacterial Community Structure of Hydrocarbon-Polluted Marine Environments as the Basis for the Definition of an Ecological Index of Hydrocarbon Exposure. *Microbes and Environments*, 29(3):269–276.

Luo W., Friedman M. S., Shedden K., Hankenson K. D., and Woolf P. J. (2009). GAGE: generally applicable gene set enrichment for pathway analysis. *BMC Bioinformatics*, 10(1):161.

Mahé F., Rognes T., Quince C., de Vargas C., and Dunthorn M. (2015). Swarm v2: highly-scalable and high-resolution amplicon clustering. *PeerJ*, 3:e1420.

Malmstrom R., Straza T., Cottrell M., and Kirchman D. (2007). Diversity, abundance, and biomass production of bacterial groups in the western Arctic Ocean. *Aquatic Microbial Ecology*, 47(July):45–55.

Malone T. C., DiGiacomo P. M., Gonçalves E., Knap A. H., Talaue-McManus L., and de Mora S. (2014). A global ocean observing system framework for sustainable development. *Marine Policy*, 43:262–272.

Malone T. C., DiGiacomo P. M., Gonçalves E., Knap A. H., Talaue-McManus L., de Mora S., and Muelbert J. (2014). Enhancing the Global Ocean Observing System to meet evidence based needs for the ecosystem-based management of coastal ecosystem services. *Natural Resources Forum*, 38(3):168–181.

Maritorena S., D'Andon O. H. F., Mangin A., and Siegel D. A. (2010). Merged satellite ocean color data products using a bio-optical model: Characteristics, benefits and issues. *Remote Sensing of Environment*, 114(8):1791–1804.

Marnela M., Rudels B., Goszczko I., Beszczynska-Möller A., and Schauer U. (2016). Fram Strait and Greenland Sea transports, water masses, and water mass transformations 1999-2010 (and beyond). *Journal of Geophysical Research: Oceans*, 121(4):2314–2346.

Marquardt M., Vader A., Stübner E. I., Reigstad M., and Gabrielsen T. M. (2016). Strong Seasonality of Marine Microbial Eukaryotes in a High-Arctic Fjord (Isfjorden, in West Spitsbergen, Norway). *Applied and Environmental Microbiology*, 82(6):1868–1880.

Martin M. (2011). Cutadapt removes adapter sequences from high-throughput sequencing reads. *EMBnet.journal*, 17(1):10.

McBride M. M., Dalpadado P., Drinkwater K. F., Godø O. R., Hobday A. J., Hollowed A. B., Kristiansen T., Murphy E. J., Ressler P. H., Subbey S., Hofmann E. E., and Loeng H. (2014). Krill, climate, and contrasting future scenarios for Arctic and Antarctic fisheries. *ICES Journal of Marine Science*, 71(7):1934–1955.

McDonald D., Clemente J. C., Kuczynski J., Rideout J. R., Stombaugh J., Wendel D., Wilke A., Huse S., Hufnagle J., Meyer F., Knight R., and Caporaso J. G. (2012). The Biological Observation Matrix (BIOM) format or: how I learned to stop worrying and love the ome-ome. *GigaScience*, 1(1):7.

McDonnell A. M. P., Boyd P. W., and Buesseler K. O. (2015). Effects of sinking velocities and microbial respiration rates on the attenuation of particulate carbon fluxes through the mesopelagic zone. *Global Biogeochemical Cycles*, 29(2):175–193.

McMurdie P. J. and Holmes S. (2013). phyloseq: An R Package for Reproducible Interactive Analysis and Graphics of Microbiome Census Data. *PLoS ONE*, 8(4):e61217.

McMurdie P. J. and Holmes S. (2014). Waste Not, Want Not: Why Rarefying Microbiome Data Is Inadmissible. *PLoS Computational Biology*, 10(4).

Medini D., Serruto D., Parkhill J., Relman D. A., Donati C., Moxon R., Falkow S., and Rappuoli R. (2008). Microbiology in the post-genomic era. *Nature Reviews Microbiology*, 6(6):419–430.

Mehrshad M., Rodriguez-Valera F., Amoozegar M. A., López-García P., and Ghai R. (2018). The enigmatic SAR202 cluster up close: Shedding light on a globally distributed dark ocean lineage involved in sulfur cycling. *ISME Journal*, 12(3):655–668.

Merbt S. N., Stahl D. A., Casamayor E. O., Martí E., Nicol G. W., and Prosser J. I. (2012). Differential photoinhibition of bacterial and archaeal ammonia oxidation. *FEMS Microbiology Letters*, 327(1):41–46.

Mestre M., Borrull E., Sala M. M., and Gasol J. M. (2017). Patterns of bacterial diversity in the marine planktonic particulate matter continuum. *The ISME Journal*, 11(4):999–1010.

Mestre M., Ferrera I., Borrull E., Ortega-Retuerta E., Mbedi S., Grossart H.-P., Gasol J. M., and Sala M. M. (2017). Spatial variability of marine bacterial and archaeal communities along the particulate matter continuum. *Molecular Ecology*, 26(24):6827–6840.

Mestre M., Ruiz-González C., Logares R., Duarte C. M., Gasol J. M., and Sala M. M. (2018). Sinking particles promote vertical connectivity in the ocean microbiome. *Proceedings of the National Academy of Sciences*, 115(29):E6799–E6807.

Metfies K., von Appen W.-J. J., Kilias E., Nicolaus A., and Nöthig E.-M. M. (2016). Biogeography and Photosynthetic Biomass of Arctic Marine Pico-Eukaroytes during Summer of the Record Sea Ice Minimum 2012. *PLOS ONE*, 11(2):e0148512.

Metfies K., Bauerfeind E., Wolf C., Sprong P., Frickenhaus S., Kaleschke L., Nicolaus A., and Nöthig E.-M. (2017). Protist Communities in Moored Long-Term Sediment Traps (Fram Strait, Arctic)–Preservation with Mercury Chloride Allows for PCR-Based Molecular Genetic Analyses. *Frontiers in Marine Science*, 4(September):1–13.

Milici M., Tomasch J., Wos-Oxley M. L., Decelle J., Jáuregui R., Wang H., Deng Z.-L., Plumeier I., Giebel H.-A., Badewien T. H., Wurst M., Pieper D. H., Simon M., and Wagner-Döbler I. (2016). Bacterioplankton Biogeography of the Atlantic Ocean: A Case Study of the Distance-Decay Relationship. *Frontiers in Microbiology*, 7(APR).

Moberly J., D'Imperio S., Parker A., and Peyton B. (2016). Microbial community signature in Lake Coeur d'Alene: Association of environmental variables and toxic heavy metal phases. *Applied Geochemistry*, 66:174–183.

Mock T., Daines S. J., Geider R., Collins S., Metodiev M., Millar A. J., Moulton V., and Lenton T. M. (2016). Bridging the gap between omics and earth system science to better understand how environmental change impacts marine microbes. *Global Change Biology*, 22(1):61–75.

Monier A., Findlay H. S., Charvet S., and Lovejoy C. (2014). Late winter under ice pelagic microbial communities in the high Arctic Ocean and the impact of short-term exposure to elevated CO 2 levels. *Frontiers in Microbiology*, 5(September):1–12.

Morey M., Fernández-Marmiesse A., Castiñeiras D., Fraga J. M., Couce M. L., and Cocho J. A. (2013). A glimpse into past, present, and future DNA sequencing. *Molecular Genetics and Metabolism*, 110(1-2):3–24.

Morris R. M., Rappe M. S., Urbach E., Connon S. a., and Giovannoni S. J. (2004). Prevalence of the Chloroflexi-Related SAR202 Bacterioplankton Cluster throughout the Mesopelagic Zone and Deep Ocean. *Applied and Environmental Microbiology*, 70(5):2836–2842.

Morris R. M., Rappé M. S., Connon S. A., Vergin K. L., Siebold W. A., Carlson C. A., and Giovannoni S. J. (2002). SAR11 clade dominates ocean surface bacterioplankton communities. *Nature*, 420(6917):806–810.

Morris R. M., Vergin K. L., Cho J. C., Rappé M. S., Carlson C. A., and Giovannoni S. J. (2005). Temporal and spatial response of bacterioplankton lineages to annual convective overturn at the Bermuda Atlantic Time-series Study site. *Limnology and Oceanography*, 50(5):1687–1696.

Morris R. M., Frazar C. D., and Carlson C. A. (2012). Basin-scale patterns in the abundance

of SAR11 subclades, marine Actinobacteria (OM1), members of the Roseobacter clade and OCS116 in the South Atlantic. *Environmental Microbiology*, 14(5):1133–1144.

Müller O., Wilson B., Paulsen M. L., Rumińska A., Armo H. R., Bratbak G., and Øvreås L. (2018). Spatiotemporal Dynamics of Ammonia-Oxidizing Thaumarchaeota in Distinct Arctic Water Masses. *Frontiers in Microbiology*, 9(January):1–13.

Muller-Karger F. E., Miloslavich P., Bax N. J., Simmons S., Costello M. J., Sousa Pinto I., Canonico G., Turner W., Gill M., Montes E., Best B. D., Pearlman J., Halpin P., Dunn D., Benson A., Martin C. S., Weatherdon L. V., Appeltans W., Provoost P., Klein E., Kelble C. R., Miller R. J., Chavez F. P., Iken K., Chiba S., Obura D., Navarro L. M., Pereira H. M., Allain V., Batten S., Benedetti-Checchi L., Duffy J. E., Kudela R. M., Rebelo L.-M., Shin Y., and Geller G. (2018). Advancing Marine Biological Observations and Data Requirements of the Complementary Essential Ocean Variables (EOVs) and Essential Biodiversity Variables (EBVs) Frameworks. *Frontiers in Marine Science*, 5(June):1–15.

Muyzer G. and Stams A. J. (2008). The ecology and biotechnology of sulphate-reducing bacteria. *Nature Reviews Microbiology*, 6(6):441–454.

Neave M., Luter H., Padovan A., Townsend S., Schobben X., and Gibb K. (2014). Multiple approaches to microbial source tracking in tropical northern Australia. *MicrobiologyOpen*, 3 (6):860–874.

Nguyen D., Maranger R., Tremblay J. r., and Gosselin M. (2012). Respiration and bacterial carbon dynamics in the Amundsen Gulf, western Canadian Arctic. *Journal of Geophysical Research: Oceans*, 117(6):1–12.

Nikrad M. P., Cottrell M. T., and Kirchman D. L. (2012). Abundance and single-cell activity of heterotrophic bacterial groups in the western Arctic Ocean in summer and winter. *Applied and Environmental Microbiology*, 78(7):2402–2409.

Nikrad M. P., Cottrell M. T., and Kirchman D. L. (2014). Growth activity of gammaproteobacterial subgroups in waters off the west Antarctic Peninsula in summer and fall. *Environmental microbiology*, 16(6):1513–1523.

Nobu M. K., Narihiro T., Rinke C., Kamagata Y., Tringe S. G., Woyke T., and Liu W.-T. (2015). Microbial dark matter ecogenomics reveals complex synergistic networks in a methanogenic bioreactor. *The ISME Journal*, 9(8):1710–1722.

Nöthig E.-M., Bracher A., Engel A., Metfies K., Niehoff B., Peeken I., Bauerfeind E., Cherkasheva A., Gäbler-Schwarz S., Hardge K., Kilias E., Kraft A., Mebrahtom Kidane Y., Lalande C., Piontek J., Thomisch K., and Wurst M. (2015). Summertime plankton ecology in Fram Strait—a compilation of long- and short-term observations. *Polar Research*, 34(1):23349.

Nöthig E.-M., Knüppel N., and Lorenzen C. Chlorophyll a measured on water bottle samples during POLARSTERN cruise PS99.2 (ARK-XXX/1.2). Technical report, 2018.

Notz D. and Stroeve J. (2016). Observed Arctic sea-ice loss directly follows anthropogenic CO 2 emission. *Science*, 354(6313):747–750.

Oksanen J. vegan: Community Ecology Package. R package version 2.4-2, 2016.

Østerhus S., Turrell W. R., Jónsson S., and Hansen B. (2005). Measured volume, heat, and salt fluxes from the Atlantic to the Arctic Mediterranean. *Geophysical Research Letters*, 32(7):1–4.

Ottesen E. A. (2016). Probing the living ocean with ecogenomic sensors. *Current Opinion in Microbiology*, 31:132–139.

Overland J. E. and Wang M. (2013). When will the summer Arctic be nearly sea ice free? *Geophysical Research Letters*, 40(10):2097–2101.

Pace N. R., Sapp J., and Goldenfeld N. (2012). Phylogeny and beyond: Scientific, historical, and conceptual significance of the first tree of life. *Proceedings of the National Academy of Sciences*, 109(4):1011–1018.

Padilla C. C., Ganesh S., Gantt S., Huhman A., Parris D. J., Sarode N., and Stewart F. J. (2015). Standard filtration practices may significantly distort planktonic microbial diversity estimates. *Frontiers in Microbiology*, 6(JUN):1–10.

Paquette R. G., Bourke R. H., Newton J. F., and Perdue W. F. (1985). The East Greenland Polar Front in autumn. *Journal of Geophysical Research*, 90(C3):4866.

Parada A. E., Needham D. M., and Fuhrman J. A. (2016). Every base matters: assessing small subunit rRNA primers for marine microbiomes with mock communities, time series and global field samples. *Environmental Microbiology*, 18(5):1403–1414.

Pawlowski J., Lejzerowicz F., Apotheloz-Perret-Gentil L., Visco J., and Esling P. (2016). Protist metabarcoding and environmental biomonitoring: Time for change. *European Journal of Protistology*, 55:12–25.

Peng G. and Meier W. N. (2017). Temporal and regional variability of Arctic sea-ice coverage from satellite data. *Annals of Glaciology*, pages 1–10.

Pereira H. M., Ferrier S., Walters M., Geller G. N., Jongman R. H. G., Scholes R. J., Bruford M. W., Brummitt N., Butchart S. H. M., Cardoso A. C., Coops N. C., Dulloo E., Faith D. P., Freyhof J., Gregory R. D., Heip C., Hoft R., Hurtt G., Jetz W., Karp D. S., McGeoch M. A., Obura D., Onoda Y., Pettorelli N., Reyers B., Sayre R., Scharlemann J. P. W., Stuart S. N., Turak E., Walpole M., and Wegmann M. (2013). Essential Biodiversity Variables. *Science*, 339(6117):277–278.

Perovich D. K. and Polashenski C. (2012). Albedo evolution of seasonal Arctic sea ice. *Geophysical Research Letters*, 39(8):1–6.

Perrette M., Yool A., Quartly G. D., and Popova E. E. (2011). Near-ubiquity of ice-edge blooms in the Arctic. *Biogeosciences*, 8(2):515–524.

Peura S., Bertilsson S., Jones R. I., and Eiler A. (2015). Resistant Microbial Cooccurrence Patterns Inferred by Network Topology. *Applied and Environmental Microbiology*, 81(6):2090–2097.

Pfirman S. L., Colony R., Nürnberg D., Eicken H., and Rigor I. (1997). Reconstructing the origin and trajectory of drifting Arctic sea ice. *Journal of Geophysical Research: Oceans*, 102(C6): 12575–12586.

Picheral M. Zooprocess Manual Version 5.08, 2008.

Picheral M., Guidi L., Stemmann L., Karl D. M., Iddaoud G., and Gorsky G. (2010). The Underwater Vision Profiler 5: An advanced instrument for high spatial resolution studies of particle size spectra and zooplankton. *Limnology and Oceanography: Methods*, 8(9):462–473.

Pinhassi J. and Hagström Å. (2000). Seasonal succession in marine bacterioplankton. *Aquatic Microbial Ecology*, 21(3):245–256.

Pinhassi J., Havskum H., Peters F., and Malits A. (2004). Changes in Bacterioplankton Composition under Different Phytoplankton Regimens. 70(11):6753–6766.

Piontek J., Sperling M., Nöthig E.-M. M., and Engel A. (2014). Regulation of bacterioplankton activity in Fram Strait (Arctic Ocean) during early summer: The role of organic matter supply and temperature. *Journal of Marine Systems*, 132:83–94.

Piontek J., Sperling M., Nöthig E.-M., and Engel A. (2015). Multiple environmental changes induce interactive effects on bacterial degradation activity in the Arctic Ocean. *Limnology and Oceanography*, 60(4):1392–1410.

Piroddi C., Teixeira H., Lynam C. P., Smith C., Alvarez M. C., Mazik K., Andonegi E., Churilova T., Tedesco L., Chifflet M., Chust G., Galparsoro I., Garcia A. C., Kämäri M., Kryvenko O., Lassalle G., Neville S., Niquil N., Papadopoulou N., Rossberg A. G., Suslin V., and Uyarra M. C. (2015). Using ecological models to assess ecosystem status in support of the European Marine Strategy Framework Directive. *Ecological Indicators*, 58:175–191.

Ploug H. and Jørgensen B. B. (1999). A net-jet flow system for mass transfer and micro electrode studies in sinking aggregates. *Mar. Ecol. Prog. Ser.*, 176(1987):279.

Ploug H., Iversen M. H., and Fischer G. (2008). Ballast, sinking velocity, and apparent diffusivity within marine snow and zooplankton fecal pellets: Implications for substrate turnover by attached bacteria. *Limnology and Oceanography*, 53(5):1878–1886.

Ploug H., Iversen M. H., Koski M., and Buitenhuis E. T. (2008). Production, oxygen respiration rates, and sinking velocity of copepod fecal pellets: Direct measurements of ballasting by opal and calcite. *Limnology and Oceanography*, 53(2):469–476.

Ploug H., Terbrüggen A., Kaufmann A., Wolf-Gladrow D., and Passow U. (2010). A novel method to measure particle sinking velocity in vitro, and its comparison to three other in vitro methods. *Limnology and Oceanography: Methods*, 8(8):386–393.

Polyak L., Alley R. B., Andrews J. T., Brigham-Grette J., Cronin T. M., Darby D. A., Dyke A. S., Fitzpatrick J. J., Funder S., Holland M., Jennings A. E., Miller G. H., O'Regan M., Savelle J., Serreze M., St. John K., White J. W., and Wolff E. (2010). History of sea ice in the Arctic. *Quaternary Science Reviews*, 29(15-16):1757–1778.

Polyakov I. V., Beszczynska A., Carmack E. C., Dmitrenko I. A., Fahrbach E., Frolov I. E., Gerdes R., Hansen E., Holfort J., Ivanov V. V., Johnson M. A., Karcher M., Kauker F., Morison J., Orvik K. A., Schauer U., Simmons H. L., Skagseth Ø., Sokolov V. T., Steele M., Timokhov L. A., Walsh D., and Walsh J. E. (2005). One more step toward a warmer Arctic. *Geophysical Research Letters*, 32(17).

Polyakov I. V., Pnyushkov A. V., Alkire M. B., Ashik I. M., Baumann T. M., Carmack E. C., Goszczko I., Guthrie J., Ivanov V. V., Kanzow T., Krishfield R., Kwok R., Sundfjord A., Morison J., Rember R., and Yulin A. (2017). Greater role for Atlantic inflows on sea-ice loss in the Eurasian Basin of the Arctic Ocean. *Science*, 356(6335):285–291.

Popova E. E., Yool A., Aksenov Y., Coward A. C., and Anderson T. R. (2014). Regional variability of acidification in the Arctic: A sea of contrasts. *Biogeosciences*, 11(2):293–308.

Popova E. E., Yool A., Coward A. C., Dupont F., Deal C., Elliott S., Hunke E., Jin M., Steele M., and Zhang J. (2012). What controls primary production in the Arctic Ocean? Results from an intercomparison of five general circulation models with biogeochemistry. *Journal of Geophysical Research: Oceans*, 117(1):1–16.

Post E., Forchhammer M. C., Syndonia Bret-Harte M., Callaghan T. V., Christensen T. R., Elberling B., Fox A. D., Gilg O., Hik D. S., Høye T. T., Ims R. A., Jeppesen E., Klein D. R., Madsen J., Mcguire A. D., Rysgaard S., Schindler D. E., Stirling I., Tamstorf M. P., Tyler N. J. C., Van Der Wal R., Welker J., Wookey P. A., Schmidt N. M., and Aastrup P. (2009). Ecological Dynamics Across the Arctic Associated with Recent Climate Change. 325(September):1355–1359.

Poulin M., Daugbjerg N., Gradinger R., Ilyash L., Ratkova T., and von Quillfeldt C. (2011). The pan-Arctic biodiversity of marine pelagic and sea-ice unicellular eukaryotes: A first-attempt assessment. *Marine Biodiversity*, 41(1):13–28.

Pruesse E., Peplies J., and Glöckner F. O. (2012). SINA: Accurate high-throughput multiple sequence alignment of ribosomal RNA genes. *Bioinformatics*, 28(14):1823–1829.

Quast C., Pruesse E., Yilmaz P., Gerken J., Schweer T., Glo F. O., and Yarza P. (2013). The SILVA ribosomal RNA gene database project : improved data processing and web-based tools. 41 (November 2012):590–596.

Quillfeldt C. V. (2005). Common Diatom Species in Arctic Spring Blooms: Their Distribution and Abundance. *Botanica Marina*, 43(6):499–516.

Rabe B., Schauer U., and Mackensen A. (2009). Freshwater components and transports in the Fram Strait- recent observations and changes since the late 1990 s. *Ocean Science*, 5:219–233.

Racault M.-F., Platt T., Sathyendranath S., A irba E., Martinez Vicente V., and Brewin R. (2014). Plankton indicators and ocean observing systems: support to the marine ecosystem state assessment. *Journal of Plankton Research*, 36(3):621–629.

Ramanan R., Kim B.-H., Cho D.-H., Oh H.-M., and Kim H.-S. (2016). Algae–bacteria interactions: Evolution, ecology and emerging applications. *Biotechnology Advances*, 34(1):14–29.

Ramírez-Castillo F., Loera-Muro A., Jacques M., Garneau P., Avelar-González F., Harel J., and Guerrero-Barrera A. (2015). Waterborne Pathogens: Detection Methods and Challenges. *Pathogens*, 4(2):307–334.

Randelhoff A., Reigstad M., Chierici M., Sundfjord A., Ivanov V., Cape M., Vernet M., Tremblay J.-É., Bratbak G., and Kristiansen S. (2018). Seasonality of the Physical and Biogeochemical Hydrography in the Inflow to the Arctic Ocean Through Fram Strait. *Frontiers in Marine Science*, 5(June):224.

Rapp J. Z., Fernández-Méndez M., Bienhold C., and Boetius A. (2018). Effects of ice-algal aggregate export on the connectivity of bacterial communities in the central Arctic Ocean. *Frontiers in Microbiology*, 9(MAY).

Rappé M. S. and Giovannoni S. J. (2003). The Uncultured Microbial Majority. *Annual Review of Microbiology*, 57(1):369–394.

Raverty S. A., Rhodes L. D., Zabek E., Eshghi A., Cameron C. E., Hanson M. B., and Schroeder J. P. (2017). Respiratory Microbiome of Endangered Southern Resident Killer Whales and Microbiota of Surrounding Sea Surface Microlayer in the Eastern North Pacific. *Scientific Reports*, 7(1):394.

Reid P., Colebrook J., Matthews J., and Aiken J. (2003). The Continuous Plankton Recorder: concepts and history, from Plankton Indicator to undulating recorders. *Progress in Oceanography*, 58(2-4):117–173.

Reid P. C., Hari R. E., Beaugrand G., Livingstone D. M., Marty C., Straile D., Barichivich J., Goberville E., Adrian R., Aono Y., Brown R., Foster J., Groisman P., Hélaouët P., Hsu H.-H., Kirby R., Knight J., Kraberg A., Li J., Lo T.-T., Myneni R. B., North R. P., Pounds J. A., Sparks T., Stübi R., Tian Y., Wiltshire K. H., Xiao D., and Zhu Z. (2016). Global impacts of the 1980s regime shift. *Global Change Biology*, 22(2):682–703.

Reigstad M. and Wassmann P. Does Phaeocystis spp. contribute significantly to vertical export of organic carbon? In *Phaeocystis, major link in the biogeochemical cycling of climate-relevant elements*, pages 217–234. Springer Netherlands, Dordrecht, 2007. ISBN 9781402062131. doi: 10.1007/978-1-4020-6214-8_16. URL `http://link.springer.com/10.1007/978-1-4020-6214-8{_}16`.

Renner A. H. H., Gerland S., Haas C., Spreen G., Beckers J. F., Hansen E., Nicolaus M., and Goodwin H. (2014). Evidence of Arctic sea ice thinning from direct observations. *Geophysical Research Letters*, 41(14):5029–5036.

Repeta D. J., Ferrón S., Sosa O. A., Johnson C. G., Repeta L. D., Acker M., DeLong E. F., and Karl D. M. (2016). Marine methane paradox explained by bacterial degradation of dissolved organic matter. *Nature Geoscience*, 9(12):884–887.

Reuter J. A., Spacek D. V., and Snyder M. P. (2015). High-Throughput Sequencing Technologies. *Molecular Cell*, 58(4):586–597.

Rich J., Gosselin M., Sherr E., Sherr B., and Kirchman D. L. (1997). High bacterial production, uptake and concentrations of dissolved organic matter in the Central Arctic Ocean. *Deep-Sea Research Part II: Topical Studies in Oceanography*, 44(8):1645–1663.

Riemann L., Steward G. F., and Azam F. (2000). Dynamics of Bacterial Community Composition and Activity during a Mesocosm Diatom Bloom. *Applied and Environmental Microbiology*, 66 (2):578–587.

Rinke C., Schwientek P., Sczyrba A., Ivanova N. N., Anderson I. J., Cheng J.-F., Darling A., Malfatti S., Swan B. K., Gies E. A., Dodsworth J. A., Hedlund B. P., Tsiamis G., Sievert S. M., Liu W.-T., Eisen J. A., Hallam S. J., Kyrpides N. C., Stepanauskas R., Rubin E. M., Hugenholtz P., and Woyke T. (2013). Insights into the phylogeny and coding potential of microbial dark matter. *Nature*, 499(7459):431–437.

Rivkin R. B., Legendre L., Deibel D., Klein B., Crocker K., Roy S., Silverberg N., Lovejoy C., Mesple F., Romero N., Anderson M. R., Matthews P., Savenkoff C., Vezina A., Therriault J.-C. J.-c., Wesson J., Berube C., Grant R., Tremblay J.-E., Klein B., Crocker K., Roy S., Silverberg N., Lovejoy C., Mespl F., Romero N., Anderson M. R., Matthews P., Savenkoff C., V zina A., Therriault J.-C. J.-c., Wesson J., B rub C., and Ingram R. G. (1996). Vertical Flux of Biogenic Carbon in the Ocean: Is There Food Web Control? *Science*, 272(5265):1163–1166.

Robinson C. (2008). Heterotrophic bacterial respiration. *Microbial ecology of the oceans*, pages 299–334.

Rognes T., Flouri T., Nichols B., Quince C., and Mahé F. (2016). VSEARCH: a versatile open source tool for metagenomics. *PeerJ*, 4:e2584.

Rooney-Varga J. N., Giewat M. W., Savin M. C., Sood S., Legresley M., and Martin J. L. (2005). Links between phytoplankton and bacterial community dynamics in a coastal marine environment. *Microbial Ecology*, 49(1):163–175.

Roullier F., Berline L., Guidi L., Durrieu De Madron X., Picheral M., Sciandra A., Pesant S., and Stemmann L. (2014). Particle size distribution and estimated carbon flux across the Arabian Sea oxygen minimum zone. *Biogeosciences*, 11(16):4541–4557.

RStudio Team . RStudio: Integrated Development Environment for R, 2015. URL `http://www.rstudio.com/`.

Rudels B. (2012). Arctic Ocean circulation and variability – Advection and external forcing encounter constraints and local processes. *Ocean Science*, 8(2):261–286.

Rudels B., Anderson L. G., and Jones E. P. (1996). Formation and evolution of the surface mixed layer and halocline of the Arctic Ocean. *Journal of Geophysical Research: Oceans*, 101(C4): 8807–8821.

Rudels B., Schauer U., Björk G., Korhonen M., Pisarev S., Rabe B., and Wisotzki A. (2013). Observations of water masses and circulation with focus on the Eurasian Basin of the Arctic Ocean from the 1990s to the late 2000s. *Ocean Science*, 9(1):147–169.

Rudels B., Nilsson J., and Winsor P. (2005). The interaction between waters from the Arctic Ocean and the Nordic Seas north of Fram Strait and along the East Greenland Current : results from the Arctic Ocean-02 Oden expedition. 55:1–30.

Russi D., Pantzar M., Kettunen M., Gitti G., Mutafoglu K., Kotulak M., and ten Brink P. (2016). Socio-Economic Benefits of the EU Marine Protected Areas (pp. 97). *More Information*.

Rysgaard S., Nielsen T. G., and Hansen B. W. (1999). Seasonal variation in nutrients, pelagic primary production and grazing in a high-Arctic coastal marine ecosystem, Young Sound, Northeast Greenland. *Marine Ecology Progress Series*, 179(Digby 1953):13–25.

Sakshaug E. *Primary and Secondary Production in the Arctic Seas*, pages 57–81. Springer Berlin Heidelberg, Berlin, Heidelberg, 2004. ISBN 978-3-642-18912-8. doi: 10.1007/978-3-642-18912-8_3. URL `https://doi.org/10.1007/978-3-642-18912-8{_}3`.

Sala M. M., Arrieta J. M., Boras J. A., Duarte C. M., and Vaqué D. (2010). The impact of ice melting on bacterioplankton in the Arctic Ocean. *Polar Biology*, 33(12):1683–1694.

Salazar G., Cornejo-Castillo F. M., Borrull E., Díez-Vives C., Lara E., Vaqué D., Arrieta J. M., Duarte C. M., Gasol J. M., and Acinas S. G. (2015). Particle-association lifestyle is a phylogenetically conserved trait in bathypelagic prokaryotes. *Molecular Ecology*, 24(22):5692–5706.

Salazar G., Cornejo-Castillo F. M., Benítez-Barrios V., Fraile-Nuez E., Álvarez-Salgado X. A., Duarte C. M., Gasol J. M., and Acinas S. G. (2016). Global diversity and biogeography of deep-sea pelagic prokaryotes. *The ISME Journal*, 10(3):596–608.

Sapp M., Schwaderer A. S., Wiltshire K. H., Hoppe H. G., Gerdts G., and Wichels A. (2007). Species-specific bacterial communities in the phycosphere of microalgae? *Microbial Ecology*, 53(4):683–699.

Sapp M., Wichels A., and Gerdts G. (2007). Impacts of cultivation of marine diatoms on the associated bacterial community. *Applied and Environmental Microbiology*, 73(9):3117–3120.

Sarmento H. and Gasol J. M. (2012). Use of phytoplankton-derived dissolved organic carbon by different types of bacterioplankton. *Environmental Microbiology*, 14(9):2348–2360.

Schafer H., Abbas B., Witte H., and Muyzer G. (2002). Genetic diversity of â€˜satelliteâ€™ bacteria present in cultures of marine diatoms. *FEMS Microbiology Ecology*, 42(1):25–35.

Schlitzer R. Ocean Data View, 2015. URL `http://odv.awi.de`.

Schoemann V., Becquevort S., Stefels J., Rousseau V., and Lancelot C. (2005). Phaeocystis blooms in the global ocean and their controlling mechanisms: a review. *Journal of Sea Research*, 53 (1-2):43–66.

Scholes R. J., Walters M., Turak E., Saarenmaa H., Heip C. H., Tuama É. Ó., Faith D. P., Mooney H. A., Ferrier S., Jongman R. H., Harrison I. J., Yahara T., Pereira H. M., Larigauderie A., and Geller G. (2012). Building a global observing system for biodiversity. *Current Opinion in Environmental Sustainability*, 4(1):139–146.

Schourup-Kristensen V., Sidorenko D., Wolf-Gladrow D. A., and Völker C. (2014). A skill assessment of the biogeochemical model REcoM2 coupled to the Finite Element Sea Ice–Ocean Model (FESOM 1.3). *Geoscientific Model Development*, 7(6):2769–2802.

Schourup-Kristensen V., Wekerle C., Wolf-Gladrow D. A., and Völker C. (2018). Arctic Ocean biogeochemistry in the high resolution FESOM 1.4-REcoM2 model. *Progress in Oceanography*, 168:65–81.

Seebens H., Schwartz N., Schupp P. J., and Blasius B. (2016). Predicting the spread of marine species introduced by global shipping. *Proceedings of the National Academy of Sciences*, 113 (20):5646–5651.

Seegers B. N., Birch J. M., Marin R., Scholin C. A., Caron D. A., Seubert E. L., Howard M. D. A., Robertson G. L., and Jones B. H. (2015). Subsurface seeding of surface harmful algal blooms observed through the integration of autonomous gliders, moored environmental sample processors, and satellite remote sensing in southern California. *Limnology and Oceanography*, 60 (3):754–764.

Segev E., Wyche T. P., Kim K. H., Petersen J., Ellebrandt C., Vlamakis H., Barteneva N., Paulson J. N., Chai L., Clardy J., and Kolter R. (2016). Dynamic metabolic exchange governs a marine algal-bacterial interaction. *eLife*, 5(NOVEMBER2016).

Sekar R., Fuchs B. M., Amann R., Pernthaler J., Planck M., and Microbiology M. (2004). Flow Sorting of Marine Bacterioplankton after Fluorescence In Situ Hybridization Flow Sorting of Marine Bacterioplankton after Fluorescence In Situ Hybridization. *Applied and environmental microbiology*, 70(10):6210–6219.

Serreze M. C. and Barry R. G. (2011). Processes and impacts of Arctic amplification: A research synthesis. *Global and Planetary Change*, 77(1-2):85–96.

Serreze M. C., Barrett A. P., Slater A. G., Woodgate R. A., Aagaard K., Lammers R. B., Steele M., Moritz R., Meredith M., and Lee C. M. (2006). The large-scale freshwater cycle of the Arctic. *Journal of Geophysical Research*, 111(C11):C11010.

Sherr B. F. and Sherr E. B. (2003). Community respiration/production and bacterial activity in the upper water column of the central Arctic Ocean. *Deep-Sea Research Part I: Oceanographic Research Papers*, 50(4):529–542.

Sherr E. B., Sherr B. F., Wheeler P. A., and Thompson K. (2003). Temporal and spatial variation in stocks of autotrophic and heterotrophic microbes in the upper water column of the central Arctic Ocean. *Deep-Sea Research Part I: Oceanographic Research Papers*, 50(5):557–571.

Siegel D., Fields E., and Buesseler K. (2008). A bottom-up view of the biological pump: Modeling source funnels above ocean sediment traps. *Deep Sea Research Part I: Oceanographic Research Papers*, 55(1):108–127.

Silvester N., Alako B., Amid C., Cerdeño-Tarrága A., Clarke L., Cleland I., Harrison P. W., Jayathilaka S., Kay S., Keane T., Leinonen R., Liu X., Martínez-Villacorta J., Menchi M., Reddy K., Pakseresht N., Rajan J., Rossello M., Smirnov D., Toribio A. L., Vaughan D., Zalunin V., and Cochrane G. (2018). The European Nucleotide Archive in 2017. *Nucleic Acids Research*, 46 (D1):D36–D40.

Simon M., Glöckner F., and Amann R. (1999). Different community structure and temperature optima of heterotrophic picoplankton in various regions of the Southern Ocean. *Aquatic Microbial Ecology*, 18(3):275–284.

Simon M., Grossart H. H.-p., Schweitzer B., and Ploug H. (2002). Microbial ecology of organic aggregates in aquatic ecosystems. *Aquatic Microbial Ecology*, 28:175–211.

Smetacek V. (2000). Oceanography: The giant diatom dump. *Nature*, 406(6796):574–575.

Smetacek V. and Nicol S. (2005). Polar ocean ecosystems in a changing world. *Nature*, 437 (7057):362–368.

Smith Jr. K., Messié M., Sherman A., Huffard C., Hobson B., Ruhl H., and Boetius A. (2015). Navigating the Uncertain Future of Global Oceanic Time Series. *Eos*, 96.

Smith Jr W. O. *Polar Oceanography: Physical science*. Academic Press, 2013. ISBN 1483289168.

Smith Jr W. O., Baumann M. E. M., Wilson D. L., and Aletsee L. (1987). Phytoplankton biomass and productivity in the marginal ice zone of the Fram Strait during summer 1984. *Journal of Geophysical Research: Oceans*, 92(C7):6777–6786.

Soltwedel T., Bauerfeind E., Bergmann M., Budaeva N., Hoste E., Jaeckisch N., von Juterzenka K., Matthiesson J., Moekievsky V., Nöthig E.-M., Quéric N.-V., Sablotny B., Sauter E., Schewe I., Urban-Malinga B., Wegner J., Maria Wlodarska-Kowalczuk M., and Klages M. (2005). HAUSGARTEN: Multidisciplinary Investigations at a Deep-Sea, Long-Term Observatory in the Arctic Ocean. *Oceanography*, 18(3):46–61.

Soltwedel T., Schauer U., Boebel O., Nothig E.-M., Bracher A., Metfies K., Schewe I., Boetius A., and Klages M. FRAM - FRontiers in Arctic marine Monitoring Visions for permanent observations in a gateway to the Arctic Ocean. In *2013 MTS/IEEE OCEANS - Bergen*, pages 1–7. IEEE, 2013. ISBN 978-1-4799-0001-5. doi: 10.1109/OCEANS-Bergen.2013.6608008. URL `http://ieeexplore.ieee.org/document/6608008/`.

Soltwedel T., Bauerfeind E., Bergmann M., Bracher A., Budaeva N., Busch K., Cherkasheva A., Fahl K., Grzelak K., Hasemann C., Jacob M., Kraft A., Lalande C., Metfies K., Nöthig E.-M., Meyer K., Quéric N.-V., Schewe I., Włodarska-Kowalczuk M., and Klages M. (2016). Natural variability or anthropogenically-induced variation? Insights from 15 years of multidisciplinary observations at the arctic marine LTER site HAUSGARTEN. *Ecological Indicators*, 65:89–102.

Søreide J. E., Leu E. V., Berge J., Graeve M., and Falk-Petersen S. (2010). Timing of blooms, algal food quality and Calanus glacialis reproduction and growth in a changing Arctic. *Global Change Biology*, 16(11):3154–3163.

Sperling M., Piontek J., Engel A., Wiltshire K. H., Niggemann J., Gerdts G., and Wichels A.

(2017). Combined Carbohydrates Support Rich Communities of Particle-Associated Marine Bacterioplankton. *Frontiers in Microbiology*, 08(January):1–14.

Spring S., Bunk B., Spröer C., Schumann P., Rohde M., Tindall B. J., and Klenk H.-p. (2016). Characterization of the first cultured representative of Verrucomicrobia subdivision 5 indicates the proposal of a novel phylum. *Nature Publishing Group*, pages 1–16.

Starke I. C., Vahjen W., Pieper R., and Zentek J. (2014). The Influence of DNA Extraction Procedure and Primer Set on the Bacterial Community Analysis by Pyrosequencing of Barcoded 16S rRNA Gene Amplicons. *Molecular Biology International*, 2014:1–10.

Steele J. A., Countway P. D., Xia L., Vigil P. D., Beman J. M., Kim D. Y., Chow C. E. T., Sachdeva R., Jones A. C., Schwalbach M. S., Rose J. M., Hewson I., Patel A., Sun F., Caron D. A., and Fuhrman J. A. (2011). Marine bacterial, archaeal and protistan association networks reveal ecological linkages. *ISME Journal*, 5(9):1414–1425.

Steele M., Morley R., and Ermold W. (2001). PHC: A global ocean hydrography with a high-quality Arctic Ocean. *Journal of Climate*, 14(9):2079–2087.

Steele M. and Dickinson S. (2016). The phenology of Arctic Ocean surface warming. *Journal of Geophysical Research: Oceans*, 121(9):6847–6861.

Steinacher M., Joos F., Frolicher T. L., Plattner G.-K., and Doney S. C. (2009). Imminent ocean acidification in the Arctic projected with the NCAR global coupled carbon cycle-climate model.

Steinberg D. K., Carlson C. A., Bates N. R., Johnson R. J., Michaels A. F., and Knap A. H. (2001). Overview of the US JGOFS Bermuda Atlantic Time-series Study (BATS): a decade-scale look at ocean biology and biogeochemistry. *Deep Sea Research Part II: Topical Studies in Oceanography*, 48(8-9):1405–1447.

Stenseth N. C., Ottersen G., Hurrell J. W., Mysterud A., Lima M., Chan K.-S., Yoccoz N. G., and Adlandsvik B. (2003). Review article. Studying climate effects on ecology through the use of climate indices: the North Atlantic Oscillation, El Nino Southern Oscillation and beyond. *Proceedings of the Royal Society B: Biological Sciences*, 270(1529):2087–2096.

Stocker R. (2012). Marine Microbes See a Sea of Gradients. *Science*, 338(6107):628–633.

Stocker R. and Seymour J. R. (2012). Ecology and Physics of Bacterial Chemotaxis in the Ocean Ecology and Physics of Bacterial Chemotaxis in the Ocean. 76(4).

Strous M., Pelletier E., Mangenot S., Rattei T., Lehner A., Taylor M. W., Horn M., Daims H., Bartol-Mavel D., Wincker P., Barbe V., Fonknechten N., Vallenet D., Segurens B., Schenowitz-Truong C., Médigue C., Collingro A., Snel B., Dutilh B. E., Op Den Camp H. J., Van Der Drift C., Cirpus I., Van De Pas-Schoonen K. T., Harhangi H. R., Van Niftrik L., Schmid M., Keltjens J., Van De Vossenberg J., Kartal B., Meier H., Frishman D., Huynen M. A., Mewes H. W., Weissenbach J., Jetten M. S., Wagner M., and Le Paslier D. (2006). Deciphering the evolution and metabolism of an anammox bacterium from a community genome. *Nature*, 440(7085):790–794.

Sun L., Perlwitz J., and Hoerling M. (2016). What caused the recent "Warm Arctic, Cold Continents" trend pattern in winter temperatures? *Geophysical Research Letters*, 43(10):5345–5352.

Sunagawa S., Coelho L. P., Chaffron S., Kultima J. R., Labadie K., Salazar G., Djahanschiri B., Zeller G., Mende D. R., Alberti A., Cornejo-Castillo F. M., Costea P. I., Cruaud C., D'Ovidio F., Engelen S., Ferrera I., Gasol J. M., Guidi L., Hildebrand F., Kokoszka F., Lepoivre C., Lima-Mendez G., Poulain J., Poulos B. T., Royo-Llonch M., Sarmento H., Vieira-Silva S., Dimier C., Picheral M., Searson S., Kandels-Lewis S., Bowler C., de Vargas C., Gorsky G., Grimsley N., Hingamp P., Iudicone D., Jaillon O., Not F., Ogata H., Pesant S., Speich S., Stemmann L., Sullivan M. B., Weissenbach J., Wincker P., Karsenti E., Raes J., Acinas S. G., Bork P., Boss E., Bowler C., Follows M., Karp-Boss L., Krzic U., Reynaud E. G., Sardet C., Sieracki M., and Velayoudon D. (2015). Structure and function of the global ocean microbiome. *Science*, 348 (6237):1261359–1261359.

Swan B. K., Martinez-Garcia M., Preston C. M., Sczyrba A., Woyke T., Lamy D., Reinthaler T., Poulton N. J., Masland E. D. P., Gomez M. L., Sieracki M. E., DeLong E. F., Herndl G. J., and Stepanauskas R. (2011). Potential for Chemolithoautotrophy Among Ubiquitous Bacteria Lineages in the Dark Ocean. *Science*, 333(6047):1296–1300.

Tada Y., Taniguchi A., Nagao I., Miki T., Uematsu M., Tsuda A., Hamasaki K., and Icrobiol A. P. P. L. E. N. M. (2011). Differing Growth Responses of Major Phylogenetic Groups of Marine Bacteria to Natural Phytoplankton Blooms in the Western North Pacific Ocean. 77(12):4055–4065.

Takahashi T., Sutherland S. C., Sweeney C., Poisson A., Metzl N., Tilbrook B., Bates N., Wanninkhof R., Feely R. A., Sabine C., Olafsson J., and Nojiri Y. (2002). Global sea-air CO2 flux based on climatological surface ocean pCO2, and seasonal biological and temperature effects. *Deep-Sea Research Part II: Topical Studies in Oceanography*, 49:1601–1622.

Tamburini C., Boutrif M., Garel M., Colwell R. R., and Deming J. W. (2013). Prokaryotic responses to hydrostatic pressure in the ocean - a review. *Environmental Microbiology*, 15(5): 1262–1274.

Tamelander T. (2013). Community composition and extracellular enzyme activity of bacteria associated with suspended and sinking particles in contrasting Arctic and sub-arctic marine environments. *Aquatic Microbial Ecology*, 69(3):211–221.

Tamminen T. and Andersen T. (2007). Seasonal phytoplankton nutrient limitation patterns as revealed by bioassays over Baltic Sea gradients of salinity and eutrophication. *Marine Ecology Progress Series*, 340(1971):121–138.

Tan B., Ng C., Nshimyimana J. P., Loh L. L., Gin K. Y.-H., and Thompson J. R. (2015). Next-generation sequencing (NGS) for assessment of microbial water quality: current progress, challenges, and future opportunities. *Frontiers in Microbiology*, 6.

Taylor A. H., Watson A. J., and Robertson J. E. (1992). The influence of the spring phytoplankton bloom on carbon dioxide and oxygen concentrations in the surface waters of the northeast Atlantic during 1989. *Deep Sea Research Part A. Oceanographic Research Papers*, 39(2):137–152.

Taylor J. D., Cottingham S. D., Billinge J., and Cunliffe M. (2014). Seasonal microbial community dynamics correlate with phytoplankton-derived polysaccharides in surface coastal waters. *ISME Journal*, 8(1):245–248.

Teeling H., Fuchs B. M., Becher D., Klockow C., Gardebrecht A., Bennke C. M., Kassabgy M., Huang S., Mann A. J., Waldmann J., Weber M., Klindworth A., Otto A., Lange J., Bernhardt J., Reinsch C., Hecker M., Peplies J., Bockelmann F. D., Callies U., Gerdts G., Wichels A., Wiltshire K. H., Glockner F. O., Schweder T., and Amann R. (2012). Substrate-Controlled Succession of Marine Bacterioplankton Populations Induced by a Phytoplankton Bloom. *Science*, 336 (6081):608–611.

Teeling H., Fuchs B. M., Bennke C. M., Krüger K., Chafee M., Kappelmann L., Reintjes G., Waldmann J., Quast C., Glöckner F. O., Lucas J., Wichels A., Gerdts G., Wiltshire K. H., and Amann R. I. (2016). Recurring patterns in bacterioplankton dynamics during coastal spring algae blooms. *eLife*, 5(APRIL2016):1–31.

Terrado R., Scarcella K., Thaler M., Vincent W. F., and Lovejoy C. (2013). Small phytoplankton in Arctic seas: vulnerability to climate change. *Biodiversity*, 14(1):2–18.

Thiele S., Fuchs B. M., Amann R., and Iversen M. H. (2015). Colonization in the Photic Zone and Subsequent Changes during Sinking Determine Bacterial Community Composition in Marine Snow. *Applied and Environmental Microbiology*, 81(4):1463–1471.

Thomas D. N. *Sea ice*. John Wiley & Sons, 2017. ISBN 1118778383.

Thomas D. N. and Dieckmann G. S. (2003). Sea Ice: an introduction to its Physics. *Chemistry, Biology, and Geology*.

Thomas T., Gilbert J., and Meyer F. (2012). Metagenomics - a guide from sampling to data analysis. *Microbial Informatics and Experimentation*, 2(1):3.

Thomsen P. F. and Willerslev E. (2015). Environmental DNA – An emerging tool in conservation for monitoring past and present biodiversity. *Biological Conservation*, 183:4–18.

Thornton D. C. (2014). Dissolved organic matter (DOM) release by phytoplankton in the contemporary and future ocean. *European Journal of Phycology*, 49(1):20–46.

Tippenhauer S., Torres-Valdes S., Fong A. A., Krauß F., Huchler M., and Wisotzki A. Physical oceanography measured on water bottle samples during POLARSTERN cruise PS99.2 (ARK-XXX/1.2). Technical report, 2017.

Tomczak M. and Godfrey J. S. *Regional oceanography: an introduction*. Elsevier, 2013. ISBN 1483287610.

Töpper B., Larsen A., Thingstad T. F., Thyrhaug R., and Sandaa R. A. (2010). Bacterial community composition in an Arctic phytoplankton mesocosm bloom: The impact of silicate and glucose. *Polar Biology*, 33(11):1557–1565.

Torres-Valdés S., Tsubouchi T., Bacon S., Naveira-Garabato A. C., Sanders R., McLaughlin F. A., Petrie B., Kattner G., Azetsu-Scott K., and Whitledge T. E. (2013). Export of nutrients from the Arctic Ocean. *Journal of Geophysical Research: Oceans*, 118(4):1625–1644.

Tremblay J.-É. and Gagnon J. The effects of irradiance and nutrient supply on the productivity of Arctic waters: a perspective on climate change. In Nihoul J. C. J. and Kostianoy A. G., editors, *Influence of Climate Change on the Changing Arctic and Sub-Arctic Conditions*, pages 73–93, Dordrecht, 2009. Springer Netherlands. ISBN 978-1-4020-9460-6. doi: 10.1007/978-1-4020-9460-6_7. URL http://link.springer.com/10.1007/978-1-4020-9460-6{_}7.

Tremblay J.-É., Anderson L. G., Matrai P., Coupel P., Bélanger S., Michel C., and Reigstad M. (2015). Global and regional drivers of nutrient supply, primary production and CO2 drawdown in the changing Arctic Ocean. *Progress in Oceanography*, 139:171–196.

Turner J. T. (2002). Zooplankton fecal pellets, mrine snow and sinking phytoplankton blooms. *Aquatic Microbial Ecology*, 27:57–102.

Turner J. W., Berthiaume C. T., Morales R., Armbrust E. V., and Strom M. S. (2016). Genomic evidence of adaptive evolution in emergent Vibrio parahaemolyticus ecotypes. *Elementa: Science of the Anthropocene*, 4:000117.

Vader A., Marquardt M., Meshram A. R., and Gabrielsen T. M. (2015). Key Arctic phototrophs are widespread in the polar night. *Polar Biology*, 38(1):13–21.

Valencia B., Landry M. R., Décima M., and Hannides C. C. S. (2016). Environmental drivers of mesozooplankton biomass variability in the North Pacific Subtropical Gyre. *Journal of Geophysical Research: Biogeosciences*, 121(12):3131–3143.

Vaughan D. G., Comiso J. C., Allison I., Carrasco J., Kaser G., Kwok R., Mote P., Murray T., Paul F., and Ren J. (2013). Observations: cryosphere. *Climate change*, 2103:317–382.

Vergin K. L., Beszteri B., Monier A., Thrash J. C., Treusch A. H., Kilpert F., Worden A. Z., and Giovannoni S. J. High resolution SAR11 ecotype dynamics at the Bermuda Atlantic Time-series Study Site as determined by phylogenetic placement of pyrosequences. In *2012 Ocean Sciences Meeting*, 2012.

Vernet M., Richardson T. L., Metfies K., Nöthig E.-M., and Peeken I. (2017). Models of Plankton Community Changes during a Warm Water Anomaly in Arctic Waters Show Altered Trophic Pathways with Minimal Changes in Carbon Export. *Frontiers in Marine Science*, 4(May):1–19.

Vezzulli L., Grande C., Reid P. C., Hélaouët P., Edwards M., Höfle M. G., Brettar I., Colwell R. R., and Pruzzo C. (2016). Climate influence on Vibrio and associated human diseases during the

past half-century in the coastal North Atlantic. *Proceedings of the National Academy of Sciences*, 113(34):E5062–E5071.

von Appen W.-J., Schauer U., Somavilla R., Bauerfeind E., and Beszczynska-Möller A. (2015). Exchange of warming deep waters across Fram Strait. *Deep Sea Research Part I: Oceanographic Research Papers*, 103:86–100.

Walczowski W., Beszczynska-Möller A., Wieczorek P., Merchel M., and Grynczel A. (2017). Oceanographic observations in the Nordic Sea and Fram Strait in 2016 under the IO PAN long-term monitoring program AREX. *Oceanologia*, 59(2):187–194.

Walsh E. A., Kirkpatrick J. B., Rutherford S. D., Smith D. C., Sogin M., and D'Hondt S. (2016). Bacterial diversity and community composition from seasurface to subseafloor. *ISME Journal*, 10(4):979–989.

Wang B., Lu L., Lv H., Jiang H., Qu G., Tian C., and Ma Y. (2014). The transcriptome landscape of Prochlorococcus MED4 and the factors for stabilizing the core genome. *BMC microbiology*, 14:11.

Wang M. and Overland J. E. (2015). Projected future duration of the sea-ice-free season in the Alaskan Arctic. *Progress in Oceanography*, 136:50–59.

Wang Q., Danilov S., Sidorenko D., Timmermann R., Wekerle C., Wang X., Jung T., and Schröter J. (2014). The Finite Element Sea Ice-Ocean Model (FESOM) v.1.4: formulation of an ocean general circulation model. *Geoscientific Model Development*, 7(2):663–693.

Wang Y. and Qian P. Y. (2009). Conservative fragments in bacterial 16S rRNA genes and primer design for 16S ribosomal DNA amplicons in metagenomic studies. *PLoS ONE*, 4(10).

Waniek J., Koeve W., and Prien R. D. (2000). Trajectories of sinking particles and the catchment areas above sediment traps in the northeast Atlantic. *Journal of Marine Research*, 58(6):983–1006.

Wassmann P., Bauerfeind E., Fortier M., Fukuchi M., Hargrave B., Moran B., Noji T., Nöthig E.-M., Olli K., Peinert R., Sasaki H., and Shevchenko V. (2004). Particulate Organic Carbon Flux to the Arctic Ocean Sea Floor. *The Organic Carbon Cycle in the Arctic Ocean*, (I):101–138.

Wassmànn P. (1997). Retention versus export food chains: Processes controlling sinking loss from marine pelagic systems. *Hydrobiologia*, 363:29–57.

Wassmann P. (2015). Overarching perspectives of contemporary and future ecosystems in the Arctic Ocean. *Progress in Oceanography*, 139:1–12.

Wassmann P. and Reigstad M. (2011). Future Arctic Ocean Seasonal Ice Zones and Implications for Pelagic-Benthic Coupling. *Oceanography*, 24(3):220–231.

Wassmann P., Andreassen I., Reigstad M., and Slagstad D. (1996). Pelagic-benthic coupling in the Nordic Seas: The role of episodic events. *Marine Ecology*, 17(1-3):447–471.

Wassmann P., Slagstad D., and Ellingsen I. (2010). Primary production and climatic variability in the European sector of the Arctic Ocean prior to 2007: Preliminary results. *Polar Biology*, 33(12):1641–1650.

Wassmann P., Duarte C. M., Agustí S., and Sejr M. K. (2011). Footprints of climate change in the Arctic marine ecosystem. *Global Change Biology*, 17(2):1235–1249.

Wear E. K., Wilbanks E. G., Nelson C. E., and Carlson C. A. (2018). Primer selection impacts specific population abundances but not community dynamics in a monthly time-series 16S rRNA gene amplicon analysis of coastal marine bacterioplankton. *Environmental Microbiology*, 00.

Weiss S., Van Treuren W., Lozupone C., Faust K., Friedman J., Deng Y., Xia L. C., Xu Z. Z., Ursell L., Alm E. J., Birmingham A., Cram J. A., Fuhrman J. A., Raes J., Sun F., Zhou J., and Knight

R. (2016). Correlation detection strategies in microbial data sets vary widely in sensitivity and precision. *The ISME Journal*, 10(7):1669–1681.

Wekerle C., Krumpen T., Dinter T., Iversen M., and Salter I. (2015). Origin and properties of sediment trap catchment areas in Fram Strait : results from Lagrangian modelling and remote sensing. *Frontiers in Marine Science*, pages 1–26.

Wekerle C., Wang Q., Danilov S., Schourup-Kristensen V., von Appen W.-J., and Jung T. (2017). Atlantic Water in the Nordic Seas: Locally eddy-permitting ocean simulation in a global setup. *Journal of Geophysical Research: Oceans*, 122(2):914–940.

Wekerle C., Wang Q., von Appen W. J., Danilov S., Schourup-Kristensen V., and Jung T. (2017). Eddy-Resolving Simulation of the Atlantic Water Circulation in the Fram Strait With Focus on the Seasonal Cycle. *Journal of Geophysical Research: Oceans*, 122(11):8385–8405.

Wells L. E. and Deming J. W. (2003). Abundance of bacteria, the Cytophaga-Flavobacterium cluster and Archaea in cold oligotrophic waters and nepheloid layers of the Northwest Passage, Canadian archipelago. *Aquatic Microbial Ecology*, 31(1):19–31.

Wemheuer B., Güllert S., Billerbeck S., Giebel H.-A. A., Voget S., Simon M., and Daniel R. (2014). Impact of a phytoplankton bloom on the diversity of the active bacterial community in the southern North Sea as revealed by metatranscriptomic approaches. *FEMS Microbiology Ecology*, 87(2):378–389.

Wenzhoefer F., Lemburg J., Hofbauer M., Lehmenhecker S., and Faerber P. TRAMPER. In *OCEANS 2016 MTS/IEEE Monterey*, pages 1–6. IEEE, 2016. ISBN 978-1-5090-1537-5. doi: 10.1109/OCEANS.2016.7761217. URL `http://ieeexplore.ieee.org/document/7761217/`.

Weydmann A., Søreide J. E., Kwasniewski S., and Widdicombe S. (2012). Influence of CO2-induced acidification on the reproduction of a key Arctic copepod Calanus glacialis. *Journal of Experimental Marine Biology and Ecology*, 428:39–42.

Whitman W. B., Coleman D. C., and Wiebe W. J. (1998). Prokaryotes: The unseen majority. *Proceedings of the National Academy of Sciences*, 95(12):6578–6583.

Wieczorek J., Bloom D., Guralnick R., Blum S., Döring M., Giovanni R., Robertson T., and Vieglais D. (2012). Darwin Core: An Evolving Community-Developed Biodiversity Data Standard. *PLoS ONE*, 7(1):e29715.

Wilkins D., Van Sebille E., Rintoul S. R., Lauro F. M., and Cavicchioli R. (2013). Advection shapes Southern Ocean microbial assemblages independent of distance and environment effects. *Nature Communications*, 4(May):1–7.

Wilkinson M. D., Dumontier M., Aalbersberg I. J., Appleton G., Axton M., Baak A., Blomberg N., Boiten J.-W., da Silva Santos L. B., Bourne P. E., Bouwman J., Brookes A. J., Clark T., Crosas M., Dillo I., Dumon O., Edmunds S., Evelo C. T., Finkers R., Gonzalez-Beltran A., Gray A. J., Groth P., Goble C., Grethe J. S., Heringa J., 't Hoen P. A., Hooft R., Kuhn T., Kok R., Kok J., Lusher S. J., Martone M. E., Mons A., Packer A. L., Persson B., Rocca-Serra P., Roos M., van Schaik R., Sansone S.-A., Schultes E., Sengstag T., Slater T., Strawn G., Swertz M. A., Thompson M., van der Lei J., van Mulligen E., Velterop J., Waagmeester A., Wittenburg P., Wolstencroft K., Zhao J., and Mons B. (2016). The FAIR Guiding Principles for scientific data management and stewardship. *Scientific Data*, 3:160018.

Williams C., Dupont A., Loevenich J., Post A., Dinasquet J., and Yager P. (2016). Pelagic microbial heterotrophy in response to a highly productive bloom of Phaeocystis antarctica in the Amundsen Sea Polynya, Antarctica. *Elementa: Science of the Anthropocene*, 4:000102.

Williams K. P. (2013). Pathogenicity Island Mobility and Gene Content. (October).

Williams T. J., Long E., Evans F., DeMaere M. Z., Lauro F. M., Raftery M. J., Ducklow H., Grzymski J. J., Murray A. E., and Cavicchioli R. (2012). A metaproteomic assessment of winter and summer bacterioplankton from Antarctic Peninsula coastal surface waters. *The ISME Journal*, 6(10):1883–1900.

Williams T. J., Wilkins D., Long E., Evans F., Demaere M. Z., Raftery M. J., and Cavicchioli R. (2013). The role of planktonic Flavobacteria in processing algal organic matter in coastal East Antarctica revealed using metagenomics and metaproteomics. *Environmental Microbiology*, 15(5):1302–1317.

Wilson B., Müller O., Nordmann E.-L., Seuthe L., Bratbak G., and Øvreås L. (2017). Changes in Marine Prokaryote Composition with Season and Depth Over an Arctic Polar Year. *Frontiers in Marine Science*, 4(April):1–17.

Wilson C. and Wallace D. W. R. (1990). Using the Nutrient Ratio No Po As a Tracer of Continental-Shelf Waters in the Central Arctic-Ocean. *Journal of Geophysical Research*, 95(C12):22193–22208.

Wittebolle L., Marzorati M., Clement L., Balloi A., Daffonchio D., Heylen K., De Vos P., Verstraete W., and Boon N. (2009). Initial community evenness favours functionality under selective stress. *Nature*, 458(7238):623–626.

Woebken D., Fuchs B. M., Kuypers M. M., and Amann R. (2007). Potential interactions of particle-associated anammox bacteria with bacterial and archaeal partners in the Namibian upwelling system. *Applied and Environmental Microbiology*, 73(14):4648–4657.

Wolf C., Iversen M., Klaas C., and Metfies K. (2016). Limited sinking of Phaeocystis during a 12 days sediment trap study. *Molecular Ecology*, 25(14):3428–3435.

Wollenburg J. E., Katlein C., Nehrke G., Nöthig E.-M., Matthiessen J., Wolf- Gladrow D. A., Nikolopoulos A., Gázquez-Sanchez F., Rossmann L., Assmy P., Babin M., Bruyant F., Beaulieu M., Dybwad C., and Peeken I. (2018). Ballasting by cryogenic gypsum enhances carbon export in a Phaeocystis under-ice bloom. *Scientific Reports*, 8(1):7703.

Woodgate R. A., Weingartner T. J., and Lindsay R. (2012). Observed increases in Bering Strait oceanic fluxes from the Pacific to the Arctic from 2001 to 2011 and their impacts on the Arctic Ocean water column. *Geophysical Research Letters*, 39(24):n/a–n/a.

Wright J. J., Mewis K., Hanson N. W., Konwar K. M., Maas K. R., and Hallam S. J. (2014). Genomic properties of Marine Group A bacteria indicate a role in the marine sulfur cycle. *ISME Journal*, 8(2):455–468.

Wulff T., Bauerfeind E., and von Appen W.-J. (2016). Physical and ecological processes at a moving ice edge in the Fram Strait as observed with an AUV. *Deep Sea Research Part I: Oceanographic Research Papers*, 115:253–264.

Xing P., Hahnke R. L., Unfried F., Markert S., Huang S., Barbeyron T., Harder J., Becher D., Schweder T., Glöckner F. O., Amann R. I., and Teeling H. (2015). Niches of two polysaccharide-degrading Polaribacter isolates from the North Sea during a spring diatom bloom. *ISME Journal*, 9(6):1410–1422.

Yang B., Wang Y., and Qian P. Y. (2016). Sensitivity and correlation of hypervariable regions in 16S rRNA genes in phylogenetic analysis. *BMC Bioinformatics*, 17(1):1–8.

Yawata Y., Cordero O. X., Menolascina F., Hehemann J.-H., Polz M. F., and Stocker R. (2014). Competition-dispersal tradeoff ecologically differentiates recently speciated marine bacterioplankton populations. *Proceedings of the National Academy of Sciences*, 111(15):5622–5627.

Yilmaz P., Kottmann R., Field D., Knight R., Cole J. R., Amaral-Zettler L., Gilbert J. A., Karsch-Mizrachi I., Johnston A., Cochrane G., Vaughan R., Hunter C., Park J., Morrison N., Rocca-Serra P., Sterk P., Arumugam M., Bailey M., Baumgartner L., Birren B. W., Blaser M. J., Bonazzi V., Booth T., Bork P., Bushman F. D., Buttigieg P. L., Chain P. S. G., Charlson E., Costello E. K., Huot-Creasy H., Dawyndt P., DeSantis T., Fierer N., Fuhrman J. A., Gallery R. E., Gevers D., Gibbs R. A., Gil I. S., Gonzalez A., Gordon J. I., Guralnick R., Hankeln W., Highlander S., Hugenholtz P., Jansson J., Kau A. L., Kelley S. T., Kennedy J., Knights D., Koren O., Kuczynski J., Kyrpides N., Larsen R., Lauber C. L., Legg T., Ley R. E., Lozupone C. A., Ludwig W., Lyons D., Maguire E., Methé B. A., Meyer F., Muegge B., Nakielny S., Nelson K. E., Nemergut D.,

Neufeld J. D., Newbold L. K., Oliver A. E., Pace N. R., Palanisamy G., Peplies J., Petrosino J., Proctor L., Pruesse E., Quast C., Raes J., Ratnasingham S., Ravel J., Relman D. A., Assunta-Sansone S., Schloss P. D., Schriml L., Sinha R., Smith M. I., Sodergren E., Spor A., Stombaugh J., Tiedje J. M., Ward D. V., Weinstock G. M., Wendel D., White O., Whiteley A., Wilke A., Wortman J. R., Yatsunenko T., and Glöckner F. O. (2011). Minimum information about a marker gene sequence (MIMARKS) and minimum information about any (x) sequence (MIxS) specifications. *Nature Biotechnology*, 29(5):415–420.

Yoshida S., Hiraga K., Takehana T., Taniguchi I., Yamaji H., Maeda Y., Toyohara K., Miyamoto K., Kimura Y., and Oda K. (2016). A bacterium that degrades and assimilates poly(ethylene terephthalate). *Science*, 351(6278):1196–1199.

Yu Z.-C., Chen X.-L., Shen Q.-T., Zhao D.-L., Tang B.-L., Su H.-N., Wu Z.-Y., Qin Q.-L., Xie B.-B., Zhang X.-Y., Yu Y., Zhou B.-C., Chen B., and Zhang Y.-Z. (2015). Filamentous phages prevalent in Pseudoalteromonas spp. confer properties advantageous to host survival in Arctic sea ice. *The ISME Journal*, 9(4):871–881.

Zamani B., Krumpen T., Smedsrud L. H., and Gerdes R. Fram Strait sea ice volume export : comparison of a high resolution sea ice-ocean model with remote sensing data. volume 20, page 18755, 2018.

Zhang J., Kobert K., Flouri T., and Stamatakis A. (2014). PEAR: a fast and accurate Illumina Paired-End reAd mergeR. *Bioinformatics*, 30(5):614–620.

Zinger L., Gobet A., and Pommier T. (2012). Two decades of describing the unseen majority of aquatic microbial diversity. *Molecular Ecology*, 21(8):1878–1896.

Zubkov M. V. and Tarran G. A. (2008). High bacterivory by the smallest phytoplankton in the North Atlantic Ocean. *Nature*, 455(7210):224–226.

Acknowledgements

I would like to thank Antje Boetius for accepting me as a PhD student to the HGF MPG Joint Research Group, and for giving me the opportunity to follow my scientific and professional aspirations throughout the last three years. Many thanks to Christina Bienhold for her dedicated guidance and support, and to Ian Salter for fruitful scientific discussions. A special thank you to all members of the HGF-MPG bridge group for Deep-Sea Ecology and Technology for great experiences both at sea and on land!

Thank you to Daniel Sher for agreeing to review my thesis, to Kai-Uwe Hinrichs, Bernhard Fuchs and Morten Iversen for taking part in my defense committee.

Finally, thanks to Verena, Laura, Rafa and my family for their friendship and encouragement throughout my PhD.

Name / *Name*: Eduard Fadeev Datum / *Date*: 15.10.18

Anschrift / *Address*: Beginenhof 3, Bremen

Erklärung gem. § 4 Abs. 1 Nr. 3 und 4
der Promotionsordnung vom 15.07.2015 /
Statement according to § 4 (1) no. 3 and 4
of the Doctoral Degree Rules and Regulations of 15.07.2015

Ich erkläre, dass ich mich weder einem Promotionsverfahren unterzogen noch ein solches beantragt habe. /
I affirm that I did not undergo a doctoral degree granting procedure, nor did I apply for the examination procedure elsewhere.

Mit einer Überprüfung der Dissertation mit qualifizierter Software zur Untersuchung von Plagiatsvorwürfen bin ich einverstanden. /
I accept scanning of the doctoral thesis with appropriate software for the detection of plagiarism.

(Unterschrift Doktorand/in / *Signature PhD student*)